

UNIVERSITÀ  
DEGLI STUDI  
DI PADOVA

Head Office: Università degli Studi di Padova

Department: Scienze chimiche

---

Ph.D. COURSE IN: MOLECULAR SCIENCES

CURRICULUM: CHEMICAL SCIENCES

SERIES: XXXII CYCLE

**Filling the Structure-Reactivity Gap: *in silico* approaches to rationalize the  
design of molecular catalysts**

Coordinator: Prof. Dr. Leonard Jan Prins

Supervisor: Prof. Dr. Laura Orian

Ph.D. student: Shah Masood Ahmad



# Contents

Acknowledgments.....	xiii
Overview of the research .....	xv
<b>Chapter 01</b>	
1. Introduction.....	1
<b>Chapter 02</b>	
2. Theories, Methods, and Models.....	7
2.1. Computational Chemistry .....	7
2.2. Methodologies for Quantum Chemistry Calculations .....	7
2.3. Density Functional Theory (DFT).....	9
2.4. Computational Details.....	11
2.5. ASA: Activation-Strain Analysis.....	11
2.6. EDA: Energy Decomposition Analysis.....	13
2.7. Turnover Frequency.....	14
<b>Chapter 03</b>	
3. <i>In Silico</i> Acetylene [2+2+2] Cycloadditions Catalyzed by Rh/Cr Indenyl Fragments.....	17
3.1. Introduction.....	17
3.2. Acetylene [2+2+2] Cycloaddition Catalyzed by Anti-[Cr(CO) <sub>3</sub> IndRh] Fragment: Reaction Mechanism and PES (Path I) .....	19
3.3. Acetylene [2+2+2] Cycloaddition Catalyzed by Syn-[Cr(CO) <sub>3</sub> IndRh] Fragment: Reaction Mechanism and PES (Path I).....	26
3.4. Acetylene [2+2+2] Cycloaddition Catalyzed by Anti-[Cr(CO) <sub>3</sub> IndRh] Fragment: Reaction Mechanism and PES (Path II) .....	30
3.5. Discussion.....	35
3.6. Conclusions.....	37
<b>Chapter 04</b>	
4. Effect of Changing the Second metal in Bimetallic [M*(CO) <sub>3</sub> IndRh] (M* = Cr, Mo, W) on the Reaction Mechanism and PESs.....	39
4.1. Introduction.....	39

4.2. Anti bimetallic catalysts: Reaction Mechanism and PES (Path 1).....	40
4.3. Syn bimetallic catalyst: Reaction Mechanism and PES (Path I).....	49
4.4. Anti bimetallic catalysts: Reaction Mechanism and PES (Path II).....	54
4.5. Turnover Frequencies (TOFs) and Structural-Activity Relationship.....	59
4.6. Conclusions.....	61

## **Chapter 05**

5. Role of the aromatic ligands in Rh(I) Half-sandwich Catalysis: Reaction Mechanism and PESs.....	63
5.1. Introduction.....	63
5.2. Reaction Mechanism and PESs (Path I).....	65
5.3. Alternative Mechanistic Path II.....	72
5.4. Turnover Frequencies (TOFs) and Structural-Activity Relationship.....	78
5.5. Conclusions.....	79

## **Chapter 06**

6. Summary and Concluding Remarks.....	81
Appendix A.....	85
Appendix B.....	107
Appendix C.....	137
<b>References.....</b>	<b>157</b>

# List of Acronyms and Abbreviations

Ab	1,2-azaborolyl
Abi	3a,7a-azaborindenyl
ASA	Activation-strain analysis
BLYP	X: Becke, C: Lee-Yang-Parr (Functional)
Cp	Cyclopentadienyl
CSD	Cambridge structural database
CpN	Cyclopentanaphthyl
Cr	Chromium
Co	Cobalt
DFT	Density functional theory
D3-BJ	Dispersion correction by Grimme with Becke-Johnson damping function
EDA	Energy decomposition analysis
Ene	Alkene, Alkyne, Allene, Arene, etc.
FN	Fluorenyl
HF	Hartee-Fock
HOMO	Highest occupied molecular orbital
Ind	Indenyl
LISP	Label independent slippage parameter
Ln	Ligand
M	Metal
Mo	Molybdenum
PES	Potential energy surface
QM	Quantum mechanics
Rh	Rhodium
SC	Small frozen core approximation
STO	Slater-type orbital
STREGA	Structure-reactivity gap

SAR	Structure-activity relationship
W	Wolframium or Tungsten
TOF	Turnover frequency
TDTS	TOF-determining transition state
TDI	TOF-determining intermediate (TDI)
TZ2P	Triple zeta with 2 polarization functions (basis set)
XC	Exchange-Correlation
ZORA	Zeroth order regular approximation

# List of Figures

<b>Figure 1.</b> Optimized structures with selected interatomic distances (Å) and angles (deg) of the intermediates and transition states located on the PES of the anti-Cr@IndRh catalyzed acetylene [2+2+2] cycloaddition to benzene (Path I, Scheme 6a). Level of theory: ZORA-BLYP/TZ2P.....	20
<b>Figure 2. (a)</b> Energy profiles of acetylene [2+2+2] cycloaddition to benzene catalyzed by CpRh (black), IndRh (red), and bimetallic anti-Cr@IndRh (blue) (Scheme 6a, Path I). <b>(b)</b> Profiles of the slippage parameters $\Delta$ (dashed line) and LISP (solid line) for the acetylene [2+2+2] cycloaddition cycles catalyzed by CpRh (black), IndRh (red), and bimetallic anti-Cr@IndRh (blue) along Path I (Scheme 6a). Level of theory: ZORA-BLYP/TZ2P.....	21
<b>Figure 3.</b> Kohn-Sham HOMOs of <b>Cp-1</b> , <b>Ind-1</b> , and <b>anti-Cr@Ind-1</b> ; the level of theory: ZORA-BLYP/TZ2P. The isodensity value is 0.03.....	22
<b>Figure 4.</b> Optimized structures with selected interatomic distances (Å) and angles (deg) of the intermediates and transition states located on the PES of the syn-Cr@IndRh catalyzed acetylene [2+2+2] cycloaddition to benzene (Path I, Scheme 6a). Level of theory: ZORA-BLYP/TZ2P.....	27
<b>Figure 5. (a)</b> Energy profile of acetylene [2+2+2] cycloaddition to benzene catalyzed by syn-Cr@IndRh (Scheme 6a, Path I). <b>(b)</b> Profiles of the slippage parameters $\Delta$ (dashed line) and LISP (solid line) along the acetylene [2+2+2] cycloaddition cycle catalyzed by syn-Cr@IndRh (Scheme 6a, Path I). Level of theory: ZORA-BLYP/TZ2P.....	28
<b>Figure 6.</b> HOMO-3 of <b>syn-Cr@Ind-1</b> ; the isodensity value is 0.03.....	30
<b>Figure 7.</b> Optimized structures with selected interatomic distances (Å) and angles (deg) of the intermediates and transition states located on the PES of the anti-Cr@IndRh(CO) catalyzed acetylene [2+2+2] cycloaddition to benzene (Path II, Scheme 6b). Level of theory: ZORA-BLYP/TZ2P.....	31
<b>Figure 8. (a)</b> Energy profiles of acetylene [2+2+2] cycloaddition to benzene catalyzed by CpRh(CO) (black), IndRh(CO) (red), and anti-Cr@IndRh(CO) (blue) (Scheme 6b, Path II). <b>(b)</b>	

Profiles of the slippage parameters  $\Delta$  (dashed line) and LISP (solid line) along the acetylene [2+2+2] cycloaddition cycles catalyzed by CpRh(CO) (black), IndRh(CO) (red), and anti-Cr@IndRh(CO) (blue) (Scheme 6b, Path II). Level of theory: ZORA-BLYP/TZ2P ..... 33

**Figure 9.** Optimized structures with selected interatomic distances ( $\text{\AA}$ ) and angles (deg) of the intermediates and transition states located on the PES of the anti-Mo@IndRh catalyzed acetylene [2+2+2] cycloaddition to benzene (Path I, Scheme 7a). Level of theory: ZORA-BLYP/TZ2P ..... 41

**Figure 10.** Optimized structures with selected interatomic distances ( $\text{\AA}$ ) and angles (deg) of the intermediates and transition states located on the PES of the anti-W@IndRh catalyzed acetylene [2+2+2] cycloaddition to benzene (Path I, Scheme 7a). Level of theory: ZORA-BLYP/TZ2P... 42

**Figure 11.** (a) Energy profiles of acetylene [2+2+2] cycloaddition to benzene catalyzed by the bimetallic anti- $M^*$ @IndRh ( $M^* = \text{Cr}$  (black), Mo (red), W (blue)) (Scheme 7a, Path I). (b) Profiles of the slippage parameters  $\Delta$  (dashed line) and LISP (solid line) along the acetylene [2+2+2] cycloaddition cycles catalyzed by the bimetallic anti- $M^*$ @IndRh ( $M^* = \text{Cr}$  (black), Mo (red), W (blue)) along Path I (Scheme 7a). Level of theory: ZORA-BLYP/TZ2P ..... 43

**Figure 12.** Profiles of the slippage parameter LISP for  $M^*$ -Bz in complexes along the acetylene [2+2+2] cycloaddition cycles catalyzed by the bimetallic anti- $M^*$ @IndRh ( $M^* = \text{Cr}$  (black), Mo (red), W (blue)) along Path I (Scheme 7a). Level of theory: ZORA-BLYP/TZ2P ..... 45

**Figure 13.** Frontier molecular orbitals (HOMOs) of **anti-Cr@Ind-1**, **anti-Mo@Ind-1**, and **anti-W@Ind-1**; the level of theory: ZORA-BLYP/TZ2P. The isodensity value is 0.03 ..... 46

**Figure 14.** Optimized structures with selected interatomic distances ( $\text{\AA}$ ) and angles (deg) of the intermediates and transition states located on the PES of the syn-Mo@IndRh catalyzed acetylene [2+2+2] cycloaddition to benzene (Path I, Scheme 7a). Level of theory: ZORA-BLYP/TZ2P... 50

**Figure 15.** Optimized structures with selected interatomic distances ( $\text{\AA}$ ) and angles (deg) of the intermediates and transition states located on the PES of the syn-W@IndRh catalyzed acetylene [2+2+2] cycloaddition to benzene (Path I, Scheme 7a). Level of theory: ZORA-BLYP/TZ2P... 51

**Figure 16.** (a) Energy profiles of acetylene [2+2+2] cycloaddition to benzene catalyzed by bimetallic syn- $M^*$ @IndRh ( $M^* = \text{Cr}$  (black), Mo (red), W (blue)) (Scheme 7a, Path I). (b) Profiles

of the slippage parameters  $\Delta$  (dashed line) and LISP (solid line) along the acetylene [2+2+2] cycloaddition cycles catalyzed by bimetallic syn-M<sup>\*</sup>@IndRh (M<sup>\*</sup> = Cr (black), Mo (red), W (blue)) along Path I (Scheme 12a). Level of theory: ZORA-BLYP/TZ2P.....52

**Figure 17.** Profiles of the slippage parameter LISP for M<sup>\*</sup>-Bz in complexes along the acetylene [2+2+2] cycloaddition cycles catalyzed by the bimetallic syn-M<sup>\*</sup>@IndRh (M<sup>\*</sup> = Cr (black), Mo (red), W (blue)) along Path I (Scheme 7a). Level of theory: ZORA-BLYP/TZ2P.....53

**Figure 18.** The frontier molecular orbitals (HOMOs) overlap in **syn-M<sup>\*</sup>@Ind-1** (M<sup>\*</sup>= Cr, Mo, W); the isodensity value is 0.03.....54

**Figure 19.** Optimized structures with selected interatomic distances ( $\text{\AA}$ ) and angles (deg) of the intermediates and transition states located on the PES of the anti-Mo@IndRh(CO) catalyzed acetylene [2+2+2] cycloaddition to benzene (Path II, Scheme 7b). Level of theory: ZORA-BLYP/TZ2P.....55

**Figure 20.** Optimized structures with selected interatomic distances ( $\text{\AA}$ ) and angles (deg) of the intermediates and transition states located on the PES of the anti-W@IndRh(CO) catalyzed acetylene [2+2+2] cycloaddition to benzene (Path II, Scheme 7b). Level of theory: ZORA-BLYP/TZ2P.....56

**Figure 21.** (a) Energy profiles of acetylene [2+2+2] cycloaddition to benzene catalyzed by bimetallic anti-Cr@IndRh(CO) (black) anti-Mo@IndRh(CO) (red), and anti-W@IndRh(CO) (blue) (Scheme 7b, Path II). (b) Profiles of the slippage parameter (LISP) along with the acetylene [2+2+2] cycloaddition cycles catalyzed by bimetallic anti-Cr@IndRh(CO) (black) anti-Mo@IndRh(CO) (red), and anti-W@IndRh(CO) (blue) along Path II (Scheme 7b). Level of theory: ZORA-BLYP/TZ2P.....57

**Figure 22.** Profiles of the slippage parameter LISP for M<sup>\*</sup>-Bz in complexes along the acetylene [2+2+2] cycloaddition cycles catalyzed by bimetallic anti-M<sup>\*</sup>@IndRh(CO) (M<sup>\*</sup> = Cr (black), Mo (red), W (blue)) along Path II (Scheme 7b). Level of theory: ZORA-BLYP/TZ2P.....58

**Figure 23.** Optimized structures with selected interatomic distances ( $\text{\AA}$ ) and angles (deg) of the intermediates and transition states located on the PES of the CpNRh catalyzed acetylene [2+2+2] cycloaddition to benzene (Path I, Scheme 9a). Level of theory: ZORA-BLYP/TZ2P.....66

<b>Figure 24.</b> Optimized structures with selected interatomic distances (Å) and angles (deg) of the intermediates and transition states located on the PES of the FNRh catalyzed acetylene [2+2+2] cycloaddition to benzene (Path I, Scheme 9a). Level of theory: ZORA-BLYP/TZ2P.....	67
<b>Figure 25. (a)</b> Energy profiles of acetylene [2+2+2] cycloaddition to benzene catalyzed by CpRh (black), IndRh (red), CpNRh (blue) and FNRh (green) (Scheme 9a, Path I). <b>(b)</b> Profiles of the slippage parameter (LISP) along with the acetylene [2+2+2] cycloaddition cycles catalyzed by CpRh (black), IndRh (red), CpNRh (blue), and FNRh (green) along Path I (Scheme 9a). Level of theory: ZORA-BLYP/TZ2P.....	68
<b>Figure 26.</b> Kohn-Sham HOMOs of <b>Cp-1</b> , <b>Ind-1</b> , <b>CpN-1</b> , and <b>FN-1</b> ; the level of theory: ZORA-BLYP/TZ2P. The isodensity value is 0.03.....	69
<b>Figure 27.</b> Kohn-Sham HOMOs of <b>Cp-2</b> , <b>Ind-2</b> , <b>CpN-2</b> , and <b>FN-2</b> ; the level of theory: ZORA-BLYP/TZ2P. The isodensity value is 0.03.....	70
<b>Figure 28.</b> Optimized structures with selected interatomic distances (Å) and angles (deg) of the intermediates and transition states located on the PES of the CpNRh(CO) catalyzed acetylene [2+2+2] cycloaddition to benzene (Path II, Scheme 9b). Level of theory: ZORA-BLYP/TZ2P.....	73
<b>Figure 29.</b> Optimized structures with selected interatomic distances (Å) and angles (deg) of the intermediates and transition states located on the PES of the FNRh(CO) catalyzed acetylene [2+2+2] cycloaddition to benzene (Path II, Scheme 9b). Level of theory: ZORA-BLYP/TZ2P.....	74
<b>Figure 30. (a)</b> Energy profiles of acetylene [2+2+2] cycloaddition to benzene catalyzed by CpRh(CO) (black), IndRh(CO) (red), CpNRh(CO) (blue), and FNRh(CO) (green) (Scheme 9b, Path II). <b>(b)</b> Profiles of the slippage parameter (LISP) along with the acetylene [2+2+2] cycloaddition cycles catalyzed by CpRh(CO) (black), IndRh(CO) (red), CpNRh(CO) (blue), and FNRh(CO) (green) along Path II (Scheme 9b). Level of theory: ZORA-BLYP/TZ2P.....	75

# List of Tables

<b>Table 1.</b> Activation strain analysis for the oxidative coupling <b>Z-1 → Z-2</b> (Path 1); all values are in kcal mol <sup>-1</sup> . The fragments are Cp'Rh (Cp' = Cp, Ind, and anti-[Cr(CO) <sub>3</sub> Ind]) and the C <sub>4</sub> H <sub>4</sub> moiety (the reference are two acetylene molecules).....	24
<b>Table 2.</b> Activation strain analysis for <b>Cp-4, Ind-4, and anti-Cr@Ind-4</b> ; all values are in kcal mol <sup>-1</sup> . The fragments are Cp'Rh (Cp' = Cp, Ind, and anti-[Cr(CO) <sub>3</sub> Ind]) and C <sub>6</sub> H <sub>6</sub> moiety (the reference is benzene).....	24
<b>Table 3.</b> Activation strain analysis (ASA) of all the intermediates and transition states of the anti-Cr@IndRh catalyzed cycle (Path I); all the values are in kcal mol <sup>-1</sup> . The fragments are Cr(CO) <sub>3</sub> and IndRhX <sub>i</sub> .....	25
<b>Table 4.</b> Activation strain analysis (ASA) of all the intermediates and transition states along the syn-Cr@IndRh catalyzed cycle (Path I); all the values are in kcal mol <sup>-1</sup> . The fragments are Cr(CO) <sub>3</sub> and IndRhX <sub>i</sub> .....	29
<b>Table 5.</b> Activation strain analysis (ASA) of <b>CO-Cp-2, CO-Ind-2, and CO-anti-Cr@Ind-2</b> ; all values are in kcal mol <sup>-1</sup> . The fragments are: CO-Cp'Rh (Cp' = Cp, Ind, and anti-[Cr(CO) <sub>3</sub> Ind]) and the C <sub>4</sub> H <sub>4</sub> moiety (the reference are two acetylene molecules) .....	34
<b>Table 6.</b> Activation strain analysis (ASA) of the transition states <b>CO-Cp-TS(2,3), CO-Ind-TS(2,3), and CO-anti-Cr@Ind-TS(2,3)</b> ; all values are in kcal mol <sup>-1</sup> . The fragments are CO-Cp'RhL <sub>n</sub> (Cp' = Cp, Ind, and anti-[Cr(CO) <sub>3</sub> Ind]) and acetylene.....	34
<b>Table 7.</b> Calculated TOF (s <sup>-1</sup> ) and slippage span ΔLISP* (Å) for the catalytic Path I and II of the [2+2+2] cycloaddition of acetylene to benzene.....	36
<b>Table 8.</b> Activation strain analysis for the first oxidative step <b>Z-1 → Z-TS(1,2)</b> (Path 1); all values are in kcal mol <sup>-1</sup> .....	44
<b>Table 9.</b> Activation strain analysis (ASA) of all the intermediates and transition states of the anti-Mo@IndRh catalyzed cycle (Path I); all the values are in kcal mol <sup>-1</sup> .....	48
<b>Table 10.</b> Activation strain analysis (ASA) of all the intermediates and transition states of the anti-W@IndRh catalyzed cycle (Path I); all the values are in kcal mol <sup>-1</sup> .....	48

<b>Table 11.</b> Calculated TOF (time <sup>-1</sup> ) and slippage span $\Delta\text{LISP}^*$ ( $\text{\AA}$ ) for the acetylene [2+2+2] cycloaddition to benzene. Level of theory: ZORA-BLYP/TZ2P.....	60
<b>Table 12.</b> Activation strain analysis for the first oxidative step <b>Z-1 → Z-TS(1,2)</b> (Path 1); all values are in kcal mol <sup>-1</sup> . The fragments are Cp'Rh (Cp' = Cp, Ind, CpN, and FN) and two acetylene molecules.....	71
<b>Table 13.</b> Activation strain analysis (ASA) of the transition states <b>CO-Z-TS(2,3)</b> ; all values are in kcal mol <sup>-1</sup> . The fragments are CO-Cp'Rh(C <sub>4</sub> H <sub>4</sub> ) (Cp' = Cp, Ind, CpN, and FN]) and acetylene.....	76
<b>Table 14.</b> Calculated TOF (time <sup>-1</sup> ) and slippage span $\Delta\text{LISP}^*$ ( $\text{\AA}$ ) for acetylene [2+2+2] cycloaddition to benzene.....	79

## **DEDICATION**

I dedicate this work to my parents and teachers, who supported me on different roads of life.



## Acknowledgements

I have no valuable words to express my gratitude and affection, although my heart feels an appreciation to those who supported me in the accomplishment of this work.

First of all, I am very thankful to my supervisor Prof. Laura Orian for her continuous support, excellence guidance, meaningful discussions, suggestions, and cooperation. Particularly, I appreciate her endless patience.

Further, I acknowledge the evaluation committee members: Prof. Antonino Polimeno, Prof. Alfonso Zoleo, and Prof. Gianfranco Pasut, for their insightful comments and encouragement.

I am truly grateful to Marco Dalla Tiezza, and Dr. Marco Bortoli, for their generosity and guidance. They helped me during the installation of software particularly ADF (Amsterdam density functional software) and the fruitful discussions related to this research work. I am also obliged to my other lab fellows for their help, cooperation, and for maintaining a peaceful co-existence with me.

Furthermore, I feel indebted to the members of my family and friends for their unending support, love and prayers that assisted me spiritually throughout writing this thesis and my life, in general.

I highly acknowledge the University of Padova for financial support. At last but not least, I am thankful to the Office staff of the DISC-UNIPD for their help with administrative matters.

Shah Masood Ahmad



# Overview of the research

The design of molecular catalysts is an ambitious task implying the fundamental issue of relating the molecular structure to the reactivity, i.e., to the catalytic activity. The rationalization of the experimental data is often not straightforward and mechanistic schemes are not transferrable when the conditions of the process are changed or the catalyst is modified even slightly. Computer-aided investigations proved to be a more and more valid support in the last decade, but in most of the cases the aim is limited to investigate in detail the catalytic mechanism of a specific reaction and no general conclusions are drawn that can be used as a guide for designing novel catalysts for the same or analogous processes.

In this Project, a computational approach has been set up to investigate the family of organometallic complexes displaying catalytic activity toward [2+2+2] cycloadditions of unsaturated molecules. In a recent book (Transition-metal-mediated aromatic ring construction, John Wiley & Sons, 2013, Chapter 4), Ken Tanaka describes Rhodium mediated [2+2+2] cycloadditions and writes ‘*...Although mechanistic aspects of these reactions attract interest, only a few studies have been reported in specific catalysts and substrates...*’. Thus this project, abbreviated with the acronym of STREGA (**Filling the Structure-Reactivity Gap: *in silico* approaches to rationalize the design of molecular catalysts**), aims at filling the gap between the goldmine of experimental data on this class of very important reactions and their mechanistic rationalization with the purpose of outlining the essential electronic and structural features of the catalyst leading to optimal performance, selectivity, and product yield.

In particular, the roles of different metal, different ancillary ligands, different aromatic ligands, and substrates have been accurately investigated; existing data from the literature were also

employed for this analysis. Larger polycyclic ligands can in principle host more than a metal center; for example, Cr can be coordinated to the benzene moiety of a rhodium indenyl complex. This might lead to interesting inter metal cooperative effects which might enhance or inhibit the catalytic activity; thus bimetallic catalysts have been considered. The effect of different cooperative metal nuclei was explored changing from Cr to Mo and W, which all belong to Group 6. Finally, the role of the polycyclic aromatic ligand was investigated and found that indeed it is an important factor since it influences rhodium hapticity and consequently its reactivity. All these results allowed to establish a solid structure-activity relationship which is of general validity for rhodium half-sandwich catalysts towards alkyne [2+2+2] cycloadditions and likely is transferrable to analogous Co, Ru, and Ir based fragments.

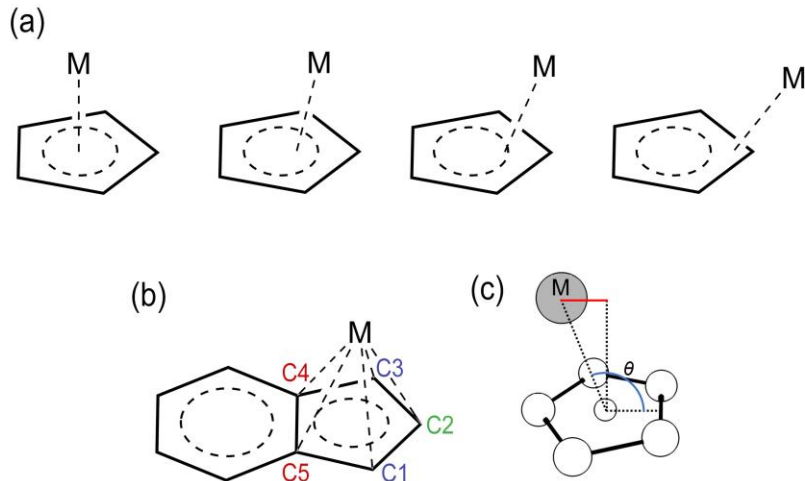


# Chapter 1

## 1. Introduction

The [2+2+2] cycloadditions of small unsaturated molecules, such as alkynes and nitriles, afford a variety of aromatic, heterocyclic, and polycyclic compounds of paramount importance in the chemical and pharmaceutical industries [1]. In 1867, the synthesis of benzene by thermal cyclotrimerization of acetylene was reported for the first time [2]. Despite the reaction being highly exothermic, it is strongly disfavored by entropic factors, and this limits its synthetic utility. Reppe and Schreckendieck demonstrated that low valent metal nuclei catalyze these [2+2+2] cycloadditions [1]. Further studies assessed that a wide variety of metals such as Ti, Zr, Ru, Co, Rh, Ir, Ni, and Pd may play an important role as catalysts in the synthesis of benzene and its derivatives and, in the past decades, experimental results and theoretical insight have been reported to establish the correct mechanism and tune the efficiency and regioselectivity [3,4,5,6,7].

One important class of catalysts for alkyne [2+2+2] cycloadditions are the half-sandwich complexes, i.e., metal-cyclopentadienyl ( $CpM$ ) or metal-ligand complexes in which the metal is coordinated to the  $Cp$  moiety of larger polycyclic ligands. These compounds possess peculiar structural features and reactivity properties; for this reason, and for their synthetic versatility, they are largely used [8,9,10,11,12,13]. They are denoted here with the general formula  $Cp'ML_n$ , where  $Cp' = Cp$ , Ind, and  $L_n$  are the ancillary ligands coordinated to the metal center (M) so that the 18-electrons rule is satisfied. Group 9 metals, i.e., cobalt, rhodium, and iridium, have been largely employed and, particularly, cobalt and rhodium have revealed significant catalytic efficiency [14,15,16,17]. The bonding mode of the metal to the  $Cp$  moiety (hapticity) is not perfectly symmetric ( $\eta^5$ ), but typically exhibits a distortion toward allylic ( $\eta^3$ ) coordination [18,19], and eventually to an extreme structure in which a  $\sigma$  metal-carbon bond forms ( $\eta^1$ ). This phenomenon is called metal slippage, and the different bonding modes are shown in Scheme 1a.



**Scheme 1.** (a) Different coordination modes (hapticities) of a metal (M) to a Cp ring. (b) Labelling scheme used in the definition of  $\Delta$  and LISP (Equations (1) and (2)). (c) Definition of  $\theta$  angle for LISP calculation.

To quantify the slippage, Basolo and coworkers [20,21] introduced the geometrical parameter  $\Delta$  [Eq. (3.1)].

$$\Delta = \frac{(M-C4 + M-C5) - (M-C1 + M-C3)}{2} \quad (1.1)$$

As shown in Scheme 9b, M-C4 and M-C5 are the longest distances between M and two adjacent C atoms of the Cp ring, and M-C3 and M-C1 are the distances between M and the C atoms adjacent to C4 and C5, respectively.

The slippage variations occurring during the catalytic cycle can be quantified referring to the value of  $\Delta$ , which changes from 0 Å ( $\eta^5$ ) to nearly 0.3 Å ( $\eta^3$ ) till 0.6 Å or even higher values ( $\eta^1$ ). Some of us have recently pointed out that this definition suitably applies to symmetric systems [22], and thus have introduced another descriptor, i.e., the label independent slippage parameter (LISP) [Eq. (3.2)].

$$LISP(\text{\AA}) = \frac{d}{N} \sum_{i=1}^N \left| \sin \left( \theta_i - \frac{\pi}{2} \right) \right| \quad (1.2)$$

LISP is actually the sum of the five average minimum distances from a normal vector passing through the centroid and the metal;  $d$  is the distance between the metal and the centroid of the ring of  $N$  atoms (Scheme 1c). Importantly, LISP is also suitable for describing non-symmetric displacements. In the same paper [22], a relationship between the catalytic activity of several half-

sandwich group 9 metal complexes for alkyne [2+2+2] cycloadditions and the slippage span expressed in terms of LISP (computed as the difference between the maximum and the minimum value of LISP along the catalytic cycle) was established. The slippage span  $\Delta$ LISP was then related to the turn-over frequency (TOF) values, calculated with the energy span model [23], and it emerged that the lower the  $\Delta$ LISP is, the higher the TOF is. Finally, in order to improve the sensitivity of  $\Delta$ LISP,  $\Delta$ LISP\* was introduced:

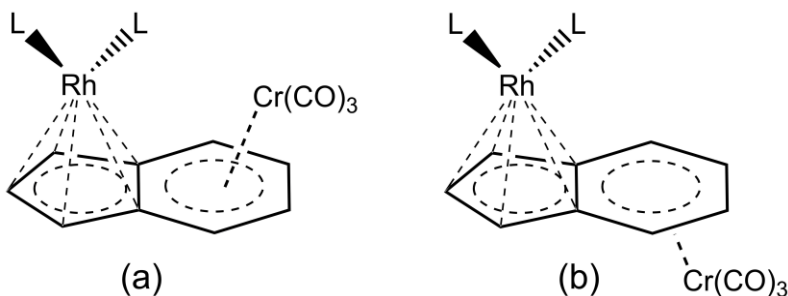
$$\Delta\text{LISP}^* (\text{\AA}) = \sum_{i=1}^{N-1} |\text{LISP}_1 - \text{LISP}_{i+1}| + \sum_{i=1}^{N-1} |\text{LISP}_i - \text{LISP}_{i+1}| + |\text{LISP}_N - \text{LISP}_1| \quad (1.3)$$

In this descriptor [Eq. (3.3)], the first term indicates how far/close each intermediate/transition state of the catalytic cycle is from/to the starting point. The second term accounts for the slippage difference between two consecutive states along the whole catalytic cycle. The last term includes the slippage variation between the last intermediate and the initial state. The availability of a flexible parameter to quantify the metal slippage, which intuitively influences the catalytic activity, and of a relationship between the metal slippage and the turn-over frequency is a valuable tool. So far, the slippage span model has been applied to monometallic Co and Rh half-sandwich catalysts for alkyne [2+2+2] cycloadditions [22]; in this work, we apply it to bimetallic Rh/Cr indenyl catalysts to assess its general validity.

Different strategies have been developed to tune the regioselectivity and the efficiency of the half-sandwich catalysts. Ingrosso et al. [24,25] experimentally studied the influence of organic moieties, i.e., cyclopentadienyl (Cp), indenyl (Ind) and fluorenyl (FN), in Rh(I) half-sandwich catalysts on alkyne [2+2+2] cycloadditions. Booth et al. [26] reported that IndRh initiates the reaction ten times faster as compared to CpRh, and this was related to the so-called *indenyl effect* (a phenomenon firstly reported by Adam J. Hart-Davis and Roger J. Mawby in 1969 [27], it was thoroughly explored and named by Fred Basolo [28]; it consists in an enhancement of the rate of the substitution reactions at the metal when indenyl is used instead of cyclopentadienyl aromatic ligand). It was also observed that the presence of an electron withdrawing group in the Cp ligand reduces the catalytic activity at low temperatures [29,30]. Based on these studies, it emerged that structural and electronic modifications to the aromatic moiety of the half-sandwich catalyst influence its efficiency.

Changing the metal also plays a role. For example, considering group 9 metals, Co is highly preferred when compared to Rh and Ir [31,32].

Finally, another modification to a half-sandwich catalyst is the coordination of a second metal to form a bimetallic complex. When the aromatic ligand is polycyclic; the second metal can be in syn or anti position. A very nice example, reported by Ceccon et al. [33,34,35], is  $[\text{Cr}(\text{CO})_3\text{IndRhL}_2]$  (Scheme 2). The idea behind the design of these compounds was that the presence of two metal centers within the same molecule may profoundly affect both the physical properties and the reactivity of the catalyst. In fact, it was found that the presence of a second metal in the anti position strongly enhances the reactivity as compared to monometallic complexes (*extra-indenyl effect*) [36].



**Scheme 2.** Anti-(a) and syn-(b)  $[\text{Cr}(\text{CO})_3\text{IndRhL}_2]$ .

Nowadays, DFT computational methodologies make it possible to investigate the mechanistic details of catalytic reactions, defining with accuracy their thermodynamic (reaction energies) as well as their kinetic (activation energies) features. After the pioneering work by Albright and co-workers on  $\text{CpCo}$  catalyzed acetylene [2+2+2] cycloaddition to benzene [37], several important computational studies were carried out by Calhorda and Kirchner on  $\text{CpRuCl}$  [38,39,40], Orian and Bickelhaupt on  $\text{CpRh}$  and  $\text{IndRh}$  [41,42,43] and analogous heteroaromatic Rh(I) catalysts [44], Koga and co-workers on  $\text{CpCo}$  [31,45,46], and Hapke et al. on  $\text{CpIr}$  [45]. To the best of our knowledge, no theoretical mechanistic investigation on the use of bimetallic half-sandwich catalysts has been reported so far. The use of bimetallic complexes as catalysts in organic synthesis is interesting because the reaction rate and selectivity can be tuned via possible inter-metal cooperative effects. Ceccon et al. have provided rather complete information on anti-and syn- $[\text{Cr}(\text{CO})_3\text{IndRhL}_2]$ . Particularly, they studied the cyclotrimerization of methylpropiolate (MP) and dimethyl-acetylenecarboxylate (DMAD) with mono and bimetallic catalysts, i.e.,

IndRh(COD), *p*-NO<sub>2</sub>-IndRh(COD), and bimetallic anti-[Cr(CO)<sub>3</sub>IndRh(COD)]. They found that the Rh/Cr catalyst leads to a greatly enhanced catalytic efficiency compared to the monometallic one. This increase of catalytic activity was ascribed to a synergic or “cooperative” interaction between the two metals in activating the substrate of interest [33-35].

The main goal of this study is the detailed investigation of the mechanism of acetylene [2+2+2] cycloaddition catalyzed by Rh/Cr indenyl fragments, particularly focusing on (i) the presence of the second metal, i.e., Cr, on the mechanism and energetics; (ii) the relationship between rhodium slippage and catalytic activity, and (iii) the outline of general guidelines for the design of Rh(I) half-sandwich catalysts based on the slippage span model. Once assessed the details of Rh/Cr indenyl catalyzed alkyne [2+2+2] cycloadditions, the role of the second metal is explored by replacing Cr with the other metals of Group 6, i. e., Mo and W. Finally, the effect of replacing the aromatic ligand, i.e., the indenyl moiety, with larger polycyclic species will be investigated. All these results will be rationalized with the aim of finding a general relationship between the structure and the reactivity of half-sandwich group 9 metal catalysts towards alkyne [2+2+2] cycloadditions providing insight for in silico design of novel functional molecules.



# Chapter 2

## Theories, Methods, and Models

### 2.1. Computational Chemistry

Chemistry is the branch of the natural sciences that deals with the properties, composition, and transformation of matter. Nowadays many chemical problems can be solved by the computer using the methods and approaches of theoretical chemistry incorporated in suitable software; this discipline is known as computational chemistry. A branch of computational chemistry is based on quantum mechanics and computer power is needed to solve numerically the Schrödinger equation for many electrons systems, i.e., atoms and molecules. Computational chemistry allows chemists to predict atomic and molecular properties, reactivity, spectroscopic observables, so providing a rational understanding of the experimental data. Quantum chemistry methods allow also to explore elementary reaction mechanisms (which is the main goal of this thesis), identifying *in silico* undetectable species like the transitions states, short-lived and unstable intermediates that cannot be traced very easily by experimental means [47].

### 2.2. Methodologies for Quantum Chemistry Calculations

Computational chemistry approaches range from approximate to very accurate methods and cover both static and dynamic conditions. So *ab initio*, *empirical* or *semi-empirical* and *molecular mechanics methods are distinguished* [48,49]. *Ab initio* means “from the beginning” or “from the first principles” and these methods are rigorously based on quantum mechanics. The *ab initio* calculations commonly rely on the Born Oppenheimer approximation by [50]. Thus only the electronic part of the system is treated. Density functional theory (DFT) methods are the most widely used methods [51].

*Empirical or semi-empirical approaches* are approximate quantum mechanics methods relying on additional empirical parameters. Semi-empirical methods are useful because much computationally cheaper than the other methods, although reliable only for very few molecular properties.

In quantum chemistry, the main goal is to gain insight into the molecular system by solving the non-relativistic time-independent Schrödinger equation ( $\hat{H}\Psi = E\Psi$ ) [52].

$$\hat{H}\Psi = E\Psi \quad (2.1)$$

The Hamiltonian operator  $\hat{H}$  includes the nuclear ( $T_n$ ) and electronic kinetic energy ( $T_e$ ) and the potential energy terms, i.e., the electrostatic attraction between nuclei and electrons ( $V_{ne}$ ), the repulsive nucleus-nucleus ( $V_{nn}$ ) and electron-electron interactions ( $V_{ee}$ ). The wavefunction ( $\Psi$ ) contains all information about the state of the system and depends on the nuclear and electronic coordinates. The Hamiltonian ( $\hat{H}$ ) can be this written as:

$$\hat{H} = T_n + T_e + V_{nn} + V_{ne} + V_{ee} \quad (2.2)$$

The Schrödinger equation can only be solved exactly for only one-electron systems. Strategies are required in order to obtain solutions for the many electrons systems. First, the Born-Oppenheimer approximation is used, since the nuclei move much slower than electrons (because the mass of a proton is approximately 1800 times bigger the mass of an electron). Thus electrons are considered to move in a field of fixed nuclei and the kinetic energy of the nuclei can be neglected. The nucleus-nucleus repulsion becomes constant.

By applying the BO approximation the Hamiltonian operator becomes the electronic Hamiltonian ( $\hat{H}_e$ ) and the electronic Schrödinger equation can be written,

$$\hat{H}_e \Psi_e = (T_e + V_{ne} + V_{ee})\Psi_e \quad (2.3)$$

Hartree–Fock method recovers nearly 99% of the total energy of the molecular system. The Hartree–Fock method assumes that the N-electrons wave function of the system can be approximated by a single Slater determinant. However, it does not take into account the Coulomb correlation [53,54,55]. As a result number of post-Hartree–Fock methods, i.e., configuration interaction (CI) [56], multi-configurational SCF approaches (MCSCF) [57], Møller-Plesset

perturbation methods (MP2, MP3, and MP4, etc.) [58], and the coupled cluster (CC) methods [59] have been developed to improve the accuracy of computed energies by recovering static and dynamic correlation energy [60].

## 2.3. Density Functional Theory

In Density Functional Theory (DFT), the total energy of the system is determined using the electron density, and not the wavefunction. Functionals of the electron density, which is spatially dependent, are employed. It is based on the first and second Hohenberg-Kohn theorems formulated in 1964. The first one states that for non-degenerate ground states, there is a unique relationship between the total energy ( $E$ ) and the corresponding electron density  $\rho(r)$ . The second one affirms the possibility to minimize the total energy using the variational principle, analogously to wave-function methods.

The electronic energy of the system is obtained by applying an energy functional to the electronic density and expressed as:

$$E[\rho] = T[\rho] + V_{ee}[\rho] + V_{ne}[\rho] \quad (2.4)$$

$T$  represents the total kinetic energy of the electrons,  $V_{ee}$  describes the electron-electron repulsion and  $V_{ne}$  is the electron nuclei attraction. The nuclear-nuclear repulsion is not taken into account due to the Born-Oppenheimer approximation. In 1965, Kohn and Sham proposed a new approach based on the one-electron approximation in order to calculate the terms,  $T[\rho]$  and  $V_{ee}[\rho]$  in a simple and accurate way [61,62]. They introduced a fictitious reference system of non-interacting electrons, moving in an effective potential  $V_S$ . The electronic wavefunction of the reference system is expressed as a single Slater determinant, which gives the Kohn-Sham orbitals  $\varphi_i$ , and by taking into account a linear combination of their densities, the total electron density can be constructed:

$$\rho(r) = \sum_i |\varphi_i|^2 \quad (2.5)$$

In this case, the total kinetic energy of the real system  $T[\rho]$  can be written as the sum of the kinetic energy of the non-interacting system  $T_S[\rho]$  and, as an amendment, the additional kinetic energy  $T_A[\rho]$  required to define the real interacting system accurately. Similarly, the term electron-electron

repulsion  $V_{ee}[\rho]$  is the sum of the classical Coulomb interaction  $J[\rho]$  (the repulsion each electron experiences from the average field due to all the electrons, including itself) and a non-classical part containing correlation and exchange  $E_{NC}[\rho]$ . The total energy can be written as:

$$E[\rho] = T_S[\rho] + T_A[\rho] + J[\rho] + E_{NC}[\rho] + V_{ne}[\rho] \quad (2.6)$$

$T_A[\rho]$ , and  $E_{NC}[\rho]$  can be combined into a single term called  $E_{XC}[\rho]$ :

$$E[\rho] = T_S[\rho] + J[\rho] + V_{ne}[\rho] + E_{XC}[\rho] \quad (2.7)$$

Unluckily, the exchange-correlation functional is not exact and has to be approximated. Furthermore, its quality determines the level of accuracy of the applied DFT. The simplest approach that represents the exchange-correlation functional is Local Density Approximation (LDA). It supposes that the energy depends only on the local density (homogeneous electron gas). LDA methods usually provide surprisingly good results with accuracy similar to those obtained by HF methods, however, an improved description is mandatory in many cases [63]. The energy also should be dependent on the gradient of density (Generalized Gradient Approximation methods (GGA)). GGA methods have a significantly increased accuracy over LDA methods and give better atomization and total energies, structural energy variances and energy barriers [64,65]. A further improvement, by using higher order density gradients and/or on the kinetic energy density leads to different more recent methods called meta-GGA (m-GGA). The use of combined exchange-correlation GGA functionals with a percentage of HF exchange is used in the hybrid functionals [66], which are superior to GGAs for many properties.

Nowadays, efficient computational formalisms and high-performance computers make it possible to determine the energy of even very large chemical systems. DFT is a much popular method than other State-of-the-art *ab initio* methods due to its relatively high accuracy at a rather low computational cost.

## 2.4. Computational Details

All computational calculations within this thesis are based on density functional theory (DFT) [67-67]. They are carried out by using the Amsterdam Density Functional (ADF2016, SCM, Vrije Universiteit: Amsterdam, The Netherlands 2016) program [68,69,70]. The equilibrium and transition state geometries along the studied catalytic cycles were fully optimized (i.e., without any imposing symmetry constraint). The BLYP [75,71,72] exchange and correlation functional developed by A.D. Becke (exchange part) and C. Lee, W. Yang and R.G. Parr (correlation term), in combination with the TZ2P basis set for all elements, was applied. The TZ2P basis set [73] is a large uncontracted set of Slater-type orbitals (STOs) of triple- $\zeta$  quality and has been augmented with two sets of polarization functions: 2p and 3d in the case of H atom, 3d and 4f in the case of C and O, 4p and 4f in the case of Cr and Co, 5p and 4f in the case of Mo and Rh and 6p and 5f in the case of W.

Since in this Project, as we are dealing with transition metals which require an accurate relativistic correction for core electrons, scalar relativistic effects were accounted by using the zeroth-order regular approximation (ZORA) [74,75]. To reduce computational time, a frozen-core approximation was adopted for core electrons: up to 1s for C and O, up to 2p for Cr and Co, up to 3d for Mo and Rh and up to 4d for W. This level of theory is mentioned in the current thesis as ZORA-BLYP/TZ2P.

Frequency calculations were computed to confirm that all the intermediates have positive frequencies, whereas the transition states have one imaginary frequency. The character of the normal mode associated with this imaginary frequency was carefully examined to verify that the correct transition state was found

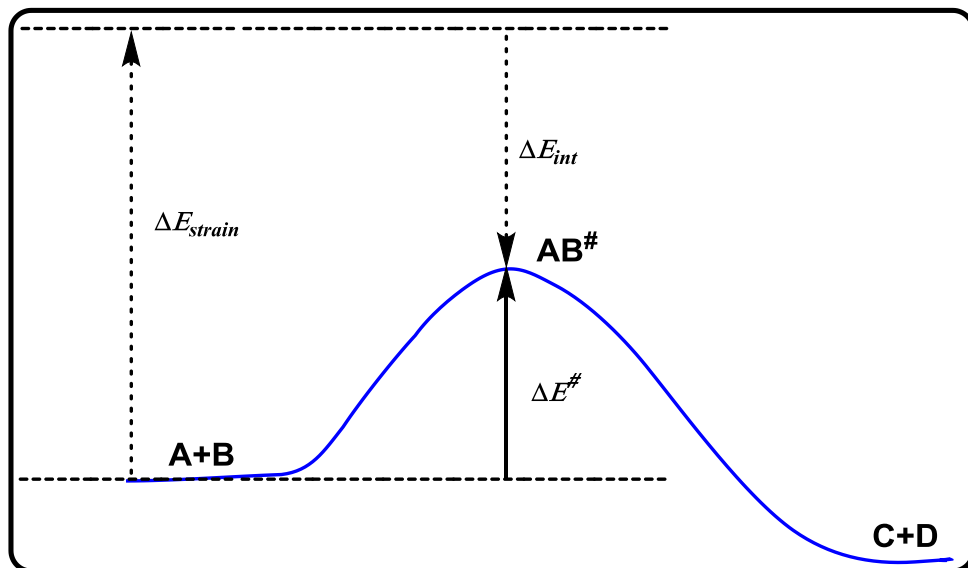
## 2.5. ASA: Activation-Strain Analysis

In the field of catalysis often we have to investigate and analyze deeply the elementary chemical reactions and the associated energy barriers. In fact, one of the objectives in this thesis is the understanding of the trends in activation barriers and transition-state geometries based on accurate calculations. The activation strain analysis (ASA) [76,77] is an important approach that

helps us to understand the nature of a chemical bonding and was introduced firstly in the 1970s by Morokuma [78] and Ziegler [79]. ASA is a fragment based approach where the energy of the complex can be written as the sum of the strain contribution ( $\Delta E_{\text{strain}}$ ) and the interaction contribution ( $\Delta E_{\text{int}}$ ) [Eq. (2.8)]; see also Scheme 3:

$$\Delta E = \Delta E_{\text{strain}} + \Delta E_{\text{int}} \quad (2.8)$$

$\Delta E_{\text{strain}}$  is the energy required for the geometrical deformation of the reacting species when they are brought from infinite distance to the acquired complex geometry, while  $\Delta E_{\text{int}}$  is the actual energy change when geometrically deformed fragments are combined to form the overall complex (Scheme 3). The strain contribution is commonly calculated as the energy difference between two fully relaxed fragments and the geometry they acquire in the activated complex and always have positive values. The remaining negative contribution derives from electronic interactions. The  $\Delta E_{\text{int}}$  can be further decomposed through the energy decomposition analysis (EDA), as explained in the next paragraph.



**Scheme 3.** ASA applied to a general elementary reaction.

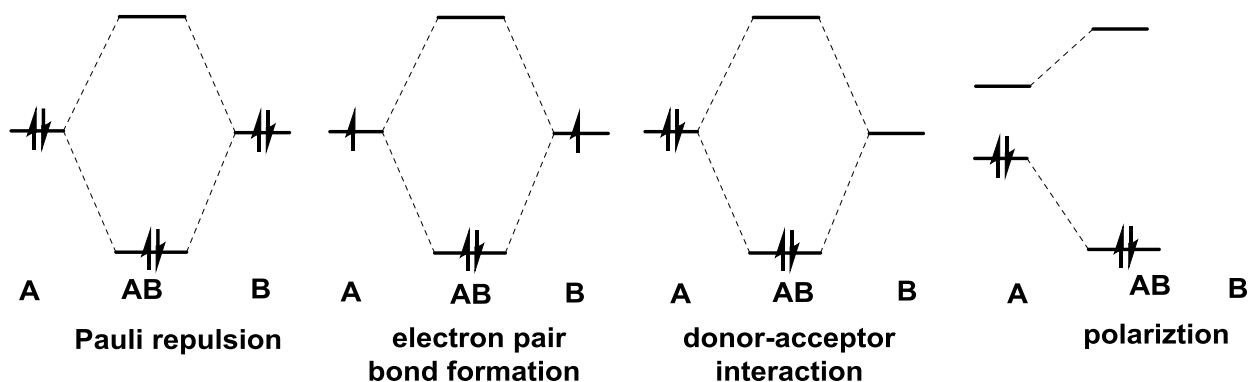
The analysis has been successfully applied to numerous systems including the study of Organometallic catalysis [80,81,82], Cycloadditions [83,84], Alder-ene reactions [85,86], Substitution, and Addition reactions [87,88,89].

## 2.6. EDA: Energy Decomposition Analysis

The energy decomposition analysis (EDA) allows to analyze the interaction energy  $\Delta E_{\text{int}}$  by decomposing it into physically meaningful terms in the framework of Kohn-Sham molecular orbital (KS-MO) model [90]. The components are electrostatic interaction ( $\Delta V_{\text{elstat}}$ ), Pauli repulsion ( $\Delta E_{\text{Pauli}}$ ), orbital interactions ( $\Delta E_{\text{oi}}$ ), and dispersion ( $\Delta E_{\text{disp}}$ ) [Eq. (2.9)]:

$$\Delta E_{\text{int}} = \Delta V_{\text{elstat}} + \Delta E_{\text{Pauli}} + \Delta E_{\text{oi}} + \Delta E_{\text{disp}} \quad (2.9)$$

First, the molecular system is divided into two fragments. When bringing these deformed fragments close to each other, a classical attractive electrostatic interaction arises ( $\Delta V_{\text{elstat}}$ ). Then, an antisymmetrization process occurs with associated energy change ( $\Delta E_{\text{Pauli}}$ ), deriving directly from the Pauli antisymmetry principle. The Pauli repulsion contains the destabilizing interactions between occupied orbitals and accounts for any steric repulsion. Both electrostatic and Pauli repulsion contributions are often summed together and provide an overall steric term. The third step is related to the relaxation of the system and interacting orbitals. It arises when fragment's orbitals are allowed to relax with electrons redistribution to achieve the final state in the entire complex. This orbital interaction ( $\Delta E_{\text{oi}}$ ) includes electron pair bonding, charge transfer (interaction between occupied orbitals on one moiety with unoccupied orbitals on the other, including the HOMO-LUMO interaction) and polarization (empty-occupied orbital mixing on one fragment due to the presence of another fragment) (Scheme 4).



**Scheme 4.** Different cases of orbital interactions.

Lastly, the long range of noncovalent interactions can be taken into account adding a dispersion term with several corrections. One of the most used is the correction D3(BJ) by Grimme (for the van der Waals-like term) and Becke-Jonson (for the damping function).

## 2.7. Turnover frequency (TOF)

Universally it is recognized that a good catalyst lowers the activation energy and shows higher efficiency by increasing the rate of a chemical reaction. Quantum mechanically, one can extract kinetic information from the obtained energy profile of any catalytic reaction. However, this approach is far to be an easy technique to relate performances or to comprehend how we can design a superior and/or a more efficient catalyst. In the field of organic and inorganic catalysis, the parameter named Turnover frequency (TOF) is ubiquitously used as a descriptor for quantifying the catalytic efficiency [91,92]. The general definition of TOF is given in [Eq. (2.10)] as the number of cycles (N) per catalyst concentration [C] per time (t):

$$\text{TOF} = \frac{N}{[C]t} \quad (2.10)$$

It was Christianen's who developed the idea 50-60 years ago to calculate the TOF from the rate constants ( $k$ ) of elementary reactions along the catalytic cycle using linear algebra [93,94]. However, the formulation of the  $k$ -representation made the equations very complicated and we know that the computational study of a catalytic cycle generates state energies (the E-representation). Amatore and Jutand created a straightforward mathematical relation from the Arrhenius rate law and the Boltzmann distribution [95]. The rate of the catalytic process, when steady-state is reached, is:

$$r = k[C_a]^n = [C_a]Ae^{\frac{-E_a}{RT}} \quad (2.11)$$

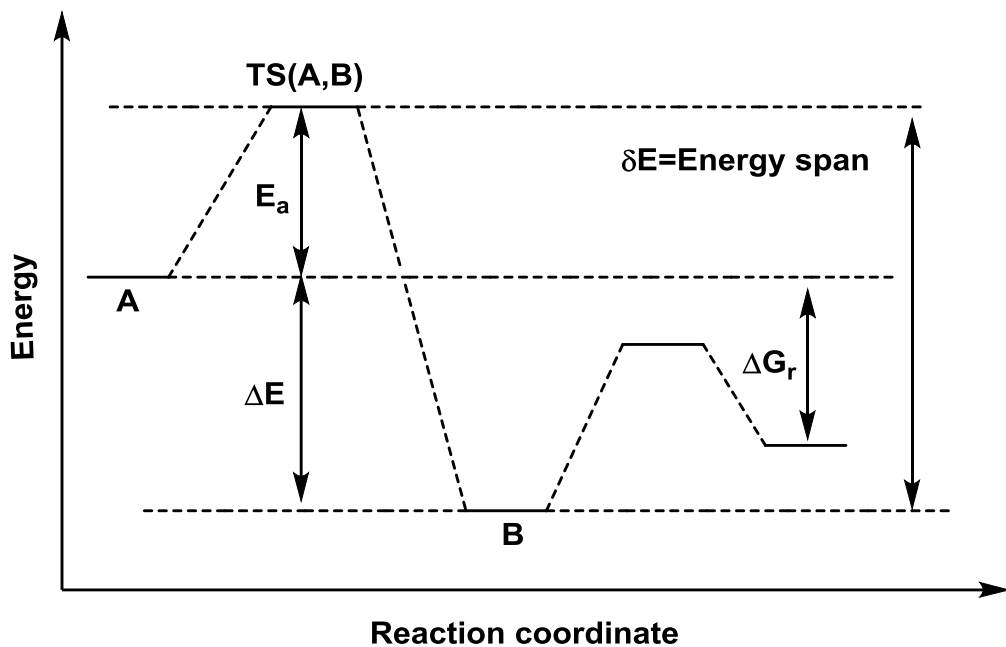
The rough estimation of the concentration of the active species  $[C_a]$  is determined by Boltzmann distribution with respect to total concentration  $[C_t]$ ,

$$[C_a] = [C_t]e^{\frac{-\Delta E}{RT}} \quad (2.12)$$

$\Delta E$  is the energy with respect to the lowest-lying intermediate (Scheme 5) along the catalytic cycle. So, by combining Equation (2.11) and (2.12), it leads to,

$$\text{TOF} = \frac{r}{[C_t]} = Ae^{\frac{-E_a - \Delta E}{RT}} = Ae^{\frac{-\delta E}{RT}} \quad (2.13)$$

$\delta E$  is called the energy span of a catalytic cycle, which is the difference between the energy of the highest energy transition state and the energy of the lowest intermediate along catalytic cycle (Scheme 5). The  $\delta E$  quantity is a suitable measure of TOF only when the energy span is much larger than the reaction energy of the cycle; the energy of the starting reactants lies at the same energy level of the final products, that is,  $\Delta G_r = 0$ .



**Scheme 5.** Schematic representation of the catalytic cycle.

Kozuch and Shaik [23,96,97] proposed a model to calculate TOF on the basis of Christianen's idea and taking into account the Eyring Transition-state theory (TST) with Eyring-Polanyi equation. The final expression is:

$$\text{TOF} = \frac{k_B T}{h} \frac{e^{\frac{-\Delta G_r}{RT}} - 1}{\sum_{i,j=1}^N e^{(TS_i - I_j - \delta G_{i,j})/RT}} \quad (2.14)$$

Where  $\Delta G_r$  is Gibb's free energy of reaction,  $TS_i$  and  $I_j$  are Gibb's free energies of the  $i^{\text{th}}$  transition state and intermediate, respectively.  $\delta G_{i,j}$ , is equal to  $\Delta G_r$  if  $i > j$  or to 0 if  $i \leq j$ .

If the reaction is exothermic, then the [Eq. (2.14)] can be simplified to [Eq. (2.15)] because the single term of the summation becomes dominate in the dominator.

$$\text{TOF} = \frac{k_B T}{h} e^{\frac{-\delta E}{RT}} \quad (2.15)$$

In this case, the  $\delta E$  called the energy span and depends upon; if TOF-determining transition state (TDTS) appears after TOF-determining intermediate (TDI), then  $\delta E = TS_{TDTS} - I_{TDI}$ . On the other hand, if TDTS appears before TDI, then it is  $\delta E = TS_{TDTS} - I_{TDI} + \Delta G_r$ .

On the PES, one can detect the TDTS and the TDI using the degree of TOF control [23], defined as [Eq. (2.16)]:

$$X_{TOF,i} = \left| \frac{1}{\text{TOF}} \frac{\partial \text{TOF}}{\partial E_i} \right| \quad (2.16)$$

In which  $E_i$  can be transition state or intermediate free energy. The bigger the degree of TOF control ( $X_{TOF,i}$ ), the higher the influence on the energy variation of the corresponding state.

The TOF ratio is a meaningful value for comparing the efficiency of different catalysts when the mechanism is identical. Instead of Gibbs free energies, electronic energies can be used, as it was demonstrated that there is no significant difference in the energy profiles and corresponding TOF ratios for the analogous catalytic cycle [44].

# Chapter 3

## *In silico* Acetylene [2+2+2] Cycloadditions Catalyzed by Rh/Cr Indenyl Fragments

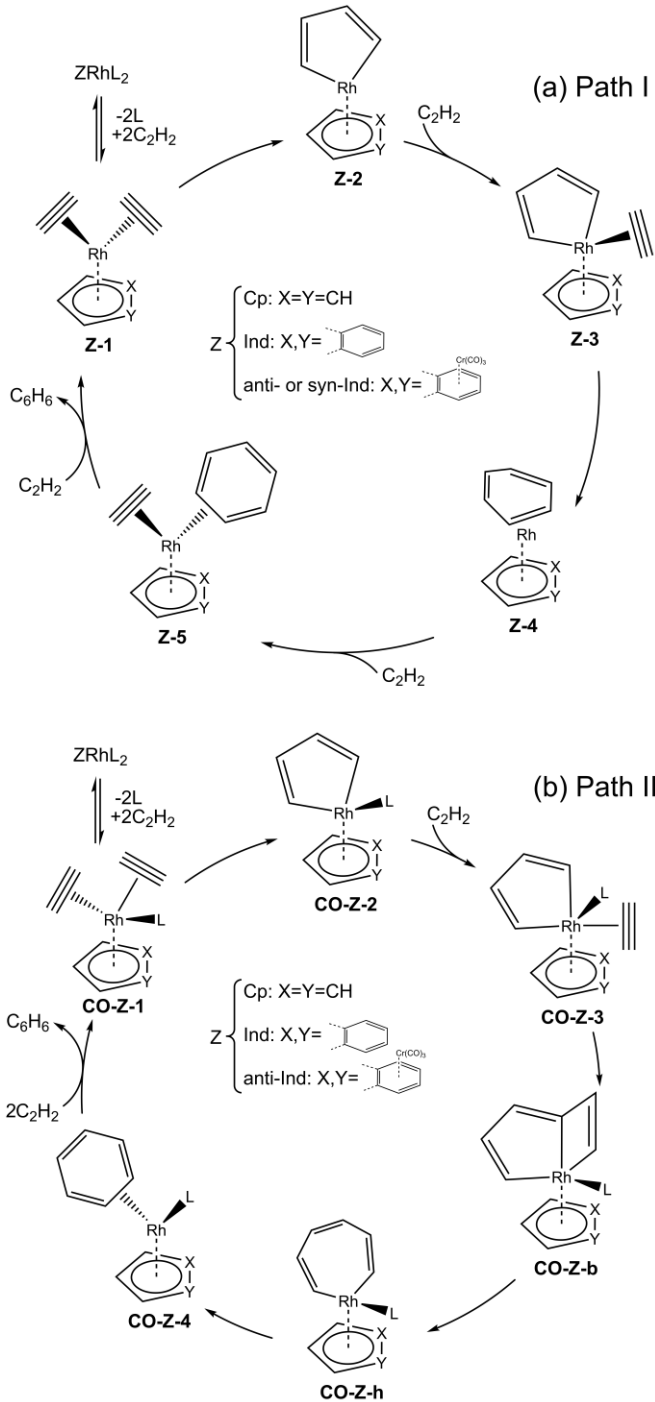
Adapted from

Shah Masood Ahmad, Marco Dalla Tiezza, and Laura Orian

*Catalysts* 2019, 9(8), 679; <https://doi.org/10.3390/catal9080679>

### 3.1. Introduction

The computational mechanistic investigation of acetylene [2+2+2] cycloaddition to benzene catalyzed by the monometallic catalysts CpRh and IndRh was first reported in 2006 [41]. In Scheme 6a (Path I), the well-known and widely accepted mechanism, proposed by Albright for CpCo catalysis [98,99] is shown. The catalytic cycle begins with the replacement of the ancillary ligands L of the catalyst precursor, i.e., Cp- or Ind-RhL<sub>2</sub> (L = CO, PPh<sub>3</sub> or COD (1,5-cyclooctadiene)) by two molecules of acetylene, leading to the bis-acetylene complex **Z-1**. The coordinated acetylene molecules undergo oxidative coupling and the unsaturated 16-electrons rhodacycle **Z-2** forms. This elementary step typically has the highest activation energy and was recently discussed in detail for group 9 metal-Cp fragments [100]. The subsequent coordination of a third acetylene molecule occurs without appreciable activation energy and leading to **Z-3**, and, after its addition to the  $\pi$ -electron system of the rhodacycle, the intermediate **Z-4** is obtained, which is characterized by an unsaturated bent six-membered ring. By further stepwise addition of two acetylene molecules, the intermediate **Z-5** first forms and then the initial catalyst is regenerated with the cleavage of benzene.



**Scheme 6.** Mechanism of acetylene [2+2+2] cycloaddition to benzene catalyzed by  $Z\text{Rh}$  ( $Z = \text{Cp}$ ,  $\text{Ind}$ , and anti or syn- $\text{Cr}@\text{Ind}$ ) (Path I) (a) and by  $\text{CO-ZRh}$  fragments ( $Z = \text{Cp}$ ,  $\text{Ind}$ , and anti- $\text{Cr}@\text{Ind}$ ;  $L = \text{CO}$ ) (Path II) (b).

An alternative mechanism was postulated by Booth and co-workers [26] on the basis of their experimental findings, which implies that a ligand of the catalyst precursor remains bonded to the metal center throughout the whole catalytic cycle; this is shown in Scheme 6b (Path II). This mechanism was rationalized by Orian et al. [43] in a recent systematic study on the *indenyl effect* and its connection to metal slippage. The presence of an ancillary ligand imposes strong hapticity variations in both CpRh and IndRh catalysis. In addition, the bicyclic **CO-Z-b**, and the heptacyclic **CO-Z-h** were located along this catalytic path, which resembles the one described for CpRuCl catalysis [38].

Inspired by the experimental work by Ceccon et al. [33-35], we chose the bimetallic catalyst  $[\text{Cr}(\text{CO})_3\text{IndRhL}_2]$ , where the second metal group  $\text{Cr}(\text{CO})_3$  can be coordinated both in anti and syn conformations and examined both paths I and II of Scheme 6. The optimized molecular structures (ZORA-BLYP/TZ2P) of anti- and syn- $[\text{Cr}(\text{CO})_3\text{IndRh}(\text{CO})_2]$  (see Appendix, Figure A1) are in good agreement with the X-ray crystallographic structures (labelled as HEXPOP [101] and HAPPOD [34] in the Cambridge database (CSD) [102]. Significant geometry parameters are compared in Table A1 (Appendix).

For simplicity, in the ongoing discussion, anti- and syn- $[\text{Cr}(\text{CO})_3\text{IndRh}]$  fragments are abbreviated as anti- or syn-Cr@IndRh (Scheme 6).

### 3.2. Acetylene [2+2+2] Cycloaddition Catalyzed by Anti-[Cr(CO)<sub>3</sub>IndRh] Fragment: Reaction Mechanism and PES (Path I)

The intermediates and transition states found for acetylene [2+2+2] cycloaddition catalyzed by the bimetallic anti-Cr@IndRh along Path I (Scheme 6a), are shown in Figure 1. Those found on the PESs of the parent monometallic catalysts, i.e., CpRh and IndRh, are in Figures A2 and A3 (Appendix), respectively. The computed energy profile for anti-Cr@RhInd is shown in Figure 2. The catalytic cycle mediated by anti-Cr@IndRh is very similar to the cycle described for the monometallic parent catalysts CpRh and IndRh [41] since the  $\text{Cr}(\text{CO})_3$  group is coordinated in anti, and thus there is no steric effect. It begins with the replacement of the ancillary ligands L by two acetylene molecules to form a bis-acetylene complex labelled **anti-Cr@Ind-1** (Scheme 6a). This process usually occurs experimentally by thermal or photochemical activation and might be dissociative or associative depending on the nature of the metal, on the electrophilicity of the ligands and on the substituents on the Cp ring [21,28,103].

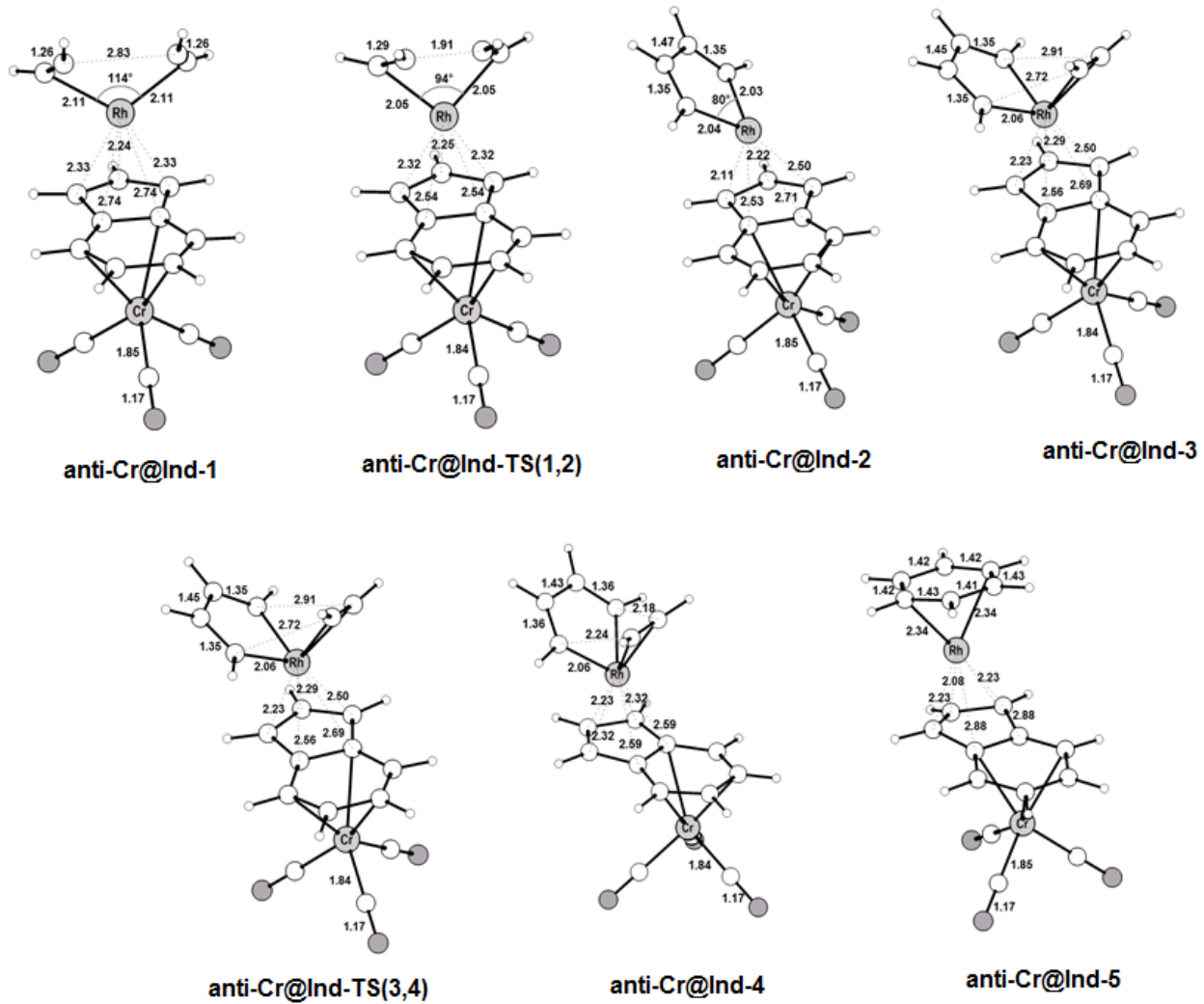


**Figure 1.** Optimized structures with selected interatomic distances ( $\text{\AA}$ ) and angles (deg) of the intermediates and transition states located on the PES of the anti-Cr@IndRh catalyzed acetylene [2+2+2] cycloaddition to benzene (Path I, Scheme 6a). Level of theory: ZORA-BLYP/TZ2P.

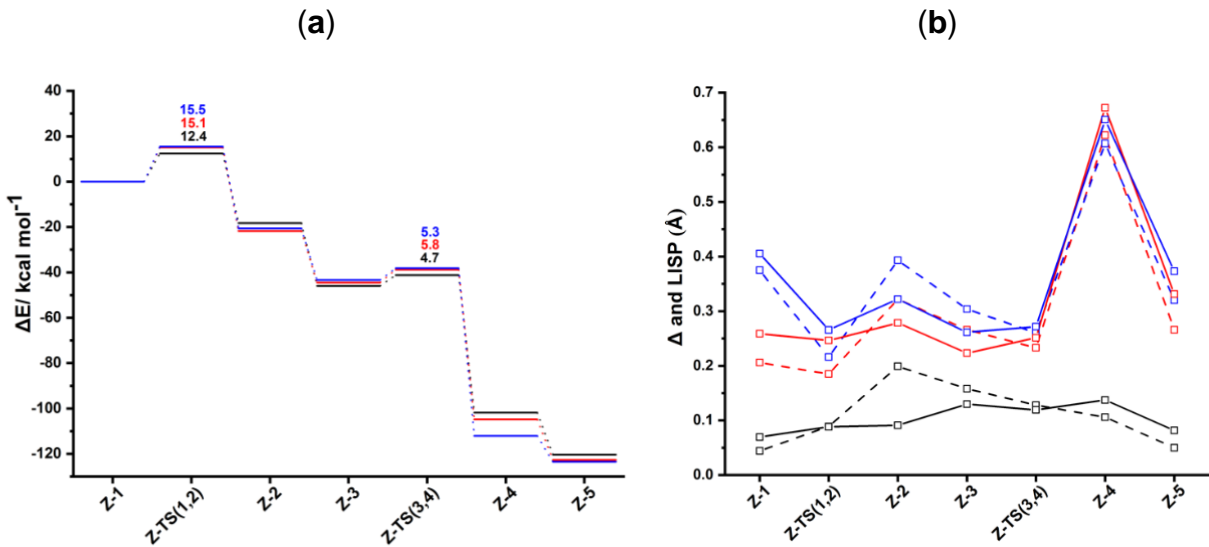


**Figure 2.** (a) Energy profiles of acetylene [2+2+2] cycloaddition to benzene catalyzed by CpRh (black), IndRh (red), and bimetallic anti-Cr@IndRh (blue) (Scheme 6a, Path I). (b) Profiles of the slippage parameters  $\Delta$  (dashed line) and LISP (solid line) for the acetylene [2+2+2] cycloaddition cycles catalyzed by CpRh (black), IndRh (red), and bimetallic anti-Cr@IndRh (blue) along Path I (Scheme 6a). Level of theory: ZORA-BLYP/TZ2P.

In **anti-Cr@Ind-1**, the acetylene molecules are slanted with respect to the plane of the indenyl ring and the C-C bond length is 1.26 Å. The Rh-C $\alpha$  and Rh-C $\beta$  bond lengths are 2.11 Å and 2.13 Å, respectively; they are shorter as compared to those of **Ind-1** (2.13 Å and 2.16 Å). This suggests that acetylene is more tightly bonded, likely due to the electron withdrawing effect of the second metal group Cr(CO)<sub>3</sub>. Additionally, the Rh-Cp coordination is more distorted in **anti-Cr@Ind-1** than in the parent **Cp-1** and **Ind-1**, as also quantified by the metal slippage parameters  $\Delta$  and LISP, which were calculated for the intermediates and the transition states along the whole catalytic cycle (Figure 2b).

By inspecting the frontier molecular orbitals of **Cp-1**, **Ind-1**, and **anti-Cr@Ind-1** shown in Figure 3, the  $\pi$ -antibonding character between Cp'- $\pi$  system and valence  $d$  orbitals of Rh is found to increase in the order **Cp-1** < **Ind-1** < **anti-Cr@Ind-1**, leading to a corresponding increase of metal slippage. Calhorda et al. have reported the same observation in their pioneering work on the nature of *indenyl effect*, which was related to the nodal characteristics of Cp'- $\pi$  orbitals of CpRh and IndRh [19,44]. Herein, it is found that the metal- $\pi$  anti-bonding nature with Ind- $\pi$  system is

further enhanced in the presence of  $\text{Cr}(\text{CO})_3$  in **anti-Cr@Ind-1** compared to the parent **Ind-1**, leading to extra slippage of rhodium in the former.

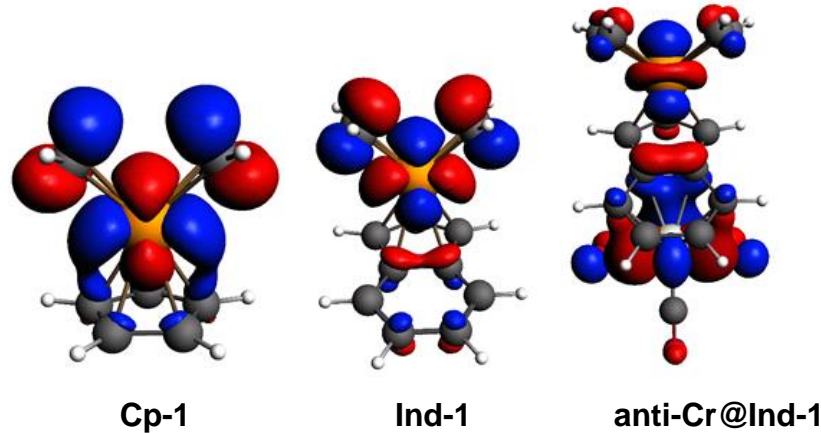


**Figure 3.** Kohn-Sham HOMOs of **Cp-1**, **Ind-1**, and **anti-Cr@Ind-1**; level of theory: ZORA-BLYP/TZ2P. The isodensity value is 0.03.

The oxidative coupling of the two coordinated acetylene molecules in **anti-Cr@Ind-1** leads to the 16-electrons unsaturated rhodacyclic intermediate **anti-Cr@Ind-2** (Figure 2a), crossing an activation barrier of  $15.5 \text{ kcal mol}^{-1}$ , which is higher than those computed for the formation of **Ind-2** ( $15.1 \text{ kcal mol}^{-1}$ ) and **Cp-2** ( $12.4 \text{ kcal mol}^{-1}$ ). This reaction step is exothermic by  $20.6 \text{ kcal mol}^{-1}$ . These metallacycles are generally described by two resonating structures, i.e., a metallacyclopentadiene, as found for  $\text{CpCo-(C}_4\text{H}_4)$  [37,49] and  $\text{CpRh-(C}_4\text{H}_4)$  [41,49], and a metallacyclopentatriene, as for  $\text{CpRuCl-(C}_4\text{H}_4)$  [38]. In **anti-Cr@Ind-2**, the  $\text{C}_\alpha\text{-C}_\beta$  and  $\text{C}_\beta\text{-C}_\beta'$  distances are  $1.35 \text{ \AA}$  and  $1.47 \text{ \AA}$ , respectively, which are rather well matched to the length of the ethylene double bond and to the length of the  $\sigma$ -bond between two carbon atoms, respectively. This suggests the character of rhodacyclopentadiene of **anti-Cr@Ind-2**.

A third acetylene molecule easily coordinates to **anti-Cr@Ind-2**, which is converted into **anti-Cr@Ind-3**. This step is barrierless and exothermic by  $22.8 \text{ kcal mol}^{-1}$ , about  $5 \text{ kcal mol}^{-1}$  less exothermic than the formation of **CpRh-3**; this value is almost identical to the reaction energy computed for the formation of **IndRh-3**. Subsequently, by Diels-Alder-like [4+2] addition of the coordinated acetylene to the rhodacycle, **anti-Cr@Ind-4** forms, with an activation energy of  $5.3 \text{ kcal mol}^{-1}$  (Figure 2a). This step is strongly exothermic by  $68.6 \text{ kcal mol}^{-1}$ ,  $8.4 \text{ kcal mol}^{-1}$  more exothermic than the same step in the IndRh catalytic cycle; conversely, the energy barriers are very

similar. Structurally, **anti-Cr@Ind-4** (Figure 1) is characterized by the presence of a six-carbon arene ring coordinated to rhodium in  $\eta^6$  fashion, while  $\eta^3$  coordination is found in the Cp-Rh moiety. A similar bonding mode of rhodium is found in **Ind-4**; conversely, in **Cp-4**,  $\eta^4$  hapticity is observed with the arene ring and  $\eta^3+\eta^2$  coordination to Cp moiety. This pronounced slippage in **Ind-4** and **anti-Cr@Ind-4** explains the spikes in the profiles of  $\Delta$  and LISP (Figure 2b). The coordination of another acetylene leads to the formation of **anti-Cr@Ind-5** (Figure 1), accompanied by a variation of hapticity from  $\eta^3$  to  $\eta^3+\eta^2$  in the anti-IndRh fragment and by the release of 11.5 kcal mol<sup>-1</sup>. The cleavage of benzene by the incoming second acetylene completes the cycle with the regeneration of the catalyst. The released energy is 16.4 kcal mol<sup>-1</sup>. Summarizing, the  $\eta^3+\eta^2$  coordination is found along the whole cycle catalyzed by anti-Cr@IndRh except in intermediate **anti-Cr@Ind-4**, where  $\eta^3$  coordination is predicted.

Consistently with CpRh and IndRh catalysis, the first step **Z-1 → Z-2**, that is the oxidative coupling of the acetylene molecules, has the highest energy barrier along the cycle (Figure 2a). To gain insight on the origin of this barrier, an activation strain analysis (ASA) has been carried out and compared to those already reported for CpRh and IndRh [49]. For this purpose, the complexes were divided into two fragments, i.e., Cp'Rh (Cp' = Cp, Ind, and anti-[Cr(CO)<sub>3</sub>Ind]) and the C<sub>4</sub>H<sub>4</sub> moiety. Being an intramolecular reaction, the activation energy  $\Delta E^\ddagger$  is conveniently given as the change, upon going from the reactant to the TS, in strain within the two fragments plus the change, upon going from the reactant to the TS, in the interaction between these two fragments [77,104].

$$\Delta E^\ddagger = \Delta\Delta E_{\text{strain}} + \Delta\Delta E_{\text{int}} \quad (3.4)$$

The results are shown in Table 1. The  $\Delta\Delta E_{\text{strain}}$  contributions increase from CpRh to IndRh and to anti-IndRh and are very similar for the Cp'Rh fragments (ranging from 2.4 to 2.7 kcal mol<sup>-1</sup>), but increase significantly for the C<sub>4</sub>H<sub>4</sub> fragment going from 33.2 to 37.0 and 37.3 kcal mol<sup>-1</sup>, respectively. Since  $\Delta\Delta E_{\text{int}}$  are very similar, varying from -23.2 kcal mol<sup>-1</sup> (CpRh) to -24.6 kcal mol<sup>-1</sup> (IndRh) and -24.5 kcal mol<sup>-1</sup> (anti-Cr@IndRh), the increase of the barrier in the indenyl catalysts is mainly due to the strain effects localized on the bis-acetylene moiety. Based on the identical  $\Delta\Delta E_{\text{int}}$  for IndRh and anti-Cr@IndRh, no influence of the second metal of the latter is found in the barrier of this oxidative coupling.

**Table 1.** Activation strain analysis for the oxidative coupling **Z-1 → Z-2** (Path 1); all values are in kcal mol<sup>-1</sup>. The fragments are Cp'Rh (Cp' = Cp, Ind, and anti-[Cr(CO)<sub>3</sub>Ind]) and the C<sub>4</sub>H<sub>4</sub> moiety (the reference are two acetylene molecules).

	$\Delta\Delta E_{strain}$			$\Delta\Delta E_{int}$	$\Delta E^\ddagger$
	2(C <sub>2</sub> H <sub>2</sub> )	Cp'Rh	Total		
<b>Cp-1/Cp-TS(1,2)</b>	33.21	2.36	35.57	-23.16	12.41
<b>Ind-1/Ind-TS(1,2)</b>	37.02	2.66	39.68	-24.59	15.09
<b>anti-Cr@Ind-1/anti-Cr@Ind-TS(1,2)</b>	37.31	2.72	40.03	-24.52	15.51
<b>syn-Cr@Ind-1/syn-Cr@Ind-TS(1,2)</b>	39.67	46.98	86.65	-71.47	15.18

We also examined **Z-4**, which was found to be more stable in the case of anti-Cr@IndRh than in the cases of IndRh and CpRh. ASA was carried out on **Z-4**, by considering these two fragments: Cp'Rh, where (Cp' = Cp, Ind, and anti-[Cr(CO)<sub>3</sub>Ind]) and the C<sub>6</sub>H<sub>6</sub> moiety; the results are listed in Table 2. A very high total  $\Delta E_{strain}$  is found in **Cp-4** compared to **Ind-4** and **anti-Cr@Ind-4**, which comes out from the benzene fragment and reflects the structural differences. In fact, benzene is bent in **Cp-4** with  $\eta^4$  coordination (see Appendix, Figure A2), while in **Ind-4** and **anti-Cr@Ind-4**, the ring is almost planar and coordinated to rhodium in  $\eta^6$  fashion and  $\eta^3$  coordination is found for the Rh coordination to the Cp ring. On the other hand, the large  $\Delta E_{strain}$  of **Cp-4** is well balanced by a large negative  $\Delta E_{int}$ , which leads to larger  $\Delta E$  by about 12.2 kcal mol<sup>-1</sup> than **Ind-4** and **anti-Cr@Ind-4**.

**Table 2.** Activation strain analysis for **Cp-4**, **Ind-4**, and **anti-Cr@Ind-4**; all values are in kcal mol<sup>-1</sup>. The fragments are Cp'Rh (Cp' = Cp, Ind, and anti-[Cr(CO)<sub>3</sub>Ind]) and C<sub>6</sub>H<sub>6</sub> moiety (the reference is benzene).

	$\Delta E_{strain}$			$\Delta E_{int}$	$\Delta E$
	C <sub>6</sub> H <sub>6</sub>	Cp'Rh	Total		
<b>Cp-4</b>	39.14	4.95	44.09	-83.44	-39.35
<b>Ind-4</b>	1.86	1.45	3.31	-30.44	-27.13
<b>anti-Cr@Ind-4</b>	1.64	1.26	2.90	-31.60	-28.70

Although the catalytic center is rhodium, we also investigated the coordination of Cr(CO)<sub>3</sub> in all the intermediates and transition states of the anti-Cr@IndRh catalyzed cycle. ASA was carried out using as fragments Cr(CO)<sub>3</sub> and IndRhX<sub>i</sub> (Table 3). Significantly larger  $\Delta E_{\text{strain}}$  values are found for **anti-Cr@Ind-TS(1,2)** and **anti-Cr@Ind-TS(3,4)**; the biggest contribution comes from the IndRhL<sub>n</sub> fragment, reflecting the changes occurring at the Rh center. The  $\Delta E_{\text{strain}}$  of Cr(CO)<sub>3</sub> fragment remains almost equal along the path, reflecting the fact that no important structural changes occur within the Cr(CO)<sub>3</sub> moiety.  $\Delta E_{\text{int}}$  values fluctuate in the range ~47–54 kcal mol<sup>-1</sup>. In **anti-Cr@Ind-4**, a sudden increase of  $\Delta E_{\text{int}}$  is computed. In fact, on the opposite side of the indenyl ligand, Rh-Cp coordination is highly slipped (Figure 1). Therefore, in order to compensate for the weakening of Rh-Cp coordination, Cr(CO)<sub>3</sub> binds more tightly the benzene moiety of the aromatic ligand. In **anti-Cr@Ind-4**, the increased  $\Delta E_{\text{int}}$  is due to a larger electrostatic contribution which is not sufficiently counterbalanced by an increase of  $\Delta E_{\text{Pauli}}$ .

**Table 3.** Activation strain analysis (ASA) of all the intermediates and transition states of the anti-Cr@IndRh catalyzed cycle (Path I); all the values are in kcal mol<sup>-1</sup>. The fragments are Cr(CO)<sub>3</sub> and IndRhX<sub>i</sub>.

	$\Delta E_{\text{strain}}$						$\Delta E_{\text{int}}$	$\Delta E$
	Cr(CO) <sub>3</sub>	IndRhX <sub>i</sub>	Total	$\Delta V_{\text{elstat}}$	$\Delta E_{\text{Pauli}}$	$\Delta E_{\text{oi}}$		
<b>anti-Cr@Ind-1</b>	1.23	2.29	3.52	-76.47	129.17	-101.20	-48.50	-44.98
<b>anti-Cr@Ind-TS(1,2)</b>	1.26	17.17	18.43	-73.37	124.90	-99.39	-47.86	-29.43
<b>anti-Cr@Ind-2</b>	1.67	1.78	3.45	-73.03	130.93	-105.13	-47.24	-43.79
<b>anti-Cr@Ind-3</b>	1.36	1.85	3.21	-73.99	129.02	-102.09	-47.06	-43.85
<b>anti-Cr@Ind-TS(3,4)</b>	1.28	7.77	9.05	-73.38	125.83	-100.03	-47.58	-38.53
<b>anti-Cr@Ind-4</b>	1.23	1.17	2.40	-80.45	128.03	-101.74	-54.16	-51.76
<b>anti-Cr@Ind-5</b>	1.25	1.65	2.90	-73.39	123.39	-97.75	-47.75	-44.85

### 3.3. Acetylene [2+2+2] Cycloaddition Catalyzed by Syn-[Cr(CO)<sub>3</sub>IndRh] Fragment: Reaction Mechanism and PES (Path I)

As stated above, the coordination of the Cr(CO)<sub>3</sub> group to the benzene moiety of IndRh catalyst may occur in anti or syn conformation [105]. Ceccon and co-workers have illuminated the stereochemistry of the syn catalyst, i.e., syn-[Cr(CO)<sub>3</sub>IndRh], and found that it is kinetically more stable because of a Rh-Cr interaction.

First, we investigated the acetylene [2+2+2] cycloaddition to benzene catalyzed by syn-Cr@IndRh catalyst along Path I (Scheme 6a). The structures of the intermediates and transition states found on the PES with their relevant parameters are shown in Figure 4, while the computed energy profile is in Figure 5a. Like for anti-Cr@IndRh catalysis, at the beginning of the cycle, the ancillary ligands L are replaced by two molecules of acetylene, leading to the formation of the bis-acetylene complex **syn-Cr@Ind-1** (Figure 4). In **syn-Cr@Ind-1**, the Rh-C<sub>α</sub> bond length is 2.15 Å, the distance C<sub>β</sub>-C<sub>β'</sub> of two acetylenes coordinated to rhodium is 2.91 Å, and the angle C<sub>α</sub>-Rh-C<sub>α'</sub> is 91°. To quantify the Rh-Cp slippage along the catalytic cycle, Δ and LISP parameters were computed for all the intermediates and transition states and are shown in Figure 5b. In **syn-Cr@Ind-1**, their values are 0.40 Å and 0.37 Å, respectively, with no appreciable difference with respect to **anti-Cr@Ind-1**; this might be ascribed to Rh-Cr interaction, despite high steric effects are present.

The oxidative coupling in **syn-Cr@Ind-1** leads to the formation of the five-membered ring rhodacycle **syn-Cr@Ind-2** with an activation energy of 15.2 kcal mol<sup>-1</sup>, nearly the same as found for anti-Cr@IndRh. Notably, in **syn-Cr@Ind-2** complex, one CO of Cr(CO)<sub>3</sub> interacts with Rh. In fact, the distance between the CO ligand and rhodium is 2.30 Å, and the distance between Cr and Rh center is smaller by 0.34 Å than in **syn-Cr@Ind-1**, implying stabilization of **syn-Cr@Ind-2**. In this situation, the rhodacycle **syn-Cr@Ind-2** is a nearly 18-electron saturated complex, in contrast to **anti-Cr@Ind-2** and the parent **Ind-2** and **Cp-2**. The conversion of **syn-Cr@Ind-1** into **syn-Cr@Ind-2** is exothermic by 26.4 kcal mol<sup>-1</sup>, about 6 kcal mol<sup>-1</sup> more than in the anti-catalyst and in the parent IndRh (Figure 2a). Finally, in this step, an hapticity shift from η<sup>3</sup>+η<sup>2</sup> to η<sup>3</sup> occurs (Figure 4).

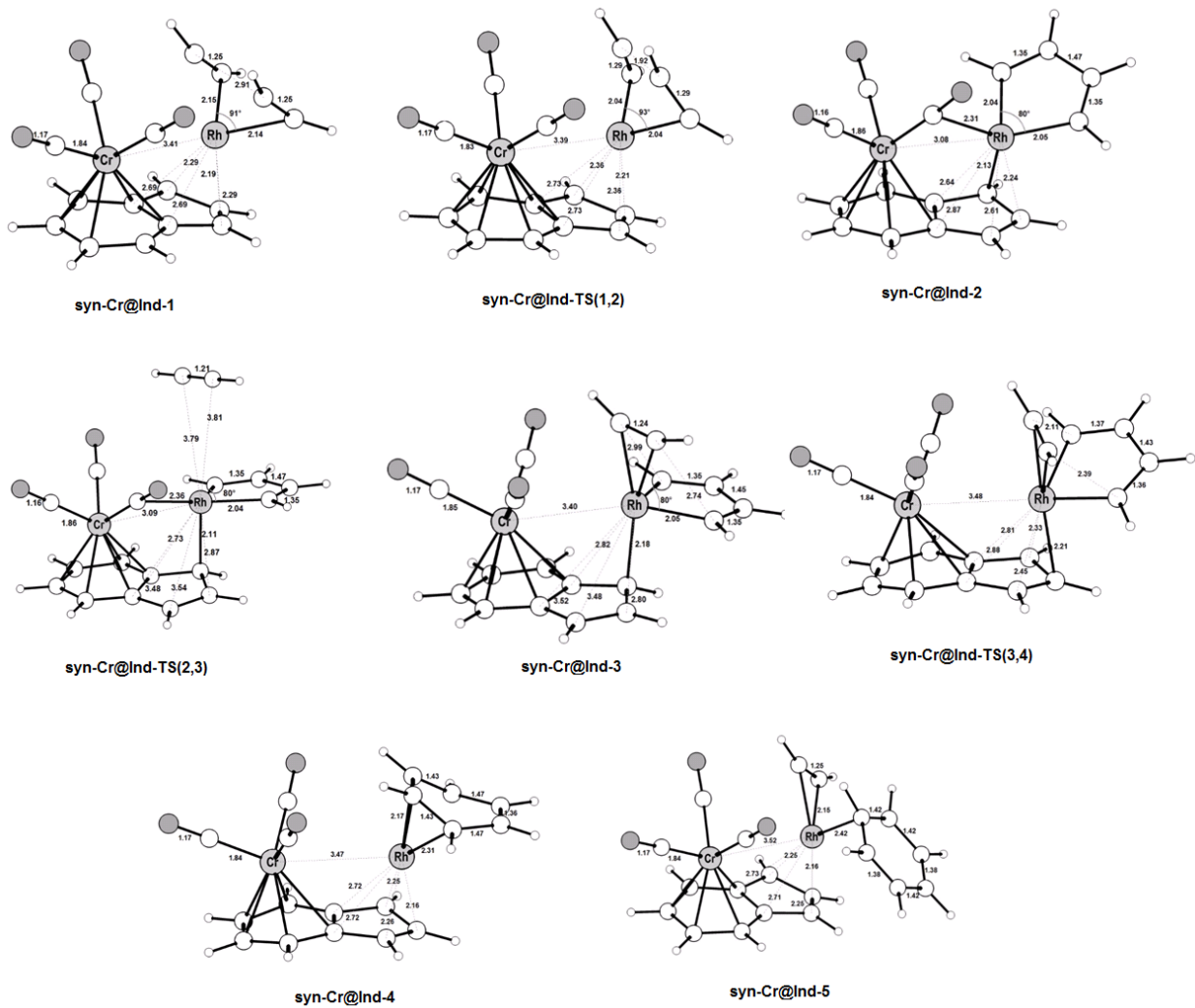


**Figure 4.** Optimized structures with selected interatomic distances ( $\text{\AA}$ ) and angles (deg) of the intermediates and transition states located on the PES of the syn-Cr@IndRh catalyzed acetylene [2+2+2] cycloaddition to benzene (Path I, Scheme 6a). Level of theory: ZORA-BLYP/TZ2P.

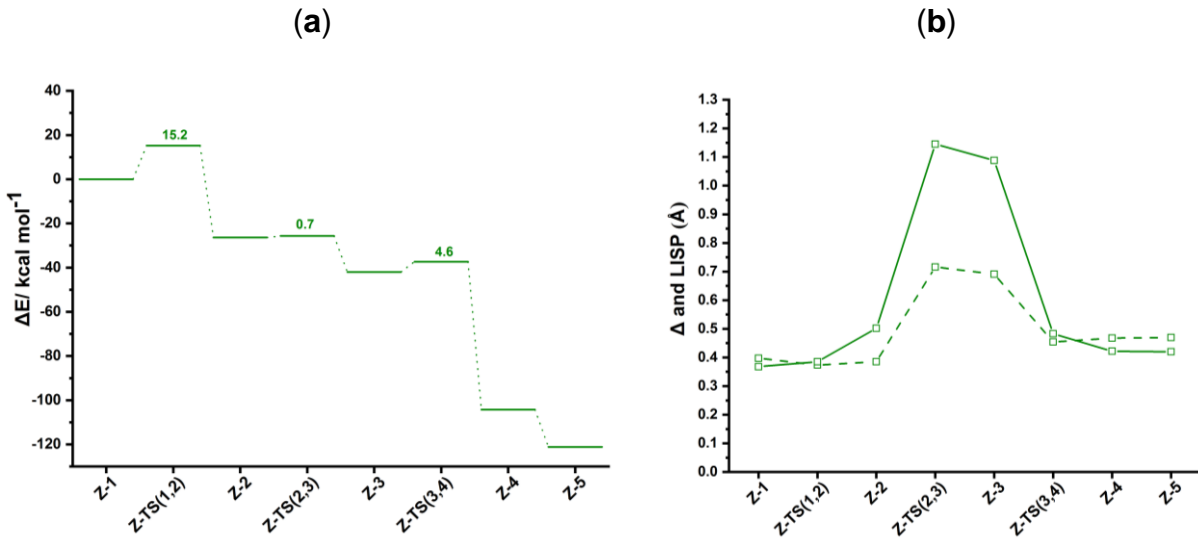


**Figure 5.** (a) Energy profile of acetylene [2+2+2] cycloaddition to benzene catalyzed by syn-Cr@IndRh (Scheme 6a, Path I). (b) Profiles of the slippage parameters  $\Delta$  (dashed line) and LISP (solid line) along the acetylene [2+2+2] cycloaddition cycle catalyzed by syn-Cr@IndRh (Scheme 6a, Path I). Level of theory: ZORA-BLYP/TZ2P.

The coordination of the third acetylene to **syn-Cr@Ind-2** occurs from the upper side with a low barrier of 0.7 kcal mol<sup>-1</sup>, via **syn-Cr@Ind-TS(2,3)** (Figure 4) and a large slippage variation (LISP changes by approximately 0.6 Å) leading to almost  $\eta^1$  coordination. The conversion **syn-Cr@Ind-2 → syn-Cr@Ind-3** occurs only with a slight modification in the carbon-carbon bonds of the rhodacycle. The reaction is exothermic by 15.6 kcal mol<sup>-1</sup>. In the next step, **syn-Cr@Ind-4** forms, crossing a barrier of 4.6 kcal mol<sup>-1</sup>. The LISP value drops from 1.09 Å to 0.42 Å (Figure 5b). **syn-Cr@Ind-4** has a six-carbon arene ring coordinated to rhodium in  $\eta^4$  fashion, while in Rh-Cp the coordination is  $\eta^3+\eta^2$ . Thus, the bonding mode of rhodium is different from **anti-Cr@Ind-4** (Figure 1), where  $\eta^6$  coordination and  $\eta^3$  coordination are found between the six-carbon arene ring and rhodium and the Cp ring and rhodium, respectively. However, **syn-Cr@Ind-4** resembles the case of the parent **Cp-4** [41]. This step is exothermic by 62.3 kcal mol<sup>-1</sup>.

Finally, the coordination of another acetylene leads to the formation of **syn-Cr@Ind-5** with no appreciable activation energy and with the release of 16.8 kcal mol<sup>-1</sup> (Figure 5a). It is less exothermic than the formation of **Ind-5** but more exothermic by 5 kcal mol<sup>-1</sup> than the formation of **anti-Cr@Ind-5**. The cleavage of benzene promoted by another acetylene completes the cycle and leads to the regeneration of the catalyst. The energy released in this last step is 18.8 kcal mol<sup>-1</sup>.

<sup>1</sup>. During the catalysis, the Rh-Cr distance varies in the range 3.05–3.51 Å, but remains close to the crystallographic value of 3.1 Å [34]. The hapticity variations along the catalytic cycle are definitively more pronounced in syn-Cr@IndRh catalysis than in the anti-Cr@IndRh one.

By inspecting the energy profile (Figure 5a), in the syn-Cr@IndRh catalyzed process the oxidative coupling **Z-1 → Z-2** has the highest energy barrier. From ASA (Table 1), a very high  $\Delta\Delta E_{\text{strain}}$  contribution to the barrier  $\Delta E^\ddagger$  has been found compared to anti-Cr@IndRh and also to the parent catalysts IndRh and CpRh. However,  $\Delta\Delta E_{\text{int}}$  is a pretty strongly stabilizing term and compensates for the strain, resulting in a lowering of  $\Delta E^\ddagger$ . In contrast to anti-Cr@IndRh, the strain arising from the Cp'Rh fragment is very high (Table 1) because of the steric effects and because Cr(CO)<sub>3</sub> undergoes deformation to interact with the Rh center.

To further assess the interaction and the role of Cr(CO)<sub>3</sub> in the syn-Cr@IndRh catalyzed process, ASA was carried out for the intermediates and transition states of the whole catalytic cycle, considering Cr(CO)<sub>3</sub> and IndRhX<sub>i</sub> fragments; the results are reported in Table 4.

**Table 4.** Activation strain analysis (ASA) of all the intermediates and transition states along the syn-Cr@IndRh catalyzed cycle (Path I); all the values are in kcal mol<sup>-1</sup>. The fragments are Cr(CO)<sub>3</sub> and IndRhX<sub>i</sub>.

	$\Delta E_{\text{strain}}$						$\Delta E_{\text{int}}$	$\Delta E$
	Cr(CO) <sub>3</sub>	IndRhX <sub>i</sub>	Total	$\Delta V_{\text{elstat}}$	$\Delta E_{\text{Pauli}}$	$\Delta E_{\text{oi}}$		
<b>syn-Cr@Ind-1</b>	1.65	5.02	6.67	-80.49	132.33	-102.88	-51.04	-44.37
<b>syn-Cr@Ind-TS(1,2)</b>	1.62	20.29	21.91	-79.52	130.84	-102.42	-51.10	-29.19
<b>syn-Cr@Ind-2</b>	2.25	4.31	6.56	-117.69	195.36	-133.21	-55.54	-48.98
<b>syn-Cr@Ind-TZ(2,3)</b>	2.57	7.56	10.13	-117.3	188.69	-129.83	-58.45	-48.32
<b>syn-Cr@Ind-3</b>	2.52	11.78	14.30	-87.65	141.15	-109.59	-56.09	-41.79
<b>syn-Ind-TS(3,4)</b>	1.82	12.54	14.36	-81.06	135.13	-105.64	-51.57	-37.21
<b>syn-Cr@Ind-4</b>	1.15	4.50	5.65	-79.61	129.57	-99.01	-49.04	-43.39
<b>syn-Cr@Ind-5</b>	1.56	5.28	6.84	-78.6	128.78	-99.76	-49.58	-42.74

$\Delta E_{\text{int}}$  are in the range ~49–58 kcal mol<sup>-1</sup>, larger than those computed for the anti-Cr@IndRh molecular species (Table 3), suggesting Rh-Cr stabilizing interaction in the former case. On the other hand,  $\Delta E_{\text{strain}}$  is also larger. This is mainly ascribed to steric factors. In particular, the contribution of Cr(CO)<sub>3</sub> to  $\Delta E_{\text{strain}}$  in **syn-Cr@Ind-2**, **syn-Cr@Ind-TS(2,3)**, and **syn-Cr@Ind-**

**3** is higher, suggesting some structural differences from the anti-analogous species. In fact, in these structures one carbonyl ligand is coordinated to Rh (Figure 4). This feature also leads to larger  $\Delta E_{\text{int}}$  in **syn-Cr@Ind-2**.

As an example of an existing favorable inter-metal interaction, in Figure 6, we show HOMO-3 of **syn-Ind-1**, which is formed by the contributions of the HOMOs of  $\text{Cr}(\text{CO})_3$  and  $\text{IndRh}(\text{C}_2\text{H}_2)_2$  fragments, whose metal *d*-based molecular orbitals (MOs) indicate stabilizing *d-d* bonding between Rh-Cr.

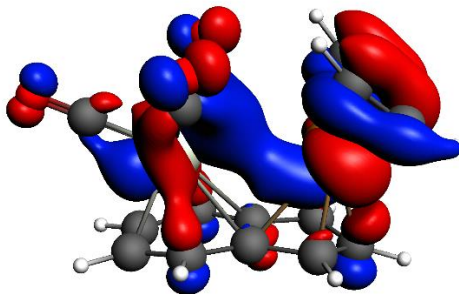


**Figure 6.** HOMO-3 of **syn-Cr@Ind-1**; the isodensity value is 0.03.

### 3.4. Acetylene [2+2+2] Cycloaddition Catalyzed by Anti-[ $\text{Cr}(\text{CO})_3\text{IndRh}$ ] Fragment: Reaction Mechanism and PES (Path II)

According to the alternative mechanistic path by Booth et al. [26], an ancillary ligand of the catalyst precursor remains bonded to rhodium during the catalytic cycle; this mechanism is denoted Path II (Scheme 6b). For  $\text{CpRh}(\text{CO})$  and  $\text{IndRh}(\text{CO})$ , this path has been thoroughly explored, making it possible to give an interpretation of the higher efficiency of the indenyl catalyst observed in the experiment [35]. Thus, here we considered the same hypothesis for anti- $\text{Cr@IndRh}(\text{CO})$  catalyzed acetylene [2+2+2] cycloaddition. The structures of the intermediates and transition states found on the PES with their relevant parameters are in Figure 7. For the parent monometallic catalysts,  $\text{CpRh}(\text{CO})$  and  $\text{IndRh}(\text{CO})$  are in Figures A4 and A5 (Appendix), respectively. The relative energy profile of the process is shown in Figure 8a.

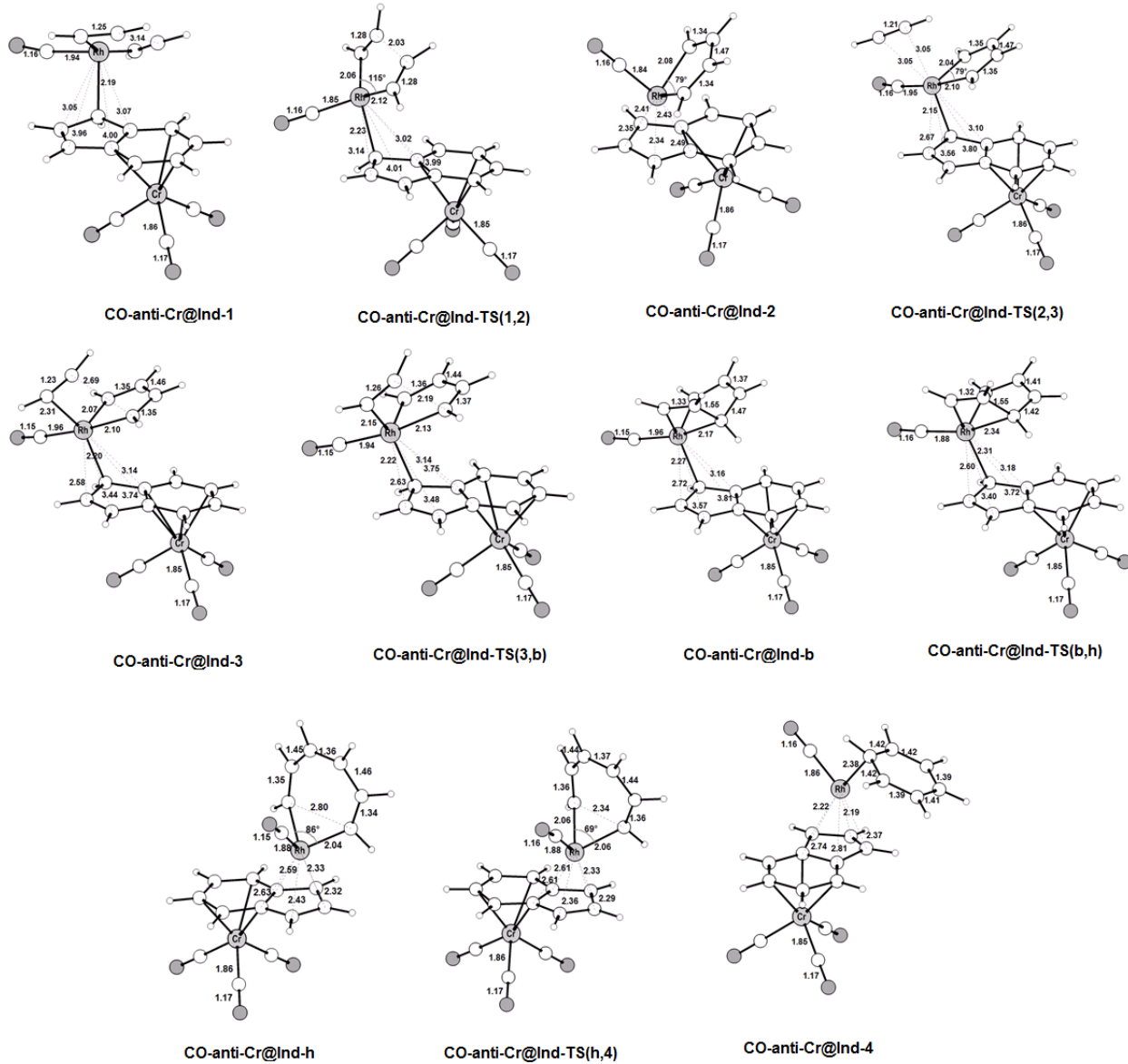


**Figure 7.** Optimized structures with selected interatomic distances ( $\text{\AA}$ ) and angles (deg) of the intermediates and transition states located on the PES of the anti-Cr@IndRh(CO) catalyzed acetylene [2+2+2] cycloaddition to benzene (Path II, Scheme 6b). Level of theory: ZORA-BLYP/TZ2P.

**CO-anti-Cr@Ind-1** is characterized by  $\eta^1$  coordination which is due to the presence of two acetylenes and the CO ligand, as observed for CpRh(CO) and IndRh(CO) catalysis [43].  $\Delta$  and LISP values are 0.92 Å and 1.60 Å, respectively (Figure 8b). The initial oxidative coupling leads to the formation of **CO-anti-Cr@Ind-2**, in which rhodium is coordinatively saturated due to the presence of CO. The energy barrier required to cross **CO-anti-Cr@Ind-TS(1,2)** is 13.9 kcal mol<sup>-1</sup> slightly higher if compared to those computed for CpRh(CO) and IndRh(CO) catalysis (by about 1–2 kcal mol<sup>-1</sup>). This is the same energy trend observed along Path I. The conversion of **CO-anti-Cr@Ind-1** into **CO-anti-Cr@Ind-2** is accompanied by the hapticity change from  $\eta^1$  to distorted  $\eta^5$  and is exothermic by 43.1 kcal mol<sup>-1</sup> (Figure 8a). About 4.5 kcal mol<sup>-1</sup> and 23.0 kcal mol<sup>-1</sup> less than the analogous step in IndRh(CO) and CpRh(CO) catalysis, respectively. The addition of the third acetylene leads to the formation of the  $\eta^1$  **CO-anti-Cr@Ind-3** with an activation energy of 9.8 kcal mol<sup>-1</sup>. The barriers for this step are much higher in the cases of IndRh(CO) and CpRh(CO) catalysis, i.e., 28.5 and 43.6 kcal mol<sup>-1</sup>, respectively. Thus, this step is kinetically favored with the bimetallic anti-IndRh(CO). In addition, the formation of **CO-anti-Cr@Ind-3** is endothermic by 4.4 kcal mol<sup>-1</sup>, which is overall less endothermic if compared to the same step in IndRh(CO) and CpRh(CO) catalysis, for which 9.3 kcal mol<sup>-1</sup> and 22.5 kcal mol<sup>-1</sup> are computed, respectively. Thus, the bimetallic catalyst has also a thermodynamic advantage. In the next step, the activation energy of 2.4 kcal mol<sup>-1</sup> is necessary to cross **CO-anti-Cr@Ind-TS(3,b)** and generate the bicyclic intermediate **CO-anti-Cr@Ind-b** (Figure 7), with negligible difference from the IndRh(CO) catalyzed step and lower by 1.2 kcal mol<sup>-1</sup> than in CpRh(CO) catalyzed step. The formation of **CO-anti-Cr@Ind-b** is accompanied by the release of 19.1 kcal mol<sup>-1</sup>, being 3.8 kcal mol<sup>-1</sup> more exothermic than the formation of the parent **CO-Ind-b** but 1.8 kcal mol<sup>-1</sup> less exothermic than **CO-Cp-b**. One can notice that the bicyclic intermediate in CpRh(CO) catalysis has higher energy while in bimetallic anti-IndRh(CO) and IndRh(CO) catalysis it lies at a lower energy (Figure 8a), suggesting a better catalytic efficiency in these latter cases. By crossing a modest barrier of 1.2 kcal mol<sup>-1</sup>, the bicyclic **CO-anti-Cr@Ind-b** readily transforms into the heptacyclic intermediate **CO-Ind-h**; this step is accompanied by the haptotropic shift  $\eta^1 \rightarrow$  distorted  $\eta^5$  and by the release of 28.0 kcal mol<sup>-1</sup>, a value lower than those computed for the parent catalysts, i.e., -37.4 kcal mol<sup>-1</sup> in the case of IndRh(CO) and -37.8 kcal mol<sup>-1</sup> in the case of CpRh(CO), respectively. **CO-anti-Cr@Ind-h** undergoes reductive elimination with an activation energy of 1.7 kcal mol<sup>-1</sup>. **CO-anti-Cr@Ind-4** forms and 46.4 kcal mol<sup>-1</sup> are released. Finally,

benzene is cleaved from **CO-anti-Cr@Ind-4** by stepwise addition of two acetylene molecules and the catalyst is regenerated.

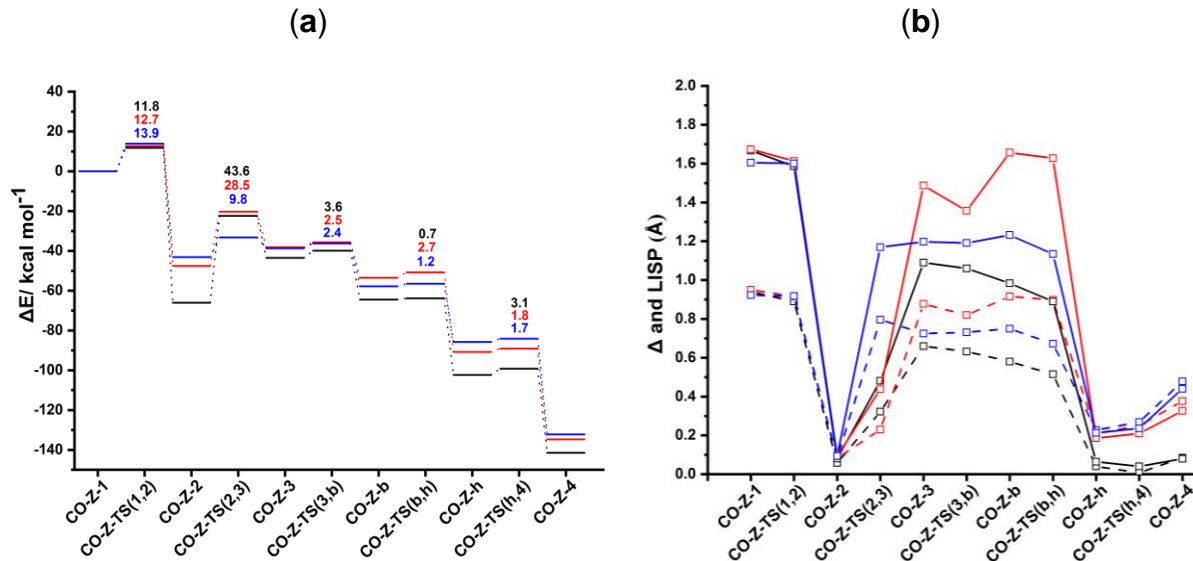


**Figure 8.** (a) Energy profiles of acetylene [2+2+2] cycloaddition to benzene catalyzed by CpRh(CO) (black), IndRh(CO) (red), and anti-Cr@IndRh(CO) (blue) (Scheme 6b, Path II). (b) Profiles of the slippage parameters  $\Delta$  (dashed line) and LISP (solid line) along the acetylene [2+2+2] cycloaddition cycles catalyzed by CpRh(CO) (black), IndRh(CO) (red), and anti-Cr@IndRh(CO) (blue) (Scheme 6b, Path II). Level of theory: ZORA-BLYP/TZ2P.

With the formation of the 18-electron intermediate **CO-Z-2**, a rather flat portion of the PES begins (Figure 8a). ASA was carried out on **CO-Z-2** considering CO-Cp'Rh (Cp' = Cp, Ind and anti-[Cr(CO)<sub>3</sub>Ind]) and the C<sub>4</sub>H<sub>4</sub> moiety as fragments; the results are listed in Table 5. The similar strain in fragment C<sub>4</sub>H<sub>4</sub> computed for **CO-Cp-2**, **CO-Ind-2**, and **CO-anti-Cr@Ind-2** (Table 5) revealed that the structure of this moiety is very similar in the three catalysts (see also Figure 7 and Appendix Figures A4–A5). The strain contribution of the fragment CO-Cp'Rh is much higher in **CO-anti-Cr@Ind-2** and **CO-Ind-2** than in **CO-Cp-2**. This is related to the least slippage predicted for this last species. The stronger interaction  $\Delta E_{\text{int}}$  in **CO-Ind-2** and **CO-anti-Cr@Ind-2** does not counterbalance their strain term and thus **CO-Cp-2** results the most stabilized among the three.

**Table 5.** Activation strain analysis (ASA) of **CO-Cp-2**, **CO-Ind-2**, and **CO-anti-Cr@Ind-2**; all values are in kcal mol<sup>-1</sup>. The fragments are: CO-Cp'Rh (Cp' = Cp, Ind, and anti-[Cr(CO)<sub>3</sub>Ind]) and the C<sub>4</sub>H<sub>4</sub> moiety (the reference are two acetylene molecules).

	$\Delta E_{strain}$			$\Delta E_{int}$	$\Delta E$
	C <sub>4</sub> H <sub>4</sub>	CO-Cp'RhL <sub>n</sub>	Total		
<b>CO-Cp-2</b>	50.63	6.08	56.71	-138.15	-81.44
<b>CO-Ind-2</b>	50.96	34.04	85.00	-153.65	-68.65
<b>CO-anti-Cr@Ind-2</b>	50.89	36.06	86.95	-149.23	-62.28

In the subsequent step, i.e., the addition of third acetylene to the 18-electrons rhodacycle **CO-Z-2**, an energy barrier is found along the catalytic Path II (Figure 7a). **CO-Z-TS(2,3)** was divided into two fragments, i.e., CO-Cp'Rh(C<sub>4</sub>H<sub>4</sub>) (Cp' = Cp, Ind and anti-[Cr(CO)<sub>3</sub>Ind] and acetylene and ASA was performed. The results are shown in Table 6. The acetylene in all cases is only slightly deformed, whereas CO-Cp'Rh(C<sub>4</sub>H<sub>4</sub>) is highly strained.

**Table 6.** Activation strain analysis (ASA) of the transition states **CO-Cp-TS(2,3)**, **CO-Ind-TS(2,3)**, and **CO-anti-Cr@Ind-TS(2,3)**; all values are in kcal mol<sup>-1</sup>. The fragments are CO-Cp'RhL<sub>n</sub> (Cp' = Cp, Ind, and anti-[Cr(CO)<sub>3</sub>Ind]) and acetylene.

	$\Delta E_{strain}$			$\Delta E_{int}$	$\Delta E$
	C <sub>2</sub> H <sub>2</sub>	CO-Cp'RhL <sub>n</sub>	Total		
<b>CO-Cp-TS(2,3)</b>	0.18	43.96	44.14	-0.50	43.64
<b>CO-Ind-TS(2,3)</b>	0.06	28.83	28.89	-0.34	28.55
<b>CO-anti-Cr@Ind-TS(2,3)</b>	0.12	14.27	14.39	-4.58	9.81

To summarize, we found that most of the steps are kinetically as well as thermodynamically more favored in the bimetallic anti-Cr@IndRh(CO) catalysis. At a glance, this can be seen also from the energy profile (Figure 8a), which is flatter in the case of anti-Cr@IndRh(CO) than in the parent IndRh(CO) and CpRh(CO) catalyzed processes. Alternatively, the slippage variations quantified with  $\Delta$  and LISP (Figure 8b) are less pronounced in anti-Cr@IndRh(CO) than those

computed for the parent monometallic catalysts. Thus, the smaller slippage variations and the flatter potential energy profile of the bimetallic anti-Cr@IndRh(CO) suggest a higher catalytic efficiency than the monometallic IndRh(CO) and CpRh(CO), which is consistent with the experimental findings [33,36]. The phenomena of *indenyl effect* for IndRh and *extra-indenyl effect* for the bimetallic anti-Cr@IndRh can be fully explained when considering the mechanism of path II.

Notably, path II has been excluded for syn-Cr@IndRh(CO) because in this particular case the rhodium center would be too much crowded.

### 3.5. Discussion

To quantify the catalytic efficiency, we calculated the turnover frequencies (TOFs) for the studied catalytic cycles by using the energy span model [23,96,97]. Calculations were run at standard room temperature (298.15 K), as well as at the reflux temperature of toluene, i.e., 383.65 K, which is occasionally used in alkyne [2+2+2] cycloadditions as solvent [25,26,29]; the values are listed in Table 7.

Following the catalytic Path I (Scheme 6a), the TOFs are in the order CpRh > IndRh > anti-Cr@IndRh, suggesting that the bimetallic catalyst anti-IndRh is worse than the monometallic parent catalysts IndRh and CpRh. This is in contrast with the experimental results [36]. Also, no appreciable difference in terms of TOF is found between IndRh and anti-IndRh, suggesting that the influence of the second metal group, i.e., Cr(CO)<sub>3</sub>, on the efficiency of the catalyst is negligible. In all these cases, the TOF determining intermediate (TDI) is the bis-acetylene intermediate **Z-1** and the TOF determining transition state (TDTS) is the subsequent transition state **Z-TS(1,2)** (Figure 2a).

Conversely, along the catalytic Path II (Scheme 6b), in terms of TOF, a significant enhancement of the catalytic activity of the bimetallic anti-Cr@IndRh(CO) is found compared to those of the parent catalysts IndRh(CO) and CpRh(CO). On the basis of the TOF values reported in Table 7, the following trend can be established anti-Cr@IndRh(CO) > IndRh(CO) > CpRh(CO), which is consistent with the experimental observation [26]. In this case, the intermediate **CO-Z-2** is the TDI and the subsequent transition state **CO-Z-TS(2,3)** is the TDTS (Figure 8a). We can thus confirm that the coordination of Cr(CO)<sub>3</sub> favors the catalytic activity.

As recently reported [22], the slippage variations in intermediates and transition states along the catalytic cycle may be related to the chemical activity of the half-metallocene catalysts in this class of reactions. For this purpose, the slippage span  $\Delta\text{LISP}^*$  was calculated. Along Path 1 (Scheme 6a),  $\Delta\text{LISP}^*$  values follow the trend anti-Cr@IndRh > IndRh > CpRh. Since TOFs' trend is reverse, i.e., anti-Cr@IndRh < IndRh < CpRh, this indicates that the higher the slippage span along the catalytic cycle is, the lower the performance of the catalyst is [22]. When following Path II,  $\Delta\text{LISP}^*$  values follow the trend anti-Cr@IndRh(CO) < IndRh(CO) < CpRh(CO), while TOFs follow the reverse trend anti-Cr@IndRh(CO) > IndRh(CO) > CpRh(CO), in agreement with the presence of extra indenyl and indenyl effect in the bimetallic and monometallic Ind catalysts, respectively.

The mechanism for syn-Cr@IndRh catalyzed acetylene [2+2+2] cycloaddition is different, and so we cannot directly compare the TOF values. However, the higher energy barriers and higher slippage variations certainly do not favor the syn catalyst.

**Table 7.** Calculated TOF ( $\text{s}^{-1}$ ) and slippage span  $\Delta\text{LISP}^*$  ( $\text{\AA}$ ) for the catalytic Path I and II of the [2+2+2] cycloaddition of acetylene to benzene.

	$\text{TOF}_{298.15 \text{ K}} (\text{s}^{-1})$	$\text{Ratio}_{298.15 \text{ K}}$	$\text{TOF}_{383.65 \text{ K}} (\text{s}^{-1})$	$\text{Ratio}_{383.65 \text{ K}}$	$\Delta\text{LISP}^* (\text{\AA})$
<i>Path I</i>					
<b>CpRh</b>	$4.83 \times 10^3$	$1.82 \times 10^2$	$6.66 \times 10^5$	$5.79 \times 10^1$	0.85
<b>IndRh</b>	$5.23 \times 10$	1.97	$2.00 \times 10^4$	1.74	1.75
<b>anti-Cr@IndRh</b>	$2.66 \times 10$	1	$1.15 \times 10^4$	1	1.81
<b>syn-Cr@IndRh</b>	$4.57 \times 10$	—	$1.78 \times 10^4$	—	3.42
<i>Path II</i>					
<b>CpRh(CO)</b>	$6.10 \times 10^{-20}$	1	$1.07 \times 10^{-12}$	1	15.59
<b>IndRh(CO)</b>	$6.41 \times 10^{-8}$	$1.05 \times 10^{12}$	$2.35 \times 10^{-3}$	$2.20 \times 10^9$	14.11
<b>anti-Cr@IndRh(CO)</b>	$3.97 \times 10^2$	$6.51 \times 10^{21}$	$9.55 \times 10^4$	$8.93 \times 10^{16}$	12.61

### 3.6. Conclusions

We performed a theoretical investigation of the bimetallic system  $[\text{Cr}(\text{CO})_3\text{IndRh}]$ -mediated [2+2+2] cycloaddition of acetylene to benzene. Through a detailed exploration of the potential energy surfaces (PESs), the intermediates and transition states were located using density functional theory (DFT) methods following two mechanistic paths, i.e., Path I and II (Scheme 6a, b). The bimetallic catalysts anti- and syn- $[\text{Cr}(\text{CO})_3\text{IndRh}]$  were tested in silico and compared to the monometallic parent catalysts CpRh and IndRh. The anti or syn coordination of  $\text{Cr}(\text{CO})_3$  affects the energetics of the cycle and also to the mechanism. The reaction energies and barriers, the turn over frequency (TOF) and the change of the slippage parameters along the catalytic cycles are discussed.

Considering Path I, the established trend for the slippage span  $\Delta\text{LISP}^*$  is anti- $\text{Cr}@\text{IndRh} > \text{IndRh} > \text{CpRh}$  while TOF values follow the opposite order, i.e.,  $\text{CpRh} > \text{IndRh} >$  anti- $\text{Cr}@\text{IndRh}$ . This leads to the conclusion that the lower slippage span along the catalytic cycle, the higher the catalytic performance. In any case, this does not explain the highest catalytic efficiency of the bimetallic Rh/Cr compound (*extra-indenyl effect*).

Conversely, if we follow the catalytic cycle along Path II, a dramatic TOF enhancement of the bimetallic system anti- $\text{Cr}@\text{IndRh}(\text{CO})$  relative to the parent  $\text{CpRh}(\text{CO})$  and  $\text{IndRh}(\text{CO})$  is found. On the basis of the TOF, the following trend of catalytic efficiency can be established anti- $\text{Cr}@\text{IndRh}(\text{CO}) > \text{IndRh}(\text{CO}) > \text{CpRh}(\text{CO})$ , in agreement with experimental findings. In this case, the slippage span is inverted, too, i.e.,  $\text{CpRh}(\text{CO}) > \text{IndRh}(\text{CO}) >$  anti- $\text{Cr}@\text{IndRh}(\text{CO})$ , which again leads us to conclude that the lower the slippage span is, the higher the catalytic efficiency is. We can thus conclude that the coordination of  $\text{Cr}(\text{CO})_3$  in the bimetallic indenyl catalyst improves the efficiency along Path II.

The hapticity variations of intermediates and transition states along the catalytic cycle are highly pronounced in the syn bimetallic conformer, implying low TOF values and leading to the conclusion that the syn- $[\text{Cr}(\text{CO})_3\text{IndRh}]$  catalyzed process is not favored.

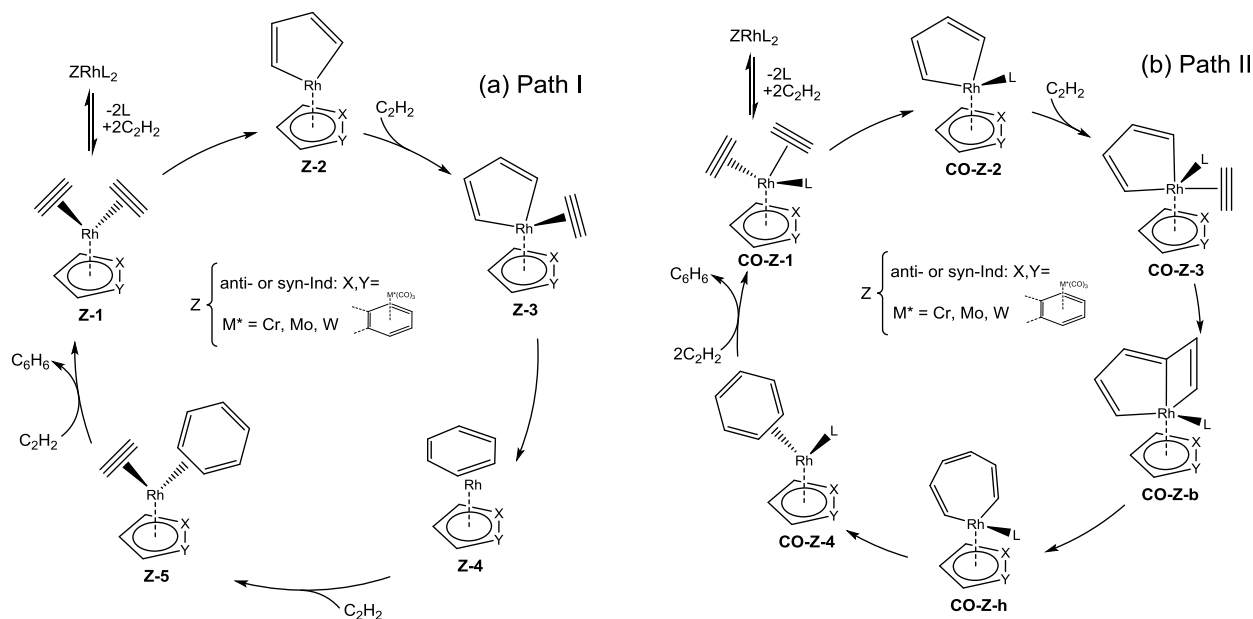


# Chapter 4

## Effect of Changing the Second metal in Bimetallic $[M^*(CO)_3IndRh]$ ( $M^* = Cr, Mo, W$ ) on the Reaction Mechanism and PES

### 4.1. Introduction

Any structural and electronic modification to the aromatic moiety of the half-sandwich IndRh catalyst may influence its catalytic efficiency as well as the mechanism [1,10,11,27,35]. In the former chapter, we have explored in detail the catalytic performance of the bimetallic  $[Cr(CO)_3IndRh]$  catalyst in its anti and syn configuration for the archetypal reaction of acetylene  $[2+2+2]$  cycloaddition to benzene and made a comparison to its analogous parent monometallic catalysts, i.e., CpRh and IndRh. Our computational investigation established that the coordination of the  $Cr(CO)_3$  group in the bimetallic IndRh catalyst favors the catalysis. Herein, we consider three bimetallic IndRh catalysts, i.e.,  $[M^*(CO)_3IndRh]$  by altering the second metal  $M^* = Cr, Mo$ , and  $W$ , with the aim of understanding how when going downward along group 6 elements, the catalysis of acetylene  $[2+2+2]$  cycloaddition to benzene is influenced. For the bimetallic anti- or syn- $[Cr(CO)_3IndRh]$  catalysts, some experimental information is present which can be correlated to our calculations [34,101,102] (Chapter 03). Conversely, for the bimetallic  $[M^*(CO)_3IndRh]$  with  $M^* = Mo$  and  $W$ , no empirical results have been reported so far. Our *in silico* assessment predicts a certain trend that may be attractive for the experimentalists, and, particularly may be used to draw structure activity relationships defining the role of the second metal in bimetallic catalysis. We examined the two well known mechanistic paths [26,88,99] outlined in Scheme 7, at the ZORA-BLYP/TZ2P level of theory. More details about these catalytic pathways are provided in Chapter 03. For the sake of simplicity, we use the abbreviation  $M^*@IndRh$  for the bimetallic  $[M^*(CO)_3IndRh]$  catalyst in the ongoing discussion, where  $M^* = Cr, Mo, W$ .



**Scheme 7.** Mechanism of acetylene [2+2+2] cycloaddition to benzene catalyzed by ZM ( $Z$  = anti or syn- $M^*$ @Ind ( $M^*$  = Cr, Mo, W, and  $M$  = Rh)) (Path 1) **(a)**, and by ZM(CO) (Path II) **(b)**.

## 4.2. Anti bimetallic catalysts: Reaction Mechanism and PES (Path 1)

The intermediates and transition states found on the PESs for acetylene [2+2+2] cycloaddition to benzene catalyzed by the bimetallic anti-Mo@IndRh and anti-W@IndRh catalysts along the mechanistic Path I (Scheme 7a) are shown in Figures 9 and 10, respectively, while those for anti-Cr@IndRh are in Figure 1, Chapter 03. All the structures and geometrical parameters have been thoroughly analyzed. It emerged that the geometries of all the intermediates and transition states have very similar bond lengths and bond angles when going from anti-Cr@IndRh to anti-Mo@IndRh and to anti-W@IndRh. This is likely due to the fact that the second metal  $M^*$  = Cr, Mo, W in these complexes belong to the same group. The most relevant difference, as expected, is the  $M^*$ -Q distance (Q = centroid of benzene) which is in the range  $\sim 1.81\text{--}1.83 \text{ \AA}$  for Cr,  $\sim 2.01\text{--}2.02 \text{ \AA}$  for Mo, and,  $\sim 1.98\text{--}1.99 \text{ \AA}$  for W. These variations are ascribed to the increasing of the atomic radius along with the group. In all cases, the  $M^*(CO)_3$  coordination to the arene ring in these complexes is found with the carbonyl groups in staggered conformation to reduce steric hindrance. The  $M^*$ -CO distance varies between  $\sim 1.96\text{--}1.98 \text{ \AA}$ .

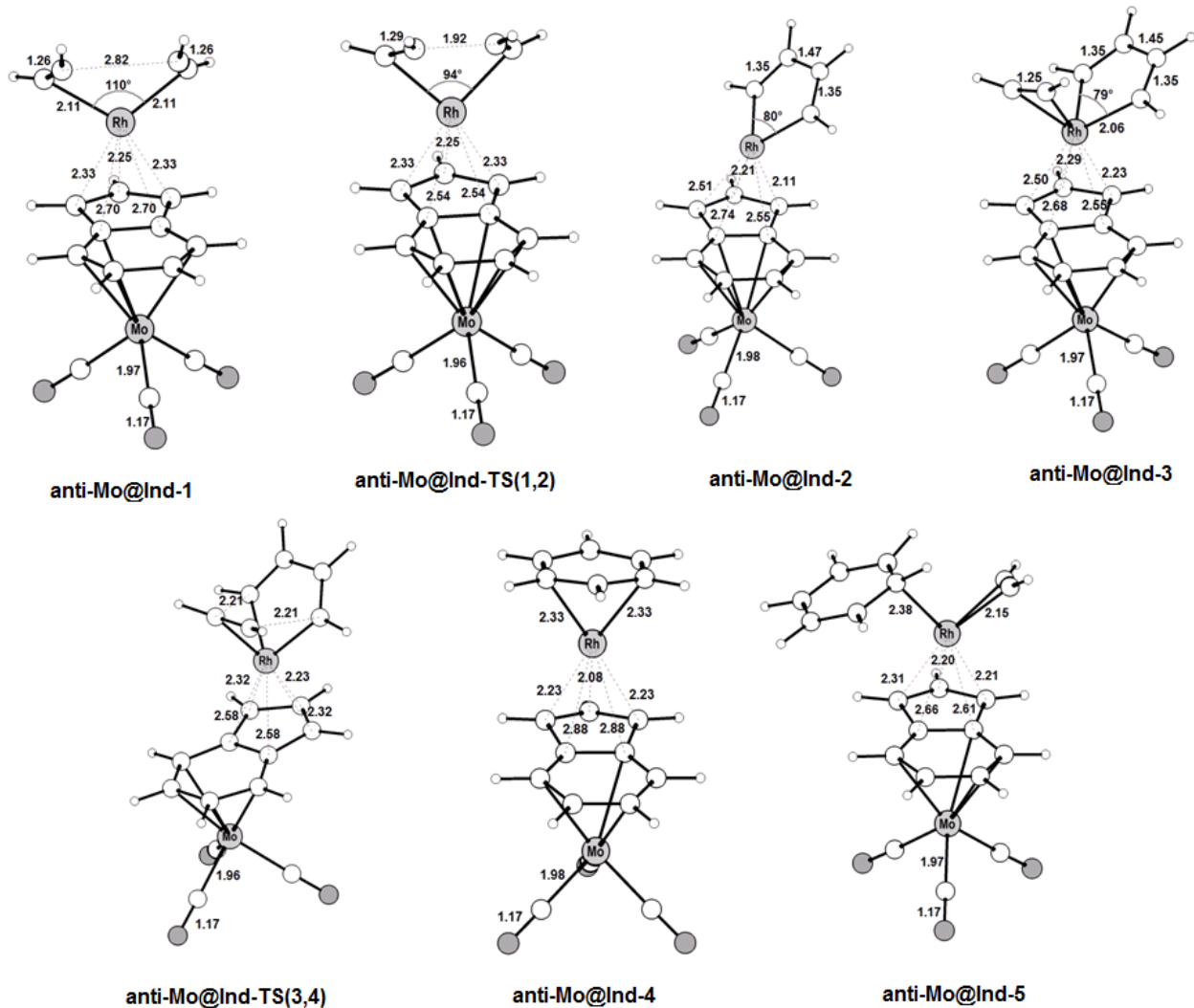


**Figure 9.** Optimized structures with selected interatomic distances ( $\text{\AA}$ ) and angles (deg) of the intermediates and transition states located on the PES of the anti-Mo@IndRh catalyzed acetylene [2+2+2] cycloaddition to benzene (Path I, Scheme 7a). Level of theory: ZORA-BLYP/TZ2P.

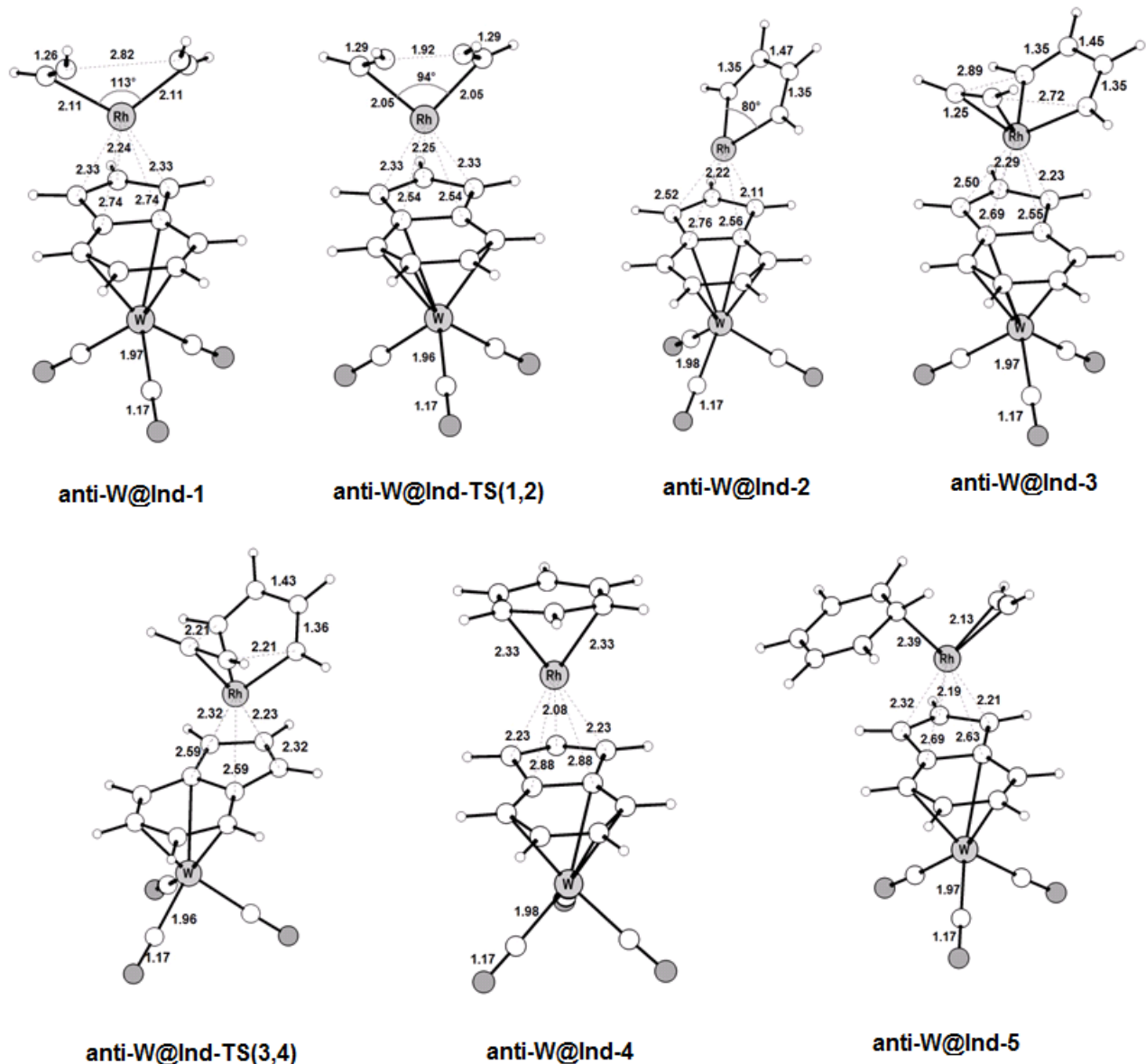


**Figure 10.** Optimized structures with selected interatomic distances ( $\text{\AA}$ ) and angles (deg) of the intermediates and transition states located on the PES of the anti-W@IndRh catalyzed acetylene [2+2+2] cycloaddition to benzene (Path I, Scheme 7a). Level of theory: ZORA-BLYP/TZ2P.

The energy profiles are shown in Figure 11a. Overall, the catalytic cycles mediated by the bimetallic anti-M<sup>\*</sup>@IndRh (M<sup>\*</sup> = Cr, Mo, W) are very similar. There are only minor energy differences falling within 1 kcal mol<sup>-1</sup>. The initial step of the catalytic path is the oxidative coupling of the two coordinated acetylene molecules in **Z-1** that leads to the 16-electrons unsaturated rhodacyclic intermediate **Z-2** (Figure 11a), crossing an activation barrier of 15.5, 14.8, and 15.1 kcal mol<sup>-1</sup> for anti-Cr@IndRh, anti-Mo@IndRh, and anti-W@IndRh, and being exothermic by -20.6, -20.8, and -21.0 kcal mol<sup>-1</sup>, respectively. **Z-1 → Z-TS(1,2)** is a key step as previously found for the CpRh, IndRh, and bimetallic anti-Cr@IndRh catalysts, characterized by the TOF determining intermediate (TDI) and transition state (TDTS) of the catalytic cycle [22,44,106].

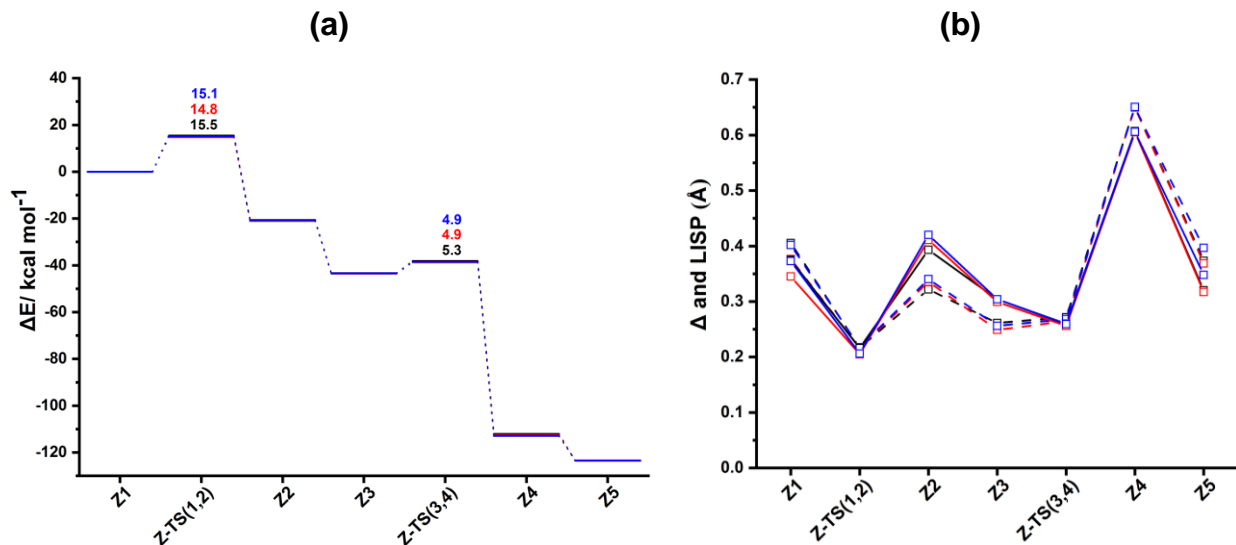


**Figure 11.** (a) Energy profiles of acetylene [2+2+2] cycloaddition to benzene catalyzed by the bimetallic anti-M<sup>\*</sup>@IndRh (M<sup>\*</sup> = Cr (black), Mo (red), W (blue)) (Scheme 7a, Path I). (b) Profiles of the slippage parameters  $\Delta$  (dashed line) and LISP (solid line) along the acetylene [2+2+2] cycloaddition cycles catalyzed by the bimetallic anti-M<sup>\*</sup>@IndRh (M<sup>\*</sup> = Cr (black), Mo (red), W (blue)) along Path I (Scheme 7a). Level of theory: ZORA-BLYP/TZ2P.

To better understand the origin of the oxidative coupling barrier, an activation strain analysis (ASA) has been performed for this catalytic step **Z-1 → Z-TS(1,2)** by dividing the complexes into two fragments: the reactant fragment consists of two acetylenes which undergo oxidative coupling (the reference energy is the sum of the energies of the isolated acetylenes) and the catalytic fragment Cp'Rh ( $\text{Cp}' = \text{anti}-[\text{M}^*(\text{CO})_3\text{Ind}]$ ) ( $\text{M}^* = \text{Cr}, \text{Mo}, \text{W}$ ). The results are given in Table 8.  $\Delta\Delta E_{\text{strain}}$  contributions to the energy barrier  $\Delta E^\ddagger$  increase when going from Cr to W. However,  $\Delta\Delta E_{\text{int}}$  increases too, compensating the deformation energy and leading to an overall decrease of the barrier going down the group.  $\Delta\Delta E_{\text{int}}$  is a little bit larger (in absolute value) in the case of anti-Mo@IndRh and this explains why the corresponding barrier is the lowest one among the three catalysts.

**Table 8.** Activation strain analysis for the first oxidative step **Z-1 → Z-TS(1,2)** (Path 1); all values are in kcal mol<sup>-1</sup>.

	$\Delta\Delta E_{\text{strain}}$			$\Delta\Delta E_{\text{int}}$	$\Delta E^\ddagger$
	2(C <sub>2</sub> H <sub>2</sub> )	Cp'Rh	Total		
<b>anti-Cr@Ind-1/anti-Cr@Ind-TS(1,2)</b>	37.31	2.72	40.03	-24.50	15.53
<b>anti-Mo@Ind-1/anti-Mo@Ind-TS(1,2)</b>	37.49	2.79	40.28	-25.48	14.80
<b>anti-W@Ind-1/anti-W@Ind-TS(1,2)</b>	37.50	2.91	40.41	-25.34	15.07

A similar energy trend is found in the catalytic step **Z3 → Z-TS(3,4)** which is related to the subsequent addition of acetylene to the  $\pi$ -electron system of the rhodacycle; the barriers of this step are 5.3, 4.9, and 4.9 kcal mol<sup>-1</sup> for anti-Cr@IndRh, anti-Mo@IndRh, and anti-W@IndRh, respectively. The exothermicity increases correspondingly, i.e., -68.6, -68.9, and -69.5 kcal mol<sup>-1</sup>. This again reveals that the activation energy decreases going down the periodic group and that the anti-Mo@IndRh catalyst is slightly kinetically more favorable. The overall catalytic cycle is exothermic by ~ -123.50 kcal mol<sup>-1</sup>.

As we know that along the catalytic cycle, the Rh position with respect to the Cp ring changes, in order to quantify the hapticity fluctuations, the  $\Delta$  and LISP parameters were calculated and are

shown in Figure 11b. We observe that the slippage variations computed with  $\Delta$  and LISP are almost identical along with the three catalytic cycles. A modest difference is found in the case of the anti-Mo@IndRh catalyst. Structurally, in all cases, the intermediates and transition states have Rh-Cp  $\eta^3+\eta^2$  coordination mode except **Z-4**, where  $\eta^3$  coordination is predicted, while Rh-benzene coordination is  $\eta^6$  (Figures 9-10). This is different from CpRh catalysis, where  $\eta^4$  hapticity was observed [41].

To quantify the drifting of the second metal  $M^* = Cr, Mo, W$  with respect to the benzene ring ( $M^*-Bz$ ) along the catalytic cycle, the LISP values have been computed and the profiles are shown in Figure 12. Interestingly, if we take into account the Rh-Cp slippage (Figure 11b) as well as  $M^*-Bz$  slippage (Figure 12), we notice that when the Rh-Cp gets more slipped, the  $M^*-Bz$  inversely gets less slipped and vice versa. This is the result of the two metals sharing the same aromatic system.

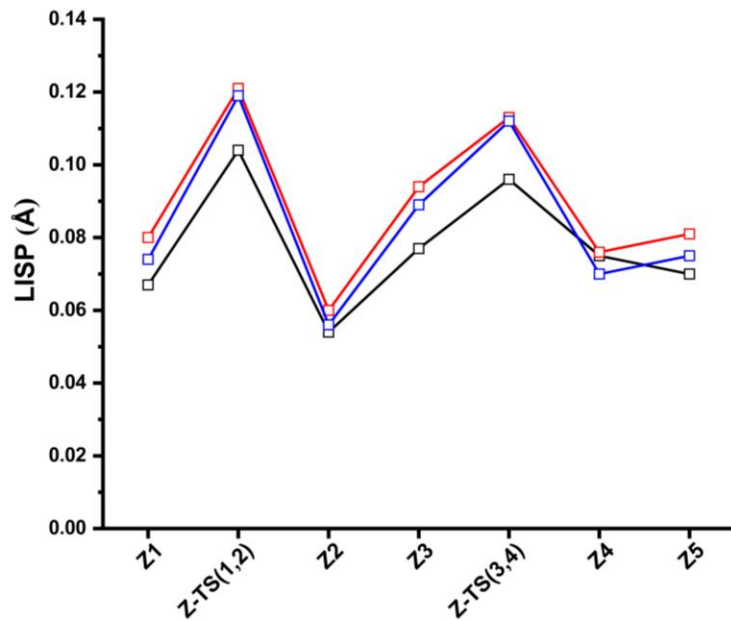


**Figure 12.** Profiles of the slippage parameter LISP for  $M^*-Bz$  in complexes along the acetylene [2+2+2] cycloaddition cycles catalyzed by the bimetallic anti- $M^*$ @IndRh ( $M^* = Cr$  (black), Mo (red), W (blue)) along Path I (Scheme 7a). Level of theory: ZORA-BLYP/TZ2P.

Figure 12 shows the isolated LISP values of the M<sup>\*</sup>-Bz in the following order: Mo > W > Cr. This non periodic trend is likely due to different electron withdrawing effects of the metals Cr, Mo, W coordinated to the arene ring. Price et al. [107] found the same unusual trend in NMR studies of arene - group 6 metal tricarbonyl complexes. The authors ascribe this non periodic trend to partial different electron withdrawing effects and to the effect of relativistic contraction in period 5 (Rb through Xe), and 6 (Cs through Rn).

The frontier molecular orbitals of **anti-Cr@Ind-1**, **anti-Mo@Ind-1**, and **anti-W@Ind-1**, shown in Figure 13, have almost similar nodal characteristics between d orbital of M<sup>\*</sup> = Cr, Mo, W, benzene ring and CpRh fragment. The  $\pi$ -antibonding character between Cp'- $\pi$  system (Cp' = anti-[M<sup>\*(CO)<sub>3</sub>Ind]] (M<sup>\*</sup> = Cr, Mo, W) and Rh valence d leads to slippage. However, it is less pronounced in **anti-Mo@IndRh-1**, because of the minor electron withdrawing nature of Mo(CO)<sub>3</sub>. Accordingly, LISP values' differences are found and LISP is  $\sim 0.03 \text{ \AA}$ , lower in **anti-Mo@Ind-1** than in **anti-Cr@Ind-1**, and **anti-W@Ind-1**. This means that the electron withdrawing nature of M<sup>\*(CO)<sub>3</sub> tunes the nodal amplitude of the  $\pi$ -anti-bonding character of the Cp'- $\pi$  system.</sup></sup>

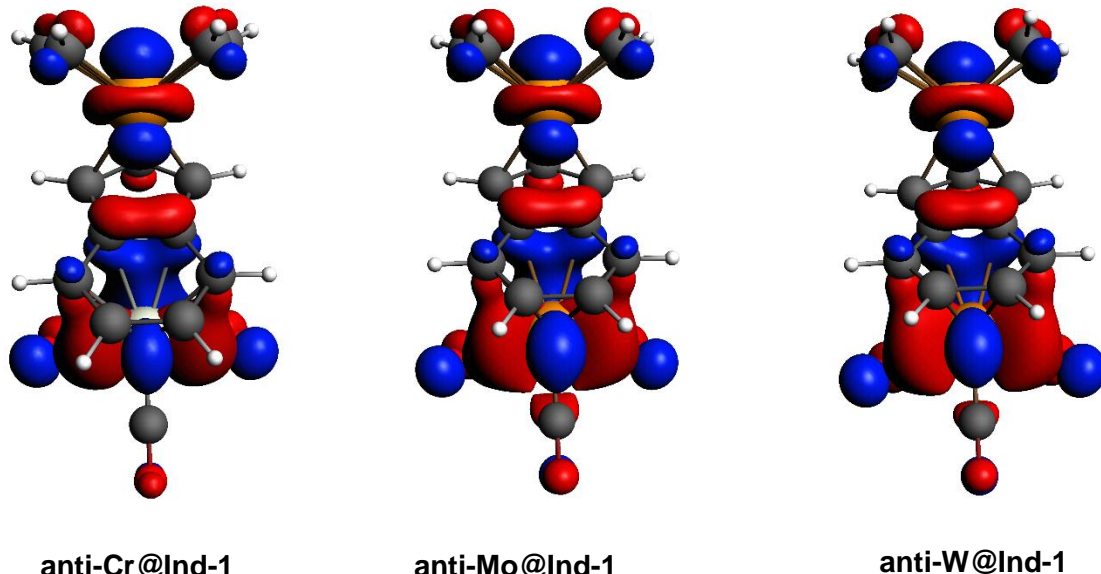


**Figure 13.** Highest occupied molecular orbitals (HOMOs) of **anti-Cr@Ind-1**, **anti-Mo@Ind-1**, and **anti-W@Ind-1**; level of theory: ZORA-BLYP/TZ2P. The isodensity value is 0.03.

To understand the role of the second metal group  $M^*(CO)_3$  in the anti-[ $M^*(CO)_3$ IndRh] catalyzed process, ASA has been carried out by dividing all the complexes of the catalytic cycle into two fragments, i.e.,  $M^*(CO)_3$  (Fg1) and IndRhX<sub>i</sub> (Fg2), where, X<sub>i</sub> is the corresponding product at the Rh active center (the reference energy for the fragment IndRhX<sub>i</sub> is relative to IndRh(C<sub>2</sub>H<sub>2</sub>)<sub>2</sub> and free acetylene). The results are reported in Tables 9 and 10 for M\* = Mo and W, respectively, while for Cr they were already given in Chapter 03, Table 3.

The total  $\Delta E_{\text{strain}}$  arises from both fragments and is destabilizing in the order syn-W@IndRh > syn-Cr@IndRh > syn-Mo@IndRh. The  $\Delta E_{\text{int}}$  interaction, which is stabilizing, also increases (larger negative values) correspondingly. Along the catalytic cycle,  $\Delta E_{\text{int}}$  fluctuates in the range  $\sim 47\text{--}54 \text{ kcal mol}^{-1}$  for anti-Cr@IndRh,  $\sim -42.56\text{--}49.08 \text{ kcal mol}^{-1}$  for anti-Mo@IndRh, and  $\sim 53.61\text{--}61.04 \text{ kcal mol}^{-1}$  for anti-Mo@IndRh, respectively. An approximately more or less equal to the experimental binding energy of Cr(CO)<sub>3</sub> coordination to the arene ring which is 53 kcal mol<sup>-1</sup> [108]. The extent of stabilizing  $\Delta E_{\text{int}}$  in the different barriers follows the order syn-Mo@IndRh > syn-W@IndRh > syn-Cr@IndRh. ASA shows that  $\Delta E_{\text{strain}}$  of fragment  $M^*(CO)_3$  remains nearly equal along the cycle, however, it increases when passing from Cr to W. In fact, it is because of the size of M\* and electron withdrawing nature which determines the strength of coordination to the benzene centroid.

In all cases, in correspondence of **anti- $M^*$ @Ind-4**, there is a sudden increase in  $\Delta E_{\text{int}}$  between  $M^*(CO)_3$  and IndRhX, because on the opposite side of the indenyl ligand, the slippage of Rh on Cp increases (Figure 11b).

**Table 9.** Activation strain analysis (ASA) of all the intermediates and transition states of the anti-Mo@IndRh catalyzed cycle (Path I); all the values are in kcal mol<sup>-1</sup>.

	$\Delta V_{\text{elstat}}$	$\Delta E_{\text{Pauli}}$	$\Delta E_{\text{oi}}$	$\Delta E_{\text{strain}}$			$\Delta E_{\text{int}}$	$\Delta E$
				Mo(CO) <sub>3</sub>	IndRhX <sub>i</sub>	Total		
<b>anti-Mo@Ind-1</b>	-87.19	141.26	-97.05	2.65	40.33	42.98	-42.98	0
<b>anti-Mo@Ind-TS(1,2)</b>	-84.38	137.07	-95.72	2.62	55.18	57.80	-43.03	14.77
<b>anti-Mo@Ind-2</b>	-85.74	146.78	-103.6	3.28	18.59	21.87	-42.56	-20.79
<b>anti-Mo@Ind-3</b>	-84.82	141.27	-98.29	2.82	-4.52	-1.73	-41.84	43.58
<b>anti-Mo@Ind-TS(3,4)</b>	-84.62	138.72	-96.76	2.68	1.28	3.96	-42.66	-38.68
<b>anti-Mo@Ind-4</b>	-93.27	143.12	-98.93	2.73	-66.18	-63.45	-49.08	-112.53
<b>anti-Mo@Ind-5</b>	-87.22	141.51	-97.52	2.67	-82.85	-80.18	-43.23	-123.41

**Table 10.** Activation strain analysis (ASA) of all the intermediates and transition states of the anti-W@IndRh catalyzed cycle (Path I); all the values are in kcal mol<sup>-1</sup>.

	$\Delta V_{\text{elstat}}$	$\Delta E_{\text{Pauli}}$	$\Delta E_{\text{oi}}$	$\Delta E_{\text{strain}}$			$\Delta E_{\text{int}}$	$\Delta E$
				W(CO) <sub>3</sub>	IndRhX <sub>i</sub>	Total		
<b>anti-W@Ind-1</b>	-109.22	174.68	-120.38	3.87	51.05	54.92	-54.92	0
<b>anti-W@Ind-TS(1,2)</b>	-105.81	169.78	-118.63	3.77	65.96	69.73	-54.66	15.07
<b>anti-W@Ind-2</b>	-107.07	179.8	-127.4	4.57	29.26	33.83	-54.67	-20.96
<b>anti-W@Ind-3</b>	-106.43	174.63	-121.81	4.05	6.17	10.22	-53.61	-43.45
<b>anti-W@Ind-TS(3,4)</b>	-105.86	171.04	-119.51	3.85	12.15	16.0	-54.33	-38.53
<b>anti-W@Ind-4</b>	-115.27	175.39	-121.16	3.85	-55.74	-51.89	-61.04	-112.93
<b>anti-W@Ind-5</b>	-109.47	175.38	-121.28	3.92	-72.05	-68.13	-55.37	-123.50

### 4.3. Syn bimetallic catalyst: Reaction Mechanism and PES (Path I)

The coordination of the  $M^*(CO)_3$  group to the benzene moiety of IndRh catalyst may also occur in syn conformation [105]. In Chapter 03, we have investigated syn-Cr@IndRh, with the idea that the presence of Cr and Rh on the same side might lead to some electronic cooperative effects and to an enhanced reactivity. We have concluded that since the rhodium center becomes overcrowded by ligands, the catalyst is less efficient and larger slippage variations occur. However, we have extended the investigation to syn-Mo@IndRh and then to syn-W@IndRh. The intermediates and transition states found on the PESs catalyzed by bimetallic syn-Mo@IndRh and syn-W@IndRh catalysts along the mechanistic Path I (Scheme 7a) are shown in Figure 14 and 15, respectively, while for syn-Cr@IndRh one should see Figure 4 (Chapter 03).

The intermediates and transition states of the acetylene [2+2+2] cycloaddition catalyzed by syn-Mo@IndRh and syn-W@IndRh are similar to those obtained with syn-Cr@IndRh catalyst. The weak differences observed in bond lengths and bond angles are due to the different size of the metals, i.e.,  $M^* = Cr < Mo < W$ . The calculated energy profiles are shown in Figure 16a. The energy differences among the catalysts syn- $M^*$ @IndRh ( $M^* = Cr, Mo, W$ ) are also very small, i.e., lower than 1 kcal mol<sup>-1</sup>. The activation energy required for the initial oxidative coupling is 15.2, 15.1 and 15.2 kcal mol<sup>-1</sup> for syn-Cr@IndRh, syn-Mo@IndRh, and syn-W@IndRh, and the step is exothermic by -26.4, -25.1, and -25.2 kcal mol<sup>-1</sup>, respectively. The combination Mo/Rh shows a comparatively lower barrier for this step. When passing from syn-Cr@IndRh to syn-Mo@IndRh and then syn-W@IndRh, on the syn side catalysis the barriers generally increase. This trend is in contrast to that described for the anti side catalysis.

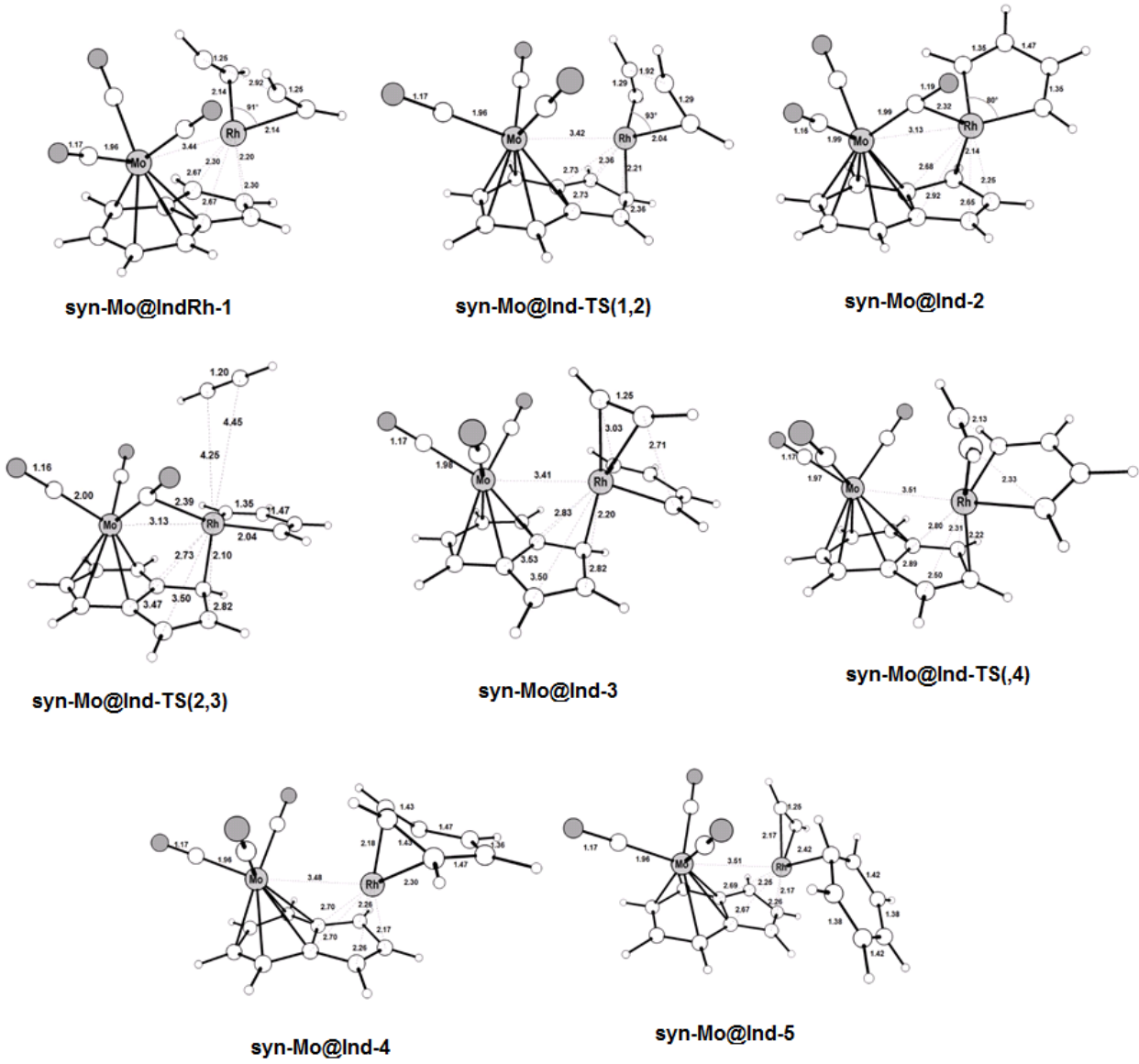


**Figure 14.** Optimized structures with selected interatomic distances ( $\text{\AA}$ ) and angles (deg) of the intermediates and transition states located on the PES of the syn-Mo@IndRh catalyzed acetylene [2+2+2] cycloaddition to benzene (Path I, Scheme 7a). Level of theory: ZORA-BLYP/TZ2P.

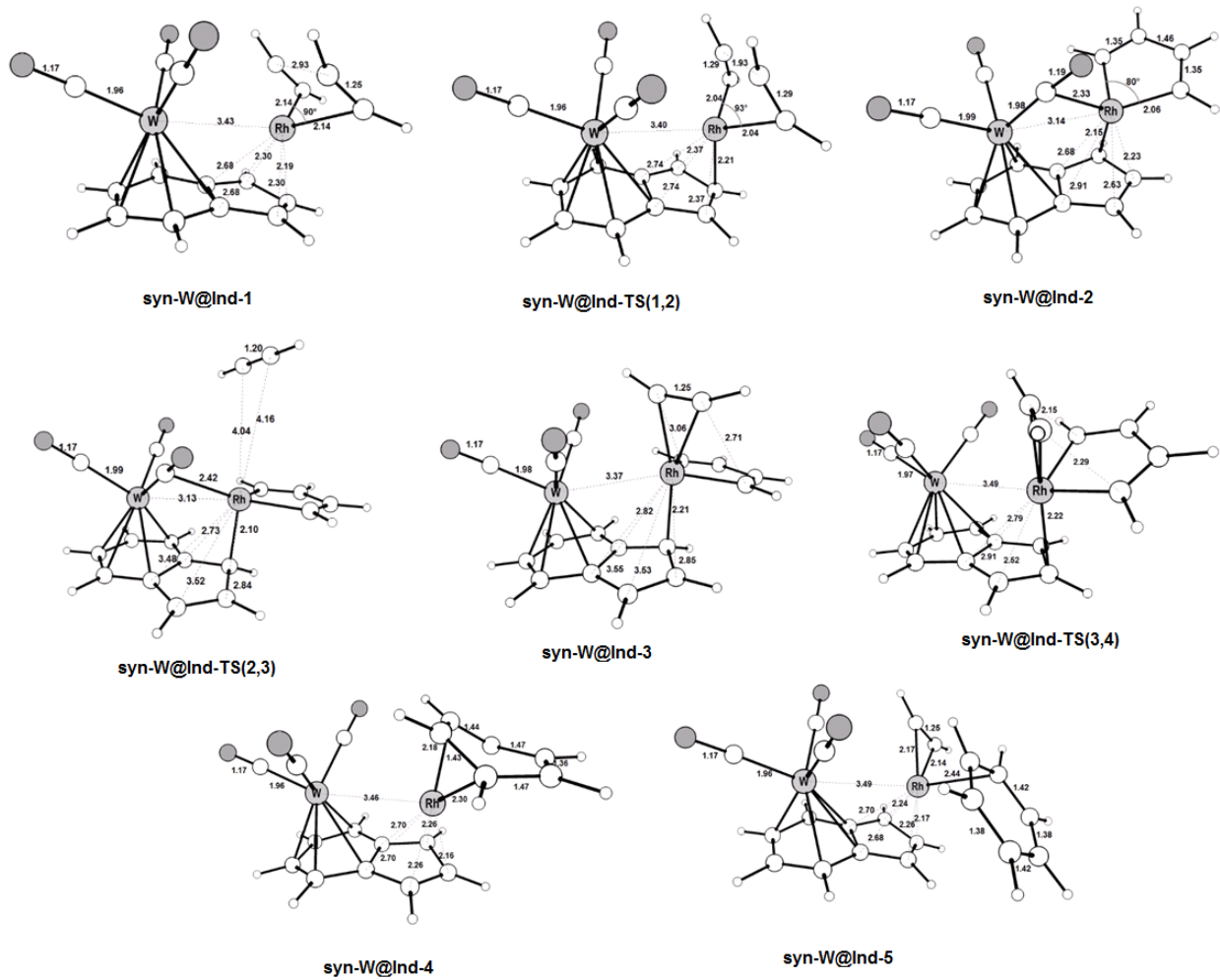


**Figure 15.** Optimized structures with selected interatomic distances ( $\text{\AA}$ ) and angles (deg) of the intermediates and transition states located on the PES of the syn-W@IndRh catalyzed acetylene [2+2+2] cycloaddition to benzene (Path I, Scheme 7a). Level of theory: ZORA-BLYP/TZ2P.

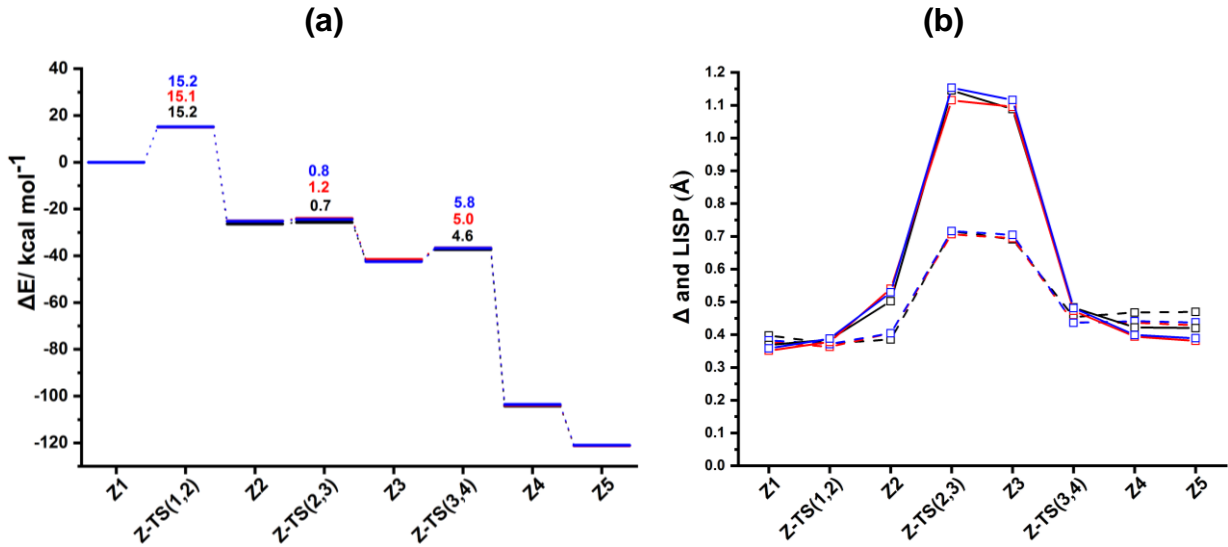


**Figure 16.** (a) Energy profiles of acetylene [2+2+2] cycloaddition to benzene catalyzed by bimetallic syn- $M^*$ @IndRh ( $M^* = \text{Cr}$  (black), Mo (red), W (blue)) (Scheme 7a, Path I). (b) Profiles of the slippage parameters  $\Delta$  (dashed line) and LISP (solid line) along the acetylene [2+2+2] cycloaddition cycles catalyzed by bimetallic syn- $M^*$ @IndRh ( $M^* = \text{Cr}$  (black), Mo (red), W (blue)) along Path I (Scheme 12a). Level of theory: ZORA-BLYP/TZ2P.

Large hapticity changes from  $\eta^3+\eta^2$  to  $\eta^3$  and to  $\eta^1$  are computed in Rh-Cp in syn complexes (Figure 16b), highly pronounced if compared to the anti analogous cases, particularly in the region from **Z2** to **Z4** of the catalytic cycle. Thus, we can conclude that the syn coordination of the second metal group is not favoring acetylene [2+2+2] cycloaddition also in the presence of Mo and W. The slippage variations of Rh-Cp along the cycle are in the following order: syn-Cr@IndRh < syn-Mo@IndRh < syn-W@IndRh.

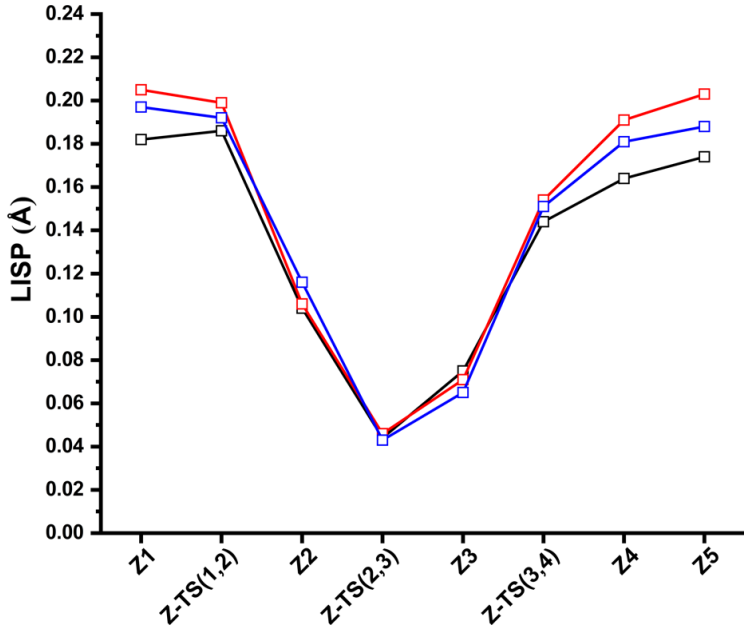


**Figure 17.** Profiles of the slippage parameter LISP for  $M^*$ -Bz in complexes along the acetylene [2+2+2] cycloaddition cycles catalyzed by the bimetallic syn- $M^*$ @IndRh ( $M^*$  = Cr (black), Mo (red), W (blue)) along Path I (Scheme 7a). Level of theory: ZORA-BLYP/TZ2P.

Figure 17 shows the LISP profiles calculated for the second metal  $M^*$ -Bz ( $M^*$  = Cr, Mo, W) along the whole cycle. When the Rh slips over Cp (Figure 16b),  $M^*$  gets closer to benzene (Figure 17) and vice versa. The trend of  $M^*$ -Bz slippage variations in syn-side catalysis are Mo > W > Cr. This non periodic trend is opposite to the anti side catalysis. The HOMOs-3 of syn-Cr@Ind-1, syn-Mo@Ind-1, and syn-W@Ind-1 are shown in Figure 18. In Rh-Mo it is less diffuse. The orbital HOMO-3 has contributions from the metal  $d$  based molecular orbitals (MOs) of the fragment  $M^*(CO)_3$  and those of Rh in the fragment IndRh( $C_2H_2$ )<sub>2</sub> and it is evident a stabilizing  $d$ - $d$  interaction between Rh and  $M^*$  in all three cases.

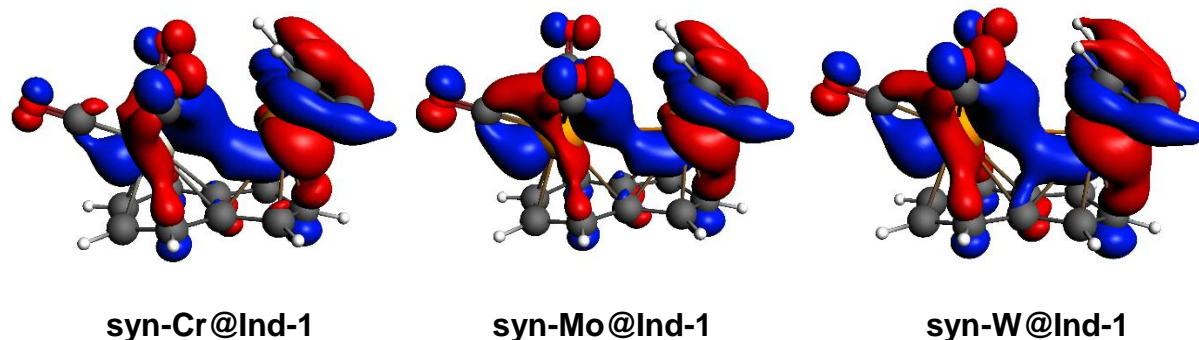


**Figure 18.** HOMOs-3 in **syn-M\*@Ind-1** ( $M^* = \text{Cr, Mo, W}$ ); the isodensity value is 0.03.

#### 4.4. Anti bimetallic catalysts: Reaction Mechanism and PES (Path II)

We also examined the activity of anti- $M^*@\text{IndRh}$  ( $M^* = \text{Cr, Mo, W}$ ) along the mechanistic Path II (Scheme 7b), in the hypothesis that one of the ligands remains bonded throughout the whole catalytic cycle. The intermediates and transition states found on the PESs for anti- $\text{Mo}@\text{IndRh}(\text{CO})$  and anti- $\text{W}@\text{IndRh}(\text{CO})$  catalysis are shown in Figures 19 and 20, respectively, while those related to anti- $\text{Cr}@\text{IndRh}(\text{CO})$  are shown in Figure 7 (Chapter 03).

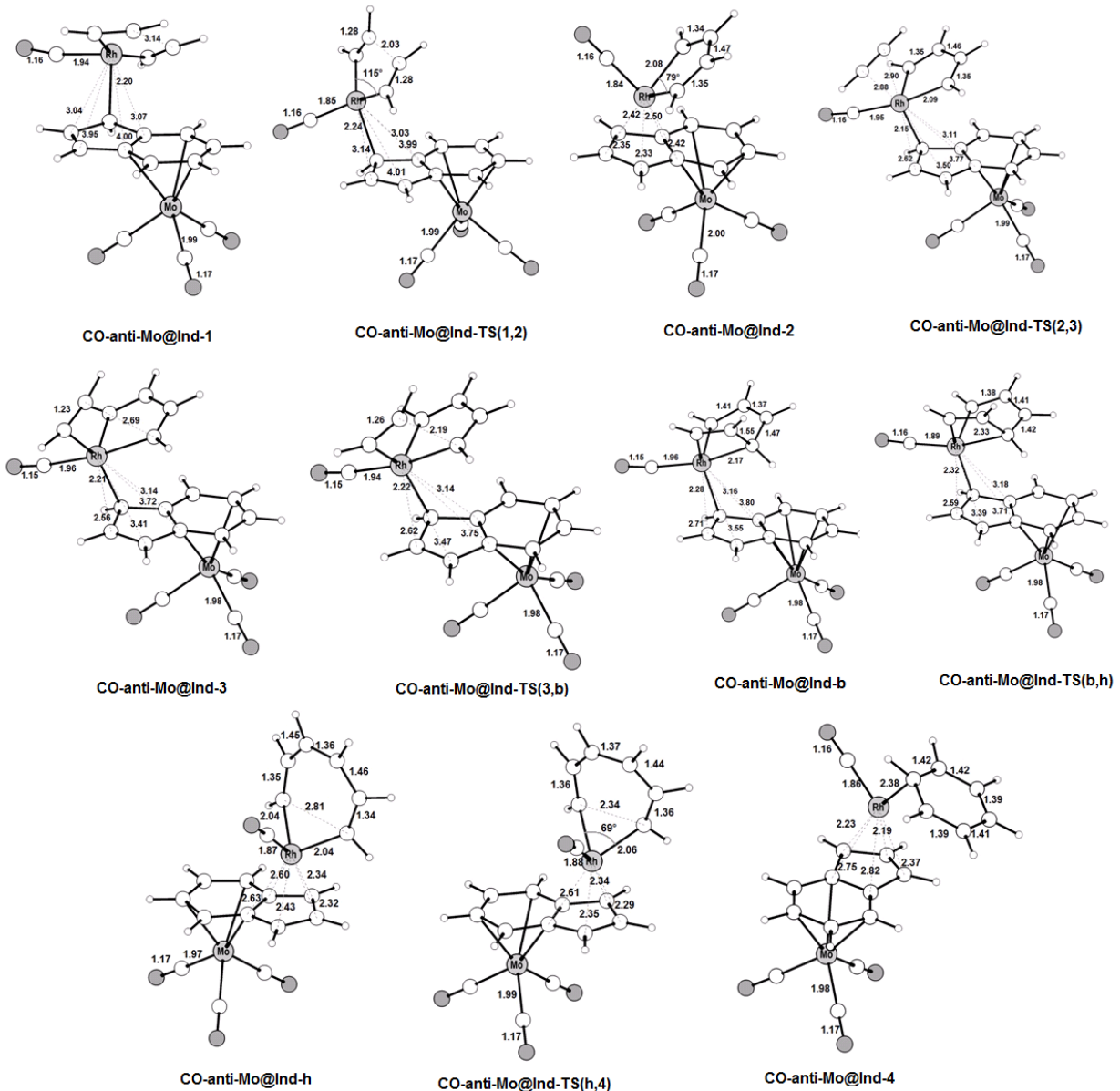


**Figure 19.** Optimized structures with selected interatomic distances ( $\text{\AA}$ ) and angles (deg) of the intermediates and transition states located on the PES of the anti-Mo@IndRh(CO) catalyzed acetylene [2+2+2] cycloaddition to benzene (Path II, Scheme 7b). Level of theory: ZORA-BLYP/TZ2P.

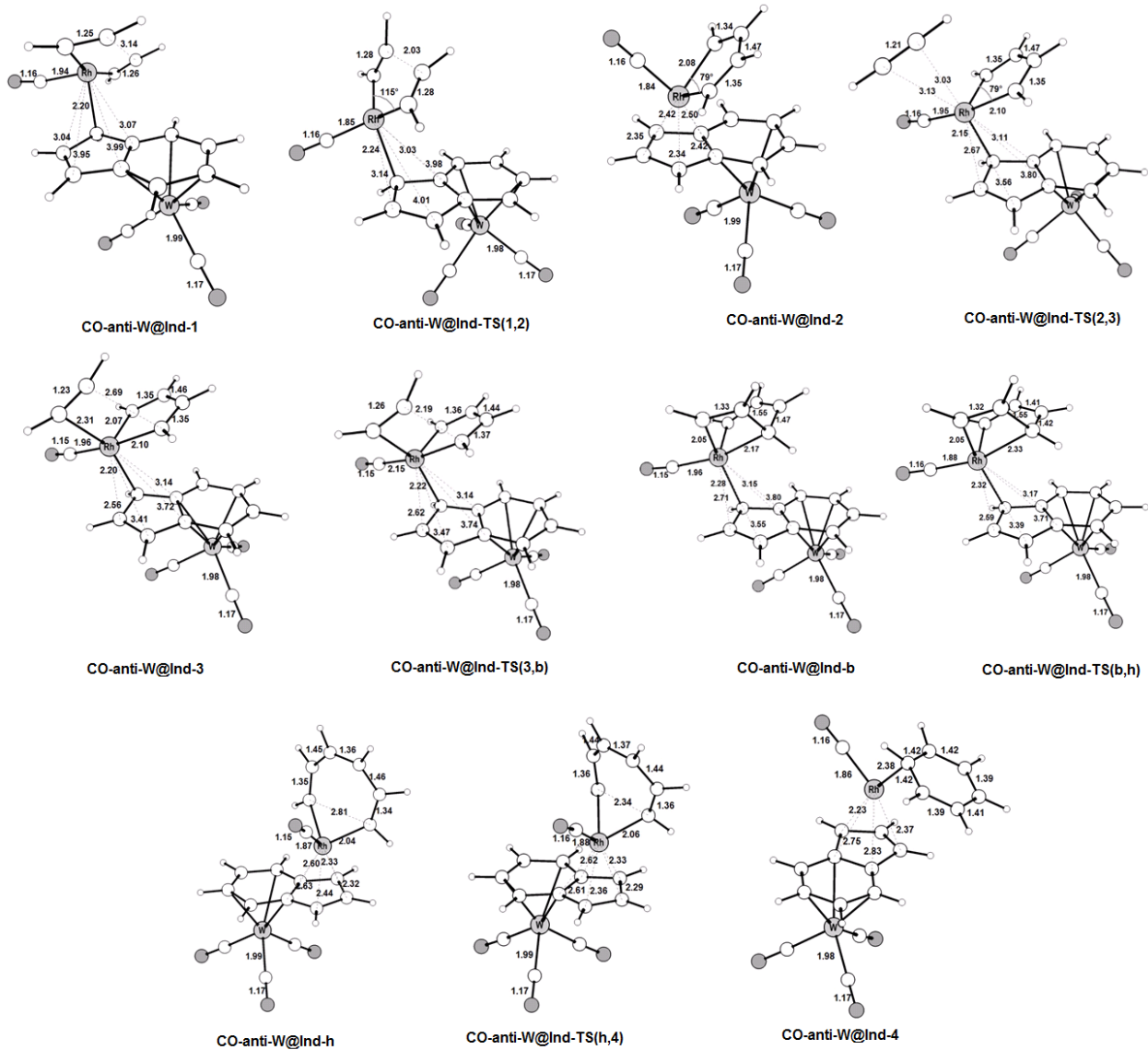


**Figure 20.** Optimized structures with selected interatomic distances ( $\text{\AA}$ ) and angles (deg) of the intermediates and transition states located on the PES of the anti-W@IndRh(CO) catalyzed acetylene [2+2+2] cycloaddition to benzene (Path II, Scheme 7b). Level of theory: ZORA-BLYP/TZ2P.

The energy profiles are presented in Figure 21a. The corresponding barriers on the PESs are quite similar. The initial oxidative coupling step (**CO-Z-1 → CO-Z-TS(1,2)**) has a barrier of 13.9, 14.1, and 14.0 kcal mol<sup>-1</sup> for anti-Cr@IndRh(CO), anti-Mo@IndRh(CO), and anti-W@IndRh(CO), and is exothermic by -43.1, -43.8, and -42.9 kcal mol<sup>-1</sup>, respectively. The rhodacycle with bonded CO is a very stable intermediate on Path II, because of the achievement of the 18-electrons configuration. This step is kinetically less but thermodynamically more favorable in the case of Mo/Rh(CO). Similarly, the next addition of acetylene to the rhodacycle (**CO-Z-2**) has a barrier of 9.9, 9.6, and 10.1 kcal mol<sup>-1</sup> for anti-Cr@IndRh(CO), anti-Mo@IndRh(CO), and anti-W@IndRh(CO), respectively that is again in favor of anti-Mo@IndRh(CO). All the other corresponding barriers on the PESs have very similar values as can be seen from the energy profiles (Figure 21a).

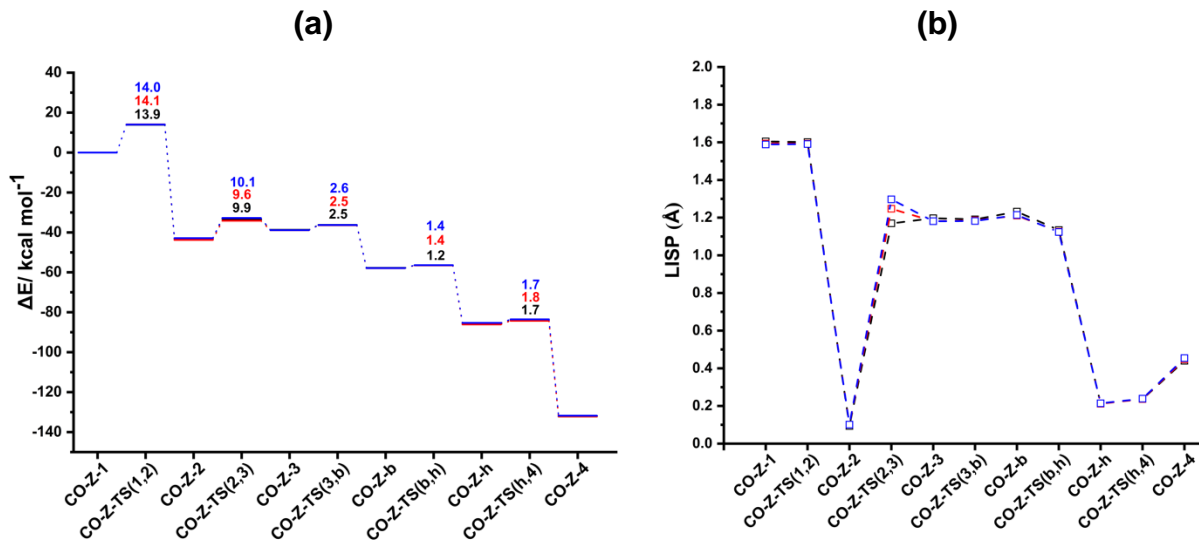


**Figure 21.** (a) Energy profiles of acetylene [2+2+2] cycloaddition to benzene catalyzed by bimetallic anti-Cr@IndRh(CO) (black) anti-Mo@IndRh(CO) (red), and anti-W@IndRh(CO) (blue) (Scheme 7b, Path II). (b) Profiles of the slippage parameter (LISP) along with the acetylene [2+2+2] cycloaddition cycles catalyzed by bimetallic anti-Cr@IndRh(CO) (black) anti-Mo@IndRh(CO) (red), and anti-W@IndRh(CO) (blue) along Path II (Scheme 7b). Level of theory: ZORA-BLYP/TZ2P.

The Rh slippage in the corresponding intermediates and transition states is unaffected when changing Cr with Mo or W, as can be seen in Figure 21b. In all cases, by having ancillary ligand CO along a cycle, a number of haptotropic shifts between  $\eta^1$  and distorted  $\eta^5$  occurs. The slippage of Rh on Cp quantified by the LISP parameter decreases in this order anti-Mo@IndRh(CO) > anti-W@IndRh(CO) > anti-Cr@IndRh(CO), similarly to Path I. Conversely, the M\*-Bz slippage variations along a cycle follow the periodic trend, i.e., Cr < Mo < W (Figure 22).

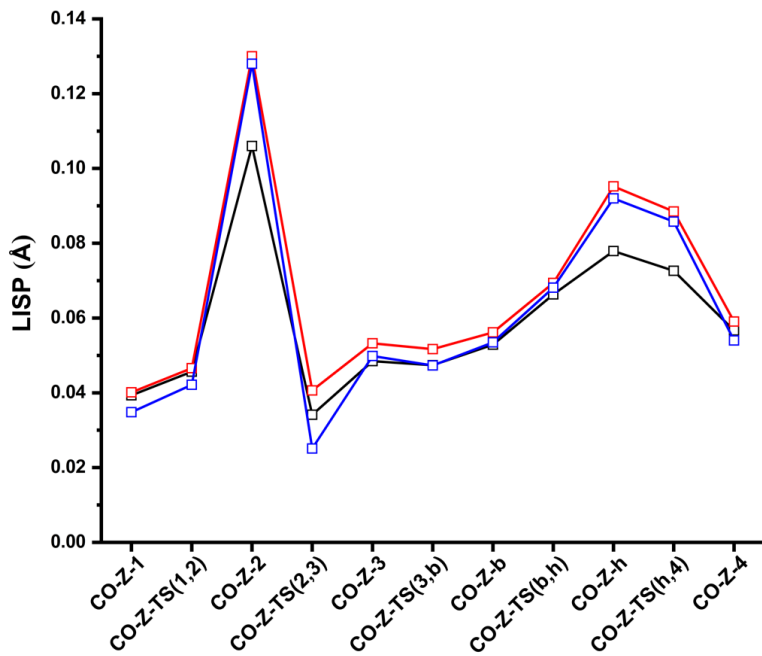


**Figure 22.** Profiles of the slippage parameter LISP for M\*-Bz in complexes along the acetylene [2+2+2] cycloaddition cycles catalyzed by bimetallic anti-M\*@IndRh(CO) (M\* = Cr (black), Mo (red), W (blue)) along Path II (Scheme 7b). Level of theory: ZORA-BLYP/TZ2P.

## 4.5. Turnover Frequencies (TOFs) and Structural-Activity Relationship

As one of the main goals of this Ph.D. project is to relate the chemical reactivity of the studied half-sandwich catalysts to their relevant structural changes, mainly the metal slippage, the search and validation of a valid relationship have been pursued. To quantify the chemical reactivity of the studied catalysts, the turn over frequencies (TOFs) have been computed from the energy profiles using the energy span model (ESM) [23,96,97] at the standard room temperature (298.15 K) as well as at the reflux temperature of toluene, i.e., 383.65 K [25,26,29]. The entity of the structural changes (metal slippage) along the catalytic cycle has been computed using the parameter  $\Delta\text{LISP}^*$  [22]. The results are listed in Table 11. Along Path 1 (Scheme 7a), the TOF ratios show that the catalytic efficiency is in the order: anti-Mo@IndRh > anti-W@IndRh > anti-Cr@IndRh, implying that the efficiency of the bimetallic catalyst anti- $\text{M}^*@\text{IndRh}$  ( $\text{M}^* = \text{Cr, Mo, W}$ ) increases when going down in the periodic group, particularly when  $\text{M}^* = \text{Mo}$ . Like already commented in Chapter 03, the TOF determining intermediate (TDI) is the initial bis-acetylene intermediate **Z-1** and the TOF determining transition state (TDTS) is the subsequent transition state **Z-TS(1,2)** that leads to five-membered ring rhodacycle **Z-2**. The computed  $\Delta\text{LISP}^*$  values are very close to each other, however, they are in the following order anti-W@IndRh > anti-Cr@IndRh > anti-Mo@IndRh. This means that anti-Mo@IndRh has the smallest slippage variation along the cycle but it has also the highest TOF value. The TOF and  $\Delta\text{LISP}^*$  trends suggest that the lower the slippage span along the catalytic cycle is, the higher the catalytic performance of the catalyst is, in agreement with the slippage span model [22].

Considering the TOF ratios, the catalytic activity of the bimetallic anti- $\text{M}^*@\text{IndRh(CO)}$  ( $\text{M}^* = \text{Cr, Mo, W}$ ) is almost similar along Path II (Scheme 7b) and reaches negligible values at the reflux temperature of toluene, i.e., 383.65 K. However, the order of catalytic efficiency is anti-Cr@IndRh > anti-W@IndRh > anti-Mo@IndRh, opposite to Path I (Scheme 7a). The trend of the  $\Delta\text{LISP}^*$  values computed for Path II is in agreement with the slippage span model [22]. In relation to the monometallic system, i.e., CpRh and IndRh as described in detail [22,44,106], the studied bimetallic anti- $\text{M}^*@\text{IndRh(CO)}$  ( $\text{M}^* = \text{Cr, Mo, W}$ ) catalysts show higher catalytic efficiency and lower slippage variations. So we can conclude that the presence of the second metal favors the catalysis.

For the syn bimetallic catalysts, in terms of TOF ratio, the syn-Mo@IndRh shows higher catalytic performance, but also higher  $\Delta LISP^*$  values due to higher slippage variations along the cycle which make them worse than the analogous anti catalysts.

**Table 11.** Calculated TOF (time<sup>-1</sup>) and slippage span  $\Delta LISP^*$  ( $\text{\AA}$ ) for the acetylene [2+2+2] cycloaddition to benzene. Level of theory: ZORA-BLYP/TZ2P.

Catalysts	TOF <sub>298.15 K</sub> (s <sup>-1</sup> )	Ratio <sub>298.15 K</sub>	TOF <sub>383.65 K</sub> (s <sup>-1</sup> )	Ratio <sub>383.65 K</sub>	$\Delta LISP^*$ (Cp-Rh)	$\Delta LISP^*$ (Bz-M*)
<i>anti side (Path I)</i>						
<b>anti-Cr@IndRh</b>	$2.66 \times 10^{01}$	1	$1.15 \times 10^{04}$	1	1.81	0.26
<b>anti-Mo@IndRh</b>	$8.67 \times 10^{01}$	3.26	$2.93 \times 10^{04}$	2.55	1.80	0.31
<b>anti-W@IndRh</b>	$5.50 \times 10^{01}$	2.07	$2.06 \times 10^{04}$	1.79	1.83	0.33
<i>syn side (Path I)</i>						
<b>syn-Cr@IndRh</b>	$4.57 \times 10^{01}$	1	$1.78 \times 10^{04}$	1	3.42	0.68
<b>syn-Mo@IndRh</b>	$5.23 \times 10^{01}$	1.16	$2.00 \times 10^{04}$	1.12	3.45	0.78
<b>syn-W@IndRh</b>	$4.64 \times 10^{01}$	1.02	$1.80 \times 10^{04}$	1.01	3.54	0.75
<i>Path II</i>						
<b>anti-Cr@IndRh(CO)</b>	$3.97 \times 10^{02}$	1.33	$9.55 \times 10^{04}$	1.25	12.61	0.45
<b>anti-Mo@IndRh(CO)</b>	$2.98 \times 10^{02}$	1	$7.64 \times 10^{04}$	1	12.52	0.58
<b>anti-W@IndRh(CO)</b>	$3.40 \times 10^{02}$	1.14	$8.43 \times 10^{04}$	1.10	12.51	0.64

## 4.6. Conclusions

We have studied *in silico* the mechanistic aspects of the acetylene [2+2+2] cycloaddition to benzene catalyzed by heterobimetallic half-sandwich complexes of general formula  $[M^*(CO)_3IndRh]$  ( $M^* = Cr, Mo, W$ ) with the aim of assessing the influence on the catalytic efficiency of the second metal when moving down the group ( $M^* = Cr, Mo$ , and  $W$ ). A detailed exploration of the potential energy surfaces (PESs) has been carried out to identify the intermediates and transition states, using an accurate density functional theory (DFT) approach along two proposed mechanistic pathways, i.e., Path I and II (Scheme 7). The reaction energies and barriers, the turn over frequency (TOF) and the slippage parameters of the complete catalytic cycles have been rationalized. The computed electronic energy profiles of the studied bimetallic catalysts, i.e.,  $[M^*(CO)_3IndRh]$  ( $M^* = Cr, Mo, W$ ) are in all cases quite similar, displaying variations within 1 kcal mol<sup>-1</sup> of the corresponding barriers along the cycle. However, taking into account these subtle energy differences, we conclude that in bimetallic catalysts when going from Cr to Mo and to W, the corresponding activation barriers decrease along the catalytic cycle. The computed TOF ratios are in the following order: anti-Mo@IndRh > anti-W@IndRh > anti-Cr@IndRh, leading to the conclusion that the presence of Mo leads to catalytic enhanced performance. The relation between the structure and the reactivity of the studied catalysts have been finally examined through the slippage span model, which confirmed that the lower the  $\Delta LISP^*$  value is, the better the performance in terms of TOF is.

Along mechanistic Path II, the TOF ratios are in the following order: anti-Cr@IndRh > anti-W@IndRh > anti-Mo@IndRh and the trend is opposite to mechanistic Path I. However, the relationship of catalytic efficiency and slippage span is in consistent to the slippage span model. The overall bimetallic  $[M^*(CO)_3IndRh]$  ( $M^* = Cr, Mo, W$ ) catalysts display higher catalytic activity than monometallic catalysts (CpRh and IndRh), and, conclude us that bimetallic catalysts favour the catalysis. The hapticity variations of the intermediates and the transition states along the catalytic cycle are highly pronounced in the syn conformers and are associated with a low TOF value, suggesting that the syn-[ $M^*(CO)_3IndRh$ ] is the worst catalyst.

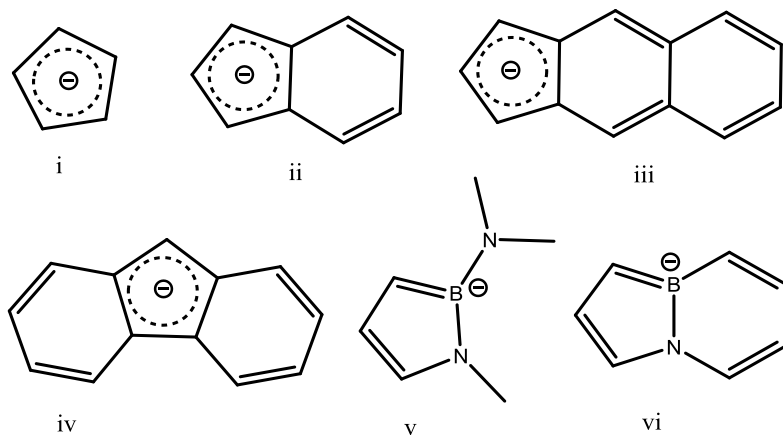


# Chapter 5

## Role of the aromatic ligands in Rh(I) Half-sandwich Catalysis: Reaction Mechanism and PESs

### 5.1. Introduction

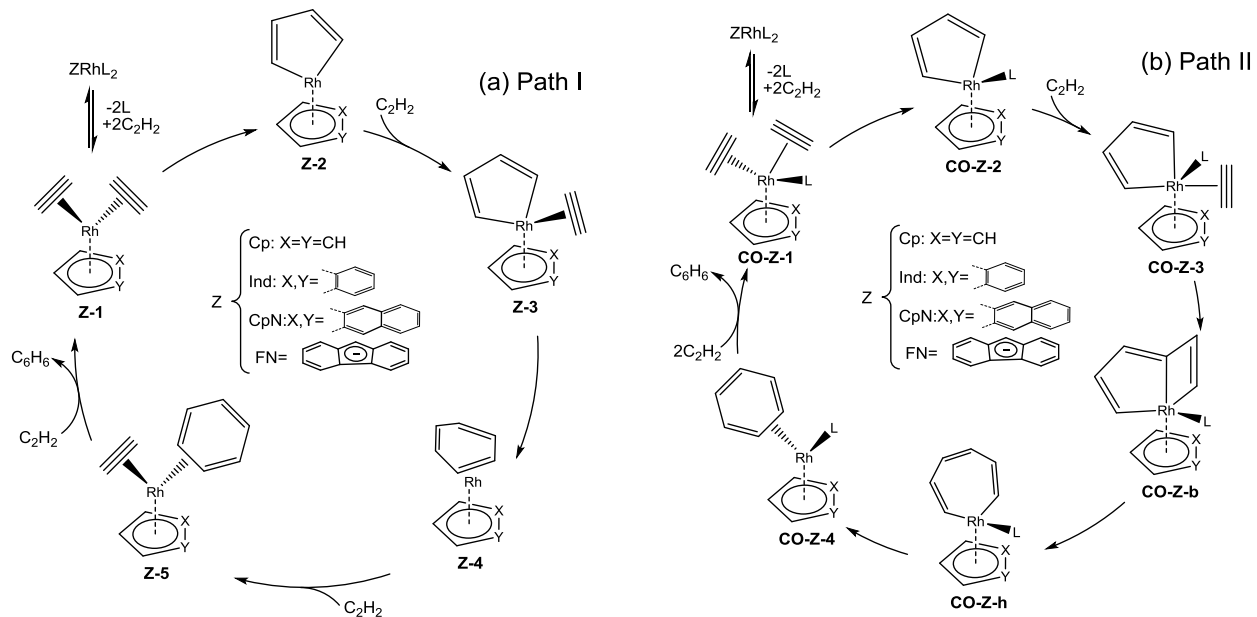
The role of the aromatic ligands ( $Cp'$ ) of the half-sandwich catalysts of general formula  $Cp'ML_n$  were investigated to gain insight on its impact on catalytic activity. Ingrosso et al. [24,25] experimentally studied the influence of the aromatic ligands ( $Cp'$ ), i.e., cyclopentadienyl ( $Cp = C_5H_5^-$ ), indenyl ( $Ind = C_9H_7^-$ ), and fluorenyl ( $FN = C_{13}H_9^-$ ) (Scheme 8) and found interesting differences in the catalytic activity toward alkyne [2+2+2] cycloadditions. Half-sandwich catalysts with heteroaromatic moieties, i.e., 1,2-azaborolyl ( $Ab$ , v) and 3a,7a-azaborindenyl ( $Abi$ , vi) (Scheme 8) were synthesized by Schmid et al. [16]. They are isoelectronic to the parent  $Cp$  and  $Ind$  anions, respectively.



**Scheme 8.** Examples of aromatic ligands ( $Cp'$ ): cyclopentadienyl (i,  $Cp$ ), indenyl (ii,  $Ind$ ), cyclopentanaphthyl (iii,  $CpN$ ), fluorenyl (iv,  $FN$ ), 1,2-azaborolyl (v,  $Ab$ ) and 3a,7a-azaborindenyl (vi,  $Abi$ ) anions.

Similarly, Booth and coworkers [26] reported that when polycyclic ligands are used in Rh(I) half-sandwich complexes, the reaction rate increases significantly. For instance, the IndRh fragment leads the reaction ten times faster than CpRh. This is ascribed to the so called *indenyl effect*, initially defined as the easier ligand substitution reactions at a metal center observed in presence of this larger aromatic ligand when compared to Cp anion. [27-28]. In the pioneering computational studies about CpRh and IndRh mediated acetylene [2+2+2] cycloaddition to benzene Orian et al. found that the less extended aromatic ligand (Cp) anion seems to be a better choice than polycyclic moieties (Ind) and surprisingly no *indenyl effect* in IndRh catalysis was found [41-42]. This observation was based on the well-known and widely accepted mechanism (Scheme 9a), proposed by Albright et al. [88,99]. However, the agreement with the experimental kinetic studies was recovered [42] when the mechanism proposed by Booth and co-workers was studied, who observed an effect on the kinetics due to the ancillary ligands and thus formulated the hypothesis that one of the ancillary ligands of the pre-catalyst might remain bonded to the metal center throughout the whole cycle [26]. This lead Orian et al. to explore *in silico* also this mechanism and indenyl effect was finally observed also *in silico* [43].

We have studied the model acetylene [2+2+2] cycloaddition to benzene mediated by Rh (I) half-sandwich catalysts with different polycyclic aromatic ligands, i.e., CpNRh and FNRh, where, ( $\text{CpN} = (\text{C}_{13}\text{H}_9)^-$ , Cyclopentanaphthyl anion, and  $\text{FN} = (\text{C}_{13}\text{H}_9)^-$ , fluorenyl anion), at ZORA-BLYP/TZ2P level of theory. CpN and FN anions have an identical molecular formula and differ in the position of the second benzene that is fused to the benzene ring of the indenyl anion in the former and to the Cp ring of indenyl anion in the latter, respectively (Scheme 8). To the best of our knowledge, the chemistry of the cyclopentanaphthyl and fluorenyl complexes of transition metals has not been explored so far as catalysts in alkyne [2+2+2] cycloadditions, this study was useful to understand the impact of larger aromatic polycyclic ligands and gain insight into the structure-activity relationship. For comparison, in this chapter, CpRh and IndRh are also included [41-42]. For consistency, we followed the same proposed mechanistic paths denoted as Path I and Path II (Scheme 9), which have been previously described in detail (Chapter 03).



**Scheme 9.** Mechanism of acetylene [2+2+2] cycloaddition to benzene catalyzed by ZM ( $Z = \text{Cp}$ , Ind, CpN, FN; M = Rh) (Path I) (a) and by CO-ZM fragments ( $Z = \text{Cp}$ , Ind, CpN, FN; L = CO) (Path II). (b).

The “coordinative flexibility” and the “metal-ligand bond” of CpN and FN were investigated. We expected enhanced coordinative flexibility of rhodium nucleus in the presence of larger and larger polycyclic ligands [18,19,28,30]. In the studied half-sandwich Rh(I) catalysts, the metal is always coordinated to the five-membered ring (Cp), but the presence of the  $\pi$ -electron clouds of the fused six-membered rings causes weakening of the bond between the Cp ring and the transition metal and leads to slippage.

## 5.2. Reaction Mechanism and PESs (Path I)

All the intermediates and transition states were successfully located on the PESs of acetylene [2+2+2] cycloaddition to benzene catalyzed by CpNRh and FN $_n$ Rh catalysts along Path I (Scheme 9a); they are displayed in Figures 23 and 24, respectively.

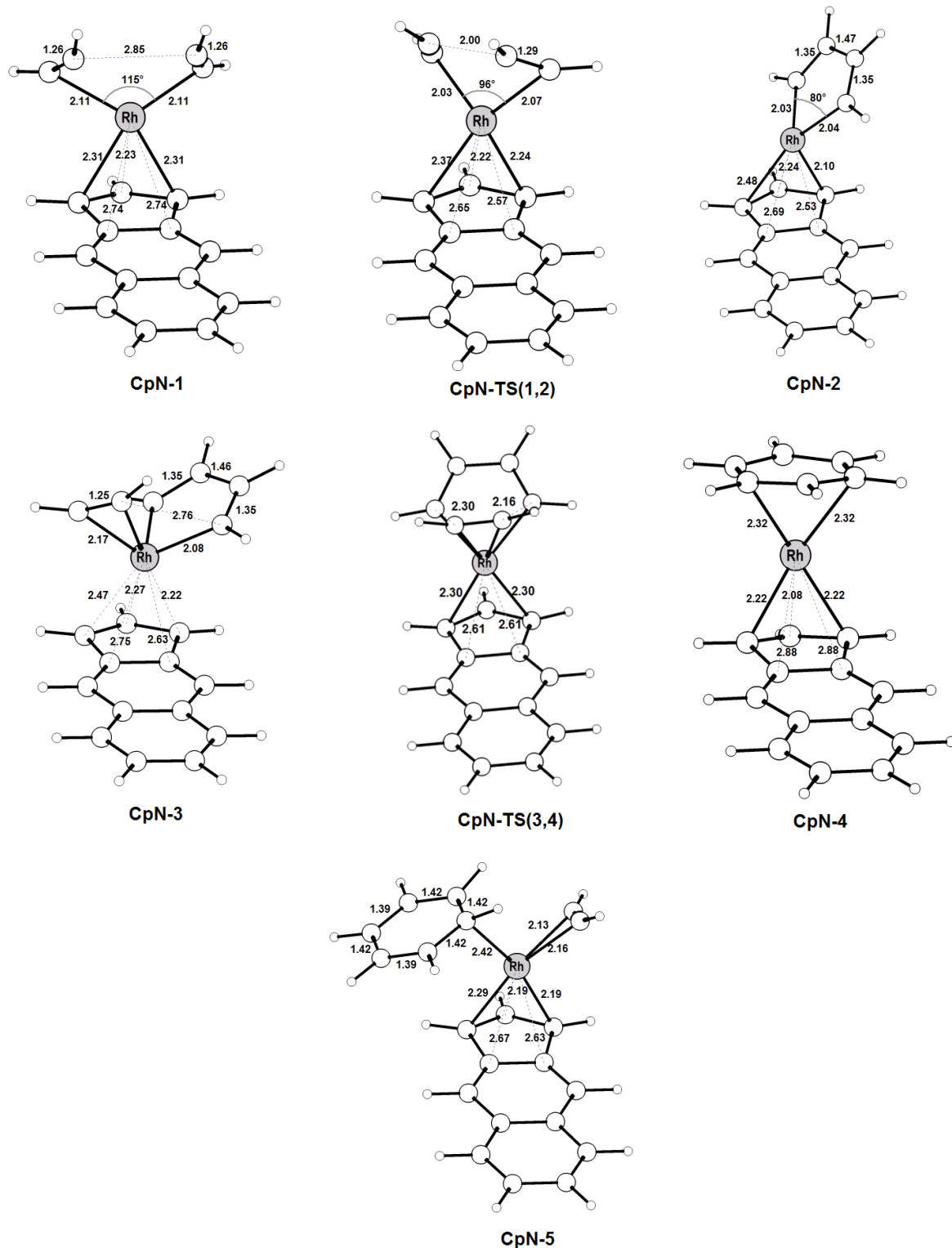


**Figure 23.** Optimized structures with selected interatomic distances ( $\text{\AA}$ ) and angles (deg) of the intermediates and transition states located on the PES of the CpNRh catalyzed acetylene [2+2+2] cycloaddition to benzene (Path I, Scheme 9a). Level of theory: ZORA-BLYP/TZ2P.

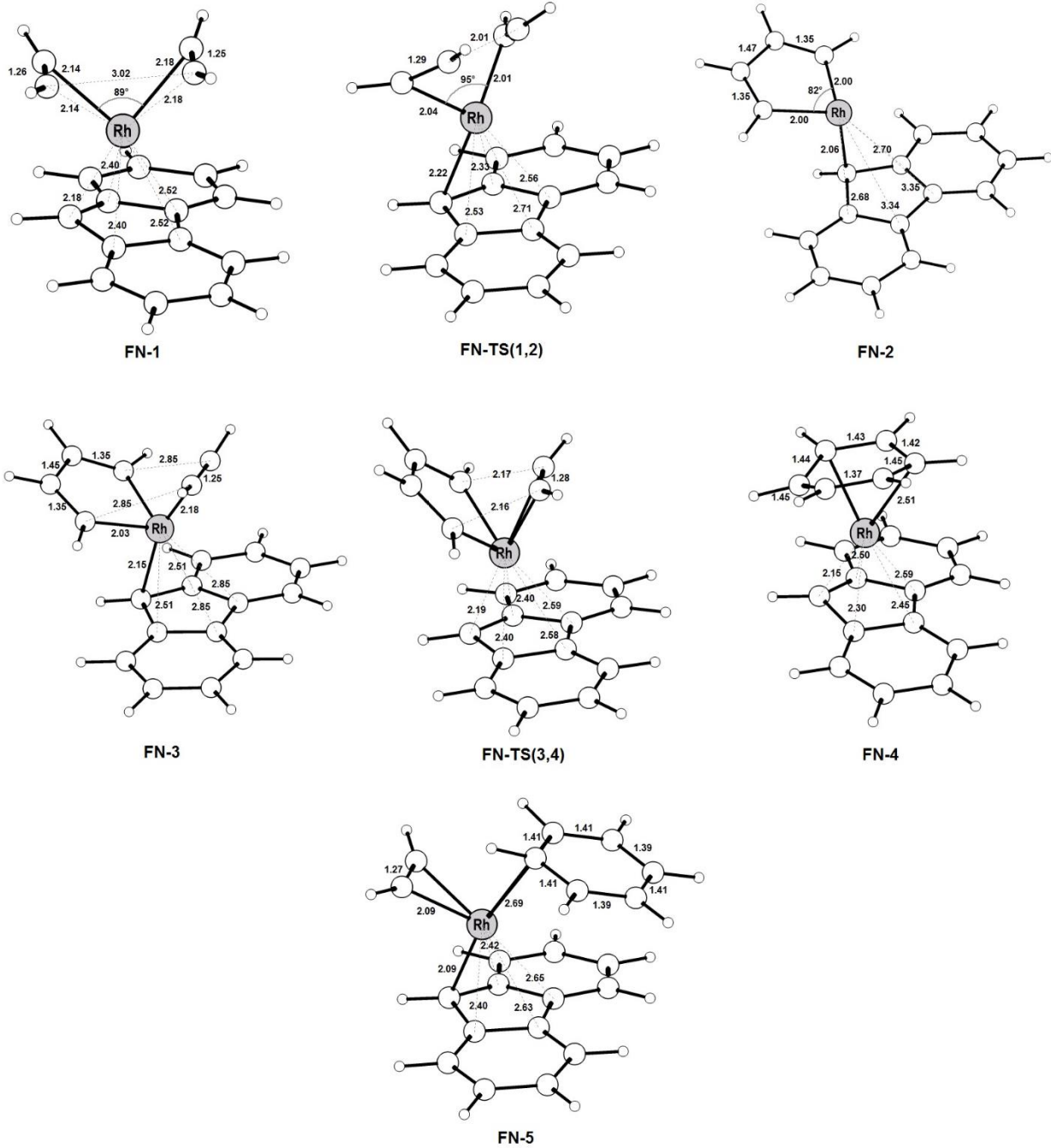


**Figure 24.** Optimized structures with selected interatomic distances ( $\text{\AA}$ ) and angles (deg) of the intermediates and transition states located on the PES of the FNRh catalyzed acetylene [2+2+2] cycloaddition to benzene (Path I, Scheme 9a). Level of theory: ZORA-BLYP/TZ2P.

The energy profiles are shown in Figure 25. At first glance, they are very similar to those computed for CpRh and IndRh catalysis. **Z-1**, by crossing an activation barrier of 16.1 and 15.7 kcal mol<sup>-1</sup> for CpNRh and FNRh, respectively, converts into the 16-electrons unsaturated rhodacyclic intermediate **Z-2**; this step is exothermic by -22.7 kcal mol<sup>-1</sup>, and -29.1 kcal mol<sup>-1</sup>, respectively. FNRh in this step is kinetically and thermodynamically more favorite than CpNRh. In contrast to our expectation, both CpNRh and FNRh show higher energy barriers than CpRh and IndRh [41-42,106], which are 12.4 kcal mol<sup>-1</sup> and 15.1 kcal mol<sup>-1</sup>, but the product formation is more exothermic (-18.2 kcal mol<sup>-1</sup> and -21.7 kcal mol<sup>-1</sup>). Thus when moving to larger polycyclic ligands the energy barriers increase indicating kinetic disadvantage; however, the thermodynamic stability of the product increases.

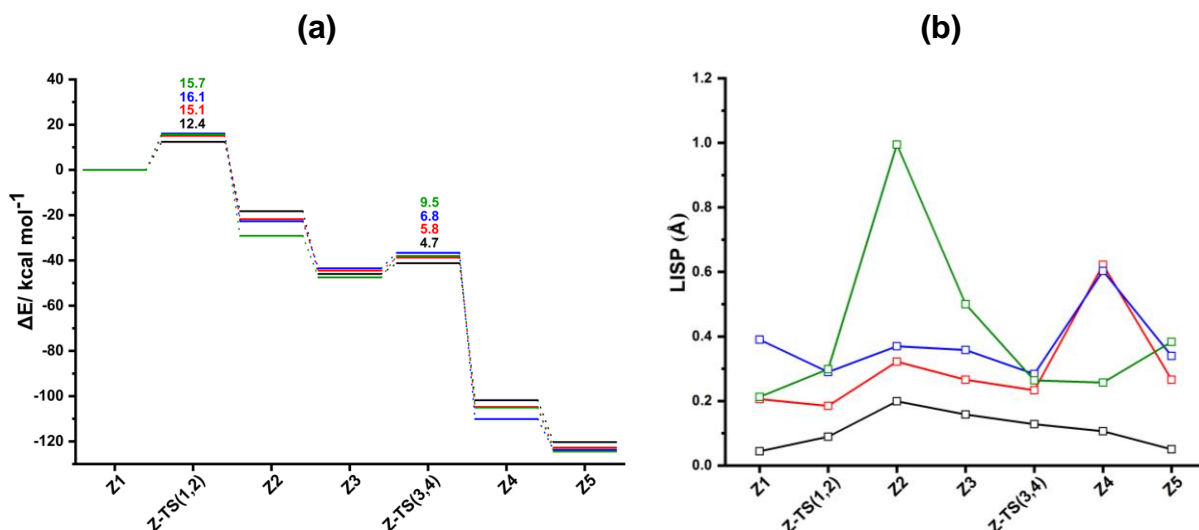


**Figure 25.** (a) Energy profiles of acetylene [2+2+2] cycloaddition to benzene catalyzed by CpRh (black), IndRh (red), CpNRh (blue) and FNRh (green) (Scheme 9a, Path I). (b) Profiles of the slippage parameter (LISP) along with the acetylene [2+2+2] cycloaddition cycles catalyzed by CpRh (black), IndRh (red), CpNRh (blue) and FNRh (green) along Path I (Scheme 9a). Level of theory: ZORA-BLYP/TZ2P.

In **CpN-1** (Figure 23), the Rh-C<sub>α</sub> and Rh-C<sub>β</sub> bond length are 2.11 Å and 2.15 Å, respectively. They are shorter than the analogous distances in **Ind-1**, which are 2.13 Å and 2.16 Å (Figure A3, Appendix). This suggests that acetylene is more tightly bonded, but Rh-Cp slippage is pronounced with LISP = 0.39 Å (Figure 25b). In **FN-1**, one acetylene is more strongly coordinated to the

rhodium center than the other one, as can be seen from the Rh-C $\alpha$  and Rh-C $\beta$  bond lengths which are 2.14 Å and 2.14 Å in the former and ~ 2.18 Å and 2.18 Å, in the latter (Figure 24). In Figure 26, the highest occupied molecular orbitals of **Cp-1**, **Ind-1**, **CpN-1**, and **FN-1** are shown. The  $\pi$ -antibonding character between Cp'- $\pi$  system (Cp' = Ind, CpN, and FN) and Rh valence  $d$  orbitals is highly pronounced in **CpN-1**, leading to much higher slippage than in the others. In **FN-1**, the two benzene rings are fused to the central Cp moiety, so that the steric hindrance is identical from both sides and the  $\pi$ -bonding character between FN- $\pi$  system and Rh valence  $d$  orbital is found to hold the metal at the center of Cp ring in **FN-1**, similarly to **Cp-1**.

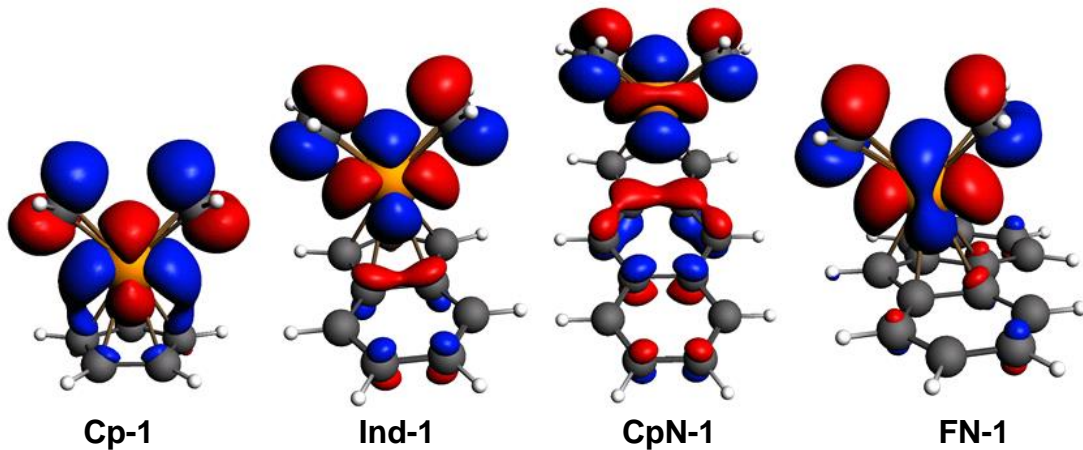


**Figure 26.** Kohn-Sham HOMOs of **Cp-1**, **Ind-1**, **CpN-1**, and **FN-1**; the level of theory: ZORA-BLYP/TZ2P. The isodensity value is 0.03.

In all cases, the C $\alpha$ -C $\beta$  and C $\beta$ -C $\beta'$  bond lengths of the rhodacycle **Z2** are very close to the ethylene double bond and  $\sigma$ -bond between two sp $^2$  carbon atoms, respectively, and this structural feature confirms the formation of rhodacyclopentadiene [37,38,49].

Figure 27 shows the overlap between Rh  $d$  orbital and Cp'- $\pi$  system which decreases in the order **Cp-2 > Ind-2 > CpN-2 > FN-2**, in opposite agreement with the trend of Rh-Cp slippage. Importantly, in **FN-2**, the anti-bonding character between Rh valence  $d$  orbitals and the Cp'- $\pi$  system is found, which leads to higher slippage and explains the big spike in the LISP profile (Figure 25b). However, Rh is less encumbered and the third acetylene coordinates easily and the

products are strongly stabilized on the PES, i.e., by  $-43.5 \text{ kcal mol}^{-1}$  and  $-47.5 \text{ kcal mol}^{-1}$ , for **CpN-2** and **FN-2**, respectively.

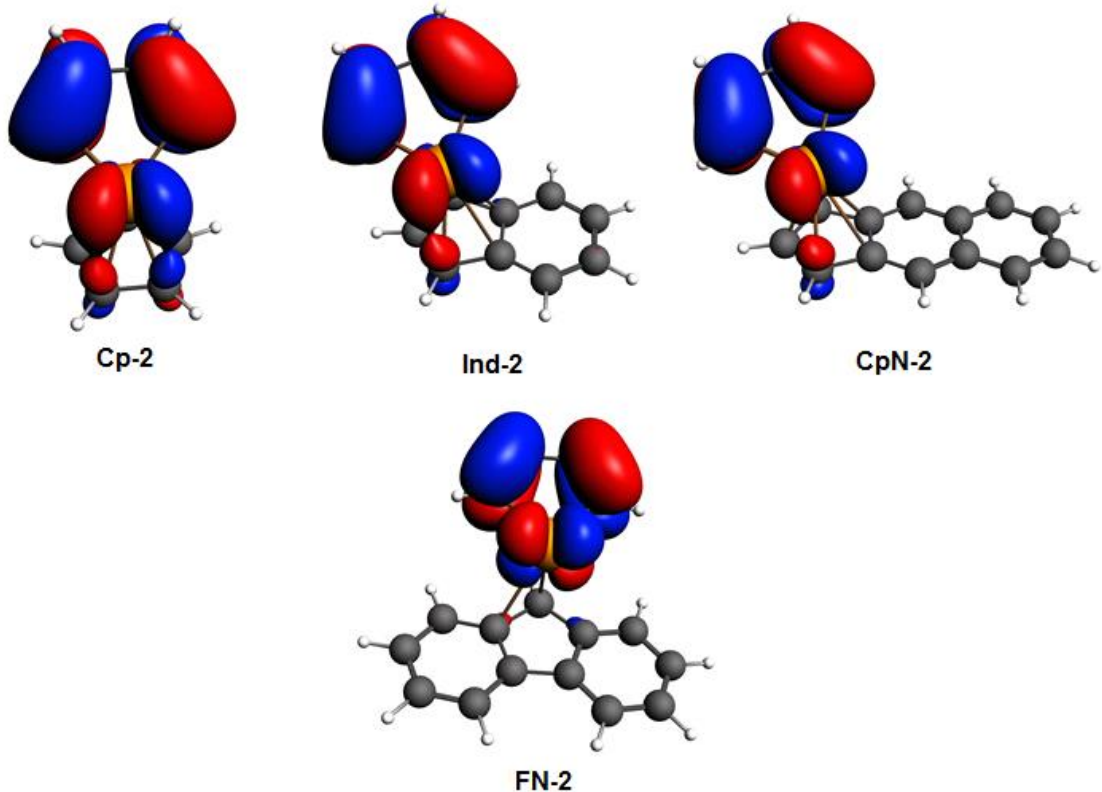


**Figure 27.** Kohn-Sham HOMOs of **Cp-2**, **Ind-2**, **CpN-2**, and **FN-2**; level of theory: ZORA-BLYP/TZ2P. The isodensity value is 0.03.

The activation strain model (ASM) was applied [83,84] to get a deeper quantitative insight into the factors ruling this oxidative coupling **Z-1 → Z-TS(1,2)**. The complexes were divided into  $\text{Cp}'\text{Rh}$  ( $\text{Cp}' = \text{CpN}$  and  $\text{FN}$ ) and the two acetylene molecules undergoing oxidative coupling (the reference energy is the sum of the energies of two isolated acetylenes). The results are shown in Table 12. For comparison, the results of  $\text{CpRh}$  and  $\text{IndRh}$  are also shown [41]. The  $\Delta\Delta E_{\text{strain}}$  contributions to the energy barrier  $\Delta E^\ddagger$  is higher for  $\text{FNRh}$  compared to  $\text{CpNRh}$ ; however,  $\Delta\Delta E_{\text{int}}$  is more stabilizing in  $\text{FNRh}$  compared to  $\text{CpNRh}$  and thus contributes to lowering the barrier.

It emerges that  $\Delta\Delta E_{\text{strain}}$  increases with increasing the size of the aromatic ligand and  $\Delta\Delta E_{\text{int}}$  also increases correspondingly, but for CpNRh the trend is inverted. This probably because of the weak coordination of Rh-Cp and antibonding character between the Cp'- $\pi$  system (Cp'= Ind, CpN, and FN) and Rh valence *d* orbitals, which is highly pronounced in **CpN-1** (Figure 26).

**Table 12.** Activation strain analysis for the first oxidative step **Z-1 → Z-TS(1,2)** (Path 1); all values are in kcal mol<sup>-1</sup>. The fragments are Cp'Rh (Cp' = Cp, Ind, CpN and FN) and two acetylene molecules.

	$\Delta\Delta E_{\text{strain}}$			$\Delta\Delta E_{\text{int}}$	$\Delta E^\ddagger$
	2(C <sub>2</sub> H <sub>2</sub> )	Cp'Rh	Total		
<b>Cp-1/Cp-TS(1,2)</b>	33.21	2.36	35.57	-23.16	12.41
<b>Ind-1/Ind-TS(1,2)</b>	37.02	2.66	39.68	-24.59	15.09
<b>CpN-1/CpN-TS(1,2)</b>	35.73	1.62	37.35	-21.25	16.10
<b>FN-1/FN-TS(1,2)</b>	37.73	2.19	39.92	-24.21	15.71

The Diels-Alder-like [4+2] addition of acetylene to the  $\pi$ -electron system of the rhodacycle **Z3** on the PESs has activation barriers of 6.8, and 9.5 kcal mol<sup>-1</sup> for CpNRh and FNRh. It is exothermic by -66.7, and -57.6 kcal mol<sup>-1</sup>, respectively. Again, both CpNRh and FNRh, show higher energy barriers than CpRh (4.7 kcal mol<sup>-1</sup>) and IndRh (5.8 kcal mol<sup>-1</sup>), while the thermodynamic stability of the product increases. Structurally, in **CpN-4** (Figure 23) we observe  $\eta^6$  coordination mode between rhodium and the six-carbon arene ring and  $\eta^3$  hapticity with the Cp ring, which is similar to what found for **Ind-4** (Figure A4, Appendix). Conversely, the coordination mode in **FN-4** (Figure 24) is  $\eta^4$  between rhodium and the arene ring and  $\eta^3 + \eta^2$  coordination is found with the Cp moiety, in agreement with the results for **Cp-4** [41,106]. The last steps along Path I reveal higher exothermicity of the product formation for those catalysts with larger aromatic ligands.

In order to quantify the Rh-Cp slippage, the LISP parameters were computed and are shown in Figure 25b. The slippage is more pronounced in FNRh and CpNRh catalysis than in CpRh and

IndRh, indicating that enhancing the aromatic character by increasing the number of aromatic benzene rings fused to the CpRh parent ligand increases the metal slippage. The higher slippage variations along the catalytic cycle are found for FNRh.

### 5.3. Alternative Mechanistic Path II

Following once again the idea proposed by Booth and co-workers that one of the ancillary ligands of the pre-catalyst remains bonded to the metal center throughout the whole cycle [24], we considered in our analysis also the alternative mechanistic Path II (Scheme 9b), keeping the ancillary ligand CO bonded to rhodium along the whole cycle [41-42]. All the intermediates and transition states were successfully located on the PESs of CpNRh(CO) and FNRh(CO) catalyzed processes and are shown in Figures 28 and 29, respectively. The energy profiles are displayed in Figure 30a.

The catalytic cycle begins with the oxidative coupling step of the two coordinated acetylene **CO-Z-1 → CO-Z-2** crossing a barrier of 14.6 kcal mol<sup>-1</sup> for CpNRh(CO) and 12.8 kcal mol<sup>-1</sup> for FNRh(CO), respectively. With FNRh(CO) the process is kinetically more favored than with CpNRh(CO) also along this mechanistic path. In analogy to what observed along Path 1, the barriers for CpNRh(CO) and FNRh(CO) are higher than those computed for IndRh(CO) (12.7 kcal mol<sup>-1</sup>) and CpRh(CO) (11.7 kcal mol<sup>-1</sup>), demonstrating that for this elementary step the presence of larger aromatic ligands is a disadvantage. Structurally, **CO-CpN-1** has LISP = 1.60 Å and **CO-FN-1** has LISP = 1.66 Å, and are both characterized by  $\eta^1$  coordination (Figure 28 and 29). The products of the oxidative coupling are 18-electrons rhodacycles, i.e., **CO-CpN-2** with LISP = 0.23 Å, and **CO-FN-2** with LISP = 0.06 Å, respectively. The electron configuration of Rh is saturated due to the presence of CO and the rhodacyle is characterized by distorted  $\eta^5$  coordination. The exothermicity is -49.2 kcal mol<sup>-1</sup> for **CO-CpN-2** and -37.5 kcal mol<sup>-1</sup> for **CO-FN-2**, which is comparatively lower than **CO-Cp-2** (-66.1 kcal mol<sup>-1</sup>) and **CO-Ind-2** (-47.5 kcal mol<sup>-1</sup>).

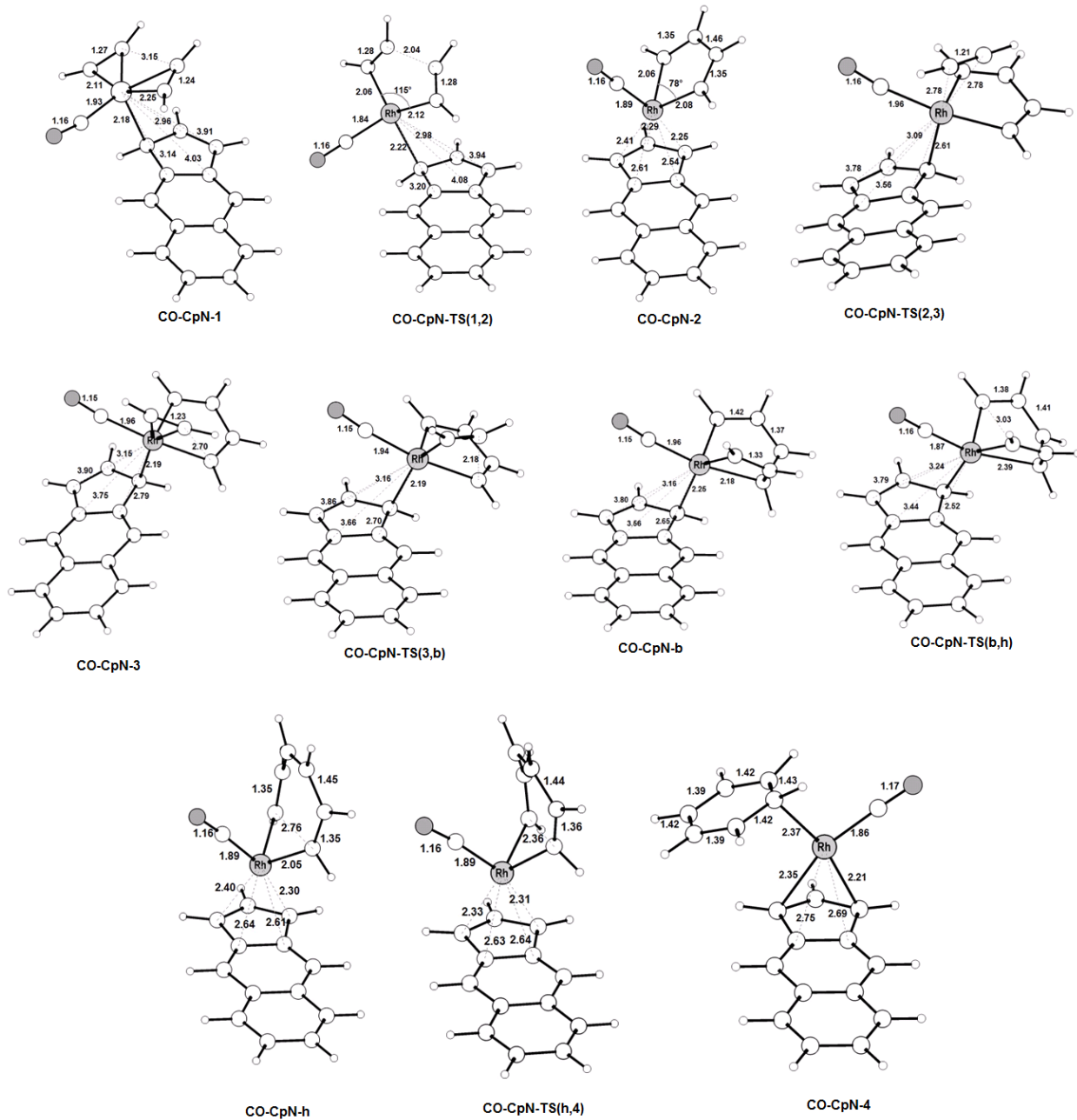


**Figure 28.** Optimized structures with selected interatomic distances ( $\text{\AA}$ ) and angles (deg) of the intermediates and transition states located on the PES of the  $\text{CpNRh}(\text{CO})$  catalyzed acetylene [2+2+2] cycloaddition to benzene (Path II, Scheme 9b). Level of theory: ZORA-BLYP/TZ2P.

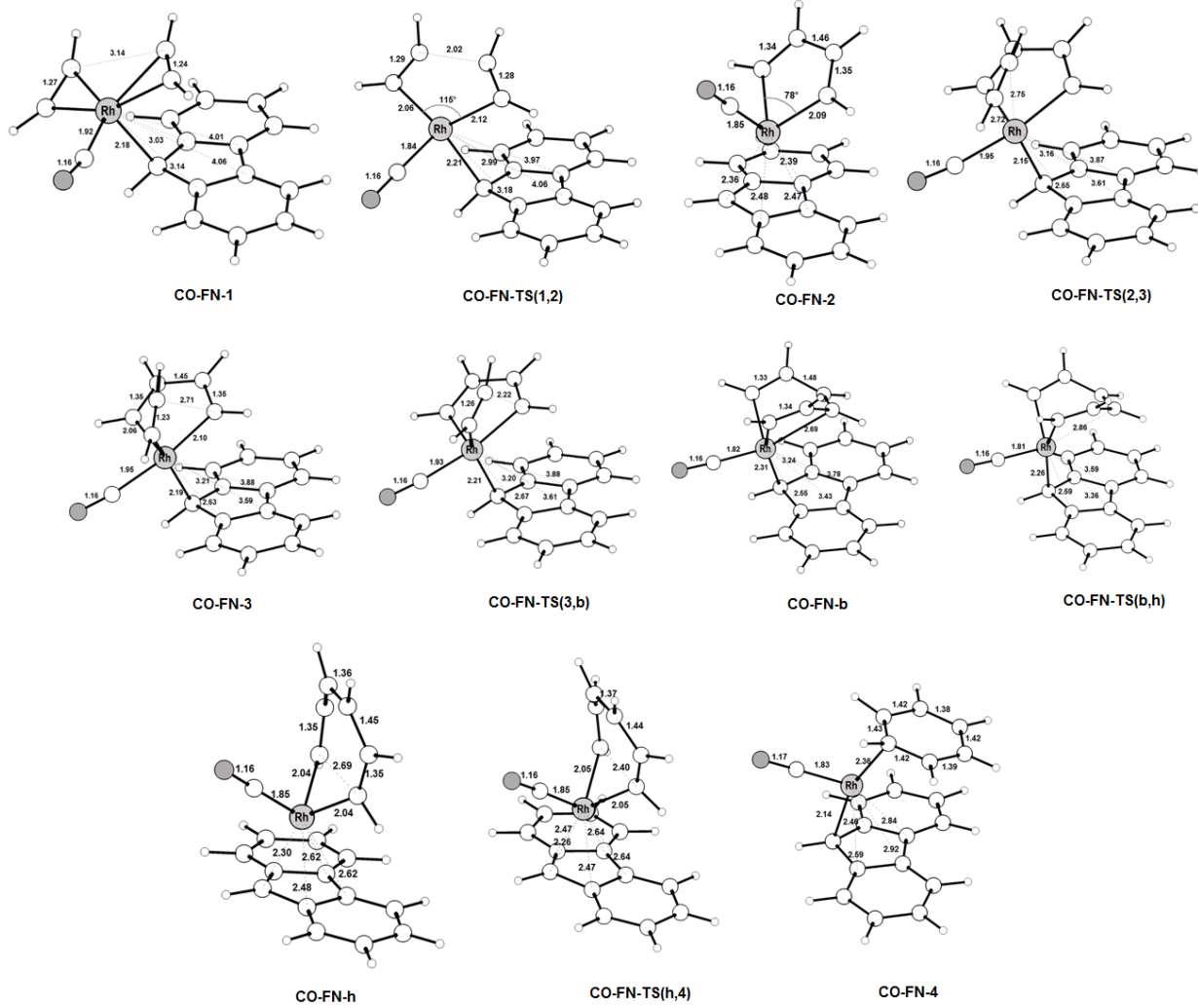


**Figure 29.** Optimized structures with selected interatomic distances ( $\text{\AA}$ ) and angles (deg) of the intermediates and transition states located on the PES of the FNRh(CO) catalyzed acetylene [2+2+2] cycloaddition to benzene (Path II, Scheme 9b). Level of theory: ZORA-BLYP/TZ2P.

The addition of the third acetylene leads to the formation of the  $\eta^1$  **CO-CpN-3** and **CO-FN-3** with an activation energy of 11.4 kcal mol<sup>-1</sup> and 4.32 kcal mol<sup>-1</sup>, respectively. This indicates that the FNRh(CO) is kinetically more favored than CpNRh(CO). For IndRh(CO) and CpRh(CO) catalysis, these barriers were estimated at 28.5 and 43.6 kcal mol<sup>-1</sup>, respectively. Notably, the catalytic barrier decreases when increasing the size of the aromatic ligand of the catalyst and the performance is FNRh(CO) > CpNRh(CO) > IndRh(CO) > CpRh(CO). Similarly to the elementary step **CO-Z2 → CO-Z-TS(2,3)** on the PESs for CpRh(CO) and IndRh(CO) catalysis which was identified as the step with the highest activation energy, and in presence of indenyl ligand the computed barrier is much smaller than in presence of the cyclopentadienyl ligand, the trend is maintained further expanding the size of the aromatic ligand, i.e., in CpNRh(CO) and FNRh(CO).

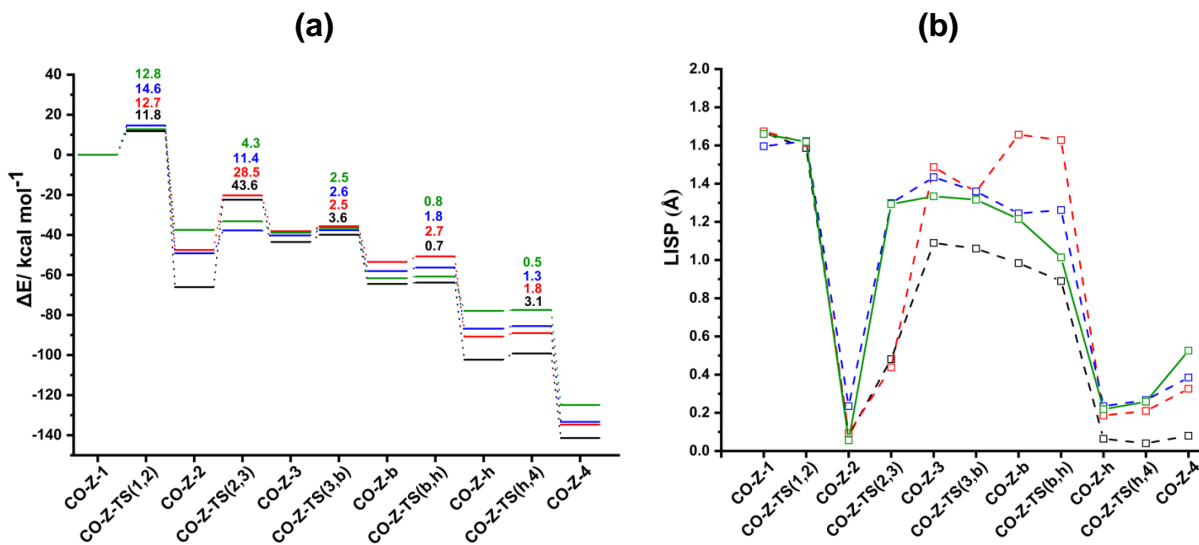


**Figure 30.** (a) Energy profiles of acetylene [2+2+2] cycloaddition to benzene catalyzed by CpRh(CO) (black), IndRh(CO) (red), CpNRh(CO) (blue) and FNRh(CO) (green) (Scheme 9b, Path II). (b) Profiles of the slippage parameter (LISP) along with the acetylene [2+2+2] cycloaddition cycles catalyzed by CpRh(CO) (black), IndRh(CO) (red), CpNRh(CO) (blue) and FNRh(CO) (green) along Path II (Scheme 9b). Level of theory: ZORA-BLYP/TZ2P.

The activation strain analysis has been performed for this elementary reaction. The natural fragments have been identified as the entering acetylene and the rhodacyle CO-Cp'Rh(C<sub>4</sub>H<sub>4</sub>) (Cp' = Cp, Ind, CpN, and FN]. The results are shown in Table 13. In all cases, the acetylene is only slightly deformed, while the rhodacyle CO-Cp'Rh(C<sub>4</sub>H<sub>4</sub>) is very much strained. The strain of this latter fragment decreases when increasing the size of the aromatic ligand; as a result, the total  $\Delta E_{\text{strain}}$  decreases according to the following trend FNRh(CO) > CpNRh(CO) > IndRh(CO) > CpRh(CO). The  $\Delta E_{\text{int}}$  generally increases for higher polycyclic ligand. The kinetic advantage of FNRh(CO) in this elementary step is due to the lower strain in the transition state.

**Table 13.** Activation strain analysis (ASA) of the transition states **CO-Z-TS(2,3)**; all values are in kcal mol<sup>-1</sup>. The fragments are CO-Cp'Rh(C<sub>4</sub>H<sub>4</sub>) (Cp' = Cp, Ind, CpN, and FN]) and acetylene.

	$\Delta E_{\text{strain}}$			$\Delta E_{\text{int}}$	$\Delta E$
	C <sub>2</sub> H <sub>2</sub>	CO-Cp'Rh(C <sub>4</sub> H <sub>4</sub> )	Total		
<b>CO-Cp-TS(2,3)</b>	0.18	43.96	44.14	-0.50	43.64
<b>CO-Ind-TS(2,3)</b>	0.06	28.83	28.89	-0.34	28.55
<b>CO-CpN-TS(2,3)</b>	0.29	18.20	18.49	-7.10	11.39
<b>CO-FN-TS(2,3)</b>	0.10	7.39	7.49	-3.17	4.32

The subsequent step is endothermic but we found that it systematically decreases in the following order **CO-Cp-3** (22.5 kcal mol<sup>-1</sup>) > **CO-Ind-3** (9.32 kcal mol<sup>-1</sup>) > **CO-CPN-3** (8.9 kcal mol<sup>-1</sup>). Interestingly in **CO-FN-3**, this step becomes exothermic by -1.41 kcal mol<sup>-1</sup>; thus, this catalyst has also a thermodynamic advantage over the others. In the subsequent step, which has an activation energy of 2.63 kcal mol<sup>-1</sup> and 2.46 kcal mol<sup>-1</sup>, rhodabicyclo[3.2.0]heptatriene **CO-Z-b** forms (Scheme 9b) accompanied by the release of 17.82 and 22.7 kcal mol<sup>-1</sup> for CpNRh(CO) and FNRh(CO) catalysis, respectively. Then breaking of the Rh-C single bond in bicyclic **CO-Z-b** readily transforms it into the 7-membered heptacyclic **CO-Z-h**, crossing a barrier of 1.8 and 0.8 kcal mol<sup>-1</sup> for CpNRh(CO) and FNRh(CO), respectively. The haptotropic shift from  $\eta^1$  to distorted  $\eta^5$  takes place with the release of 28.7 kcal mol<sup>-1</sup> for **CO-CpN-h** and 16.3 kcal mol<sup>-1</sup> for **CO-FN-h**, values which are smaller than those computed for the Cp and Ind catalysts (**CO-Ind-h** = -37.4

$\text{kcal mol}^{-1}$  and **CO-Cp-h** = -37.8  $\text{kcal mol}^{-1}$ ) [42,106]. Finally, **CO-Z-h** undergoes reductive elimination to form **CO-Z-4**, which has the required benzene product in  $\eta^2$  coordination. The activation energies are 1.3, and 0.45  $\text{kcal mol}^{-1}$  and the reaction is accompanied by the release of 47.9 and 47.0  $\text{kcal mol}^{-1}$  for CpNRh(CO) and FNRh(CO), respectively. The last two steps are clearly more favorable for FNRh(CO) catalysis as it goes smoothly to the product formation with almost negligible barriers.

By stepwise addition of two acetylene molecules to rhodium, benzene is cleaved from **CO-Z-4**, and the catalyst is ready for the next cycle. This catalytic pathway shows many similarities to Ru(II)-catalyzed acetylene [2+2+2] cycloaddition reported by Calhorda and Kirchner [38]. Like for Ru-catalyzed cyclotrimerization, we did not find an acetylene insertion or a Diels–Alder type mechanism starting from rhodacyclopentadienes (**CO-Z2**).

Summarizing, most of the steps on the PESs of Path II are kinetically as well as thermodynamically more favorable for those catalysts having larger polycyclic ligands and the order of efficiency is FNRh(CO) > CpNRh(CO) > IndRh(CO) > CpRh(CO). This indicates that the *indenyl effect* described for IndRh, is more pronounced for CpNRh and FNRh and we may define a *super indenyl effect* as long as we increase the size of the aromatic ligand of these half-sandwich Rh(I) catalytic fragments. In addition, we also found that FNRh(CO) is more efficient than CpNRh(CO) along Path I as well as Path II.

Structurally, the LISP profiles shown in Figure 30b are smoother in the presence of larger aromatic ligands.

## 5.4. Turnover Frequencies (TOFs) and Structural-Activity Relationship

As we were interested to find out a structure-activity relationship, the turn over frequencies (TOFs) have been calculated from the energy profiles of the studied catalyzed processes using the energy span model (ESM) [23,96] at the standard room temperature (298.15 K) as well as at toluene reflux temperature , i.e., 383.65 K [25,26]. The structural changes along the catalytic cycles have been quantified using the slippage span model [22]. The results are presented in Table 14. By applying the energy span model (ESM), we quantify the kinetic performance of the studied catalytic cycles. The higher the TOF value is, the higher the efficiency [47]. The TOF ratios are in the following order CpRh > IndRh > FNRh > CpNRh (Table 14), along mechanistic Path I. The results are the same as those derived by inspecting the energy profiles. The increase of the size of the aromatic ligand does not increase the catalytic efficiency if we follow Path I. This observation is in contrast to experimental kinetic studies [24-26]; however, it is consistent with previous theoretical results [41-44]. According to the slippage span model, the  $\Delta\text{LISP}^*$  computed from the LISP values of intermediate and transition states along the whole cycle, is in the following order: FNRh > IndRh > CpNRh > CpRh.

For CpRh, IndRh, and FNRh catalysts, the same trend is observed as predicted by the slippage span model, i.e., the smaller the slippage span along the catalytic cycle is, the higher the catalytic performance of the catalyst is. However, CpNRh deviates from the trend. By comparing the TOF ratios of CPNRh and FNRh, we notice that FNRh catalysis is more favored, despite the slippage variation is much larger. In all the studied catalysts, the TOF determining intermediate (TDI) is the initial bis-acetylene intermediate **Z-1** and the TOF determining transition state (TDTS) is the subsequent transition state **Z-TS(1,2)** of the oxidative coupling.

On the other hand, along Path II, the catalytic efficiency based on the TOF ratios follows the trend FNRh > CpNRh > IndRh > CpRh (Table 14). This means that the agreement with the experimental kinetic studies is well recovered along Path II. In addition, the  $\Delta\text{LISP}^*$  is in the following order CpRh > IndRh > FNRh > CpNRh. This further validates the predictions of the slippage span model. Along Path II, differently from CpRh(CO) and IndRh(CO) catalysis [42,101], for CpNRh(CO) and FNRh(CO), the TOF determining intermediate (TDI) is the initial

bis-acetylene intermediate **CO-Z-1** and the TOF determining transition state (TDTS) is the subsequent transition state **CO-Z-TS(1,2)** as in Path I.

**Table 14.** Calculated TOF (time<sup>-1</sup>) and slippage span  $\Delta LISP^*$  (Å) for acetylene [2+2+2] cycloaddition to benzene.

Catalysts	TOF <sub>298.15 K</sub> (s <sup>-1</sup> )	Ratio <sub>298.15 K</sub>	TOF <sub>383.65 K</sub> (s <sup>-1</sup> )	Ratio <sub>383.65 K</sub>	$\Delta LISP^*$
<i>Path I</i>					
<b>CpRh</b>	$4.83 \times 10^{03}$	$5.01 \times 10^{02}$	$6.66 \times 10^{05}$	$1.25 \times 10^{02}$	0.85
<b>IndRh</b>	$5.23 \times 10^{01}$	5.42	$2.00 \times 10^{04}$	3.76	1.75
<b>CpNRh</b>	9.65	1	$5.32 \times 10^{03}$	1	1.42
<b>FNRh</b>	$1.87 \times 10^{01}$	1.94	$8.87 \times 10^{03}$	1.67	3.25
<i>Path II</i>					
<b>CpRh(CO)</b>	$6.10 \times 10^{-20}$	1	$1.07 \times 10^{-12}$	1	15.59
<b>IndRh(CO)</b>	$6.41 \times 10^{-08}$	$1.05 \times 10^{12}$	$2.35 \times 10^{-03}$	$2.20 \times 10^{09}$	14.11
<b>CpNRh(CO)</b>	$1.16 \times 10^{02}$	$1.90 \times 10^{21}$	$3.66 \times 10^{04}$	$3.42 \times 10^{16}$	11.88
<b>FNRh(CO)</b>	$2.63 \times 10^{02}$	$4.31 \times 10^{21}$	$4.15 \times 10^{05}$	$3.88 \times 10^{17}$	13.19

## 5.5. Conclusions

DFT calculations have been used to investigate the acetylene [2+2+2] cycloaddition to benzene mediated by CpNRh and FNRh with the ambition of understanding the role of the aromatic ligand. For comparative analysis, the parent systems CpRh and IndRh were also included. Through a detailed exploration of the potential energy surfaces (PESs), the intermediates and transition states were located following two mechanistic paths, i.e., Path I and II (Scheme 9b). By applying the energy span model (ESM) we quantified the kinetic performance of the catalytic cycles. The calculated TOF ratios follow this order of catalytic efficiency: CpRh > IndRh > FNRh > CpNRh along Path I. This suggests that increasing the size of the aromatic ligand by increasing the number of benzene rings fused to the parent CpRh moiety worsens efficiency. Reverse *indenyl effect* was thus noted, which is consistent with previous theoretical results and in contrast to experimental

evidence. The structure-reactivity relation was also drawn and, according to the slippage span model, which predicts that the lower the slippage variations along the catalytic cycle are, the higher the catalytic efficiency is. The computed  $\Delta$ LISP\* parameters are in the following order FNRh > IndRh > CpNRh > CpRh.

Conversely, following Path II, the agreement with the experimental observation is recovered and catalysts with larger polycyclic moieties have higher efficiency. Combining the information from the energy profiles and TOF ratios this trend of catalytic efficiency is established: FNRh > CpNRh > IndRh > CpRh. The  $\Delta$ LISP\* parameters increase in following order CpRh < IndRh < FNRh < CpNRh. By relating the above described trends, we come to the conclusion that the lower the slippage span along the catalytic cycle is, the higher the catalytic efficiency is. The FNRh is the most efficient catalyst along Path I as well as Path II.

# Chapter 6

## 6.1. Summary and Concluding remarks

Metal-catalyzed alkyne [2+2+2] cycloadditions provide a variety of substantial aromatic compounds of interest in the chemical and pharmaceutical industries. As explained in the introduction about alkyne [2+2+2] cycloadditions, among the different catalysts that can be employed, the role of group 9 metal half-sandwich complexes is largely recognized by numerous experimental and theoretical studies (Chapter 1). Descriptors that can measure the drifting of the metal form the centroid of Cp in half-sandwich complexes along the catalytic cycle and the link between this structural change with the activity (TOF) of the catalyst (structural-activity relationship) have been designed in this thesis. Relativistic density functional theory (DFT) methods have been employed to obtain structural, energy and mechanistic information (Chapter 2). The implementation of quantitative models to analyze chemical bonding (activation strain model and energy decomposition analysis) allowed us to get a deeper insight into the factors ruling energy barriers.

The main objectives of the STREGA (**Filling the Structure-Reactivity Gap: *in silico* approaches to rationalize the design of molecular catalysts**) project were to outline the essential electronic and structural features of half-sandwich metal complexes as catalysts for alkyne [2+2+2] cycloadditions and to assess the role of a second metal which is not directly involved in the process. Particularly, the metals of group 6 have been considered, coordinated to different polycyclic aromatic ligands and different mechanistic paths have been investigated. All these aspects have been tackled in Chapters 3, 4, and 5.

In Chapter 3, we have studied *in silico* the mechanistic aspects of the archetypal acetylene [2+2+2] cycloaddition to benzene mediated by heterobimetallic half-sandwich catalysts  $[\text{Cr}(\text{CO})_3\text{Ind}\text{Rh}]$  ( $\text{Ind}=(\text{C}_9\text{H}_7)^-$ , indenyl anion). Since the coordination of the second metal group, i.e.,  $\text{Cr}(\text{CO})_3$ , to the benzene moiety of the indenyl ligand may occur in syn or in anti conformation, both cases have been considered. Through a detailed exploration of the potential energy surfaces (PESs), the intermediates and transition states were located using density functional theory (DFT) methods along two mechanistic paths, i.e., Path I and II (Scheme 6a,b). The anti or syn coordination of

$\text{Cr}(\text{CO})_3$  affects not only the energetics of the cycle but also the mechanism. The reaction energies and barriers, the turn over frequency (TOF) and the variations of the slippage parameter along the catalytic cycles were discussed including in the analysis, for comparison, the monometallic parent systems, i.e.,  $\text{CpRh}$  ( $\text{Cp} = (\text{C}_5\text{H}_5)^-$ , cyclopentadienyl anion) and  $\text{IndRh}$ .

These are the major outcomes:

- Along Path I, the trend of the slippage parameter  $\Delta\text{LISP}^*$  is  $\text{anti-Cr@IndRh} > \text{IndRh} > \text{CpRh}$ ; in contrast, TOF values follow the opposite order, i.e.,  $\text{CpRh} > \text{IndRh} > \text{anti-Cr@IndRh}$ . This indicates that the larger the slippage variation along the catalytic cycle is, the lower the catalytic performance is. In addition, this does not explain the experimentally observed highest catalytic efficiency of the bimetallic Rh/Cr compound (*extra-indenyl effect*).
- Conversely, if we follow the catalytic cycle along Path II, a dramatic TOF enhancement for the bimetallic system  $\text{anti-Cr@IndRh}(\text{CO})$  is found compared to the parent  $\text{CpRh}(\text{CO})$  and  $\text{IndRh}(\text{CO})$ . On the basis of the TOF, the following trend of catalytic efficiency can be established  $\text{anti-Cr@IndRh}(\text{CO}) > \text{IndRh}(\text{CO}) > \text{CpRh}(\text{CO})$ , in agreement with the experimental findings. In this case, the trend of the slippage parameter is inverted, too, i.e.,  $\text{CpRh}(\text{CO}) > \text{IndRh}(\text{CO}) > \text{anti-Cr@IndRh}(\text{CO})$ , which leads us to conclude that the lower the slippage span is, the higher the catalytic efficiency is. We can thus assess that the coordination of  $\text{Cr}(\text{CO})_3$  in the bimetallic indenyl catalyst improves the catalytic efficiency along Path II.
- The hapticity variations of the intermediates and transition states along the catalytic cycle are highly pronounced in the syn bimetallic conformer, implying low TOF values and so we concluded, in agreement with the experimental works, that the syn-[ $\text{Cr}(\text{CO})_3\text{IndRh}$ ] catalyzed process is not favored.

Once rationalized the structural and mechanistic aspects of the bimetallic  $[\text{Cr}(\text{CO})_3\text{IndRh}]$  catalyst on the basis of the available experimental results, we were interested to see the influence of second metal ( $M^*$ ) in bimetallic catalysis by moving downward along group 6, and this was done in Chapter 4. We have studied *in silico* the mechanistic aspects of the simple acetylene [2+2+2] cycloaddition to benzene catalyzed by heterobimetallic half-sandwich complexes of general

formula  $[M^*(CO)_3IndRh]$  ( $M^* = Cr, Mo, W$ ). The same two proposed mechanistic paths, i.e., Path I and II, were investigated. The reaction energies and barriers, the turn over frequency (TOF) and the slippage parameters of the complete catalytic cycles have been rationalized. The computed electronic energy profiles of the studied bimetallic catalysts, i.e.,  $[M^*(CO)_3IndRh]$  ( $M^* = Cr, Mo, W$ ) are in all cases quite similar, displaying variations within 1 kcal mol<sup>-1</sup> along the cycle. However, taking into account these small energy differences, we concluded that;

- When going from Cr to Mo and W, the corresponding activation barriers decrease along Path I. The computed TOF ratios are in the following order: anti-Mo@IndRh > anti-W@IndRh > anti-Cr@IndRh, suggesting that the presence of Mo leads to catalytic enhanced performance. The relation between the structure and the reactivity of the studied catalysts has been finally examined through the slippage span model, which confirmed that the lower the  $\Delta LISP^*$  value is, the better the performance in terms of TOF is.
- Along Path II, the TOF ratios are in the following order: anti-Cr@IndRh > anti-W@IndRh > anti-Mo@IndRh and the trend is opposite to mechanistic Path I. However, the relationship of catalytic efficiency and slippage span remains consistent with the prediction of the slippage span model.
- The bimetallic  $[M^*(CO)_3IndRh]$  ( $M^* = Cr, Mo, W$ ) catalysts display higher catalytic efficiency than the monometallic catalysts (CpRh and IndRh), and we came to the conclusion that the presence of the second metal favors the catalysis. The hapticity variations of the intermediates and the transition states along the catalytic cycle are highly pronounced in the syn conformers and are associated with a low TOF value, suggesting that the syn-[ $M^*(CO)_3IndRh$ ] are the worst catalysts.

Any structural and electronic modification can influence the efficiency of the half-sandwich catalyst. The effect of using different aromatic ligands has been explored and described in Chapter 5, which deals with the mechanistic aspects of the acetylene [2+2+2] cycloaddition mediated by monometallic catalysts having different polycyclic aromatic ligands, i.e., CpNRh and FNRh, where (CpN =  $(C_{13}H_9)^-$ , CyclopentaNaphthyl anion and FN =  $(C_{13}H_9)^-$ , Fluorenyl anion). For comparison, the parent systems CpRh and IndRh were also included. Through a detailed exploration of the potential energy surfaces (PESs), the intermediates and transition states were located following two mechanistic paths, i.e., Path I and II. By applying the energy span model

(ESM), we quantified the kinetic performance of the catalytic cycles and we could draw these conclusions.

- The calculated TOF ratios follow this order of catalytic efficiency: CpRh > IndRh > FNRh > CpNRh along Path I. This suggests that increasing the size of the aromatic ligand by increasing the number of benzene rings fused to the parent CpRh moiety lowers efficiency. Reverse *indenyl effect* was thus noted, which is consistent with previous theoretical results but in contrast to experimental evidence. The structure-reactivity relation is in agreement with the slippage span model, which predicts that the lower the slippage variations along the catalytic cycle are, the higher the catalytic efficiency is. The computed  $\Delta\text{LISP}^*$  parameters are in the following order FNRh > IndRh > CpNRh > CpRh.
- Conversely, following Path II, the agreement with the experimental observation is recovered and catalysts with larger polycyclic moieties appear to have higher efficiency. Combining the information from the energy profiles and the TOF ratios, this trend of catalytic efficiency is established: FNRh > CpNRh > IndRh > CpRh. The  $\Delta\text{LISP}^*$  parameters increase in following order CpRh < IndRh < FNRh < CpNRh.
- FNRh is the most efficient catalyst along Path I as well as Path II.

By relating the above described trends, we assessed that “the lower the slippage span along the catalytic cycle is, the higher the catalytic efficiency is” which is the essence of the slippage span model that has been validated also for polynuclear systems and with aromatic ligands larger than Cp and Ind. The obtainment of a relation of general validity like the slippage span model, which combines structural and energy features of a catalytic cycle with the catalyst’s performance in terms of TOF is undoubtedly a sound achievement and was the main goal of the STREGA project (**Filling the Structure-Reactivity Gap: *in silico* approaches to rationalize the design of molecular catalysts**).

Future perspectives will deal with changing the catalytic center, i.e., moving to cobalt, which is more used than rhodium and will require the study of catalytic paths in different electronic states, because, differently from rhodium and iridium, some intermediates in CpCo catalyzed alkyne [2+2+2] cycloadditions are more stable in the triplet state.

# Appendix A

## Associated to Chapter 3

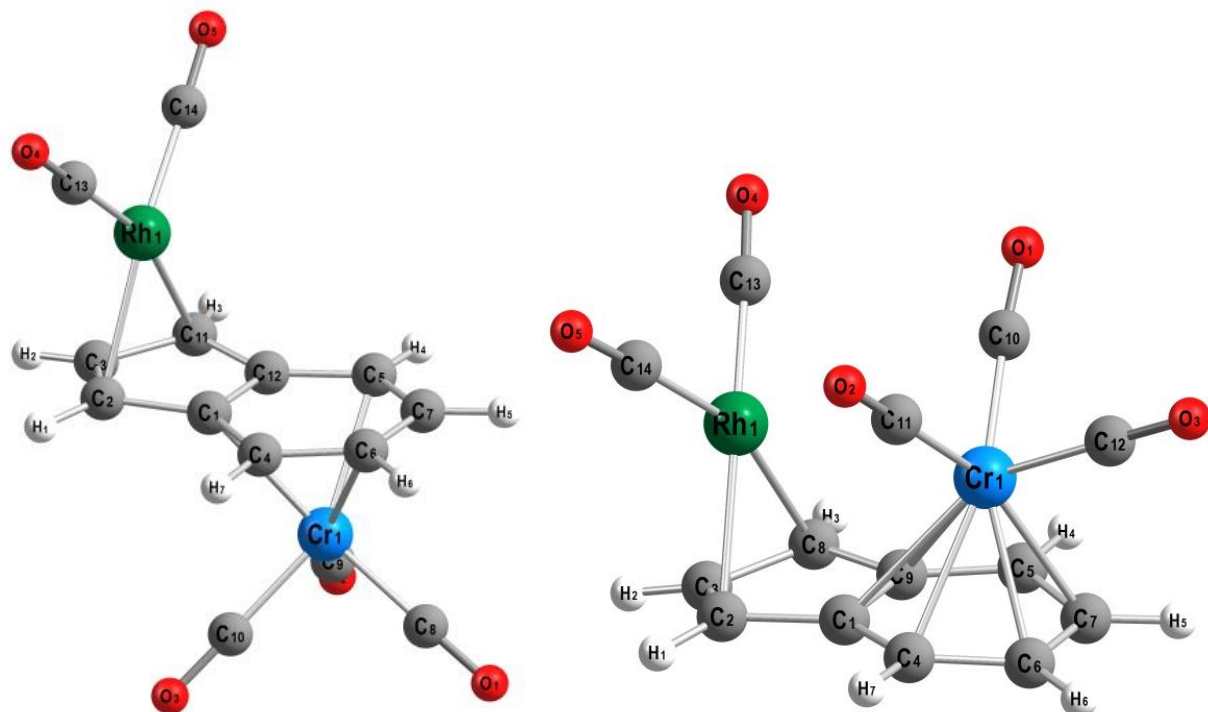


**Figure A1.** A representative optimized geometries of the bimetallic catalysts anti- and syn-[Cr(CO)<sub>3</sub>IndRh].

**Table A1.** Selected geometrical parameters of the optimized bimetallic catalyst anti- and syn-[Cr(CO)<sub>3</sub>IndRh]L<sub>2</sub>, where L=CO at ZORA-BLYP/TZ2P level of theory. The little difference between computational and reported experimental X-ray crystallographic structures is because we have carried out calculations in the gas phase.

anti-[Cr(CO) <sub>3</sub> IndRh]L <sub>2</sub>			syn-[Cr(CO) <sub>3</sub> IndRh]L <sub>2</sub>		
Bond distances (Å)	Calculated	Exp [33,34]	Bond distances (Å)	Calculated	Exp [101]
Cr1-C12	2.36	2.28	Cr1-C9	2.49	2.37
Cr1-C5	2.29	2.25	Cr1-C5	2.30	2.24
Cr1-C7	2.26	2.23	Cr1-C7	2.24	2.18
Cr1-C6	2.26	2.22	Cr1-C6	2.24	2.19
Cr1-C4	2.29	2.23	Cr1-C4	2.31	2.25
Cr1-C1	2.36	2.26	Cr1-C1	2.48	2.40
Rh1-C11	2.30	2.21	Rh1-C2	2.28	2.20
Rh1-C3	2.26	2.23	Rh1-C3	2.21	2.19
Rh1-C2	2.30	2.23	Rh1-C8	2.29	2.25
Rh1-C1	2.62	2.41	Rh1-C9	2.69	2.58
Rh1-C12	2.62	2.45	Rh1-C1	2.69	2.54
Rh1-C13	1.89	1.85	Rh1-C13	1.89	1.87
Rh1-C14	1.89	1.86	Rh1-C14	1.89	1.88
Cr1-Rh1	4.77	4.47	Cr1-Rh1	3.30	3.08
Bond angles (°)			Bond angles (°)		
C8-Cr-C9	89.2	55.3	C12-Cr-C11	86.4	85.7
C10-Cr-C11	89.1	90.3	C10-Cr-C11	93.5	95.5
Cr1-C9-O2	179.0	177.1	Cr1-C10-O1	176.3	175.3
Cr1-C8-O1	179.1	178.3	Cr1-C12-O3	179.4	177.9
Cr1-C10-O3	179.1	179.2	Cr1-C11-O2	176.3	178.5
Rh1-C14-O5	178.4	172.5	Rh1-C13-O4	177.0	177.3
Rh1-C13-O4	178.4	177.3	Rh1-C14-O5	177.1	176.7
Parameters			Parameters		
ΔRh (Å) <sup>a</sup>	0.32	0.20	ΔRh (Å)	0.40	0.34
ΔCr (Å)	0.07	0.04	ΔCr (Å)	0.18	0.14
HA <sub>Rh</sub> (°) <sup>b</sup>	11.7	11	HA <sub>Rh</sub> (°)	13.7	11.8

<sup>a</sup>Δ indicates Basolo slippage parameter; [Eq. (3.1)]. <sup>b</sup> HA indicates the hinge angle = The angle between planes C1, C2, C3, and C3, C4, C5, C1.

**Table A2.** Cartesian coordinates (in Å) and ADF total energies (in kcal mol<sup>-1</sup>) of all stationary points as well as imaginary frequencies of transition states (in cm<sup>-1</sup>) along the Path I catalyzed by anti-[Cr(CO)<sub>3</sub>IndRh], computed at ZORA-BLYP/TZ2P. For CpRh and IndRh the coordinates have been grabbed from reported literature;

a) L. Orian, J. N. P Van Stralen, F. M. Bickelhaupt, *Organometallics* **2007**, *26*, 3816–3830; (b) L. Orian, L. P. Wolters, F. M. Bickelhaupt, *Chem. Eur. J.* **2013**, *19*, 13337–13347; (c) L. Orian, M. Swart, F. M. Bickelhaupt, *ChemPhysChem.* **2014**, *15*, 219–228.

### anti-Cr@Ind-1

$$E = -4709.12 \text{ kcal mol}^{-1}$$

C	-0.101707000000	0.073784000000	-0.721569000000
C	0.743258000000	-1.039092000000	-1.147626000000
C	1.099656000000	-1.807171000000	0.000589000000
Rh	2.532252000000	-0.082372000000	-0.000083000000
C	3.728037000000	0.983902000000	1.415549000000
C	3.681517000000	-0.225772000000	1.760419000000
C	3.676770000000	-0.216730000000	-1.764676000000
C	3.727916000000	0.990146000000	-1.410829000000
H	0.866851000000	-1.354711000000	-2.176823000000
H	1.543532000000	-2.794612000000	0.000956000000
H	0.867504000000	-1.352693000000	2.177702000000
H	4.110774000000	1.994387000000	-1.467010000000
H	3.874365000000	-1.041886000000	-2.428156000000
H	3.883274000000	-1.055290000000	2.417196000000
H	4.107661000000	1.988970000000	1.478591000000
C	-0.827149000000	1.070455000000	-1.436254000000
C	-0.827159000000	1.071541000000	1.435379000000
C	-1.475332000000	2.097669000000	-0.715037000000
C	-1.475282000000	2.098259000000	0.713405000000
H	-0.864402000000	1.058762000000	2.520480000000
H	-2.019138000000	2.870670000000	1.247653000000
H	-2.019209000000	2.869659000000	-1.249875000000
H	-0.864390000000	1.056861000000	-2.521345000000
C	-4.068369000000	0.847777000000	-0.001112000000
C	-2.886023000000	-1.065206000000	1.305977000000

C	-2.885290000000	-1.067421000000	-1.304318000000
O	-5.141555000000	1.310626000000	-0.001763000000
O	-3.199349000000	-1.824952000000	2.136056000000
O	-3.198135000000	-1.828591000000	-2.133277000000
Cr	-2.361194000000	0.144358000000	-0.000048000000
C	0.743405000000	-1.038088000000	1.148249000000
C	-0.101691000000	0.074314000000	0.721470000000

### anti-Cr@Ind-TS(1,2)

$$E = -4693.61 \text{ kcal mol}^{-1} \quad -447.22 \text{ cm}^{-1}$$

C	-0.034123000000	-0.084252000000	-0.731582000000
C	0.731432000000	-1.229137000000	-1.158685000000
C	1.128239000000	-1.965074000000	0.001888000000
Rh	2.415212000000	-0.115669000000	0.000039000000
C	3.827353000000	1.239244000000	0.960971000000
C	3.797586000000	0.066662000000	1.503036000000
C	3.796301000000	0.066774000000	-1.504185000000
C	3.826622000000	1.239275000000	-0.961984000000
H	0.875619000000	-1.542042000000	-2.185214000000
H	1.612963000000	-2.933176000000	0.002739000000
H	0.875852000000	-1.537903000000	2.188262000000
H	3.905482000000	2.287302000000	-1.224960000000
H	4.123449000000	-0.558402000000	-2.319691000000
H	4.125339000000	-0.558767000000	2.318103000000
H	3.906578000000	2.287223000000	1.224017000000
C	-0.748844000000	0.938096000000	-1.439595000000
C	-0.748976000000	0.940566000000	1.438223000000

C	-1.318029000000	2.006443000000	-0.716972000000	H	-0.560012000000	0.425364000000	2.538452000000
C	-1.318128000000	2.007640000000	0.713699000000	H	-1.900479000000	2.462925000000	1.970731000000
H	-0.798929000000	0.925827000000	2.522611000000	H	-2.304287000000	3.073271000000	-0.412109000000
H	-1.820762000000	2.810133000000	1.244215000000	H	-1.305874000000	1.745430000000	-2.274988000000
H	-1.820592000000	2.808037000000	-1.248909000000	C	-4.121617000000	0.751249000000	-0.007294000000
H	-0.798622000000	0.921540000000	-2.523968000000	C	-2.973209000000	-1.029848000000	1.473954000000
C	-3.988489000000	0.938639000000	-0.000367000000	C	-2.816274000000	-1.196732000000	-1.135220000000
C	-2.944874000000	-1.036941000000	1.316246000000	O	-5.206928000000	1.171592000000	-0.084842000000
C	-2.945249000000	-1.038181000000	-1.315191000000	O	-3.332209000000	-1.736810000000	2.328130000000
O	-5.033343000000	1.465997000000	-0.000577000000	O	-3.073496000000	-2.011990000000	-1.926643000000
O	-3.314378000000	-1.765237000000	2.151090000000	Cr	-2.389899000000	0.109631000000	0.123301000000
O	-3.315028000000	-1.767230000000	-2.149292000000	C	0.869124000000	-1.148547000000	0.457865000000
Cr	-2.337068000000	0.127972000000	-0.000119000000	C	-0.069539000000	-0.024453000000	0.458634000000
C	0.731423000000	-1.227045000000	1.161146000000				
C	-0.034170000000	-0.082987000000	0.732034000000				

### anti-Cr@Ind-3

$$E = -5261.28 \text{ kcal mol}^{-1}$$

### anti-Cr@Ind-2

$$E = -4729.74 \text{ kcal mol}^{-1}$$

C	-0.290362000000	0.351703000000	-0.930641000000	C	0.266751000000	-0.070985000000	-0.544934000000
C	0.461053000000	-0.579892000000	-1.767746000000	C	-0.408205000000	1.129369000000	-1.019786000000
C	1.061448000000	-1.536593000000	-0.940686000000	C	-0.580979000000	1.998548000000	0.116552000000
Rh	2.347025000000	0.155601000000	-0.293146000000	Rh	-2.173808000000	0.347871000000	0.096461000000
C	4.669724000000	0.302140000000	1.408725000000	C	-4.379247000000	1.415040000000	-1.433855000000
C	3.397631000000	0.749223000000	1.355879000000	C	-3.599020000000	1.715384000000	-0.375635000000
C	4.064762000000	-0.884382000000	-0.568517000000	C	-3.068320000000	-0.549221000000	-1.534014000000
C	5.043531000000	-0.616256000000	0.317170000000	C	-4.079013000000	0.152113000000	-2.090107000000
H	0.461280000000	-0.579392000000	-2.850834000000	H	-0.519070000000	1.418833000000	-2.056739000000
H	1.580770000000	-2.428721000000	-1.268173000000	H	-0.947329000000	3.016275000000	0.071006000000
H	1.084866000000	-1.773018000000	1.317029000000	H	-0.241159000000	1.699754000000	2.297343000000
H	6.047551000000	-1.038499000000	0.231797000000	H	-4.632333000000	-0.190678000000	-2.966275000000
H	4.158269000000	-1.551198000000	-1.427994000000	H	-2.728720000000	-1.528464000000	-1.877114000000
H	2.960803000000	1.409761000000	2.110623000000	H	-3.692430000000	2.596956000000	0.258182000000
H	5.382499000000	0.581524000000	2.187672000000	H	-5.181589000000	2.074836000000	-1.769636000000
C	-1.107370000000	1.471734000000	-1.243627000000	C	0.789827000000	-1.224369000000	-1.213069000000
C	-0.691026000000	0.721782000000	1.501972000000	C	0.970717000000	-1.028604000000	1.651631000000
C	-1.672599000000	2.221023000000	-0.181188000000	C	1.278438000000	-2.300841000000	-0.442971000000
C	-1.439180000000	1.878733000000	1.181529000000	H	1.083800000000	-0.947377000000	2.728319000000
				H	1.791793000000	-3.028734000000	1.545167000000

H	1.646565000000	-3.192891000000	-0.939764000000	H	0.954025000000	-0.433294000000	2.742679000000
H	0.768168000000	-1.288893000000	-2.296342000000	H	1.794833000000	-2.679249000000	2.050878000000
C	4.082674000000	-1.511246000000	0.013153000000	H	1.838685000000	-3.337590000000	-0.353938000000
C	3.375658000000	0.641153000000	1.280159000000	H	1.041024000000	-1.767235000000	-2.121587000000
C	3.181037000000	0.527130000000	-1.328265000000	C	4.163469000000	-1.423581000000	0.450078000000
O	5.050575000000	-2.164591000000	-0.025979000000	C	3.314657000000	0.919804000000	1.168161000000
O	3.889076000000	1.359410000000	2.042837000000	C	3.354912000000	0.238559000000	-1.371917000000
O	3.570786000000	1.174322000000	-2.216906000000	O	5.143304000000	-2.035534000000	0.630927000000
Cr	2.538224000000	-0.505397000000	0.079324000000	O	3.745900000000	1.798219000000	1.803792000000
C	-0.203236000000	1.309792000000	1.287496000000	O	3.811887000000	0.685639000000	-2.348041000000
C	0.373737000000	0.034453000000	0.902180000000	Cr	2.607060000000	-0.481774000000	0.171246000000
C	-3.381317000000	-1.115207000000	1.107485000000	C	-0.319788000000	1.418406000000	0.800052000000
C	-3.326914000000	-0.121892000000	1.867299000000	C	0.333808000000	0.133086000000	0.717126000000
H	-3.558619000000	0.477820000000	2.729003000000	C	-3.397650000000	-1.362546000000	-0.409520000000
H	-3.739803000000	-2.066583000000	0.757414000000	C	-3.427324000000	-1.063175000000	0.841298000000
				H	-3.643869000000	-1.363102000000	1.852568000000
				H	-3.597468000000	-2.072507000000	-1.193659000000

### anti-Cr@Ind-TS(3,4)

E = -5255.99 kcal mol<sup>-1</sup> -328.373 cm<sup>-1</sup>

C	0.358307000000	-0.252706000000	-0.690682000000
C	-0.283421000000	0.802694000000	-1.438374000000
C	-0.609433000000	1.863520000000	-0.529986000000
Rh	-2.112840000000	0.271524000000	-0.117595000000
C	-4.655520000000	1.587446000000	0.324109000000
C	-3.608006000000	1.102359000000	1.049352000000
C	-3.584025000000	0.567306000000	-1.532569000000
C	-4.645779000000	1.290084000000	-1.079274000000
H	-0.365028000000	0.847683000000	-2.517165000000
H	-0.973980000000	2.844943000000	-0.805008000000
H	-0.438711000000	2.005302000000	1.702247000000
H	-5.460541000000	1.595769000000	-1.737411000000
H	-3.444556000000	0.266842000000	-2.568880000000
H	-3.486165000000	1.254067000000	2.119801000000
H	-5.472849000000	2.140867000000	0.788934000000
C	0.971524000000	-1.490572000000	-1.074080000000
C	0.922087000000	-0.730553000000	1.698940000000
C	1.414210000000	-2.379100000000	-0.072626000000
C	1.389168000000	-2.001736000000	1.306287000000

### anti-Cr@Ind-4

E = -5329.93 kcal mol<sup>-1</sup>

C	-0.475755000000	-0.220828000000	0.725234000000
C	0.426079000000	0.870092000000	1.147023000000
C	0.708150000000	1.702167000000	-0.000005000000
Rh	2.258865000000	0.322536000000	0.000000000000
C	3.584435000000	-1.527247000000	-0.703809000000
C	4.004302000000	-0.356294000000	-1.404727000000
C	4.004299000000	-0.356287000000	1.404735000000
C	3.584432000000	-1.527242000000	0.703822000000
H	0.501873000000	1.204517000000	2.176834000000
H	0.943076000000	2.760855000000	-0.000006000000
H	0.501878000000	1.204514000000	-2.176843000000
H	3.246816000000	-2.399285000000	1.255663000000
H	3.971047000000	-0.344295000000	2.490616000000
H	3.971053000000	-0.344308000000	-2.490608000000
H	3.246820000000	-2.399293000000	-1.255646000000
C	-1.207548000000	-1.182540000000	1.433517000000
C	-1.207552000000	-1.182539000000	-1.433525000000

C	-1.941750000000	-2.176351000000	0.705044000000	C	1.941937000000	3.552680000000	-0.311516000000
C	-1.941752000000	-2.176351000000	-0.705052000000	C	1.876370000000	2.889669000000	-1.571408000000
H	-1.236146000000	-1.176054000000	-2.519436000000	C	2.936312000000	2.115615000000	-2.016304000000
H	-2.520780000000	-2.918385000000	-1.245450000000	C	4.105547000000	1.983384000000	-1.227336000000
H	-2.520776000000	-2.918386000000	1.245443000000	C	4.187420000000	2.606287000000	0.007312000000
H	-1.236139000000	-1.176056000000	2.519428000000	H	2.547408000000	-0.036235000000	2.920174000000
C	-4.058628000000	-0.203492000000	-1.291765000000	H	0.008434000000	0.606294000000	3.614623000000
C	-2.758099000000	1.667578000000	0.000004000000	C	-1.910518000000	0.261130000000	1.264394000000
C	-4.058621000000	-0.203492000000	1.291768000000	H	1.240925000000	4.355366000000	-0.105460000000
O	-4.892106000000	-0.226930000000	-2.111536000000	H	1.000402000000	3.031754000000	-2.200655000000
O	-2.759846000000	2.835946000000	0.000007000000	H	2.884770000000	1.629514000000	-2.988362000000
O	-4.892094000000	-0.226930000000	2.111543000000	H	2.615522000000	-0.334528000000	0.240790000000
Cr	-2.733383000000	-0.190994000000	-0.000002000000	C	-0.197173000000	-0.372331000000	-0.948778000000
C	0.426081000000	0.870091000000	-1.147032000000	H	3.266218000000	4.035096000000	1.350696000000
C	-0.475755000000	-0.220828000000	-0.725243000000	H	4.944973000000	1.401037000000	-1.601583000000
C	4.503151000000	0.774147000000	0.708051000000	H	5.094930000000	2.528001000000	0.602193000000
C	4.503152000000	0.774143000000	-0.708048000000	H	1.860122000000	3.425442000000	4.047804000000
H	4.863504000000	1.637676000000	-1.259349000000	H	-0.368728000000	4.550688000000	2.063635000000
H	4.863501000000	1.637684000000	1.259348000000	C	-1.592316000000	-0.233235000000	-1.130825000000
				C	-2.445420000000	0.088386000000	-0.031895000000
				H	0.437502000000	-0.651217000000	-1.783988000000
				H	-2.026668000000	-0.414872000000	-2.108857000000
				H	-3.518202000000	0.146801000000	-0.185110000000
				H	-2.567880000000	0.462607000000	2.104798000000
				C	-2.582827000000	-2.882243000000	-0.313765000000
				C	-1.705186000000	-2.556398000000	2.113047000000
				C	-0.040068000000	-3.128966000000	0.190137000000
				O	-3.398795000000	-3.550655000000	-0.817619000000
Rh	1.287997000000	2.107033000000	1.465055000000	O	-1.953842000000	-3.016254000000	3.157466000000
C	1.297645000000	3.436506000000	3.128811000000	O	0.770012000000	-3.951534000000	0.013140000000
C	0.405878000000	3.857731000000	2.348403000000	Cr	-1.306142000000	-1.799969000000	0.465341000000

### anti-Cr@Ind-5

E = -5850.18 kcal mol<sup>-1</sup>

C	-0.497893000000	0.204018000000	1.448374000000				
C	0.368153000000	0.449704000000	2.604082000000				
C	1.713984000000	0.090718000000	2.240652000000				
C	1.745706000000	-0.066231000000	0.827774000000				
C	0.365096000000	-0.115353000000	0.335380000000				
Rh	1.287997000000	2.107033000000	1.465055000000				
C	1.297645000000	3.436506000000	3.128811000000				
C	0.405878000000	3.857731000000	2.348403000000				
C	3.104432000000	3.388952000000	0.494208000000				

**Table A3.** Cartesian coordinates (in Å) and ADF total energies (in kcal mol<sup>-1</sup>) of all stationary points as well as imaginary frequencies of transition states (in cm<sup>-1</sup>) along Path I, catalyzed by syn-IndRh.

**syn-Cr@Ind-1**

E = -4708.53 kcal mol<sup>-1</sup>

C	-0.094221000000	1.732326000000	0.756253000000
C	1.300310000000	1.781006000000	1.154561000000
C	2.091741000000	2.024483000000	-0.017834000000
Rh	1.667817000000	-0.128449000000	-0.057001000000
C	1.858576000000	-1.693823000000	-1.554668000000
C	2.862800000000	-0.951319000000	-1.636650000000
C	2.942097000000	-1.020083000000	1.420332000000
C	1.933407000000	-1.758439000000	1.357999000000
H	1.645702000000	1.857530000000	2.178905000000
H	3.130239000000	2.329974000000	-0.037182000000
H	1.534029000000	1.960153000000	-2.194339000000
H	1.298708000000	-2.585949000000	1.620692000000
H	3.898294000000	-0.695252000000	1.791097000000
H	3.798609000000	-0.608436000000	-2.041531000000
H	1.210865000000	-2.510191000000	-1.820334000000
C	-1.313979000000	1.695150000000	1.493232000000
C	-1.386984000000	1.763209000000	-1.367020000000
C	-2.537411000000	1.892534000000	0.810187000000
C	-2.573791000000	1.926533000000	-0.613946000000
H	-1.429708000000	1.742053000000	-2.451739000000
H	-3.524534000000	2.035974000000	-1.125380000000
H	-3.460687000000	1.976340000000	1.374130000000
H	-1.301472000000	1.622529000000	2.576502000000
Cr	-1.736354000000	-0.050200000000	0.030412000000
C	1.241259000000	1.835331000000	-1.158430000000
C	-0.131243000000	1.766547000000	-0.692216000000
C	-1.402582000000	-1.243222000000	-1.349816000000
O	-1.258237000000	-1.995350000000	-2.233543000000
C	-1.333741000000	-1.307048000000	1.333522000000
O	-1.146068000000	-2.099974000000	2.172328000000
C	-3.436516000000	-0.742118000000	0.057845000000

O -4.521921000000 -1.177137000000 0.075512000000

**syn-Cr@Ind-TS(1,2)**

E = -4693.35 kcal mol<sup>-1</sup> -444.37 cm<sup>-1</sup>

C	-0.186080000000	1.811021000000	0.730412000000
C	1.173867000000	1.974406000000	1.160852000000
C	1.989980000000	2.191853000000	0.000000000000
Rh	1.721119000000	-0.006503000000	0.000000000000
C	2.185000000000	-1.903486000000	-0.958930000000
C	2.806031000000	-0.897007000000	-1.483648000000
C	2.806031000000	-0.897007000000	1.483648000000
C	2.185000000000	-1.903486000000	0.958930000000
H	1.496445000000	2.084371000000	2.188872000000
H	3.015522000000	2.538591000000	0.000000000000
H	1.496445000000	2.084371000000	-2.188872000000
H	1.657204000000	-2.804586000000	1.246257000000
H	3.469079000000	-0.541119000000	2.255881000000
H	3.469079000000	-0.541119000000	-2.255881000000
H	1.657204000000	-2.804586000000	-1.246257000000
C	-1.424683000000	1.682081000000	1.432346000000
C	-1.424683000000	1.682081000000	-1.432346000000
C	-2.637407000000	1.768737000000	0.713964000000
C	-2.637407000000	1.768737000000	-0.713964000000
H	-1.438458000000	1.630097000000	-2.516937000000
H	-3.580806000000	1.784937000000	-1.250058000000
H	-3.580806000000	1.784937000000	1.250058000000
H	-1.438458000000	1.630097000000	2.516937000000
Cr	-1.664460000000	-0.121869000000	0.000000000000
C	1.173867000000	1.974406000000	-1.160852000000
C	-0.186080000000	1.811021000000	-0.730412000000
C	-1.179351000000	-1.305468000000	-1.346659000000
O	-0.924602000000	-2.059638000000	-2.202098000000
C	-1.179351000000	-1.305468000000	1.346659000000

O	-0.924602000000	-2.059638000000	2.202098000000
C	-3.295720000000	-0.962153000000	0.000000000000
O	-4.337590000000	-1.494008000000	0.000000000000

O	-3.804757000000	-1.803827000000	-1.104767000000
---	-----------------	-----------------	-----------------

### **syn-Cr@Ind-2**

E = -4734.92 kcal mol<sup>-1</sup>

C	-0.252915000000	1.721978000000	0.761704000000
C	1.207888000000	1.817066000000	0.822372000000
C	1.634727000000	2.356482000000	-0.462057000000
Rh	1.469169000000	0.122669000000	-0.449993000000
C	4.188932000000	-0.816441000000	-0.229503000000
C	3.463217000000	0.066005000000	-0.944390000000
C	2.154342000000	-1.217467000000	0.928289000000
C	3.462519000000	-1.524055000000	0.829134000000
H	1.782671000000	1.860105000000	1.740407000000
H	2.636106000000	2.708344000000	-0.674073000000
H	0.568705000000	2.689333000000	-2.385766000000
H	3.951511000000	-2.261681000000	1.469067000000
H	1.465055000000	-1.649371000000	1.655311000000
H	3.843331000000	0.640247000000	-1.792155000000
H	5.242195000000	-1.020258000000	-0.437534000000
C	-1.233801000000	1.360326000000	1.718367000000
C	-2.007997000000	1.926458000000	-0.987210000000
C	-2.608336000000	1.368687000000	1.351213000000
C	-2.976997000000	1.599601000000	0.003820000000
H	-2.315976000000	2.097999000000	-2.013858000000
H	-4.023813000000	1.541133000000	-0.277946000000
H	-3.366156000000	1.129346000000	2.089784000000
H	-0.944445000000	1.113542000000	2.735652000000
Cr	-1.551413000000	-0.154007000000	0.045778000000
C	0.540734000000	2.392619000000	-1.344534000000
C	-0.654956000000	2.049417000000	-0.605719000000
C	-0.403316000000	-1.026949000000	-1.136906000000
O	0.240404000000	-1.635215000000	-1.928453000000
C	-1.353954000000	-1.498082000000	1.299925000000
O	-1.274171000000	-2.332755000000	2.111495000000
C	-2.935075000000	-1.168005000000	-0.662708000000

### **syn-Cr@Ind-TS(2,3)**

E = -5242.98 kcal mol<sup>-1</sup> -47.554397 cm<sup>-1</sup>

C	-0.575000000000	-2.137800000000	-0.379800000000
C	0.884500000000	-2.128800000000	-0.110600000000
C	0.987800000000	-2.516600000000	1.314600000000
Rh	1.143300000000	-0.033400000000	-0.109700000000
C	3.871000000000	-0.210400000000	-1.011300000000
C	3.158900000000	-0.174500000000	0.136500000000
C	1.728800000000	-0.093700000000	-2.032300000000
C	3.060800000000	-0.154700000000	-2.233700000000
H	1.574400000000	-2.558200000000	-0.835200000000
H	1.937800000000	-2.667400000000	1.816400000000
H	-0.451600000000	-2.798800000000	2.944900000000
H	3.506400000000	-0.120900000000	-3.229600000000
H	0.972100000000	-0.004700000000	-2.815300000000
H	3.605000000000	-0.203200000000	1.135200000000
H	4.961600000000	-0.250600000000	-1.045100000000
C	-1.324700000000	-1.932300000000	-1.560400000000
C	-2.662600000000	-2.256600000000	0.954900000000
C	-2.745200000000	-1.910900000000	-1.490900000000
C	-3.399900000000	-2.025900000000	-0.244500000000
H	-3.183200000000	-2.356400000000	1.902900000000
H	-4.481800000000	-1.945300000000	-0.199200000000
H	-3.326800000000	-1.743000000000	-2.392000000000
H	-0.824200000000	-1.785600000000	-2.512300000000
Cr	-1.932300000000	-0.287700000000	-0.085200000000
C	-0.241800000000	-2.604900000000	1.898700000000
C	-1.260500000000	-2.352100000000	0.883900000000
C	-0.785300000000	0.577000000000	1.111500000000
O	-0.180200000000	1.075400000000	1.995600000000
C	-1.734200000000	0.992000000000	-1.406100000000
O	-1.634100000000	1.794400000000	-2.249400000000
C	-3.304500000000	0.763200000000	0.597100000000
O	-4.173800000000	1.413300000000	1.017700000000
C	1.103300000000	3.686300000000	-0.820600000000

C	1.930500000000	3.695600000000	0.057000000000	O	-4.167740000000	-1.689068000000	-0.609900000000
H	2.670500000000	3.728000000000	0.827200000000	C	1.623142000000	-1.975875000000	-1.467724000000
H	0.359900000000	3.669300000000	-1.593900000000	C	2.496574000000	-1.316108000000	-2.060730000000

### syn-Cr@Ind-3

$$E = -5259.27 \text{ kcal mol}^{-1}$$

C	-0.226002000000	1.636642000000	0.728136000000
C	1.181896000000	1.904783000000	0.418304000000
C	1.140076000000	2.749982000000	-0.778332000000
Rh	1.689597000000	0.017871000000	-0.557889000000
C	4.360629000000	0.322460000000	0.491707000000
C	3.628706000000	0.688278000000	-0.583106000000
C	2.366399000000	-0.762135000000	1.159687000000
C	3.654115000000	-0.493448000000	1.465445000000
H	1.907958000000	2.071332000000	1.209472000000
H	2.023920000000	3.184911000000	-1.232662000000
H	-0.454183000000	3.401510000000	-2.152617000000
H	4.132296000000	-0.882449000000	2.366103000000
H	1.690363000000	-1.416667000000	1.710486000000
H	4.007633000000	1.255588000000	-1.435542000000
H	5.407833000000	0.603152000000	0.618376000000
C	-0.858869000000	0.967050000000	1.809338000000
C	-2.449900000000	2.102736000000	-0.287317000000
C	-2.270545000000	0.936360000000	1.886758000000
C	-3.053843000000	1.468532000000	0.826108000000
H	-3.065523000000	2.500580000000	-1.088699000000
H	-4.135429000000	1.384655000000	0.870367000000
H	-2.757955000000	0.447481000000	2.724090000000
H	-0.261080000000	0.507657000000	2.591294000000
Cr	-1.674635000000	-0.083520000000	-0.067253000000
C	-0.145519000000	2.888975000000	-1.248475000000
C	-1.039557000000	2.226672000000	-0.323158000000
C	-1.253864000000	-0.338675000000	-1.862382000000
O	-1.069688000000	-0.457419000000	-3.008713000000
C	-0.972549000000	-1.688993000000	0.526247000000
O	-0.616719000000	-2.726044000000	0.937063000000
C	-3.201109000000	-1.068420000000	-0.405994000000

### syn-Cr@Ind-TS(3,4)

$$E = -5254.66 \text{ kcal mol}^{-1} \quad -325.80 \text{ cm}^{-1}$$

C	-0.426855000000	1.594328000000	0.993930000000
C	0.976813000000	1.763815000000	1.286449000000
C	1.566559000000	2.452372000000	0.174908000000
Rh	1.654330000000	0.328243000000	-0.413385000000
C	4.518350000000	-0.077670000000	-0.341908000000
C	3.580128000000	0.654876000000	-1.001615000000
C	2.645717000000	-1.138822000000	0.658680000000
C	4.008290000000	-1.035376000000	0.594029000000
H	1.435286000000	1.623491000000	2.257302000000
H	2.543096000000	2.919813000000	0.175342000000
H	0.764215000000	2.973279000000	-1.855571000000
H	4.665357000000	-1.669710000000	1.190778000000
H	2.117444000000	-1.804666000000	1.338315000000
H	3.799899000000	1.416891000000	-1.748639000000
H	5.584956000000	0.020634000000	-0.550607000000
C	-1.526852000000	1.130998000000	1.775031000000
C	-1.965323000000	2.003117000000	-0.919885000000
C	-2.838605000000	1.261090000000	1.264754000000
C	-3.055981000000	1.697579000000	-0.076372000000
H	-2.141849000000	2.286165000000	-1.953426000000
H	-4.067474000000	1.744215000000	-0.466990000000
H	-3.686702000000	0.986975000000	1.883881000000
H	-1.368310000000	0.758530000000	2.782629000000
Cr	-1.777557000000	-0.151199000000	-0.112370000000
C	0.615536000000	2.499928000000	-0.892880000000
C	-0.647715000000	2.050546000000	-0.372590000000
C	-1.398926000000	-0.740284000000	-1.834373000000
O	-1.216477000000	-1.089211000000	-2.932372000000
C	-0.943270000000	-1.587531000000	0.715740000000

O	-0.476739000000	-2.507343000000	1.267831000000	O	3.545225000000	-3.136490000000	0.088824000000
C	-3.275446000000	-1.215250000000	-0.187884000000	C	0.813848000000	-1.465269000000	1.416715000000
O	-4.231336000000	-1.886525000000	-0.230128000000	O	0.221537000000	-1.969549000000	2.291432000000
C	1.849030000000	-1.684680000000	-1.216846000000	C	0.778867000000	-1.524209000000	-1.241540000000
C	2.098329000000	-0.842261000000	-2.137290000000	O	0.164165000000	-2.066923000000	-2.076949000000
H	2.216731000000	-0.586904000000	-3.174118000000	C	-4.052986000000	1.528466000000	0.771641000000
H	1.467005000000	-2.646183000000	-0.921631000000	C	-3.012019000000	0.737729000000	1.434449000000
				H	-2.882905000000	0.840601000000	2.509446000000
				H	-4.761331000000	2.102999000000	1.364089000000

### syn-Cr@Ind-4

$$E = -5321.55 \text{ kcal mol}^{-1}$$

C	1.353452000000	1.658522000000	-0.709514000000
C	0.175167000000	2.403426000000	-1.141536000000
C	-0.379063000000	3.072133000000	0.005318000000
Rh	-1.191721000000	1.070175000000	0.056433000000
C	-2.553241000000	-0.484989000000	-0.613390000000
C	-2.532630000000	-0.463518000000	0.815120000000
C	-4.072721000000	1.508368000000	-0.584973000000
C	-3.050326000000	0.698403000000	-1.253782000000
H	-0.049478000000	2.639591000000	-2.175284000000
H	-1.082955000000	3.894558000000	-0.002577000000
H	0.007780000000	2.730846000000	2.192407000000
H	-2.953053000000	0.769017000000	-2.334741000000
H	-4.798310000000	2.065218000000	-1.173384000000
H	-2.123961000000	-1.282080000000	1.398699000000
H	-2.162194000000	-1.321371000000	-1.183645000000
C	2.394832000000	0.996468000000	-1.418910000000
C	2.433646000000	1.058112000000	1.441332000000
C	3.527462000000	0.535009000000	-0.705764000000
C	3.546839000000	0.565907000000	0.718249000000
H	2.437757000000	1.036992000000	2.526975000000
H	4.404001000000	0.170902000000	1.253709000000
H	4.369872000000	0.116477000000	-1.246726000000
H	2.369655000000	0.928606000000	-2.502353000000
Cr	1.800594000000	-0.689101000000	0.056578000000
C	0.205789000000	2.452124000000	1.163832000000
C	1.372555000000	1.688874000000	0.732409000000
C	2.859590000000	-2.188208000000	0.076298000000

### syn-Cr@Ind-5

$$E = -5847.20 \text{ kcal mol}^{-1}$$

C	1.370114000000	1.870008000000	-0.371523000000
C	0.473471000000	2.840346000000	-0.998683000000
C	-0.219032000000	3.549276000000	0.047015000000
Rh	-1.356416000000	1.743848000000	-0.293685000000
C	-3.575441000000	1.993096000000	0.646786000000
C	-3.732604000000	3.062379000000	1.574624000000
C	-2.699345000000	0.603026000000	2.467782000000
C	-3.063078000000	0.742530000000	1.095240000000
H	0.559450000000	3.165119000000	-2.029521000000
H	-0.735196000000	4.496248000000	-0.046700000000
H	-0.467695000000	3.025834000000	2.216048000000
H	-3.187726000000	-0.154301000000	0.495778000000
H	-2.343598000000	-0.359939000000	2.820459000000
H	-4.174668000000	3.997093000000	1.235670000000
H	-4.078765000000	2.058656000000	-0.311006000000
C	2.463550000000	1.111443000000	-0.866245000000
C	1.722415000000	0.931477000000	1.891443000000
C	3.274340000000	0.397708000000	0.052717000000
C	2.905535000000	0.309599000000	1.425329000000
H	1.426300000000	0.822203000000	2.930430000000
H	3.511864000000	-0.275435000000	2.109113000000
H	4.167330000000	-0.108115000000	-0.299474000000
H	2.728133000000	1.141080000000	-1.918769000000
Cr	1.259901000000	-0.569645000000	0.159173000000
C	-0.066082000000	2.771648000000	1.242971000000

C	1.010549000000	1.806687000000	1.024315000000	C	-3.370007000000	2.900858000000	2.899550000000
C	2.112295000000	-2.195081000000	0.158995000000	H	-3.511108000000	3.715154000000	3.607801000000
O	2.666002000000	-3.225437000000	0.162821000000	H	-2.588166000000	1.533734000000	4.397853000000
C	-0.081242000000	-1.419949000000	1.110044000000	C	-2.205137000000	0.736089000000	-2.008417000000
O	-0.884934000000	-2.018816000000	1.714332000000	C	-2.339157000000	1.969739000000	-2.189839000000
C	0.497635000000	-1.089352000000	-1.447656000000	H	-2.602601000000	2.855841000000	-2.741382000000
O	0.069193000000	-1.460986000000	-2.470278000000	H	-2.277876000000	-0.300636000000	-2.289420000000
C	-2.845529000000	1.661187000000	3.348160000000				

**Table A4.** Cartesian coordinates (in Å) and ADF total energies (in kcal mol<sup>-1</sup>) of all stationary points as well as imaginary frequencies of transition states (in cm<sup>-1</sup>) along Path II catalyzed by anti-IndRh(CO).

### CO-anti-Cr@Ind-1

E = -5054.68 kcal mol<sup>-1</sup>

C	1.777851000000	0.171665000000	-3.657102000000
C	1.596578000000	-0.313469000000	-2.326292000000
C	1.537711000000	0.599450000000	-1.259709000000
C	1.711409000000	2.016854000000	-1.512256000000
C	1.920720000000	2.490503000000	-2.820694000000
C	1.948054000000	1.552325000000	-3.897114000000
C	1.652031000000	2.703217000000	-0.223910000000
C	1.438112000000	1.787019000000	0.756200000000
C	1.305669000000	0.414388000000	0.206589000000
Rh	-0.703100000000	-0.373459000000	0.599371000000
C	-1.842906000000	1.385177000000	-0.036321000000
C	-1.851918000000	0.588457000000	-1.004313000000
C	-0.621079000000	-2.251150000000	-0.473891000000
C	-0.122805000000	-2.444632000000	0.669640000000
H	1.782542000000	3.772068000000	-0.091356000000
H	1.383427000000	2.004640000000	1.816801000000
H	1.883382000000	-0.367985000000	0.696990000000
H	-2.122146000000	0.280331000000	-1.998162000000
H	-2.076661000000	2.309577000000	0.459923000000
H	0.333472000000	-3.080060000000	1.409877000000
H	-0.926153000000	-2.611757000000	-1.441827000000

H 1.496492000000 -1.378865000000 -2.146123000000

H 1.832248000000 -0.530009000000 -4.483344000000

H 2.126644000000 1.902914000000 -4.908859000000

H 2.087750000000 3.546088000000 -3.013778000000

C -0.582115000000 0.043514000000 2.487205000000

O -0.688131000000 0.192308000000 3.630613000000

Cr 3.534941000000 0.889784000000 -2.424733000000

C 4.818190000000 1.801233000000 -3.411070000000

C 4.493401000000 -0.669437000000 -2.731747000000

C 4.546717000000 1.188491000000 -0.887542000000

O 5.174252000000 1.370877000000 0.076714000000

O 5.613370000000 2.378545000000 -4.039041000000

O 5.082424000000 -1.655795000000 -2.934297000000

### CO-anti-Cr@Ind-TS(1,2)

E = -5040.78 kcal mol<sup>-1</sup> -348.75 cm<sup>-1</sup>

C 1.942823000000 -0.155180000000 -3.458847000000

C 1.774720000000 -0.426867000000 -2.066742000000

C 1.605675000000 0.644940000000 -1.171423000000

C 1.650094000000 2.011420000000 -1.656068000000

C 1.853177000000 2.275543000000 -3.025300000000

C 1.989332000000 1.176606000000 -3.927180000000

C 1.470837000000 2.891688000000 -0.503242000000

C	1.313007000000	2.130407000000	0.614466000000	C	0.880645000000	-0.074980000000	-3.390322000000
C	1.334301000000	0.681435000000	0.296528000000	C	1.516389000000	-0.674631000000	-2.285544000000
Rh	-0.620425000000	-0.344242000000	0.619759000000	Rh	-0.375003000000	0.119283000000	0.606200000000
C	-1.526751000000	1.258084000000	-0.438188000000	C	-1.015540000000	-0.622756000000	2.161583000000
C	-2.079662000000	0.300355000000	-1.078704000000	O	-1.417275000000	-1.075266000000	3.148094000000
C	-2.432110000000	-1.494868000000	-0.210392000000	C	-2.135389000000	1.220193000000	0.411041000000
C	-1.495444000000	-2.187646000000	0.330159000000	C	-3.095743000000	0.607610000000	-0.304057000000
H	1.494455000000	3.975650000000	-0.548037000000	H	0.984091000000	2.847087000000	0.778022000000
H	1.192075000000	2.511898000000	1.622953000000	H	2.115985000000	0.849207000000	2.177595000000
H	1.988902000000	0.068600000000	0.914044000000	H	2.435817000000	-1.287296000000	0.568171000000
H	-2.499857000000	0.052437000000	-2.042191000000	H	-4.052211000000	1.081555000000	-0.534612000000
H	-1.247458000000	2.295858000000	-0.552417000000	H	-2.226919000000	2.206949000000	0.863122000000
H	-1.345474000000	-3.160842000000	0.772587000000	H	1.934324000000	-1.672958000000	-2.365955000000
H	-3.490757000000	-1.547186000000	-0.419639000000	H	0.826150000000	-0.611276000000	-4.332382000000
H	1.769194000000	-1.452788000000	-1.710621000000	H	-0.033885000000	1.721806000000	-4.212525000000
H	2.079707000000	-0.976378000000	-4.155180000000	H	0.197757000000	3.063050000000	-2.120742000000
H	2.158132000000	1.367939000000	-4.982359000000	C	-2.790306000000	-0.752853000000	-0.757108000000
H	1.922594000000	3.294671000000	-3.394168000000	C	-1.593682000000	-1.244321000000	-0.391960000000
C	-0.002286000000	-0.730311000000	2.319685000000	H	-3.499095000000	-1.326592000000	-1.358211000000
O	0.326312000000	-0.894427000000	3.422286000000	H	-1.222101000000	-2.244606000000	-0.609941000000
Cr	3.600617000000	0.923200000000	-2.358749000000	Cr	2.575134000000	1.279179000000	-2.798395000000
C	4.809904000000	1.808584000000	-3.450805000000	C	3.073347000000	1.507544000000	-4.554559000000
C	4.706889000000	-0.561884000000	-2.414099000000	C	4.231260000000	0.491462000000	-2.461040000000
C	4.534873000000	1.535193000000	-0.873387000000	C	3.304101000000	2.949842000000	-2.408313000000
O	5.108734000000	1.916023000000	0.067998000000	O	3.373667000000	1.646679000000	-5.675208000000
O	5.557953000000	2.368973000000	-4.150074000000	O	3.750214000000	3.997226000000	-2.158972000000
O	5.389984000000	-1.508097000000	-2.457631000000	O	5.260643000000	-0.009887000000	-2.244420000000

## CO-anti-Cr@Ind-2

E = -5097.75 kcal mol<sup>-1</sup>

C	1.967814000000	-0.350767000000	0.293994000000
C	1.509981000000	0.007837000000	-1.018239000000
C	0.999324000000	1.388120000000	-0.946976000000
C	1.191782000000	1.849656000000	0.413536000000
C	1.809728000000	0.795438000000	1.139631000000
C	0.527571000000	2.029727000000	-2.148134000000
C	0.386022000000	1.265391000000	-3.321950000000

## CO-anti-Cr@Ind-TS(2,3)

E = -5596.71 kcal mol<sup>-1</sup> -57.79 cm<sup>-1</sup>

C	1.767700000000	-0.065000000000	-3.503600000000
C	1.634100000000	-0.452700000000	-2.136100000000
C	1.554900000000	0.542000000000	-1.151800000000
C	1.663800000000	1.941800000000	-1.515700000000
C	1.811400000000	2.317200000000	-2.866400000000
C	1.843300000000	1.297800000000	-3.864600000000
C	1.619200000000	2.717600000000	-0.282900000000

C	1.498400000000	1.863400000000	0.780600000000	C	1.608710000000	1.829494000000	-1.506426000000
C	1.374500000000	0.460600000000	0.322100000000	C	1.745704000000	2.187668000000	-2.868957000000
Rh	-0.654900000000	0.300300000000	1.012500000000	C	1.782660000000	1.165896000000	-3.856283000000
C	-1.457300000000	0.882000000000	-0.834300000000	C	1.560512000000	2.616688000000	-0.289686000000
C	-1.967800000000	-0.141500000000	-1.552600000000	C	1.467428000000	1.767097000000	0.792085000000
C	-1.778600000000	-1.469700000000	-0.963100000000	C	1.355125000000	0.366423000000	0.345236000000
C	-1.146000000000	-1.521100000000	0.227100000000	Rh	-0.727825000000	0.430770000000	1.051564000000
H	1.706300000000	3.798200000000	-0.231600000000	C	-1.457434000000	0.762262000000	-0.886312000000
H	1.540900000000	2.160000000000	1.824100000000	C	-1.849366000000	-0.354388000000	-1.542180000000
H	1.919200000000	-0.323300000000	0.844600000000	C	-1.693667000000	-1.595349000000	-0.797750000000
H	-2.483400000000	-0.023700000000	-2.509200000000	C	-1.197691000000	-1.493247000000	0.455550000000
H	-1.536300000000	1.924100000000	-1.162400000000	H	1.625103000000	3.699269000000	-0.250661000000
H	-0.920900000000	-2.432400000000	0.779800000000	H	1.558049000000	2.077484000000	1.827473000000
H	-2.139000000000	-2.377900000000	-1.454200000000	H	1.868806000000	-0.425148000000	0.885003000000
H	1.582700000000	-1.503600000000	-1.869600000000	H	-2.271182000000	-0.349453000000	-2.549691000000
H	1.837400000000	-0.827800000000	-4.272900000000	H	-1.558850000000	1.767132000000	-1.304666000000
H	1.972500000000	1.571400000000	-4.907200000000	H	-1.072131000000	-2.322992000000	1.149267000000
H	1.918300000000	3.360500000000	-3.149300000000	H	-1.979201000000	-2.563302000000	-1.218142000000
C	-0.113000000000	-0.515600000000	2.697100000000	H	1.631972000000	-1.623479000000	-1.822124000000
O	0.125900000000	-1.129600000000	3.647400000000	H	1.873913000000	-0.965401000000	-4.224138000000
Cr	3.515300000000	0.855300000000	-2.389500000000	H	1.890390000000	1.427593000000	-4.903864000000
C	4.722400000000	1.880000000000	-3.357600000000	H	1.820107000000	3.230865000000	-3.163203000000
C	4.558800000000	-0.632700000000	-2.769400000000	C	-0.146470000000	-0.234714000000	2.801503000000
C	4.533500000000	1.148500000000	-0.858400000000	O	0.136791000000	-0.793346000000	3.771192000000
O	5.162300000000	1.332400000000	0.105800000000	Cr	3.496155000000	0.809078000000	-2.394208000000
O	5.473200000000	2.526800000000	-3.973500000000	C	4.641599000000	2.125750000000	-3.021793000000
O	5.203700000000	-1.573600000000	-3.012600000000	C	4.617977000000	-0.448775000000	-3.166014000000
C	-3.494200000000	1.214800000000	1.657000000000	C	4.489950000000	0.704244000000	-0.825983000000
C	-2.984100000000	1.226900000000	2.752900000000	O	5.091803000000	0.640472000000	0.170743000000
H	-2.606900000000	1.250700000000	3.751800000000	O	5.352135000000	2.959008000000	-3.426080000000
H	-3.929200000000	1.200100000000	0.681300000000	O	5.313390000000	-1.243547000000	-3.662496000000
				C	-3.019041000000	0.779432000000	1.304408000000
				C	-2.465725000000	1.511262000000	2.125470000000
				H	-2.273922000000	2.171057000000	2.947436000000
				H	-3.702056000000	0.234597000000	0.686597000000

### CO-anti-Cr@Ind-3

E = -5602.15 kcal mol<sup>-1</sup>

C	1.776683000000	-0.194798000000	-3.465455000000
C	1.645454000000	-0.574363000000	-2.098694000000
C	1.534916000000	0.432020000000	-1.125183000000

### CO-anti-Cr@Ind-TS(3,b)

E = -5599.68 kcal mol<sup>-1</sup> -270.09 cm<sup>-1</sup>

C	1.731811000000	-0.164086000000	-3.438161000000
C	1.622342000000	-0.553559000000	-2.071000000000
C	1.540019000000	0.444903000000	-1.086639000000
C	1.611360000000	1.845581000000	-1.460005000000
C	1.724509000000	2.214054000000	-2.820511000000
C	1.742197000000	1.198936000000	-3.817273000000
C	1.583118000000	2.625112000000	-0.236120000000
C	1.503544000000	1.769233000000	0.838349000000
C	1.384855000000	0.370990000000	0.386135000000
Rh	-0.717930000000	0.376011000000	1.090431000000
C	-1.573108000000	0.788255000000	-0.811581000000
C	-1.837717000000	-0.343351000000	-1.534673000000
C	-1.617338000000	-1.581282000000	-0.841869000000
C	-1.092337000000	-1.501263000000	0.414663000000
H	1.646973000000	3.707396000000	-0.190814000000
H	1.586164000000	2.071731000000	1.876699000000
H	1.910143000000	-0.420013000000	0.915334000000
H	-2.199070000000	-0.323150000000	-2.564632000000
H	-1.677977000000	1.794649000000	-1.215773000000
H	-0.959474000000	-2.359509000000	1.072351000000
H	-1.869394000000	-2.546382000000	-1.287986000000
H	1.608403000000	-1.604827000000	-1.803179000000
H	1.810163000000	-0.929446000000	-4.204258000000
H	1.834959000000	1.468293000000	-4.864394000000
H	1.799305000000	3.259218000000	-3.107518000000
C	-0.160235000000	-0.280508000000	2.829816000000
O	0.113369000000	-0.796401000000	3.825945000000
Cr	3.476186000000	0.817711000000	-2.389846000000
C	4.617714000000	2.106224000000	-3.078582000000
C	4.572738000000	-0.474409000000	-3.140088000000
C	4.498920000000	0.758367000000	-0.838370000000
O	5.119977000000	0.721779000000	0.148044000000
O	5.324526000000	2.923580000000	-3.520505000000
O	5.250466000000	-1.292441000000	-3.623560000000
C	-2.948307000000	1.046735000000	0.873177000000

C	-2.372851000000	1.488922000000	1.902681000000
H	-2.468739000000	1.909943000000	2.888973000000
H	-3.826488000000	0.736607000000	0.338139000000

### CO-anti-Cr@Ind-b

E = -5621.21 kcal mol<sup>-1</sup>

C	1.731012000000	-0.123488000000	-3.412298000000
C	1.673132000000	-0.524947000000	-2.048033000000
C	1.621727000000	0.466020000000	-1.046424000000
C	1.663027000000	1.873042000000	-1.412076000000
C	1.736312000000	2.249404000000	-2.776164000000
C	1.721315000000	1.245206000000	-3.781176000000
C	1.635314000000	2.642295000000	-0.185821000000
C	1.583840000000	1.771648000000	0.883009000000
C	1.501053000000	0.384587000000	0.416627000000
Rh	-0.652540000000	0.235179000000	1.128113000000
C	-1.619358000000	0.715158000000	-0.756392000000
C	-2.176243000000	-0.538033000000	-1.295212000000
C	-2.109428000000	-1.645897000000	-0.485696000000
C	-1.419340000000	-1.483872000000	0.738901000000
H	1.676804000000	3.724866000000	-0.130760000000
H	1.660126000000	2.065611000000	1.924676000000
H	1.995253000000	-0.418063000000	0.958687000000
H	-2.641487000000	-0.578304000000	-2.283269000000
H	-1.131242000000	1.351772000000	-1.500317000000
H	-1.375079000000	-2.295788000000	1.467809000000
H	-2.571643000000	-2.599653000000	-0.748256000000
H	1.678105000000	-1.579854000000	-1.791137000000
H	1.786030000000	-0.881890000000	-4.187433000000
H	1.775174000000	1.523539000000	-4.828597000000
H	1.792897000000	3.297457000000	-3.057267000000
C	-0.239763000000	-0.195463000000	2.990758000000
O	-0.112416000000	-0.518253000000	4.091232000000
Cr	3.512703000000	0.861021000000	-2.426863000000
C	4.620886000000	2.206016000000	-3.056185000000
C	4.586224000000	-0.360871000000	-3.311229000000
C	4.592172000000	0.688683000000	-0.924390000000

O	5.249884000000	0.583004000000	0.033188000000	Cr	3.513663000000	0.806636000000	-2.450009000000
O	5.307118000000	3.058784000000	-3.463212000000	C	4.544848000000	2.295140000000	-2.846732000000
O	5.249498000000	-1.135978000000	-3.879260000000	C	4.632733000000	-0.183886000000	-3.538019000000
C	-2.663124000000	1.496784000000	0.079485000000	C	4.619271000000	0.427437000000	-1.005490000000
C	-2.400028000000	1.287488000000	1.364278000000	O	5.294430000000	0.190499000000	-0.083987000000
H	-2.880094000000	1.651228000000	2.268238000000	O	5.183830000000	3.237085000000	-3.108342000000
H	-3.447827000000	2.112245000000	-0.373502000000	O	5.326622000000	-0.812029000000	-4.237245000000

### CO-anti-Cr@Ind-TS(b,h)

$$E = -5619.68 \text{ kcal mol}^{-1} \quad -227.82 \text{ cm}^{-1}$$

C	1.780857000000	-0.297697000000	-3.382157000000
C	1.753272000000	-0.666825000000	-2.011967000000
C	1.638846000000	0.345772000000	-1.029617000000
C	1.612954000000	1.742760000000	-1.429437000000
C	1.667108000000	2.087266000000	-2.808351000000
C	1.689698000000	1.063249000000	-3.786611000000
C	1.546885000000	2.538051000000	-0.226522000000
C	1.548041000000	1.683951000000	0.867931000000
C	1.525269000000	0.293035000000	0.426415000000
Rh	-0.666986000000	0.351455000000	1.155017000000
C	-1.700511000000	0.790617000000	-0.893049000000
C	-1.822518000000	-0.528211000000	-1.399683000000
C	-1.856589000000	-1.636038000000	-0.526383000000
C	-1.359764000000	-1.445075000000	0.748681000000
H	1.526238000000	3.621990000000	-0.194173000000
H	1.653126000000	2.005279000000	1.898916000000
H	1.990333000000	-0.505098000000	0.997694000000
H	-1.797754000000	-0.702951000000	-2.479198000000
H	-1.361385000000	1.539689000000	-1.611639000000
H	-1.324849000000	-2.254300000000	1.478740000000
H	-2.181794000000	-2.620114000000	-0.868979000000
H	1.828126000000	-1.712529000000	-1.729381000000
H	1.874935000000	-1.070360000000	-4.139378000000
H	1.722443000000	1.317332000000	-4.841089000000
H	1.669933000000	3.129880000000	-3.114800000000
C	-0.374297000000	-0.030188000000	2.976688000000
O	-0.232726000000	-0.310200000000	4.089952000000

### CO-anti-Cr@Ind-h

$$E = -5649.23 \text{ kcal mol}^{-1}$$

C	1.308821000000	3.312495000000	2.277462000000
C	-0.056074000000	2.952830000000	2.523885000000
C	-1.122199000000	3.586721000000	1.758862000000
C	-0.795746000000	4.570333000000	0.770663000000
C	0.561422000000	4.815520000000	0.469758000000
C	1.608023000000	4.184805000000	1.210635000000
C	-2.376986000000	3.015236000000	2.205898000000
C	-2.084241000000	2.156945000000	3.321002000000
C	-0.685637000000	2.038325000000	3.466206000000
Rh	-1.451981000000	1.045224000000	1.379802000000
C	-1.739942000000	1.255962000000	-0.632446000000
C	-1.979321000000	0.387187000000	-1.633787000000
C	-0.360024000000	-0.461347000000	1.141166000000
O	0.354393000000	-1.364573000000	1.056079000000
C	-3.152334000000	-0.085146000000	1.376372000000
C	-3.549491000000	-1.121522000000	0.617037000000
C	-2.957577000000	-1.689358000000	-0.585002000000
C	-2.280438000000	-1.033714000000	-1.564165000000
H	-3.361671000000	3.345616000000	1.900636000000
H	-3.173298000000	-2.744996000000	-0.754363000000
H	-4.452304000000	-1.636111000000	0.965952000000
H	-2.005276000000	-1.613535000000	-2.446146000000
H	-1.917711000000	0.790863000000	-2.650535000000

H	-3.762852000000	0.196301000000	2.235771000000	H	-2.913030000000	-2.872738000000	-0.600118000000
H	-1.557260000000	2.303623000000	-0.892172000000	H	-4.469886000000	-1.588035000000	0.793296000000
H	-2.821029000000	1.662306000000	3.941871000000	H	-1.620110000000	-1.771615000000	-2.290098000000
H	-0.166762000000	1.458457000000	4.219354000000	H	-1.833260000000	0.650538000000	-2.622660000000
H	-1.580574000000	5.089857000000	0.229902000000	H	-4.040014000000	0.589334000000	1.648002000000
H	0.817398000000	5.535488000000	-0.301187000000	H	-2.101737000000	2.232706000000	-0.859696000000
H	2.641435000000	4.433544000000	0.992320000000	H	-2.738807000000	1.640828000000	3.989621000000
H	2.107240000000	2.877446000000	2.870573000000	H	-0.064437000000	1.404414000000	4.085548000000
Cr	0.281669000000	5.308531000000	2.648255000000	H	-1.691268000000	5.173175000000	0.314545000000
C	0.839838000000	5.250457000000	4.422654000000	H	0.673617000000	5.652761000000	-0.324627000000
C	-1.204663000000	6.302027000000	3.170596000000	H	2.566100000000	4.515382000000	0.836367000000
C	1.230235000000	6.877311000000	2.439701000000	H	2.134030000000	2.876456000000	2.670589000000
O	1.193248000000	5.199991000000	5.532607000000	Cr	0.287572000000	5.314593000000	2.641856000000
O	1.836718000000	7.864427000000	2.292819000000	C	0.874599000000	5.173491000000	4.401463000000
O	-2.143597000000	6.914230000000	3.490115000000	C	-1.164425000000	6.318148000000	3.229979000000
				C	1.264520000000	6.872020000000	2.474673000000
				O	1.243108000000	5.068946000000	5.502990000000
				O	1.888395000000	7.851568000000	2.352104000000
				O	-2.084958000000	6.937214000000	3.589724000000

### CO-anti-Cr@Ind-TS(h,4)

$$E = -5647.57 \text{ kcal mol}^{-1} \quad -251.10 \text{ cm}^{-1}$$

C	1.304705000000	3.333070000000	2.139261000000
C	-0.043872000000	2.966473000000	2.446159000000
C	-1.145749000000	3.626124000000	1.768126000000
C	-0.877056000000	4.639773000000	0.795196000000
C	0.461384000000	4.904634000000	0.432506000000
C	1.545756000000	4.253660000000	1.097242000000
C	-2.375945000000	3.030103000000	2.264169000000
C	-2.035747000000	2.141429000000	3.335412000000
C	-0.625267000000	1.997976000000	3.374200000000
Rh	-1.484466000000	1.062986000000	1.390673000000
C	-1.990890000000	1.176012000000	-0.600529000000
C	-1.921264000000	0.262805000000	-1.602459000000
C	-0.396653000000	-0.463025000000	1.228461000000
O	0.343185000000	-1.351587000000	1.241057000000
C	-3.271952000000	0.102970000000	1.044288000000
C	-3.534760000000	-1.105454000000	0.490382000000
C	-2.765004000000	-1.796735000000	-0.512332000000
C	-2.024030000000	-1.167217000000	-1.478482000000
H	-3.374825000000	3.365569000000	2.012719000000

### CO-anti-Cr@Ind-4

$$E = -5695.62 \text{ kcal/mol}$$

H	-1.361731000000	2.786196000000	1.926957000000
H	-2.007291000000	0.179715000000	2.049412000000
C	0.476476000000	-1.555489000000	2.323673000000
H	-4.176736000000	1.320338000000	-0.948056000000
H	-4.554411000000	-0.943236000000	-0.004529000000
H	-2.799821000000	-2.699966000000	-0.222235000000
H	1.305448000000	2.971541000000	1.566302000000
C	2.661038000000	0.275129000000	1.959138000000
H	-2.133418000000	1.784845000000	-2.276536000000
H	-0.689956000000	-2.212666000000	-1.431378000000
H	-0.404725000000	-0.027561000000	-2.585694000000
C	2.906970000000	-1.114664000000	2.183358000000
C	1.831699000000	-2.009626000000	2.374961000000
H	3.492742000000	0.964107000000	1.845817000000
H	3.928094000000	-1.475643000000	2.250740000000

H	2.035956000000	-3.054412000000	2.587033000000
H	-0.338317000000	-2.253064000000	2.491240000000
C	0.577030000000	2.440254000000	-1.460565000000
O	1.124971000000	3.195128000000	-2.156637000000
C	1.332371000000	0.731233000000	1.883569000000
C	0.223873000000	-0.195885000000	2.065758000000
C	-3.405636000000	0.557551000000	-1.028625000000
C	-2.198779000000	0.861324000000	-1.709855000000
C	-1.207868000000	-0.148892000000	-1.864147000000
C	-3.617580000000	-0.710867000000	-0.506420000000
C	-2.623672000000	-1.707795000000	-0.632169000000
C	-1.437809000000	-1.434019000000	-1.300015000000
C	0.740189000000	2.047476000000	1.592743000000
C	-1.011677000000	0.574342000000	1.887054000000
C	-0.676934000000	1.953874000000	1.820820000000
Rh	-0.288788000000	1.326970000000	-0.241833000000
Cr	1.664669000000	-0.379895000000	3.926710000000
C	3.155517000000	0.170566000000	4.879008000000
C	0.628666000000	0.831027000000	4.878704000000
C	1.350112000000	-1.651558000000	5.237223000000
O	1.152971000000	-2.466211000000	6.050420000000
O	4.105840000000	0.512142000000	5.465673000000
O	-0.033515000000	1.600236000000	5.456094000000

## Acetylene

$$E = -508.77 \text{ kcal mol}^{-1}$$

## Benzene

$$E = -1666.21 \text{ kcal mol}^{-1}$$

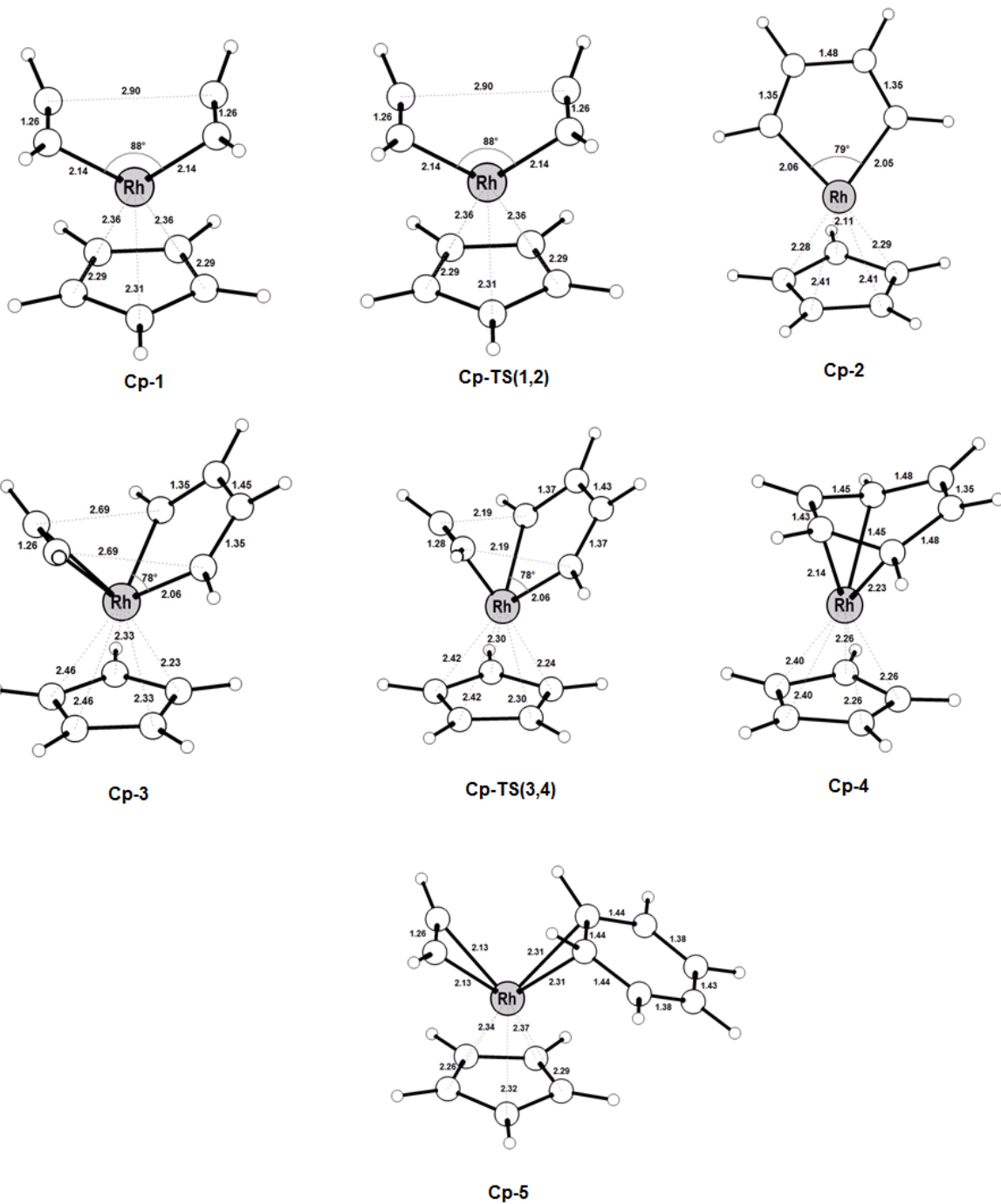


**Figure A2.** Optimized structures with selected interatomic distances ( $\text{\AA}$ ) and angles (deg) of the intermediates and transition states located on the PES of the CpRh catalyzed acetylene [2+2+2] cycloaddition to benzene (Path I, Scheme 6a). Level of theory: ZORA-BLYP/TZ2P.

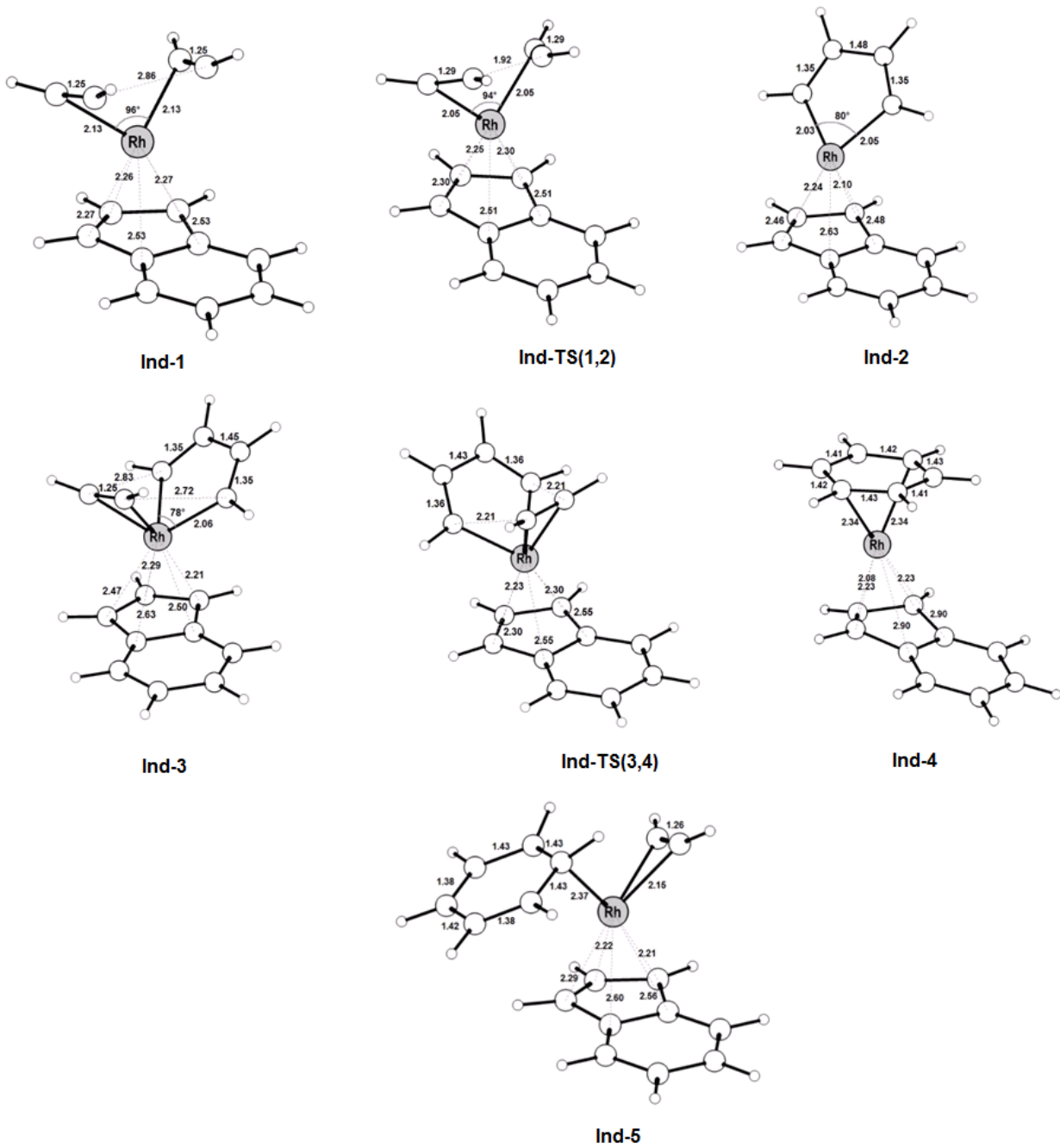


**Figure A3.** Optimized structures with selected interatomic distances ( $\text{\AA}$ ) and angles (deg) of the intermediates and transition states located on the PES of the InRh catalyzed acetylene [2+2+2] cycloaddition to benzene (Path I, Scheme 6a). Level of theory: ZORA-BLYP/TZ2P.

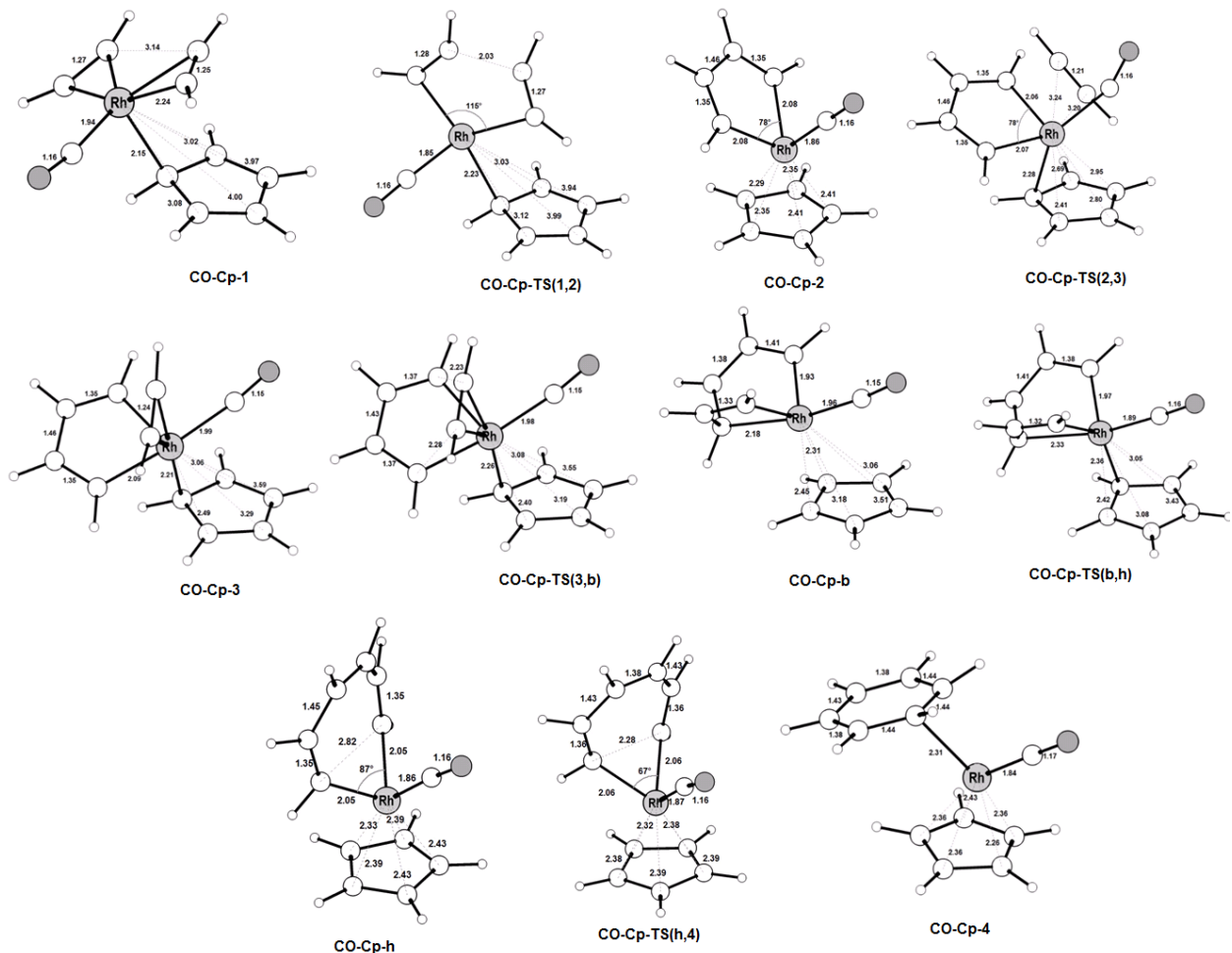


**Figure A4.** Optimized structures with selected interatomic distances ( $\text{\AA}$ ) and angles (deg) of the intermediates and transition states located on the PES of the  $\text{CpRh}(\text{CO})$  catalyzed acetylene [2+2+2] cycloaddition to benzene (Path II, Scheme 6b). Level of theory: ZORA-BLYP/TZ2P.

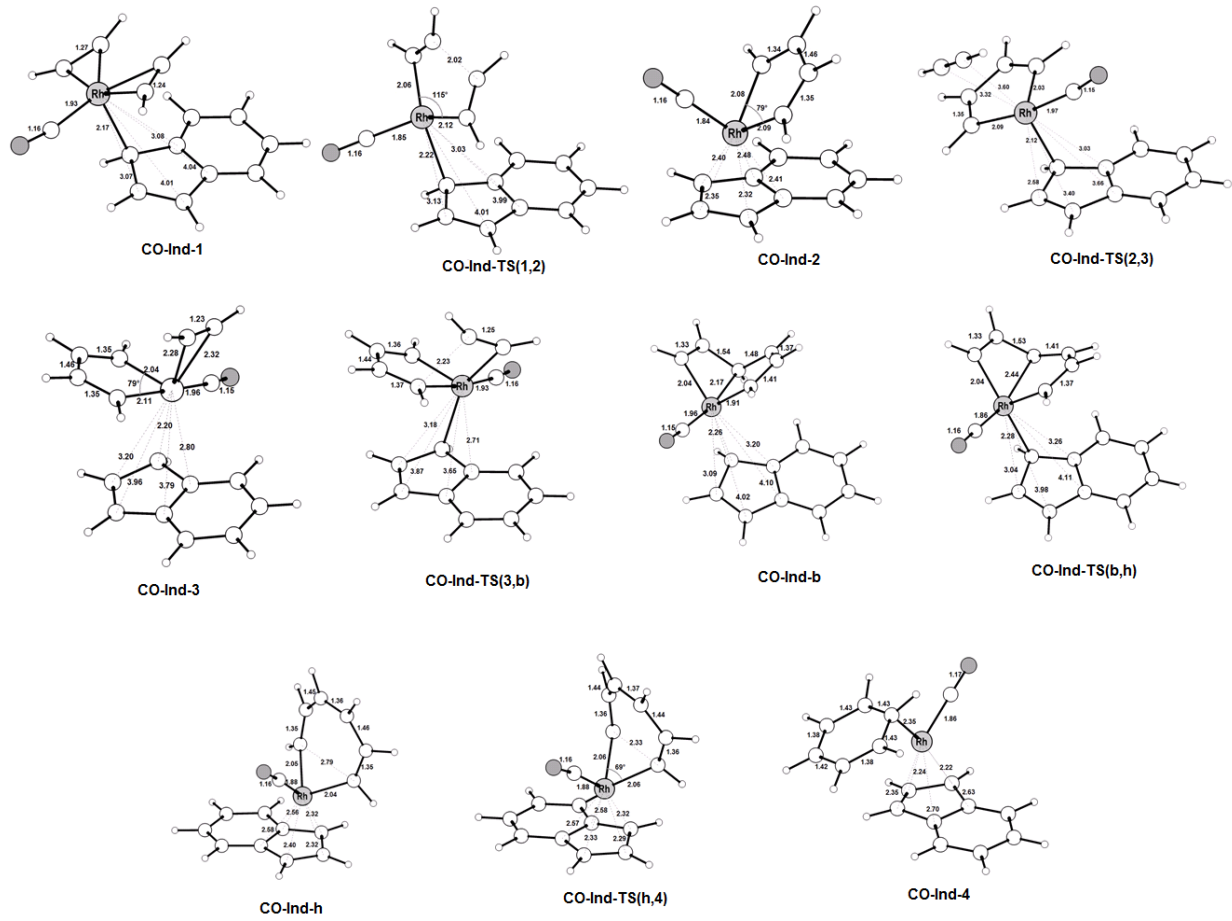


**Figure A5.** Optimized structures with selected interatomic distances ( $\text{\AA}$ ) and angles (deg) of the intermediates and transition states located on the PES of the IndRh(CO) catalyzed acetylene [2+2+2] cycloaddition to benzene (Path II, Scheme 6b). Level of theory: ZORA-BLYP/TZ2P.



# Appendix B

## Associated to Chapter 4

**Table B1.** Cartesian coordinates (in Å) and ADF total energies (in kcal mol<sup>-1</sup>) of all stationary points as well as imaginary frequencies of transition states (in cm<sup>-1</sup>) along the Path I catalyzed by anti-[Mo(CO)<sub>3</sub>IndRh], computed at ZORA-BLYP/TZ2P.

### Mo@Ind-1

E = -4728.50 kcal mol<sup>-1</sup>

C	-0.001142000000	0.067742000000	-0.723186000000
C	0.839917000000	-1.045527000000	-1.149337000000
C	1.205416000000	-1.808524000000	0.000000000000
Rh	2.602418000000	-0.049083000000	0.000000000000
C	3.785040000000	1.045986000000	1.408855000000
C	3.799324000000	-0.169967000000	1.732286000000
C	3.799324000000	-0.169967000000	-1.732286000000
C	3.785039000000	1.045986000000	-1.408855000000
H	0.968700000000	-1.358419000000	-2.178754000000
H	1.660147000000	-2.790915000000	0.000000000000
H	0.968700000000	-1.358419000000	2.178754000000
H	4.114044000000	2.068028000000	-1.481477000000
H	4.052852000000	-1.001649000000	-2.368001000000
H	4.052852000000	-1.001649000000	2.368001000000
H	4.114045000000	2.068028000000	1.481478000000
C	-0.708551000000	1.083454000000	-1.439605000000
C	-0.708550000000	1.083454000000	1.439605000000
C	-1.329411000000	2.126664000000	-0.716479000000
C	-1.329410000000	2.126665000000	0.716479000000
H	-0.725641000000	1.084319000000	2.525294000000
H	-1.835827000000	2.924848000000	1.249794000000
H	-1.835828000000	2.924848000000	-1.249794000000
H	-0.725642000000	1.084319000000	-2.525295000000
C	-4.244961000000	0.894748000000	0.000000000000

C -3.091576000000 -1.170504000000 1.384355000000

C -3.091576000000 -1.170503000000 -1.384355000000

O -5.298830000000 1.402512000000 0.000000000000

O -3.440591000000 -1.907955000000 2.220923000000

O -3.440590000000 -1.907954000000 -2.220923000000

Mo -2.441553000000 0.098903000000 0.000000000000

C 0.839917000000 -1.045527000000 1.149336000000

C -0.001141000000 0.067742000000 0.723186000000

### Mo@Ind-TS(1,2)

E = -4713.70 kcal mol<sup>-1</sup> -450.29 cm<sup>-1</sup>

C	0.304627000000	-0.093817000000	-0.732890000000
C	1.046336000000	-1.252212000000	-1.160387000000
C	1.436125000000	-1.994330000000	0.000000000000
Rh	2.737451000000	-0.156670000000	0.000000000000
C	4.173512000000	1.175618000000	0.961305000000
C	4.123923000000	0.002172000000	1.501040000000
C	4.123923000000	0.002172000000	-1.501040000000
C	4.173512000000	1.175618000000	-0.961305000000
H	1.188074000000	-1.564658000000	-2.187473000000
H	1.905661000000	-2.969719000000	0.000000000000
H	1.188074000000	-1.564658000000	2.187473000000
H	4.275520000000	2.222530000000	-1.221002000000
H	4.446539000000	-0.628311000000	-2.314432000000
H	4.446539000000	-0.628311000000	2.314432000000
H	4.275520000000	2.222530000000	1.221002000000

C	-0.380150000000	0.953824000000	-1.442657000000	H	-4.123680000000	1.232747000000	-0.321194000000
C	-0.380150000000	0.953824000000	1.442657000000	H	-2.239321000000	2.193226000000	1.120758000000
C	-0.918667000000	2.036434000000	-0.718074000000	H	1.901483000000	-1.739450000000	-2.253918000000
C	-0.918667000000	2.036434000000	0.718074000000	H	0.777201000000	-0.737239000000	-4.244008000000
H	-0.409038000000	0.952192000000	2.528023000000	H	-0.140187000000	1.579642000000	-4.171541000000
H	-1.377503000000	2.864792000000	1.248486000000	H	0.052030000000	2.968547000000	-2.105567000000
H	-1.377503000000	2.864792000000	-1.248486000000	C	-2.911167000000	-0.604247000000	-0.726182000000
H	-0.409038000000	0.952192000000	-2.528023000000	C	-1.719030000000	-1.148974000000	-0.426660000000
C	-3.902567000000	1.058766000000	0.000000000000	H	-3.644277000000	-1.111675000000	-1.356968000000
C	-2.946897000000	-1.081108000000	1.399343000000	H	-1.373068000000	-2.135493000000	-0.732737000000
C	-2.946897000000	-1.081108000000	-1.399343000000	Mo	2.672428000000	1.303753000000	-2.835181000000
O	-4.912555000000	1.650497000000	0.000000000000	C	3.168683000000	1.500635000000	-4.721242000000
O	-3.365428000000	-1.770919000000	2.243296000000	C	4.489229000000	0.531289000000	-2.534193000000
O	-3.365428000000	-1.770919000000	-2.243296000000	C	3.428939000000	3.128290000000	-2.548959000000
Mo	-2.183979000000	0.112951000000	0.000000000000	O	3.437832000000	1.607392000000	-5.854525000000
C	1.046336000000	-1.252212000000	1.160387000000	O	3.840610000000	4.204106000000	-2.367840000000
C	0.304627000000	-0.093817000000	0.732890000000	O	5.535049000000	0.052302000000	-2.344291000000

## Mo@Ind-2

$$E = -5117.75 \text{ kcal mol}^{-1}$$

C	1.917427000000	-0.350115000000	0.373365000000
C	1.460811000000	-0.027704000000	-0.944950000000
C	0.914173000000	1.341041000000	-0.901117000000
C	1.092447000000	1.832529000000	0.450861000000
C	1.724266000000	0.805640000000	1.202498000000
C	0.428020000000	1.950712000000	-2.118633000000
C	0.309615000000	1.160758000000	-3.277145000000
C	0.839138000000	-0.173737000000	-3.318393000000
C	1.481916000000	-0.739861000000	-2.200219000000
Rh	-0.449115000000	0.092781000000	0.660083000000
C	-1.077111000000	-0.770766000000	2.162066000000
O	-1.471512000000	-1.296302000000	3.114470000000
C	-2.182303000000	1.247119000000	0.583916000000
C	-3.174038000000	0.719498000000	-0.156176000000
H	0.857144000000	2.830942000000	0.795702000000
H	2.024162000000	0.884816000000	2.240432000000
H	2.398758000000	-1.273458000000	0.669210000000

## Mo@Ind-3

$$E = -5280.85 \text{ kcal mol}^{-1}$$

C	-2.413448000000	0.205661000000	-0.017121000000
C	-1.199547000000	0.077562000000	-0.725582000000
C	0.037289000000	0.063286000000	0.004481000000
C	0.019655000000	0.083587000000	1.461412000000
C	-1.237201000000	0.080774000000	2.158529000000
C	-2.432040000000	0.201706000000	1.417600000000
C	1.425398000000	0.051300000000	-0.411391000000
C	2.235946000000	-0.002653000000	0.742662000000
C	1.402299000000	0.116955000000	1.912782000000
Rh	1.441164000000	2.137732000000	0.968148000000
C	1.023236000000	3.203192000000	2.683308000000
C	2.092805000000	3.765740000000	3.285180000000
C	3.361411000000	3.540569000000	2.610915000000
C	3.295150000000	2.791189000000	1.491577000000
H	1.771579000000	0.004299000000	-1.436743000000
H	3.312029000000	-0.120460000000	0.755314000000
H	1.732670000000	0.002599000000	2.937090000000

H	4.131588000000	2.544942000000	0.837965000000	H	3.175360000000	-0.100617000000	1.694111000000
H	-0.006851000000	3.293775000000	3.033377000000	H	1.129528000000	0.115520000000	3.442653000000
H	4.303139000000	3.950221000000	2.981302000000	H	2.948901000000	3.014791000000	-0.936924000000
H	2.022367000000	4.343425000000	4.208505000000	H	1.808631000000	3.187357000000	3.710212000000
H	-1.262585000000	0.060081000000	3.243515000000	H	4.532888000000	4.370030000000	0.536296000000
H	-3.383657000000	0.259907000000	1.936404000000	H	3.917513000000	4.462652000000	3.045552000000
H	-3.350298000000	0.270786000000	-0.561195000000	H	-1.844259000000	0.091382000000	3.069149000000
H	-1.197491000000	0.056749000000	-1.811078000000	H	-3.618002000000	0.227708000000	1.316626000000
C	0.630468000000	3.930057000000	0.098985000000	H	-3.028821000000	0.143073000000	-1.108178000000
C	1.548926000000	3.552208000000	-0.663294000000	H	-0.651329000000	-0.081060000000	-1.839252000000
H	-0.107682000000	4.608524000000	0.487622000000	C	0.447384000000	3.959100000000	1.544388000000
H	2.231320000000	3.606687000000	-1.492375000000	C	0.752148000000	3.912438000000	0.295902000000
C	-3.163090000000	-2.861069000000	0.714629000000	H	-0.135789000000	4.399602000000	2.334817000000
C	-0.818806000000	-3.167123000000	2.096778000000	H	0.606418000000	4.286591000000	-0.702931000000
C	-0.832055000000	-3.165000000000	-0.686064000000	C	-3.129379000000	-2.917022000000	0.264639000000
O	-4.196248000000	-3.409210000000	0.715510000000	C	-1.195681000000	-3.164209000000	2.177980000000
O	-0.434698000000	-3.886466000000	2.931502000000	C	-0.541415000000	-3.262096000000	-0.539201000000
O	-0.456698000000	-3.882763000000	-1.526455000000	O	-4.136157000000	-3.470948000000	0.043078000000
Mo	-1.453669000000	-1.886813000000	0.708986000000	O	-1.034529000000	-3.849580000000	3.109159000000
				O	0.012779000000	-4.007507000000	-1.246329000000
				Mo	-1.465479000000	-1.940580000000	0.629750000000

### Mo@Ind-TS(3,4)

$$E = -5275.95 \text{ kcal mol}^{-1} \quad -332.71 \text{ cm}^{-1}$$

C	-2.235472000000	0.116064000000	-0.367968000000
C	-0.894536000000	-0.018573000000	-0.782940000000
C	0.152781000000	0.035842000000	0.201607000000
C	-0.192345000000	0.086070000000	1.621293000000
C	-1.575110000000	0.079941000000	2.017307000000
C	-2.574171000000	0.164759000000	1.025889000000
C	1.592106000000	0.054844000000	0.107514000000
C	2.132156000000	0.028088000000	1.435819000000
C	1.043663000000	0.135162000000	2.363353000000
Rh	1.362491000000	2.100603000000	1.174133000000
C	2.188088000000	3.234151000000	2.691547000000
C	3.323067000000	3.895794000000	2.327455000000
C	3.664455000000	3.844259000000	0.935946000000
C	2.815475000000	3.139070000000	0.135723000000
H	2.162938000000	-0.036178000000	-0.808175000000

### Mo@Ind-4

$$E = -5349.80 \text{ kcal mol}^{-1}$$

C	0.181541000000	-0.049551000000	-0.046215000000
C	-0.378775000000	0.278119000000	1.258343000000
C	0.766603000000	0.498054000000	2.163125000000
C	1.963754000000	0.009578000000	1.518080000000
C	1.649222000000	-0.017844000000	0.107977000000
Rh	1.901306000000	2.016027000000	0.987676000000
C	1.373567000000	4.205202000000	1.570843000000
C	1.223444000000	4.140754000000	0.163651000000
C	2.311742000000	3.660582000000	-0.605824000000
C	3.576827000000	3.396458000000	0.002432000000
C	3.749597000000	3.577747000000	1.393293000000
C	2.636540000000	3.942289000000	2.184063000000
H	0.653420000000	0.607912000000	3.236985000000

H	2.853546000000	-0.382118000000	1.998607000000	C	3.140570000000	3.452135000000	0.480458000000
H	2.327860000000	-0.371090000000	-0.661881000000	C	1.967782000000	3.634094000000	-0.307007000000
H	0.531080000000	4.497742000000	2.191359000000	C	1.878970000000	2.985068000000	-1.573110000000
H	0.277481000000	4.389759000000	-0.306336000000	C	2.925863000000	2.207563000000	-2.041301000000
H	2.199068000000	3.529609000000	-1.678465000000	C	4.105980000000	2.058228000000	-1.270948000000
H	2.738356000000	4.033932000000	3.261535000000	C	4.210949000000	2.667011000000	-0.031435000000
H	4.716689000000	3.399517000000	1.854781000000	H	2.600255000000	0.032934000000	2.913547000000
H	4.408263000000	3.064768000000	-0.612677000000	H	0.066163000000	0.678704000000	3.623883000000
C	-0.659543000000	-0.250436000000	-1.148768000000	C	-1.869981000000	0.361806000000	1.278848000000
C	-1.765075000000	0.396980000000	1.425089000000	H	1.278697000000	4.442685000000	-0.084581000000
C	-2.082295000000	-0.111593000000	-0.976602000000	H	0.995668000000	3.141667000000	-2.188506000000
C	-2.624469000000	0.205618000000	0.285832000000	H	2.856713000000	1.732800000000	-3.017846000000
H	-2.195191000000	0.641299000000	2.392182000000	H	2.651025000000	-0.267678000000	0.233475000000
H	-3.698903000000	0.304838000000	0.403646000000	C	-0.165738000000	-0.270674000000	-0.950356000000
H	-2.740620000000	-0.256003000000	-1.827384000000	H	3.321921000000	4.090737000000	1.338716000000
H	-0.254302000000	-0.495198000000	-2.126460000000	H	4.935534000000	1.474253000000	-1.664187000000
C	-2.840116000000	-2.730537000000	1.665640000000	H	5.126849000000	2.576294000000	0.548622000000
C	-0.096049000000	-3.049355000000	1.408861000000	H	1.943780000000	3.493949000000	4.039502000000
C	-1.783801000000	-3.343527000000	-0.775005000000	H	-0.313223000000	4.620269000000	2.088213000000
O	-3.679348000000	-3.195333000000	2.335078000000	C	-1.560152000000	-0.106729000000	-1.125904000000
O	0.730401000000	-3.691923000000	1.929316000000	C	-2.408820000000	0.223071000000	-0.020864000000
O	-1.987920000000	-4.176131000000	-1.570973000000	H	0.466235000000	-0.524076000000	-1.795535000000
Mo	-1.454192000000	-1.889336000000	0.528404000000	H	-1.997086000000	-0.244891000000	-2.109993000000
				H	-3.477498000000	0.327942000000	-0.177826000000
				H	-2.520106000000	0.587766000000	2.118860000000
				C	-2.683207000000	-3.030295000000	-0.412440000000
				C	-1.876111000000	-2.753051000000	2.190196000000
				C	-0.032892000000	-3.372138000000	0.224669000000
				O	-3.495147000000	-3.668942000000	-0.961655000000
				O	-2.195552000000	-3.218460000000	3.213364000000
				O	0.763931000000	-4.211342000000	0.062324000000
				Mo	-1.339636000000	-1.896139000000	0.479027000000

## Mo@Ind-5

E = -5869.45 kcal mol<sup>-1</sup>

C	-0.454109000000	0.279278000000	1.460983000000				
C	0.418999000000	0.519528000000	2.611308000000				
C	1.762920000000	0.160920000000	2.239181000000				
C	1.785199000000	0.001139000000	0.826101000000				
C	0.402278000000	-0.042953000000	0.341093000000				
Rh	1.332966000000	2.177441000000	1.463807000000				
C	1.367221000000	3.504301000000	3.129250000000				
C	0.464444000000	3.926157000000	2.361753000000				

**Table B2.** Cartesian coordinates (in Å) and ADF total energies (in kcal mol<sup>-1</sup>) of all stationary points as well as imaginary frequencies of transition states (in cm<sup>-1</sup>) along the Path I catalyzed by anti-[W(CO)<sub>3</sub>IndRh], computed at ZORA-BLYP/TZ2P.

**anti-W@Ind-1**

$$E = -4724.41 \text{ kcal mol}^{-1}$$

C	-0.024672000000	0.078169000000	-0.723193000000
C	0.825883000000	-1.029893000000	-1.148286000000
C	1.190863000000	-1.793929000000	0.000189000000
Rh	2.609795000000	-0.057927000000	0.000052000000
C	3.796950000000	1.021904000000	1.411278000000
C	3.764127000000	-0.187999000000	1.757656000000
C	3.764298000000	-0.188588000000	-1.757393000000
C	3.797084000000	1.021432000000	-1.411420000000
H	0.952250000000	-1.344084000000	-2.177545000000
H	1.640316000000	-2.778767000000	0.000286000000
H	0.952186000000	-1.343680000000	2.177830000000
H	4.166580000000	2.030396000000	-1.473175000000
H	3.977685000000	-1.015175000000	-2.414254000000
H	3.977444000000	-1.014365000000	2.414817000000
H	4.166440000000	2.030889000000	1.472726000000
C	-0.740396000000	1.089406000000	-1.441077000000
C	-0.740402000000	1.089678000000	1.440886000000
C	-1.363951000000	2.136211000000	-0.717532000000
C	-1.363991000000	2.136314000000	0.717127000000
H	-0.762498000000	1.087136000000	2.526227000000
H	-1.876313000000	2.929843000000	1.251211000000
H	-1.876250000000	2.929652000000	-1.251767000000
H	-0.762480000000	1.086662000000	-2.526419000000
C	-4.256348000000	0.877288000000	0.000312000000
C	-3.060100000000	-1.174122000000	1.384956000000
C	-3.060514000000	-1.173703000000	-1.385227000000
O	-5.314750000000	1.379992000000	0.000514000000
O	-3.376530000000	-1.920826000000	2.228921000000
O	-3.377219000000	-1.920132000000	-2.229320000000
W	-2.439791000000	0.108958000000	-0.000037000000
C	0.825859000000	-1.029677000000	1.148509000000

C -0.024691000000 0.078305000000 0.723186000000

**anti-W@Ind-TS(1,2)**

$$E = -4709.34 \text{ kcal mol}^{-1} \quad -434.4 \text{ cm}^{-1}$$

C	0.049474000000	-0.077815000000	-0.733141000000
C	0.818029000000	-1.219488000000	-1.159584000000
C	1.223837000000	-1.951861000000	0.001062000000
Rh	2.485359000000	-0.086012000000	-0.000070000000
C	3.888136000000	1.280620000000	0.961435000000
C	3.868109000000	0.105909000000	1.500455000000
C	3.865220000000	0.110995000000	-1.502728000000
C	3.886416000000	1.283832000000	-0.959723000000
H	0.966225000000	-1.529190000000	-2.186505000000
H	1.715020000000	-2.916540000000	0.001438000000
H	0.965989000000	-1.527566000000	2.188294000000
H	3.959913000000	2.333534000000	-1.217865000000
H	4.202746000000	-0.509424000000	-2.317784000000
H	4.207495000000	-0.517553000000	2.312412000000
H	3.962166000000	2.329390000000	1.223183000000
C	-0.665906000000	0.951584000000	-1.443846000000
C	-0.666280000000	0.952437000000	1.443722000000
C	-1.217355000000	2.033925000000	-0.718884000000
C	-1.217557000000	2.034331000000	0.717961000000
H	-0.700173000000	0.947959000000	2.528634000000
H	-1.693267000000	2.852524000000	1.248890000000
H	-1.692911000000	2.851814000000	-1.250417000000
H	-0.699501000000	0.946463000000	-2.528765000000
C	-4.168871000000	0.984454000000	-0.000397000000
C	-3.136240000000	-1.130184000000	1.398758000000
C	-3.136000000000	-1.130745000000	-1.398512000000
O	-5.192330000000	1.557117000000	-0.000625000000
O	-3.512564000000	-1.838223000000	2.250086000000
O	-3.512151000000	-1.839113000000	-2.249579000000

W	-2.421303000000	0.092639000000	-0.000059000000	O	3.442798000000	1.613105000000	-5.855722000000
C	0.817732000000	-1.218694000000	1.161129000000	O	3.818863000000	4.193302000000	-2.314319000000
C	0.049315000000	-0.077376000000	0.733827000000	O	5.503645000000	0.034214000000	-2.287216000000

### anti-W@Ind-2

$$E = -5113.20 \text{ kcal mol}^{-1}$$

C	1.928855000000	-0.348947000000	0.369691000000
C	1.473917000000	-0.022919000000	-0.948874000000
C	0.930099000000	1.348598000000	-0.902056000000
C	1.108858000000	1.835773000000	0.451590000000
C	1.737659000000	0.805313000000	1.200625000000
C	0.451309000000	1.964686000000	-2.121999000000
C	0.309969000000	1.168338000000	-3.280326000000
C	0.836881000000	-0.167239000000	-3.324505000000
C	1.498242000000	-0.730659000000	-2.208827000000
Rh	-0.436625000000	0.096793000000	0.656434000000
C	-1.069091000000	-0.759263000000	2.160324000000
O	-1.466175000000	-1.280707000000	3.113862000000
C	-2.171035000000	1.248507000000	0.567029000000
C	-3.157711000000	0.715751000000	-0.176082000000
H	0.876152000000	2.833989000000	0.798602000000
H	2.036806000000	0.881293000000	2.239053000000
H	2.408314000000	-1.273826000000	0.663538000000
H	-4.106794000000	1.227133000000	-0.349899000000
H	-2.232216000000	2.197390000000	1.098477000000
H	1.918318000000	-1.729551000000	-2.266028000000
H	0.769775000000	-0.731254000000	-4.249235000000
H	-0.143552000000	1.589222000000	-4.171685000000
H	0.081219000000	2.984385000000	-2.107970000000
C	-2.890450000000	-0.611150000000	-0.737226000000
C	-1.699975000000	-1.153794000000	-0.427741000000
H	-3.619460000000	-1.122323000000	-1.369757000000
H	-1.351646000000	-2.141900000000	-0.725917000000
W	2.658301000000	1.299536000000	-2.840136000000
C	3.173727000000	1.505201000000	-4.720160000000
C	4.467548000000	0.525183000000	-2.508782000000
C	3.416458000000	3.117240000000	-2.524795000000

### anti-W@Ind-3

$$E = -5276.63 \text{ kcal mol}^{-1}$$

C	-2.425507000000	0.192366000000	-0.023222000000
C	-1.206392000000	0.054970000000	-0.729971000000
C	0.030598000000	0.048257000000	0.003980000000
C	0.009668000000	0.070891000000	1.461982000000
C	-1.249971000000	0.061752000000	2.157565000000
C	-2.447081000000	0.189250000000	1.412673000000
C	1.421044000000	0.039075000000	-0.407924000000
C	2.228267000000	-0.013013000000	0.747744000000
C	1.392186000000	0.110353000000	1.915521000000
Rh	1.438640000000	2.128618000000	0.966904000000
C	1.020243000000	3.190459000000	2.685463000000
C	2.091140000000	3.745583000000	3.291720000000
C	3.360028000000	3.518135000000	2.618418000000
C	3.292596000000	2.773904000000	1.495784000000
H	1.769218000000	-0.011135000000	-1.432384000000
H	3.304146000000	-0.132032000000	0.763187000000
H	1.720125000000	-0.003238000000	2.940647000000
H	4.128432000000	2.526993000000	0.841648000000
H	-0.010206000000	3.284481000000	3.033725000000
H	4.302841000000	3.922825000000	2.991443000000
H	2.021704000000	4.319579000000	4.217419000000
H	-1.278105000000	0.037668000000	3.242121000000
H	-3.399436000000	0.244873000000	1.929959000000
H	-3.360867000000	0.253612000000	-0.569859000000
H	-1.202521000000	0.027840000000	-1.815039000000
C	0.638310000000	3.924890000000	0.097716000000
C	1.537066000000	3.528679000000	-0.678620000000
H	-0.082844000000	4.617032000000	0.494157000000
H	2.202994000000	3.566810000000	-1.521910000000
C	-3.156062000000	-2.866263000000	0.720037000000
C	-0.795464000000	-3.140993000000	2.096692000000

C	-0.816744000000	-3.145416000000	-0.685232000000
O	-4.192189000000	-3.413146000000	0.724639000000
O	-0.388849000000	-3.840669000000	2.940027000000
O	-0.424533000000	-3.848531000000	-1.532869000000
W	-1.455529000000	-1.875019000000	0.708407000000

C	-3.124728000000	-2.916938000000	0.296190000000
C	-1.157387000000	-3.146216000000	2.188948000000
C	-0.532687000000	-3.224546000000	-0.533484000000
O	-4.135459000000	-3.470283000000	0.079402000000
O	-0.965461000000	-3.821649000000	3.123921000000
O	0.038431000000	-3.946392000000	-1.254617000000
W	-1.467849000000	-1.923844000000	0.648306000000

### anti-W@Ind-TS(3,4)

$$E = -5271.61 \text{ kcal mol}^{-1} \quad -331.78 \text{ cm}^{-1}$$

C	-2.255873000000	0.114632000000	-0.333122000000
C	-0.915181000000	-0.028847000000	-0.762357000000
C	0.144150000000	0.033113000000	0.211766000000
C	-0.185930000000	0.077097000000	1.636203000000
C	-1.566278000000	0.056870000000	2.047515000000
C	-2.579823000000	0.156726000000	1.065177000000
C	1.582775000000	0.059800000000	0.102712000000
C	2.136974000000	0.030298000000	1.424714000000
C	1.058663000000	0.130599000000	2.364405000000
Rh	1.360282000000	2.101784000000	1.178400000000
C	2.205867000000	3.228163000000	2.690156000000
C	3.335490000000	3.891464000000	2.313494000000
C	3.658111000000	3.846758000000	0.917040000000
C	2.798681000000	3.145938000000	0.124447000000
H	2.143759000000	-0.026481000000	-0.819440000000
H	3.183372000000	-0.095887000000	1.671051000000
H	1.156136000000	0.106958000000	3.442563000000
H	2.917953000000	3.027045000000	-0.950465000000
H	1.839861000000	3.176535000000	3.713443000000
H	4.521633000000	4.373888000000	0.508636000000
H	3.940119000000	4.454373000000	3.026152000000
H	-1.824456000000	0.058071000000	3.101858000000
H	-3.620085000000	0.216360000000	1.368363000000
H	-3.056231000000	0.142998000000	-1.065384000000
H	-0.683530000000	-0.092076000000	-1.820935000000
C	0.447884000000	3.956385000000	1.567909000000
C	0.737728000000	3.915763000000	0.315405000000
H	-0.125022000000	4.394478000000	2.367198000000
H	0.581218000000	4.295976000000	-0.679568000000

### anti-W@Ind-4

$$E = -5346.11 \text{ kcal mol}^{-1}$$

C	0.176394000000	-0.061902000000	-0.046762000000
C	-0.385024000000	0.266266000000	1.258113000000
C	0.759931000000	0.487025000000	2.163146000000
C	1.957421000000	-0.001641000000	1.518768000000
C	1.643945000000	-0.029869000000	0.108531000000
Rh	1.896603000000	2.004187000000	0.988631000000
C	1.368141000000	4.192624000000	1.572525000000
C	1.218421000000	4.128827000000	0.165154000000
C	2.307173000000	3.650081000000	-0.604588000000
C	3.571922000000	3.385069000000	0.003733000000
C	3.743737000000	3.563648000000	1.395141000000
C	2.630680000000	3.928695000000	2.185985000000
H	0.645679000000	0.595010000000	3.237060000000
H	2.845587000000	-0.395985000000	2.000128000000
H	2.322437000000	-0.385628000000	-0.660244000000
H	0.525386000000	4.484719000000	2.192889000000
H	0.272483000000	4.377773000000	-0.304914000000
H	2.194653000000	3.520139000000	-1.677376000000
H	2.732237000000	4.019311000000	3.263557000000
H	4.710457000000	3.384103000000	1.856898000000
H	4.403571000000	3.053930000000	-0.611368000000
C	-0.666160000000	-0.266401000000	-1.151375000000
C	-1.774550000000	0.381988000000	1.424923000000
C	-2.091257000000	-0.125803000000	-0.981164000000
C	-2.635336000000	0.192180000000	0.283628000000
H	-2.205380000000	0.619532000000	2.393117000000
H	-3.709921000000	0.285883000000	0.402256000000

H	-2.749156000000	-0.275807000000	-1.830981000000	H	2.636114000000	-0.011127000000	2.843666000000
H	-0.260693000000	-0.517819000000	-2.126990000000	H	0.121671000000	0.643239000000	3.612555000000
C	-2.828410000000	-2.721828000000	1.671549000000	C	-1.864617000000	0.345754000000	1.303256000000
C	-0.081988000000	-3.021198000000	1.405355000000	H	1.264931000000	4.474338000000	-0.008773000000
C	-1.771889000000	-3.337702000000	-0.775641000000	H	0.859098000000	3.224415000000	-2.123584000000
O	-3.668518000000	-3.177716000000	2.349387000000	H	2.661767000000	1.822065000000	-3.085577000000
O	0.761805000000	-3.642559000000	1.928444000000	H	2.633610000000	-0.275986000000	0.160171000000
O	-1.971698000000	-4.166674000000	-1.579318000000	C	-0.200681000000	-0.260899000000	-0.967767000000
W	-1.451184000000	-1.878708000000	0.524801000000	H	3.381251000000	4.080617000000	1.290394000000
				H	4.811322000000	1.525428000000	-1.857429000000
				H	5.133694000000	2.581143000000	0.363516000000
				H	2.140681000000	3.344295000000	4.078136000000

### anti-W@Ind-5

E = -5865.45 kcal mol<sup>-1</sup>

C	-0.444768000000	0.271125000000	1.457357000000	H	-0.159119000000	4.631744000000	2.284294000000
C	0.453406000000	0.501615000000	2.590182000000	C	-1.606256000000	-0.105773000000	-1.109901000000
C	1.788499000000	0.138648000000	2.186620000000	C	-2.433885000000	0.235321000000	0.007036000000
C	1.782214000000	-0.003909000000	0.771895000000	H	0.412494000000	-0.511300000000	-1.827002000000
C	0.388750000000	-0.044976000000	0.314883000000	H	-2.061978000000	-0.245754000000	-2.085171000000
Rh	1.378777000000	2.170221000000	1.476529000000	H	-3.505051000000	0.341671000000	-0.127310000000
C	1.527703000000	3.416974000000	3.194889000000	H	-2.498451000000	0.558856000000	2.158881000000
C	0.605810000000	3.900612000000	2.488662000000	C	-2.536039000000	-3.064150000000	-0.543318000000
C	3.154863000000	3.471479000000	0.421508000000	C	-2.071718000000	-2.711784000000	2.128850000000
C	1.941836000000	3.675122000000	-0.293825000000	C	0.034503000000	-3.297648000000	0.434203000000
C	1.775512000000	3.052194000000	-1.563331000000	O	-3.259734000000	-3.729369000000	-1.181113000000
C	2.789953000000	2.277702000000	-2.105915000000	O	-2.507097000000	-3.160145000000	3.118574000000
C	4.009448000000	2.107174000000	-1.407595000000	O	0.889192000000	-4.096233000000	0.395921000000
C	4.188151000000	2.690941000000	-0.163159000000	W	-1.346946000000	-1.869516000000	0.482213000000

**Table B3.** Cartesian coordinates (in Å) and ADF total energies (in kcal mol<sup>-1</sup>) of all stationary points as well as imaginary frequencies of transition states (in cm<sup>-1</sup>) along the Path II catalyzed by syn-[Mo(CO)<sub>3</sub>IndRh], computed at ZORA-BLYP/TZ2P

**syn-Mo@Ind-1**

$$E = -4730.10 \text{ kcal mol}^{-1}$$

C	-0.014703000000	1.818787000000	0.757471000000
C	1.378003000000	1.851389000000	1.154987000000
C	2.175449000000	2.069263000000	-0.018649000000
Rh	1.686727000000	-0.073704000000	-0.056128000000
C	1.826319000000	-1.645872000000	-1.555640000000
C	2.850484000000	-0.930523000000	-1.637392000000
C	2.929148000000	-0.999332000000	1.423169000000
C	1.901323000000	-1.711520000000	1.362043000000
H	1.726211000000	1.918648000000	2.178954000000
H	3.221136000000	2.348744000000	-0.038642000000
H	1.614856000000	2.021806000000	-2.195126000000
H	1.252787000000	-2.528108000000	1.625180000000
H	3.894562000000	-0.702830000000	1.794001000000
H	3.796015000000	-0.616512000000	-2.043336000000
H	1.164164000000	-2.450609000000	-1.821277000000
C	-1.238129000000	1.810896000000	1.497514000000
C	-1.311119000000	1.879189000000	-1.369640000000
C	-2.457189000000	2.035855000000	0.813506000000
C	-2.493582000000	2.069962000000	-0.614638000000
H	-1.352916000000	1.879995000000	-2.454695000000
H	-3.439578000000	2.221743000000	-1.124123000000
H	-3.375878000000	2.161959000000	1.377121000000
H	-1.224741000000	1.760020000000	2.582106000000
Mo	-1.752699000000	-0.118808000000	0.029058000000
C	1.319091000000	1.906111000000	-1.159078000000
C	-0.051666000000	1.853206000000	-0.693218000000
C	-1.466771000000	-1.440113000000	-1.422995000000
O	-1.322536000000	-2.201685000000	-2.299361000000
C	-1.394022000000	-1.507279000000	1.400056000000
O	-1.206634000000	-2.309050000000	2.231253000000
C	-3.596093000000	-0.792304000000	0.060878000000

O -4.701390000000 -1.175189000000 0.080723000000

**syn-Mo@Ind-TS(1,2)**

$$E = -4715.01 \text{ kcal mol}^{-1} \quad -446.127 \text{ cm}^{-1}$$

C	0.162222000000	1.905913000000	0.731753000000
C	1.528856000000	1.965194000000	1.161271000000
C	2.362184000000	2.108001000000	0.000000000000
Rh	1.905214000000	-0.057137000000	0.000000000000
C	2.206438000000	-1.989469000000	-0.962414000000
C	2.909881000000	-1.037510000000	-1.483554000000
C	2.909881000000	-1.037510000000	1.483554000000
C	2.206438000000	-1.989469000000	0.962414000000
H	1.859757000000	2.046707000000	2.189318000000
H	3.412284000000	2.370569000000	0.000000000000
H	1.859757000000	2.046707000000	-2.189318000000
H	1.615434000000	-2.850605000000	1.248404000000
H	3.602794000000	-0.740425000000	2.254619000000
H	3.602794000000	-0.740425000000	-2.254619000000
H	1.615434000000	-2.850605000000	-1.248404000000
C	-1.085985000000	1.889223000000	1.436681000000
C	-1.085985000000	1.889223000000	-1.436681000000
C	-2.287112000000	2.072424000000	0.716510000000
C	-2.287112000000	2.072424000000	-0.716510000000
H	-1.102577000000	1.861954000000	-2.522278000000
H	-3.224737000000	2.185983000000	-1.250967000000
H	-3.224737000000	2.185983000000	1.250967000000
H	-1.102577000000	1.861954000000	2.522278000000
Mo	-1.510460000000	-0.081526000000	0.000000000000
C	1.528856000000	1.965194000000	-1.161271000000
C	0.162222000000	1.905913000000	-0.731753000000
C	-1.137561000000	-1.423125000000	-1.417691000000
O	-0.936370000000	-2.201410000000	-2.266505000000
C	-1.137561000000	-1.423125000000	1.417691000000

O	-0.936370000000	-2.201410000000	2.266505000000
C	-3.330110000000	-0.816063000000	0.000000000000
O	-4.420718000000	-1.240280000000	0.000000000000

O	-3.962583000000	-1.900585000000	-1.173799000000
---	-----------------	-----------------	-----------------

### **syn-Mo@Ind-2**

E = -4755.23 kcal mol<sup>-1</sup>

C	-0.218748000000	1.797307000000	0.748450000000
C	1.245235000000	1.841175000000	0.780281000000
C	1.664443000000	2.367190000000	-0.510085000000
Rh	1.477063000000	0.126373000000	-0.486912000000
C	4.207055000000	-0.774519000000	-0.231744000000
C	3.474374000000	0.076497000000	-0.976671000000
C	2.170254000000	-1.170004000000	0.922533000000
C	3.482669000000	-1.461922000000	0.840385000000
H	1.836594000000	1.870751000000	1.688280000000
H	2.671236000000	2.693293000000	-0.736775000000
H	0.574523000000	2.753218000000	-2.411397000000
H	3.974622000000	-2.177031000000	1.503084000000
H	1.474824000000	-1.588548000000	1.651717000000
H	3.850529000000	0.629068000000	-1.840365000000
H	5.264168000000	-0.970200000000	-0.426937000000
C	-1.195955000000	1.482798000000	1.728203000000
C	-2.004487000000	2.089745000000	-0.965365000000
C	-2.580960000000	1.560499000000	1.390226000000
C	-2.966432000000	1.800947000000	0.048522000000
H	-2.329572000000	2.298027000000	-1.979901000000
H	-4.021707000000	1.804340000000	-0.207759000000
H	-3.333309000000	1.378725000000	2.150489000000
H	-0.898347000000	1.245624000000	2.745547000000
Mo	-1.592951000000	-0.201065000000	0.036222000000
C	0.554599000000	2.451832000000	-1.371323000000
C	-0.635979000000	2.144814000000	-0.614745000000
C	-0.341065000000	-1.144520000000	-1.181905000000
O	0.406439000000	-1.678559000000	-1.938810000000
C	-1.406490000000	-1.665103000000	1.349316000000
O	-1.333580000000	-2.503659000000	2.159080000000
C	-3.080930000000	-1.283072000000	-0.730497000000

### **syn-Mo@Ind-TS(2,3)**

E = -5262.83 kcal mol<sup>-1</sup> -25.7 cm<sup>-1</sup>

C	-0.529460000000	-2.201963000000	-0.446502000000
C	0.925778000000	-2.202292000000	-0.159131000000
C	1.013902000000	-2.640296000000	1.251998000000
Rh	1.175731000000	-0.118850000000	-0.006191000000
C	3.887973000000	-0.229551000000	-0.956396000000
C	3.195893000000	-0.293625000000	0.202580000000
C	1.732188000000	-0.011744000000	-1.934122000000
C	3.060992000000	-0.065259000000	-2.157722000000
H	1.629293000000	-2.593778000000	-0.891945000000
H	1.958592000000	-2.803853000000	1.759319000000
H	-0.440877000000	-2.989684000000	2.855747000000
H	3.493828000000	0.055617000000	-3.153153000000
H	0.963187000000	0.156776000000	-2.691296000000
H	3.662211000000	-0.396241000000	1.186910000000
H	4.978356000000	-0.262433000000	-1.011362000000
C	-1.268641000000	-1.989172000000	-1.635409000000
C	-2.636848000000	-2.434801000000	0.853429000000
C	-2.693820000000	-2.019182000000	-1.587134000000
C	-3.365137000000	-2.185085000000	-0.354381000000
H	-3.169635000000	-2.606991000000	1.784187000000
H	-4.450258000000	-2.163421000000	-0.327981000000
H	-3.265981000000	-1.866895000000	-2.496946000000
H	-0.758620000000	-1.821700000000	-2.578943000000
Mo	-1.948518000000	-0.219915000000	-0.094264000000
C	-0.221857000000	-2.754032000000	1.819960000000
C	-1.232667000000	-2.475647000000	0.803531000000
C	-0.725053000000	0.769063000000	1.133437000000
O	-0.097079000000	1.326306000000	1.968504000000
C	-1.816362000000	1.215946000000	-1.444651000000
O	-1.751203000000	2.044521000000	-2.267272000000
C	-3.405799000000	0.877460000000	0.715233000000
O	-4.271343000000	1.495337000000	1.188528000000
C	0.977606000000	3.985064000000	-1.095608000000

C 1.919084000000 4.248916000000 -0.391764000000  
H 2.754350000000 4.479638000000 0.230912000000  
H 0.141182000000 3.738064000000 -1.712514000000

### **syn@Mo@Ind-3**

$$E = -5280.58 \text{ kcal mol}^{-1}$$

-5276.62 kcal/mol

C -0.171442000000 1.717647000000 0.752175000000  
C 1.231250000000 1.959709000000 0.419331000000  
C 1.188481000000 2.799339000000 -0.779732000000  
Rh 1.692262000000 0.038822000000 -0.551131000000  
C 4.353682000000 0.335981000000 0.539073000000  
C 3.641850000000 0.713831000000 -0.544325000000  
C 2.343170000000 -0.742143000000 1.173353000000  
C 3.627805000000 -0.481679000000 1.497984000000  
H 1.977891000000 2.104670000000 1.194696000000  
H 2.074192000000 3.212411000000 -1.250440000000  
H -0.412985000000 3.478956000000 -2.132606000000  
H 4.090273000000 -0.876529000000 2.404320000000  
H 1.654245000000 -1.390121000000 1.715755000000  
H 4.037657000000 1.291325000000 -1.381907000000  
H 5.399621000000 0.611631000000 0.686553000000  
C -0.801955000000 1.078872000000 1.858771000000  
C -2.408537000000 2.245537000000 -0.220961000000  
C -2.212772000000 1.086995000000 1.964121000000  
C -3.004706000000 1.620801000000 0.904683000000  
H -3.030788000000 2.676731000000 -0.999688000000  
H -4.087202000000 1.577412000000 0.978603000000  
H -2.696950000000 0.638904000000 2.825773000000  
H -0.199608000000 0.632805000000 2.645155000000  
Mo -1.678796000000 -0.128691000000 -0.086178000000

C -3.333054000000 -1.168676000000 -0.419859000000  
O -4.320673000000 -1.763506000000 -0.596128000000  
C 1.599720000000 -1.921564000000 -1.519998000000  
C 2.537830000000 -1.273789000000 -2.026381000000  
H 3.422963000000 -1.096361000000 -2.609478000000  
H 0.957686000000 -2.760512000000 -1.326755000000

### **syn-Mo@Ind-TS(3,4)**

$$E = -5275.49 \text{ kcal mol}^{-1} \quad -341.096 \text{ cm}^{-1}$$

C -0.362354000000 1.696221000000 0.993743000000  
C 1.046947000000 1.866713000000 1.248972000000  
C 1.609130000000 2.536051000000 0.109016000000  
Rh 1.665846000000 0.383561000000 -0.412953000000  
C 4.508893000000 -0.149243000000 -0.237692000000  
C 3.631134000000 0.639012000000 -0.921507000000  
C 2.548758000000 -1.151772000000 0.640017000000  
C 3.917429000000 -1.113345000000 0.637199000000  
H 1.529055000000 1.742340000000 2.210444000000  
H 2.591453000000 2.989781000000 0.074739000000  
H 0.753779000000 3.051264000000 -1.898880000000  
H 4.517022000000 -1.806454000000 1.229013000000  
H 1.961678000000 -1.817323000000 1.269741000000  
H 3.920779000000 1.413218000000 -1.631089000000  
H 5.587070000000 -0.089027000000 -0.394867000000  
C -1.449561000000 1.258232000000 1.815017000000  
C -1.958912000000 2.126418000000 -0.878299000000  
C -2.774292000000 1.402348000000 1.341270000000  
C -3.026402000000 1.834790000000 -0.000634000000  
H -2.164366000000 2.429532000000 -1.900826000000  
H -4.050011000000 1.911598000000 -0.353229000000  
H -3.608873000000 1.164655000000 1.992981000000  
H -1.267891000000 0.911468000000 2.827992000000  
Mo -1.777699000000 -0.213036000000 -0.116896000000  
C 0.625321000000 2.597045000000 -0.924107000000  
C -0.620637000000 2.151251000000 -0.370992000000  
C -1.424997000000 -0.907956000000 -1.950442000000  
O -1.256399000000 -1.272175000000 -3.045839000000

C	-0.951452000000	-1.798988000000	0.749036000000	C	2.966872000000	-2.299578000000	0.077431000000
O	-0.496713000000	-2.726381000000	1.298220000000	O	3.698621000000	-3.213913000000	0.090045000000
C	-3.406396000000	-1.315023000000	-0.183346000000	C	0.763930000000	-1.662691000000	1.491920000000
O	-4.385894000000	-1.952465000000	-0.211188000000	O	0.180630000000	-2.185290000000	2.363210000000
C	1.825520000000	-1.589117000000	-1.318361000000	C	0.727552000000	-1.726243000000	-1.309124000000
C	2.210970000000	-0.720111100000	-2.164064000000	O	0.121445000000	-2.288743000000	-2.138938000000
H	2.418619000000	-0.409860000000	-3.171220000000	C	-4.026641000000	1.524898000000	0.772651000000
H	1.366729000000	-2.538668000000	-1.109817000000	C	-2.966816000000	0.753838000000	1.432667000000
				H	-2.837149000000	0.859756000000	2.507339000000
				H	-4.746627000000	2.081964000000	1.367684000000

### syn-Mo@Ind-4

$$E = -5342.65 \text{ kcal mol}^{-1}$$

C	1.330084000000	1.799244000000	-0.713262000000
C	0.142090000000	2.522527000000	-1.144915000000
C	-0.438133000000	3.166320000000	0.003217000000
Rh	-1.163765000000	1.124701000000	0.054246000000
C	-2.494442000000	-0.464615000000	-0.613319000000
C	-2.472542000000	-0.442585000000	0.814561000000
C	-4.047768000000	1.504176000000	-0.582938000000
C	-3.007945000000	0.713451000000	-1.251735000000
H	-0.093086000000	2.749430000000	-2.178280000000
H	-1.172839000000	3.961142000000	-0.004083000000
H	-0.038069000000	2.840912000000	2.190550000000
H	-2.912390000000	0.786354000000	-2.332703000000
H	-4.786347000000	2.043037000000	-1.171886000000
H	-2.057584000000	-1.257201000000	1.398469000000
H	-2.098084000000	-1.297606000000	-1.184148000000
C	2.388500000000	1.158839000000	-1.424524000000
C	2.423792000000	1.218163000000	1.441923000000
C	3.529689000000	0.720883000000	-0.709571000000
C	3.547226000000	0.750376000000	0.717904000000
H	2.436231000000	1.214052000000	2.527836000000
H	4.420909000000	0.391389000000	1.252062000000
H	4.390281000000	0.339622000000	-1.249478000000
H	2.374322000000	1.109832000000	-2.509272000000
Mo	1.771466000000	-0.745998000000	0.056715000000
C	0.171414000000	2.571478000000	1.161865000000
C	1.348003000000	1.829294000000	0.730961000000

### syn-Mo@Ind-5

$$E = -5868.79 \text{ kcal mol}^{-1}$$

C	1.305517000000	1.965076000000	-0.437417000000
C	0.379882000000	2.892638000000	-1.081314000000
C	-0.332059000000	3.605152000000	-0.052085000000
Rh	-1.368981000000	1.715813000000	-0.305338000000
C	-3.582721000000	1.894226000000	0.668970000000
C	-3.772755000000	2.988414000000	1.561688000000
C	-2.616604000000	0.609790000000	2.521795000000
C	-3.009293000000	0.684074000000	1.152268000000
H	0.435994000000	3.180447000000	-2.124958000000
H	-0.895489000000	4.521286000000	-0.173833000000
H	-0.527142000000	3.156869000000	2.138804000000
H	-3.102768000000	-0.237453000000	0.586378000000
H	-2.215972000000	-0.324754000000	2.902401000000
H	-4.261423000000	3.890078000000	1.198135000000
H	-4.104611000000	1.902711000000	-0.281141000000
C	2.410962000000	1.213097000000	-0.924930000000
C	1.718148000000	1.113013000000	1.855799000000
C	3.252535000000	0.549690000000	0.006413000000
C	2.909611000000	0.505910000000	1.391003000000
H	1.452649000000	1.049856000000	2.906881000000
H	3.552549000000	-0.023106000000	2.086956000000
H	4.162868000000	0.070408000000	-0.338468000000
H	2.669066000000	1.227835000000	-1.979446000000
Mo	1.185451000000	-0.650168000000	0.147989000000

C	-0.123837000000	2.885762000000	1.171180000000	C	-2.796511000000	1.690825000000	3.367187000000
C	0.968911000000	1.942141000000	0.968355000000	C	-3.383561000000	2.889602000000	2.884995000000
C	2.173852000000	-2.342210000000	0.204365000000	H	-3.550780000000	3.720920000000	3.567259000000
O	2.786078000000	-3.339009000000	0.242516000000	H	-2.518172000000	1.612160000000	4.416291000000
C	-0.182999000000	-1.621975000000	1.200757000000	C	-2.194532000000	0.594219000000	-1.968029000000
O	-0.960964000000	-2.218640000000	1.840762000000	C	-2.393077000000	1.813755000000	-2.184811000000
C	0.380046000000	-1.359980000000	-1.515498000000	H	-2.717737000000	2.664161000000	-2.759708000000
O	-0.058416000000	-1.788399000000	-2.512542000000	H	-2.229230000000	-0.451885000000	-2.219530000000

**Table B5.** Cartesian coordinates (in Å) and ADF total energies (in kcal mol<sup>-1</sup>) of all stationary points as well as imaginary frequencies of transition states (in cm<sup>-1</sup>) along the Path II catalyzed by syn-[W(CO)<sub>3</sub>IndRh], computed at ZORA-BLYP/TZ2P.

### syn-W@Ind-1

E = -4726.24 kcal mol<sup>-1</sup>

C	-0.020949000000	1.820368000000	0.757988000000
C	1.371882000000	1.842355000000	1.155072000000
C	2.170564000000	2.055276000000	-0.018999000000
Rh	1.677641000000	-0.083100000000	-0.056594000000
C	1.829866000000	-1.648297000000	-1.561993000000
C	2.859608000000	-0.939662000000	-1.628086000000
C	2.934738000000	-1.009388000000	1.413841000000
C	1.902942000000	-1.716440000000	1.365202000000
H	1.719773000000	1.908162000000	2.179169000000
H	3.216783000000	2.332569000000	-0.038990000000
H	1.608767000000	2.010701000000	-2.195946000000
H	1.250411000000	-2.525987000000	1.640498000000
H	3.905719000000	-0.715863000000	1.772045000000
H	3.812714000000	-0.629717000000	-2.018965000000
H	1.162899000000	-2.444323000000	-1.842134000000
C	-1.246107000000	1.807083000000	1.498227000000
C	-1.318897000000	1.874371000000	-1.371009000000
C	-2.468957000000	2.038951000000	0.813781000000
C	-2.505235000000	2.072530000000	-0.615455000000
H	-1.361273000000	1.869601000000	-2.455750000000
H	-3.450623000000	2.221827000000	-1.126337000000

H -3.387077000000 2.163062000000 1.378338000000

H -1.233539000000 1.751567000000 2.582315000000

W -1.747015000000 -0.091431000000 0.030113000000

C 1.313152000000 1.896629000000 -1.159746000000

C -0.057805000000 1.854425000000 -0.693989000000

C -1.446298000000 -1.402095000000 -1.429102000000

O -1.289009000000 -2.148503000000 -2.318732000000

C -1.374406000000 -1.469342000000 1.408581000000

O -1.173904000000 -2.257006000000 2.252794000000

C -3.582204000000 -0.789708000000 0.060478000000

O -4.688627000000 -1.175633000000 0.079764000000

### syn-W@Ind-TS(1,2)

E = -4711.07 kcal mol<sup>-1</sup> -444.72 cm<sup>-1</sup>

C	0.378667000000	1.916363000000	0.732375000000
C	1.745291000000	1.973519000000	1.161411000000
C	2.578377000000	2.116601000000	0.000003000000
Rh	2.135632000000	-0.051168000000	-0.000001000000
C	2.464634000000	-1.975900000000	-0.962629000000
C	3.158486000000	-1.015106000000	-1.481268000000
C	3.158486000000	-1.015110000000	1.481264000000
C	2.464633000000	-1.975902000000	0.962622000000
H	2.075688000000	2.055460000000	2.189499000000

H	3.627632000000	2.382655000000	0.000003000000	H	3.972811000000	-2.196066000000	1.476956000000
H	2.075691000000	2.055465000000	-2.189495000000	H	1.478031000000	-1.586593000000	1.638686000000
H	1.880067000000	-2.840226000000	1.252671000000	H	3.857770000000	0.628932000000	-1.850505000000
H	3.852153000000	-0.708294000000	2.247840000000	H	5.265290000000	-0.987764000000	-0.450124000000
H	3.852152000000	-0.708286000000	-2.247844000000	C	-1.232187000000	1.476716000000	1.690212000000
H	1.880068000000	-2.840222000000	-1.252681000000	C	-1.972367000000	2.074829000000	-1.027719000000
C	-0.870716000000	1.882953000000	1.437491000000	C	-2.611179000000	1.565038000000	1.321195000000
C	-0.870715000000	1.882953000000	-1.437491000000	C	-2.961709000000	1.794605000000	-0.034817000000
C	-2.077469000000	2.062887000000	0.716789000000	H	-2.272490000000	2.272813000000	-2.051672000000
C	-2.077468000000	2.062886000000	-0.716792000000	H	-4.009586000000	1.794948000000	-0.319086000000
H	-0.887657000000	1.849962000000	-2.522634000000	H	-3.382038000000	1.386776000000	2.063203000000
H	-3.015470000000	2.166131000000	-1.252249000000	H	-0.959446000000	1.238226000000	2.713993000000
H	-3.015471000000	2.166132000000	1.252246000000	W	-1.603311000000	-0.191177000000	0.001339000000
H	-0.887660000000	1.849963000000	2.522633000000	C	0.595215000000	2.452215000000	-1.365700000000
W	-1.266628000000	-0.061602000000	0.000000000000	C	-0.611187000000	2.146826000000	-0.640297000000
C	1.745293000000	1.973521000000	-1.161408000000	C	-0.346680000000	-1.115297000000	-1.217281000000
C	0.378668000000	1.916364000000	-0.732374000000	O	0.448301000000	-1.603276000000	-1.963516000000
C	-0.863472000000	-1.386760000000	-1.424196000000	C	-1.402290000000	-1.643822000000	1.324791000000
O	-0.638420000000	-2.147233000000	-2.285777000000	O	-1.318542000000	-2.467776000000	2.151190000000
C	-0.863476000000	-1.386756000000	1.424199000000	C	-3.103187000000	-1.276719000000	-0.727468000000
O	-0.638427000000	-2.147227000000	2.285783000000	O	-4.001363000000	-1.889503000000	-1.149286000000
C	-3.067772000000	-0.841352000000	0.000000000000				
O	-4.154483000000	-1.281290000000	0.000001000000				

### Syn-W@Ind-TS(2,3)

$$E = -5259.42 \text{ kcal mol}^{-1} \quad -39.73 \text{ cm}^{-1}$$

C	-0.524400000000	-2.203400000000	-0.411800000000
C	0.931000000000	-2.179800000000	-0.121800000000
C	1.019400000000	-2.595900000000	1.295700000000
Rh	1.181100000000	-0.089100000000	-0.051300000000
C	3.884100000000	-0.304000000000	-1.024100000000
C	3.203700000000	-0.283000000000	0.143700000000
C	1.722100000000	-0.087500000000	-1.984000000000
C	3.046300000000	-0.182500000000	-2.222200000000
H	1.635200000000	-2.588800000000	-0.844800000000
H	1.965200000000	-2.738000000000	1.807200000000
H	-0.433200000000	-2.944800000000	2.900800000000
H	3.468000000000	-0.121800000000	-3.227700000000
H	0.948700000000	0.058300000000	-2.742100000000

### Syn-W@Ind-2

$$E = -4751.39 \text{ kcal mol}^{-1}$$

C	-0.228630000000	1.797037000000	0.734636000000
C	1.232394000000	1.837675000000	0.802754000000
C	1.686462000000	2.360240000000	-0.475405000000
Rh	1.485246000000	0.136623000000	-0.491752000000
C	4.210098000000	-0.786135000000	-0.250843000000
C	3.480803000000	0.073852000000	-0.988842000000
C	2.174913000000	-1.170670000000	0.909289000000
C	3.484442000000	-1.473355000000	0.819821000000
H	1.802718000000	1.853987000000	1.724207000000
H	2.697579000000	2.691517000000	-0.673500000000
H	0.641485000000	2.757774000000	-2.403523000000

H	3.682200000000	-0.349300000000	1.125900000000	H	4.075383000000	-0.826403000000	2.414396000000
H	4.972000000000	-0.374700000000	-1.090800000000	H	1.642976000000	-1.363287000000	1.734646000000
C	-1.266400000000	-2.003200000000	-1.605700000000	H	4.016954000000	1.277398000000	-1.407477000000
C	-2.634500000000	-2.428500000000	0.891300000000	H	5.379227000000	0.639065000000	0.673471000000
C	-2.693200000000	-2.046800000000	-1.559600000000	C	-0.778626000000	1.069300000000	1.848865000000
C	-3.363700000000	-2.200000000000	-0.322600000000	C	-2.422819000000	2.243281000000	-0.203201000000
H	-3.166200000000	-2.584300000000	1.825500000000	C	-2.190499000000	1.069447000000	1.975882000000
H	-4.449000000000	-2.178000000000	-0.296300000000	C	-2.999734000000	1.600422000000	0.926665000000
H	-3.265700000000	-1.902000000000	-2.470200000000	H	-3.059251000000	2.671707000000	-0.971556000000
H	-0.755500000000	-1.839500000000	-2.549000000000	H	-4.080618000000	1.540605000000	1.009941000000
W	-1.954600000000	-0.247300000000	-0.082800000000	H	-2.660176000000	0.607132000000	2.837810000000
C	-0.215000000000	-2.720900000000	1.862300000000	H	-0.162106000000	0.618363000000	2.620892000000
C	-1.226800000000	-2.467000000000	0.840600000000	W	-1.663414000000	-0.107534000000	-0.085705000000
C	-0.753500000000	0.709500000000	1.181300000000	C	-0.131989000000	2.983430000000	-1.239314000000
O	-0.091300000000	1.204000000000	2.030900000000	C	-1.009129000000	2.329678000000	-0.292039000000
C	-1.775400000000	1.177500000000	-1.440500000000	C	-1.270004000000	-0.420483000000	-2.012630000000
O	-1.676500000000	1.990400000000	-2.278600000000	O	-1.090432000000	-0.530824000000	-3.162255000000
C	-3.443700000000	0.852900000000	0.660200000000	C	-0.969148000000	-1.861766000000	0.518769000000
O	-4.340000000000	1.461200000000	1.092500000000	O	-0.612216000000	-2.899290000000	0.930845000000
C	1.052400000000	3.719600000000	-0.979000000000	C	-3.318278000000	-1.141360000000	-0.442857000000
C	1.888800000000	3.896100000000	-0.129700000000	O	-4.313756000000	-1.724452000000	-0.625274000000
H	2.631400000000	4.055900000000	0.619700000000	C	1.557181000000	-1.939548000000	-1.516720000000
H	0.299000000000	3.556500000000	-1.718800000000	C	2.535667000000	-1.322880000000	-1.985642000000
				H	3.448381000000	-1.179243000000	-2.534520000000
				H	0.885336000000	-2.761697000000	-1.355214000000

### syn-W@nd-3

E = -5277.47 kcal mol<sup>-1</sup>

C	-0.167014000000	1.724463000000	0.738161000000
C	1.229289000000	1.969261000000	0.382139000000
C	1.163838000000	2.817166000000	-0.810368000000
Rh	1.671555000000	0.022014000000	-0.556433000000
C	4.335125000000	0.355215000000	0.528212000000
C	3.622549000000	0.709448000000	-0.562633000000
C	2.328410000000	-0.720935000000	1.181025000000
C	3.611859000000	-0.448949000000	1.501122000000
H	1.986371000000	2.115968000000	1.146815000000
H	2.041636000000	3.231116000000	-1.295082000000
H	-0.459490000000	3.502366000000	-2.132972000000

### syn-W@Ind-TS(3,4)

E = -348.877 kcal mol<sup>-1</sup>

C	-0.324208000000	1.709573000000	1.009320000000
C	1.090500000000	1.875973000000	1.237366000000
C	1.627859000000	2.555936000000	0.090853000000
Rh	1.678309000000	0.394317000000	-0.422829000000
C	4.514313000000	-0.175364000000	-0.194889000000
C	3.661276000000	0.637429000000	-0.884039000000
C	2.521777000000	-1.174179000000	0.605249000000
C	3.890632000000	-1.156079000000	0.635782000000
H	1.589373000000	1.749532000000	2.189832000000

H	2.610568000000	3.007058000000	0.039716000000	C	-3.008897000000	0.717559000000	-1.252018000000
H	0.733469000000	3.092047000000	-1.893270000000	H	-0.090972000000	2.730064000000	-2.177748000000
H	4.466172000000	-1.878196000000	1.216768000000	H	-1.171653000000	3.940615000000	-0.001846000000
H	1.910027000000	-1.849703000000	1.199497000000	H	-0.034509000000	2.818765000000	2.191763000000
H	3.980184000000	1.426448000000	-1.564197000000	H	-2.912726000000	0.798492000000	-2.332391000000
H	5.596822000000	-0.121635000000	-0.321657000000	H	-4.786675000000	2.048767000000	-1.162258000000
C	-1.394157000000	1.248194000000	1.842810000000	H	-2.068500000000	-1.277471000000	1.383273000000
C	-1.958780000000	2.155697000000	-0.829492000000	H	-2.112120000000	-1.300438000000	-1.200651000000
C	-2.732804000000	1.397658000000	1.398191000000	C	2.390098000000	1.134430000000	-1.426811000000
C	-3.011781000000	1.847314000000	0.066396000000	C	2.428909000000	1.196003000000	1.442322000000
H	-2.184973000000	2.467393000000	-1.844700000000	C	3.537738000000	0.698955000000	-0.712638000000
H	-4.041550000000	1.920036000000	-0.268024000000	C	3.557227000000	0.729735000000	0.716602000000
H	-3.552747000000	1.142513000000	2.061423000000	H	2.440694000000	1.188301000000	2.527906000000
H	-1.191461000000	0.882321000000	2.844781000000	H	4.429276000000	0.367583000000	1.250836000000
W	-1.748563000000	-0.170611000000	-0.098899000000	H	4.394955000000	0.313034000000	-1.254188000000
C	0.623659000000	2.632801000000	-0.918665000000	H	2.372525000000	1.079927000000	-2.510968000000
C	-0.611032000000	2.183141000000	-0.345382000000	W	1.775536000000	-0.727075000000	0.058565000000
C	-1.389749000000	-0.819467000000	-1.946632000000	C	0.174590000000	2.551217000000	1.162584000000
O	-1.213045000000	-1.145456000000	-3.054815000000	C	1.354383000000	1.814671000000	0.731051000000
C	-0.927414000000	-1.767543000000	0.747834000000	C	2.948522000000	-2.299313000000	0.078327000000
O	-0.472876000000	-2.698208000000	1.296066000000	O	3.679805000000	-3.216738000000	0.089099000000
C	-3.371153000000	-1.280075000000	-0.191847000000	C	0.758362000000	-1.622887000000	1.502080000000
O	-4.355109000000	-1.913954000000	-0.229785000000	O	0.169700000000	-2.122894000000	2.385388000000
C	1.842557000000	-1.540336000000	-1.400765000000	C	0.718346000000	-1.687801000000	-1.313083000000
C	2.291914000000	-0.651563000000	-2.192975000000	O	0.105186000000	-2.228419000000	-2.154777000000
H	2.540942000000	-0.302218000000	-3.177653000000	C	-4.024513000000	1.517972000000	0.777863000000
H	1.353208000000	-2.484734000000	-1.245657000000	C	-2.964953000000	0.739022000000	1.430757000000
				H	-2.832057000000	0.837804000000	2.505711000000
				H	-4.743682000000	2.070293000000	1.378292000000

### syn-W@Ind-4

$$E = -5338.59 \text{ kcal mol}^{-1}$$

C	1.335343000000	1.784787000000	-0.714221000000
C	0.144310000000	2.503345000000	-1.144421000000
C	-0.437125000000	3.145764000000	0.004687000000
Rh	-1.160212000000	1.105705000000	0.052780000000
C	-2.503135000000	-0.469265000000	-0.623303000000
C	-2.479767000000	-0.456960000000	0.804868000000
C	-4.047346000000	1.506618000000	-0.577270000000

### syn-W@Ind-5

$$E = -5864.80 \text{ kcal mol}^{-1}$$

C	1.379083000000	1.997470000000	-0.356337000000
C	0.468076000000	2.945728000000	-0.993024000000
C	-0.260180000000	3.634135000000	0.042066000000
Rh	-1.308490000000	1.769062000000	-0.289720000000
C	-3.547914000000	1.962034000000	0.656697000000

C	-3.734861000000	3.035935000000	1.573383000000		W	1.223114000000	-0.596094000000	0.148563000000
C	-2.644329000000	0.611181000000	2.492449000000		C	-0.083819000000	2.875807000000	1.247361000000
C	-3.007114000000	0.729681000000	1.118481000000		C	1.007950000000	1.932735000000	1.040819000000
H	0.550013000000	3.264278000000	-2.025979000000		C	2.171598000000	-2.314056000000	0.157557000000
H	-0.810357000000	4.560281000000	-0.062868000000		O	2.772739000000	-3.320464000000	0.171812000000
H	-0.505751000000	3.119662000000	2.214230000000		C	-0.181033000000	-1.572947000000	1.150070000000
H	-3.099920000000	-0.173389000000	0.523439000000		O	-0.981911000000	-2.165043000000	1.769006000000
H	-2.268659000000	-0.340572000000	2.855265000000		C	0.435235000000	-1.221897000000	-1.558400000000
H	-4.198449000000	3.956305000000	1.224102000000		O	0.013095000000	-1.591303000000	-2.587617000000
H	-4.045935000000	2.006613000000	-0.304997000000		C	-2.820201000000	1.673336000000	3.362777000000
C	2.490950000000	1.251691000000	-0.842518000000		C	-3.373656000000	2.895511000000	2.901204000000
C	1.724501000000	1.060333000000	1.917486000000		H	-3.538308000000	3.712129000000	3.601635000000
C	3.306500000000	0.547632000000	0.088492000000		H	-2.564813000000	1.561447000000	4.414726000000
C	2.929013000000	0.461056000000	1.463885000000		C	-2.126915000000	0.718704000000	-2.000851000000
H	1.429748000000	0.960591000000	2.957579000000		C	-2.308496000000	1.947443000000	-2.177049000000
H	3.546774000000	-0.100341000000	2.156905000000		H	-2.614452000000	2.821405000000	-2.726269000000
H	4.218061000000	0.067960000000	-0.251921000000		H	-2.164915000000	-0.317032000000	-2.292094000000
H	2.773124000000	1.295580000000	-1.889737000000					

**Table B5.** Cartesian coordinates (in Å) and ADF total energies (in kcal mol<sup>-1</sup>) of all stationary points as well as imaginary frequencies of transition states (in cm<sup>-1</sup>) along the Path II catalyzed by anti-[Mo(CO)<sub>3</sub>IndRh(CO)], computed at ZORA-BLYP/TZ2P.

### CO-anti-Mo@Ind-1

E = -5073.99 kcal mol<sup>-1</sup>

C	1.646121000000	0.191841000000	-3.652845000000		C	-1.941206000000	0.619256000000	-0.946247000000
C	1.507192000000	-0.309771000000	-2.318644000000		C	-0.736048000000	-2.242106000000	-0.486676000000
C	1.464277000000	0.591741000000	-1.239468000000		C	-0.217500000000	-2.461400000000	0.643270000000
C	1.626744000000	2.017988000000	-1.483561000000		H	1.698242000000	3.759678000000	-0.047122000000
C	1.787770000000	2.509927000000	-2.793659000000		H	1.328340000000	1.971414000000	1.847982000000
C	1.803373000000	1.577493000000	-3.881031000000		H	1.812129000000	-0.395097000000	0.708478000000
C	1.575622000000	2.691063000000	-0.188197000000		H	-2.233890000000	0.328543000000	-1.938931000000
C	1.376058000000	1.763715000000	0.785045000000		H	-2.120463000000	2.317528000000	0.550692000000
C	1.241819000000	0.396013000000	0.224565000000		H	0.244703000000	-3.116342000000	1.362612000000
Rh	-0.775481000000	-0.383775000000	0.622656000000		H	-1.065189000000	-2.582542000000	-1.454077000000
C	-1.906217000000	1.399792000000	0.033812000000		H	1.395628000000	-1.376188000000	-2.150780000000
					H	1.662401000000	-0.499293000000	-4.489443000000
					H	1.930615000000	1.942606000000	-4.895569000000
					H	1.913272000000	3.571678000000	-2.983943000000

C	-0.631005000000	-0.004516000000	2.515331000000	C	-0.065937000000	-0.803087000000	2.325963000000
O	-0.725915000000	0.122859000000	3.662448000000	O	0.269740000000	-0.998356000000	3.421297000000
Mo	3.622976000000	0.898041000000	-2.440639000000	Mo	3.687753000000	0.946305000000	-2.376164000000
C	4.973480000000	1.821421000000	-3.568484000000	C	4.975692000000	1.773861000000	-3.637771000000
C	4.678450000000	-0.756905000000	-2.743833000000	C	4.883346000000	-0.635325000000	-2.355631000000
C	4.783153000000	1.286929000000	-0.861983000000	C	4.772671000000	1.704753000000	-0.888951000000
O	5.430113000000	1.522960000000	0.078345000000	O	5.373202000000	2.158530000000	0.003064000000
O	5.736773000000	2.376153000000	-4.254704000000	O	5.702960000000	2.267911000000	-4.406567000000
O	5.265904000000	-1.746601000000	-2.937590000000	O	5.556538000000	-1.590351000000	-2.355194000000

### CO-anti-Mo@Ind-TS(1,2)

$$E = -5059.92 \text{ kcal mol}^{-1} \quad -348.837 \text{ cm}^{-1}$$

C	1.794683000000	-0.106910000000	-3.474429000000
C	1.676338000000	-0.411895000000	-2.080978000000
C	1.530728000000	0.637026000000	-1.151628000000
C	1.570341000000	2.019248000000	-1.606251000000
C	1.719208000000	2.320245000000	-2.976979000000
C	1.838829000000	1.239098000000	-3.907419000000
C	1.407120000000	2.869828000000	-0.429255000000
C	1.263136000000	2.080142000000	0.671204000000
C	1.275073000000	0.640188000000	0.317713000000
Rh	-0.693298000000	-0.369997000000	0.640527000000
C	-1.596375000000	1.266283000000	-0.369438000000
C	-2.162873000000	0.329511000000	-1.028602000000
C	-2.523000000000	-1.485308000000	-0.201780000000
C	-1.587460000000	-2.198061000000	0.313952000000
H	1.429607000000	3.954523000000	-0.447427000000
H	1.155261000000	2.436751000000	1.690245000000
H	1.923009000000	0.003853000000	0.917516000000
H	-2.595145000000	0.108807000000	-1.993369000000
H	-1.310790000000	2.304626000000	-0.460220000000
H	-1.441387000000	-3.182878000000	0.731335000000
H	-3.583461000000	-1.523683000000	-0.404710000000
H	1.656574000000	-1.447579000000	-1.754049000000
H	1.885288000000	-0.911198000000	-4.197371000000
H	1.955329000000	1.456674000000	-4.964833000000
H	1.750232000000	3.347721000000	-3.327036000000

### CO-anti-Mo@Ind-2

$$E = -5117.75 \text{ kcal mol}^{-1}$$

C	1.917427000000	-0.350115000000	0.373365000000
C	1.460811000000	-0.027704000000	-0.944950000000
C	0.914173000000	1.341041000000	-0.901117000000
C	1.092447000000	1.832529000000	0.450861000000
C	1.724266000000	0.805640000000	1.202498000000
C	0.428020000000	1.950712000000	-2.118633000000
C	0.309615000000	1.160758000000	-3.277145000000
C	0.839138000000	-0.173737000000	-3.318393000000
C	1.481916000000	-0.739861000000	-2.200219000000
Rh	-0.449115000000	0.092781000000	0.660083000000
C	-1.077111000000	-0.770766000000	2.162066000000
O	-1.471512000000	-1.296302000000	3.114470000000
C	-2.182303000000	1.247119000000	0.583916000000
C	-3.174038000000	0.719498000000	-0.156176000000
H	0.857144000000	2.830942000000	0.795702000000
H	2.024162000000	0.884816000000	2.240432000000
H	2.398758000000	-1.273458000000	0.669210000000
H	-4.123680000000	1.232747000000	-0.321194000000
H	-2.239321000000	2.193226000000	1.120758000000
H	1.901483000000	-1.739450000000	-2.253918000000
H	0.777201000000	-0.737239000000	-4.244008000000
H	-0.140187000000	1.579642000000	-4.171541000000
H	0.052030000000	2.968547000000	-2.105567000000
C	-2.911167000000	-0.604247000000	-0.726182000000
C	-1.719030000000	-1.148974000000	-0.426660000000

H	-3.644277000000	-1.111675000000	-1.356968000000	C	-0.180400000000	-0.278700000000	2.822800000000
H	-1.373068000000	-2.135493000000	-0.732737000000	O	0.023200000000	-0.765500000000	3.851600000000
Mo	2.672428000000	1.303753000000	-2.835181000000	Mo	3.592200000000	0.832700000000	-2.437000000000
C	3.168683000000	1.500635000000	-4.721242000000	C	4.871200000000	2.176800000000	-3.152600000000
C	4.489229000000	0.531289000000	-2.534193000000	C	4.785000000000	-0.548400000000	-3.217800000000
C	3.428939000000	3.128290000000	-2.548959000000	C	4.690800000000	0.739300000000	-0.778400000000
O	3.437832000000	1.607392000000	-5.854525000000	O	5.279200000000	0.680300000000	0.227700000000
O	3.840610000000	4.204106000000	-2.367840000000	O	5.599900000000	2.980700000000	-3.582800000000
O	5.535049000000	0.052302000000	-2.344291000000	O	5.455200000000	-1.374500000000	-3.698100000000
				C	-3.488400000000	1.011200000000	1.542500000000
				C	-2.921200000000	1.536800000000	2.474400000000
				H	-2.511200000000	2.019000000000	3.334800000000
				H	-3.992100000000	0.561900000000	0.714400000000

### CO-anti-Mo@Ind-TS(2,3)

$$E = -5616.89 \text{ kcal mol}^{-1} \quad -65.28 \text{ cm}^{-1}$$

C	1.663100000000	-0.162700000000	-3.488100000000
C	1.548200000000	-0.530500000000	-2.111800000000
C	1.479700000000	0.488400000000	-1.146600000000
C	1.543700000000	1.886400000000	-1.542000000000
C	1.657200000000	2.231200000000	-2.910800000000
C	1.666800000000	1.195500000000	-3.891900000000
C	1.499500000000	2.684100000000	-0.329400000000
C	1.413100000000	1.850300000000	0.759700000000
C	1.313700000000	0.438500000000	0.333600000000
Rh	-0.712700000000	0.348100000000	1.050500000000
C	-1.519700000000	0.725700000000	-0.844400000000
C	-2.002100000000	-0.372800000000	-1.465500000000
C	-1.809800000000	-1.631700000000	-0.742500000000
C	-1.206700000000	-1.551100000000	0.461700000000
H	1.560400000000	3.767500000000	-0.303200000000
H	1.487800000000	2.172400000000	1.793200000000
H	1.860700000000	-0.332300000000	0.872000000000
H	-2.511800000000	-0.355400000000	-2.432400000000
H	-1.623300000000	1.731900000000	-1.264100000000
H	-1.001200000000	-2.396700000000	1.117000000000
H	-2.150800000000	-2.589100000000	-1.146400000000
H	1.497700000000	-1.576300000000	-1.826000000000
H	1.717900000000	-0.942200000000	-4.242400000000
H	1.732600000000	1.447000000000	-4.945500000000
H	1.709700000000	3.271900000000	-3.219600000000

### CO-anti-Mo@Ind-3

$$E = -5621.69 \text{ kcal mol}^{-1}$$

C	1.665785000000	-0.213786000000	-3.450739000000
C	1.560324000000	-0.596314000000	-2.078812000000
C	1.468038000000	0.411648000000	-1.103468000000
C	1.514992000000	1.814912000000	-1.488167000000
C	1.616863000000	2.172814000000	-2.856936000000
C	1.635044000000	1.147696000000	-3.845365000000
C	1.464727000000	2.600036000000	-0.273256000000
C	1.391120000000	1.748761000000	0.812311000000
C	1.296865000000	0.348701000000	0.366780000000
Rh	-0.789470000000	0.427897000000	1.077618000000
C	-1.528485000000	0.758768000000	-0.856026000000
C	-1.932167000000	-0.356813000000	-1.506626000000
C	-1.781442000000	-1.597651000000	-0.760543000000
C	-1.280545000000	-1.496623000000	0.490807000000
H	1.511359000000	3.683518000000	-0.235186000000
H	1.493730000000	2.061090000000	1.845800000000
H	1.806876000000	-0.442966000000	0.909112000000
H	-2.362380000000	-0.350922000000	-2.510633000000
H	-1.629008000000	1.763215000000	-1.275560000000
H	-1.160477000000	-2.326099000000	1.185868000000
H	-2.075792000000	-2.564064000000	-1.178472000000

H	1.537078000000	-1.645777000000	-1.804214000000	H	-2.288920000000	-0.315442000000	-2.524157000000
H	1.735255000000	-0.984890000000	-4.212187000000	H	-1.754184000000	1.798456000000	-1.173512000000
H	1.689524000000	1.408277000000	-4.897306000000	H	-1.035967000000	-2.363034000000	1.102069000000
H	1.647499000000	3.216771000000	-3.156608000000	H	-1.958252000000	-2.541661000000	-1.254723000000
C	-0.213753000000	-0.237313000000	2.830217000000	H	1.517411000000	-1.625495000000	-1.768896000000
O	0.061246000000	-0.795227000000	3.802657000000	H	1.676765000000	-0.967520000000	-4.181132000000
Mo	3.587441000000	0.819379000000	-2.414050000000	H	1.636854000000	1.426175000000	-4.865244000000
C	4.806268000000	2.220053000000	-3.114584000000	H	1.623112000000	3.235900000000	-3.124006000000
C	4.791095000000	-0.495460000000	-3.282227000000	C	-0.210197000000	-0.291947000000	2.853913000000
C	4.735307000000	0.697843000000	-0.790252000000	O	0.072172000000	-0.815441000000	3.843566000000
O	5.365707000000	0.626482000000	0.188959000000	Mo	3.569397000000	0.824894000000	-2.414020000000
O	5.495490000000	3.058121000000	-3.546366000000	C	4.783169000000	2.187732000000	-3.191495000000
O	5.466810000000	-1.284339000000	-3.815241000000	C	4.755456000000	-0.536045000000	-3.233298000000
C	-3.069932000000	0.780360000000	1.348040000000	C	4.737605000000	0.780108000000	-0.801941000000
C	-2.510210000000	1.537220000000	2.142446000000	O	5.379637000000	0.754642000000	0.172287000000
H	-2.312548000000	2.222307000000	2.942143000000	O	5.469573000000	3.004650000000	-3.666639000000
H	-3.764282000000	0.219634000000	0.757260000000	O	5.420394000000	-1.353779000000	-3.736097000000
				C	-3.007877000000	1.041202000000	0.919813000000
				C	-2.425857000000	1.486089000000	1.944994000000
				H	-2.515896000000	1.908009000000	2.931474000000
				H	-3.891564000000	0.726706000000	0.396150000000

### CO-anti-Mo@Ind-TS(3,b)

$$E = -5619.17 \text{ kcal mol}^{-1} \quad -272.697 \text{ cm}^{-1}$$

C	1.624354000000	-0.195388000000	-3.419420000000
C	1.539828000000	-0.576302000000	-2.044040000000
C	1.472959000000	0.431623000000	-1.066899000000
C	1.515607000000	1.835223000000	-1.454953000000
C	1.593858000000	2.192168000000	-2.823405000000
C	1.597313000000	1.165228000000	-3.812706000000
C	1.481520000000	2.622919000000	-0.238724000000
C	1.421790000000	1.774349000000	0.845325000000
C	1.325205000000	0.371948000000	0.406090000000
Rh	-0.778984000000	0.372660000000	1.120956000000
C	-1.648339000000	0.790762000000	-0.772889000000
C	-1.919834000000	-0.338723000000	-1.497003000000
C	-1.699539000000	-1.578694000000	-0.807813000000
C	-1.167854000000	-1.503054000000	0.446365000000
H	1.524878000000	3.706524000000	-0.202933000000
H	1.510141000000	2.087507000000	1.879966000000
H	1.853913000000	-0.410839000000	0.943371000000

### CO-anti-Mo@Ind-b

$$E = -5640.7 \text{ kcal mol}^{-1}$$

C	1.617603000000	-0.138796000000	-3.393330000000
C	1.581863000000	-0.539735000000	-2.025589000000
C	1.554724000000	0.456040000000	-1.024566000000
C	1.570599000000	1.867314000000	-1.395303000000
C	1.614803000000	2.239941000000	-2.765104000000
C	1.579621000000	1.230890000000	-3.767637000000
C	1.535038000000	2.637238000000	-0.172610000000
C	1.501638000000	1.767733000000	0.900975000000
C	1.441576000000	0.380455000000	0.438222000000
Rh	-0.715421000000	0.232446000000	1.157070000000
C	-1.689871000000	0.699070000000	-0.727380000000
C	-2.248688000000	-0.557829000000	-1.254187000000
C	-2.186539000000	-1.658326000000	-0.433283000000

C	-1.495541000000	-1.486927000000	0.788913000000	Rh	-0.731384000000	0.338160000000	1.180609000000
H	1.557488000000	3.720503000000	-0.120108000000	C	-1.766887000000	0.762047000000	-0.863471000000
H	1.583662000000	2.066205000000	1.940785000000	C	-1.908840000000	-0.560832000000	-1.358656000000
H	1.934240000000	-0.419650000000	0.984873000000	C	-1.948799000000	-1.657860000000	-0.473537000000
H	-2.712674000000	-0.607064000000	-2.242480000000	C	-1.448031000000	-1.454801000000	0.799076000000
H	-1.205861000000	1.331309000000	-1.477599000000	H	1.433345000000	3.616124000000	-0.151617000000
H	-1.454399000000	-2.292248000000	1.525306000000	H	1.589388000000	1.985126000000	1.930192000000
H	-2.652551000000	-2.612608000000	-0.687034000000	H	1.924199000000	-0.520373000000	1.013750000000
H	1.572846000000	-1.594313000000	-1.767618000000	H	-1.899740000000	-0.745837000000	-2.436673000000
H	1.643313000000	-0.899193000000	-4.168268000000	H	-1.424515000000	1.500946000000	-1.590917000000
H	1.585015000000	1.505925000000	-4.817310000000	H	-1.422590000000	-2.255328000000	1.539205000000
H	1.632117000000	3.288122000000	-3.051575000000	H	-2.283956000000	-2.642980000000	-0.803345000000
C	-0.301275000000	-0.182373000000	3.022809000000	H	1.700406000000	-1.714987000000	-1.727608000000
O	-0.175126000000	-0.491299000000	4.127332000000	H	1.717830000000	-1.052355000000	-4.135036000000
Mo	3.604554000000	0.868099000000	-2.450716000000	H	1.542959000000	1.340595000000	-4.819194000000
C	4.789477000000	2.304322000000	-3.130795000000	H	1.533545000000	3.145950000000	-3.081049000000
C	4.751222000000	-0.399469000000	-3.449489000000	C	-0.432958000000	-0.026930000000	3.006362000000
C	4.838647000000	0.657158000000	-0.904134000000	O	-0.289398000000	-0.295487000000	4.122051000000
O	5.524187000000	0.533667000000	0.032720000000	Mo	3.605927000000	0.823652000000	-2.470316000000
O	5.458103000000	3.166553000000	-3.548896000000	C	4.730625000000	2.384844000000	-2.949487000000
O	5.392993000000	-1.161614000000	-4.059548000000	C	4.776732000000	-0.237266000000	-3.657739000000
C	-2.732052000000	1.485594000000	0.106919000000	C	4.869093000000	0.422587000000	-0.985634000000
C	-2.460371000000	1.288896000000	1.391532000000	O	5.573147000000	0.182014000000	-0.085960000000
H	-2.935223000000	1.657604000000	2.296188000000	O	5.363683000000	3.319849000000	-3.250763000000
H	-3.522284000000	2.092880000000	-0.347195000000	O	5.435016000000	-0.875429000000	-4.382893000000
				C	-2.835001000000	1.347790000000	0.091151000000
				C	-2.566702000000	1.230808000000	1.379698000000
				H	-3.140152000000	1.526736000000	2.252006000000
				H	-3.711020000000	1.822999000000	-0.363200000000

### CO-anti-Mo@Ind-TS(b,h)

E =	-5639.29	kcal mol <sup>-1</sup>	-226.12	cm <sup>-1</sup>
C	1.659671000000	-0.283775000000	-3.369819000000	
C	1.649461000000	-0.665329000000	-2.000524000000	
C	1.570682000000	0.344351000000	-1.008467000000	
C	1.530329000000	1.748684000000	-1.399204000000	
C	1.559573000000	2.101915000000	-2.779939000000	
C	1.554344000000	1.081938000000	-3.765357000000	
C	1.463054000000	2.532668000000	-0.192147000000	
C	1.475264000000	1.669954000000	0.898479000000	
C	1.465435000000	0.283986000000	0.446468000000	

### CO-anti-Mo@Ind-h

E =	-5668.8	kcal mol <sup>-1</sup>	
C	1.294636000000	3.231090000000	2.218768000000
C	-0.073435000000	2.877811000000	2.485205000000
C	-1.147456000000	3.513239000000	1.729947000000
C	-0.829145000000	4.491913000000	0.726997000000
C	0.525500000000	4.728830000000	0.407318000000

C	1.582711000000	4.095688000000	1.141596000000
C	-2.396295000000	2.938006000000	2.183489000000
C	-2.094778000000	2.069917000000	3.288897000000
C	-0.693593000000	1.958152000000	3.426527000000
Rh	-1.469315000000	0.965153000000	1.344044000000
C	-1.744712000000	1.177827000000	-0.669352000000
C	-1.992726000000	0.314059000000	-1.673057000000
C	-0.380190000000	-0.538795000000	1.098934000000
O	0.330510000000	-1.444473000000	1.008394000000
C	-3.169480000000	-0.166604000000	1.341409000000
C	-3.571836000000	-1.196831000000	0.576188000000
C	-2.987334000000	-1.759786000000	-0.631605000000
C	-2.307725000000	-1.104006000000	-1.609021000000
H	-3.383958000000	3.264663000000	1.883734000000
H	-3.211707000000	-2.812560000000	-0.807291000000
H	-4.474882000000	-1.710948000000	0.925131000000
H	-2.040143000000	-1.681747000000	-2.494686000000
H	-1.926426000000	0.720486000000	-2.688379000000
H	-3.776096000000	0.108284000000	2.205612000000
H	-1.546289000000	2.223374000000	-0.926690000000
H	-2.826213000000	1.571274000000	3.912815000000
H	-0.168113000000	1.376218000000	4.173516000000
H	-1.619239000000	4.993277000000	0.176758000000
H	0.775620000000	5.424171000000	-0.387789000000
H	2.614320000000	4.320700000000	0.891020000000
H	2.099701000000	2.777582000000	2.788899000000
Mo	0.291316000000	5.400622000000	2.708630000000
C	0.916746000000	5.403877000000	4.600885000000
C	-1.239669000000	6.553201000000	3.261936000000
C	1.336418000000	7.050012000000	2.463144000000
O	1.294190000000	5.370073000000	5.704082000000
O	1.970585000000	8.016146000000	2.287601000000
O	-2.157384000000	7.208044000000	3.560162000000

### CO-anti-Mo@Ind-TS(h,4)

$$E = -5667 \text{ kcal mol}^{-1} \quad -254.02 \text{ cm}^{-1}$$

C	1.274875000000	3.242093000000	2.094960000000
C	-0.079398000000	2.891297000000	2.417883000000
C	-1.180847000000	3.555174000000	1.740811000000
C	-0.910394000000	4.555497000000	0.748138000000
C	0.428466000000	4.800720000000	0.371071000000
C	1.515671000000	4.144126000000	1.036129000000
C	-2.410903000000	2.959263000000	2.234144000000
C	-2.073803000000	2.062923000000	3.300254000000
C	-0.662192000000	1.921729000000	3.342551000000
Rh	-1.510459000000	0.988491000000	1.357593000000
C	-1.993041000000	1.102021000000	-0.639927000000
C	-1.910252000000	0.190807000000	-1.642897000000
C	-0.417664000000	-0.531152000000	1.199585000000
O	0.327306000000	-1.415466000000	1.213065000000
C	-3.292661000000	0.027150000000	0.985291000000
C	-3.547660000000	-1.181321000000	0.427401000000
C	-2.765456000000	-1.870843000000	-0.566388000000
C	-2.013314000000	-1.239275000000	-1.522871000000
H	-3.409411000000	3.293784000000	1.979711000000
H	-2.912921000000	-2.946555000000	-0.658392000000
H	-4.486338000000	-1.664522000000	0.718029000000
H	-1.600790000000	-1.841978000000	-2.331379000000
H	-1.811795000000	0.580817000000	-2.661244000000
H	-4.068619000000	0.512774000000	1.579471000000
H	-2.102987000000	2.159201000000	-0.897672000000
H	-2.778183000000	1.561504000000	3.952219000000
H	-0.102434000000	1.325720000000	4.052736000000
H	-1.724502000000	5.072708000000	0.249816000000
H	0.642265000000	5.518181000000	-0.414856000000
H	2.535498000000	4.373810000000	0.744802000000
H	2.104055000000	2.765582000000	2.608935000000
Mo	0.299688000000	5.400460000000	2.702895000000
C	0.979653000000	5.331343000000	4.573888000000
C	-1.196982000000	6.548197000000	3.346317000000
C	1.355965000000	7.047700000000	2.477739000000

O	1.387289000000	5.253676000000	5.664380000000	H	-0.439388000000	-2.233077000000	2.391918000000
O	1.994420000000	8.012596000000	2.311492000000	C	0.568142000000	2.444608000000	-1.549088000000
O	-2.097324000000	7.201372000000	3.698459000000	O	1.116576000000	3.190591000000	-2.254178000000
<b>CO-Mo@Ind-4</b>							
E = -5714.86 kcal mol <sup>-1</sup>							
H	-1.291366000000	2.848537000000	1.847808000000	C	-3.432734000000	0.610602000000	-1.086853000000
H	-2.024254000000	0.266448000000	2.000425000000	C	-2.227266000000	0.895819000000	-1.777837000000
C	0.397227000000	-1.558515000000	2.239605000000	C	-1.250525000000	-0.127184000000	-1.934649000000
H	-4.193519000000	1.383395000000	-1.003930000000	C	-3.656569000000	-0.652875000000	-0.557174000000
H	-4.592452000000	-0.871234000000	-0.047313000000	C	-2.676305000000	-1.662505000000	-0.685482000000
H	-2.861773000000	-2.650537000000	-0.269750000000	C	-1.491859000000	-1.406521000000	-1.363414000000
H	1.376453000000	2.940231000000	1.457340000000	C	0.781246000000	2.035744000000	1.499407000000
C	2.646144000000	0.197302000000	1.847972000000	C	-1.017619000000	0.625176000000	1.823551000000
H	-2.152796000000	1.817125000000	-2.346981000000	C	-0.636894000000	1.992389000000	1.739228000000
H	-0.754724000000	-2.194992000000	-1.496556000000	Rh	-0.296162000000	1.341764000000	-0.320370000000
H	-0.449205000000	-0.017434000000	-2.660150000000	Mo	1.679094000000	-0.396551000000	4.024301000000
C	2.847231000000	-1.205542000000	2.051595000000	C	3.249899000000	0.289566000000	5.019057000000
C	1.740707000000	-2.057324000000	2.275460000000	C	0.536013000000	0.801494000000	5.125623000000
H	3.499757000000	0.851833000000	1.697321000000	C	1.505122000000	-1.766341000000	5.445486000000
H	3.854496000000	-1.608364000000	2.071984000000	O	1.406137000000	-2.602673000000	6.255468000000
H	1.909369000000	-3.113679000000	2.461113000000	O	4.197688000000	0.689825000000	5.573117000000
				O	-0.161390000000	1.519918000000	5.727799000000

**Table B6.** Cartesian coordinates (in Å) and ADF total energies (in kcal mol<sup>-1</sup>) of all stationary points as well as imaginary frequencies of transition states (in cm<sup>-1</sup>) along the Path II catalyzed by anti-[W(CO)<sub>3</sub>IndRh(CO)], computed at ZORA-BLYP/TZ2P.

<b>CO-anti-W@Ind-1</b>							
E = -5070.31 kcal mol <sup>-1</sup>							
C	1.652020000000	0.196590000000	-3.657986000000	C	1.598228000000	2.683555000000	-0.177558000000
C	1.522247000000	-0.311264000000	-2.322851000000	C	1.398618000000	1.751832000000	0.791483000000
C	1.479942000000	0.588180000000	-1.237088000000	C	1.259093000000	0.387311000000	0.225872000000
C	1.643445000000	2.016657000000	-1.476453000000	Rh	-0.764936000000	-0.382525000000	0.617400000000
C	1.805271000000	2.514795000000	-2.787188000000	C	-1.890264000000	1.399995000000	0.015936000000
C	1.815431000000	1.585059000000	-3.880237000000	C	-1.919457000000	0.616521000000	-0.962065000000
				C	-0.716064000000	-2.244862000000	-0.485179000000
				C	-0.207215000000	-2.460274000000	0.649923000000
				H	1.725080000000	3.750961000000	-0.031798000000

H	1.354997000000	1.954693000000	1.855530000000	H	1.167882000000	2.424336000000	1.703583000000
H	1.823492000000	-0.409395000000	0.707086000000	H	1.924427000000	-0.008507000000	0.922510000000
H	-2.206020000000	0.323553000000	-1.955903000000	H	-2.583931000000	0.133448000000	-1.995488000000
H	-2.107827000000	2.319415000000	0.528478000000	H	-1.312263000000	2.312510000000	-0.433336000000
H	0.248884000000	-3.112579000000	1.375559000000	H	-1.435353000000	-3.189308000000	0.701757000000
H	-1.037482000000	-2.589902000000	-1.453586000000	H	-3.569764000000	-1.529238000000	-0.443808000000
H	1.415896000000	-1.378469000000	-2.158172000000	H	1.662888000000	-1.450632000000	-1.756551000000
H	1.669733000000	-0.491035000000	-4.497160000000	H	1.875516000000	-0.906163000000	-4.202288000000
H	1.947680000000	1.953411000000	-4.892751000000	H	1.956829000000	1.466859000000	-4.959695000000
H	1.937637000000	3.576228000000	-2.973028000000	H	1.759279000000	3.354288000000	-3.313324000000
C	-0.632633000000	0.004220000000	2.509779000000	C	-0.070259000000	-0.814726000000	2.327069000000
O	-0.734212000000	0.136528000000	3.655763000000	O	0.262363000000	-1.016549000000	3.422250000000
W	3.612141000000	0.897499000000	-2.439717000000	W	3.660801000000	0.942062000000	-2.373349000000
C	4.965358000000	1.820792000000	-3.565088000000	C	4.949321000000	1.751945000000	-3.646565000000
C	4.665396000000	-0.759575000000	-2.737861000000	C	4.851347000000	-0.643174000000	-2.329483000000
C	4.761990000000	1.286859000000	-0.857474000000	C	4.739119000000	1.720582000000	-0.893871000000
O	5.392622000000	1.526441000000	0.095500000000	O	5.324734000000	2.191046000000	0.001876000000
O	5.722415000000	2.382025000000	-4.255934000000	O	5.667266000000	2.239626000000	-4.430675000000
O	5.242784000000	-1.757781000000	-2.929688000000	O	5.512256000000	-1.608878000000	-2.315355000000

## CO-anti-W@Ind-TS(1,2)

$$E = -5056.32 \text{ kcal mol}^{-1} \quad -348.837 \text{ cm}^{-1}$$

C	1.784676000000	-0.104925000000	-3.476429000000
C	1.677667000000	-0.414265000000	-2.080597000000
C	1.532102000000	0.633829000000	-1.144551000000
C	1.573667000000	2.018447000000	-1.595363000000
C	1.721486000000	2.325907000000	-2.967665000000
C	1.836373000000	1.245515000000	-3.903723000000
C	1.416341000000	2.864957000000	-0.414160000000
C	1.272339000000	2.071235000000	0.682993000000
C	1.279446000000	0.632590000000	0.324985000000
Rh	-0.691879000000	-0.373799000000	0.641901000000
C	-1.593498000000	1.272054000000	-0.353543000000
C	-2.155027000000	0.341715000000	-1.026448000000
C	-2.512287000000	-1.486915000000	-0.226711000000
C	-1.579420000000	-2.200698000000	0.292647000000
H	1.442625000000	3.949518000000	-0.428360000000

## CO-anti-W@Ind-2

$$E = -5113.2 \text{ kcal mol}^{-1}$$

C	1.928855000000	-0.348947000000	0.369691000000
C	1.473917000000	-0.022919000000	-0.948874000000
C	0.930099000000	1.348598000000	-0.902056000000
C	1.108858000000	1.835773000000	0.451590000000
C	1.737659000000	0.805313000000	1.200625000000
C	0.451309000000	1.964686000000	-2.121999000000
C	0.309969000000	1.168338000000	-3.280326000000
C	0.836881000000	-0.167239000000	-3.324505000000
C	1.498242000000	-0.730659000000	-2.208827000000
Rh	-0.436625000000	0.096793000000	0.656434000000
C	-1.069091000000	-0.759263000000	2.160324000000
O	-1.466175000000	-1.280707000000	3.113862000000
C	-2.171035000000	1.248507000000	0.567029000000
C	-3.157711000000	0.715751000000	-0.176082000000
H	0.876152000000	2.833989000000	0.798602000000

H	2.036806000000	0.881293000000	2.239053000000	H	1.446000000000	2.189500000000	1.810000000000
H	2.408314000000	-1.273826000000	0.663538000000	H	1.872400000000	-0.303900000000	0.874300000000
H	-4.106794000000	1.227133000000	-0.349899000000	H	-2.623200000000	0.050800000000	-2.463000000000
H	-2.232216000000	2.197390000000	1.098477000000	H	-1.617900000000	1.961000000000	-1.105200000000
H	1.918318000000	-1.729551000000	-2.266028000000	H	-1.005000000000	-2.439000000000	0.737800000000
H	0.769775000000	-0.731254000000	-4.249235000000	H	-2.263100000000	-2.328500000000	-1.472700000000
H	-0.143552000000	1.589222000000	-4.171685000000	H	1.536600000000	-1.531200000000	-1.841700000000
H	0.081219000000	2.984385000000	-2.107970000000	H	1.738900000000	-0.875200000000	-4.261700000000
C	-2.890450000000	-0.611150000000	-0.737226000000	H	1.824000000000	1.518400000000	-4.927500000000
C	-1.699975000000	-1.153794000000	-0.427741000000	H	1.780300000000	3.333700000000	-3.185000000000
H	-3.619460000000	-1.122323000000	-1.369757000000	C	-0.157700000000	-0.547500000000	2.692200000000
H	-1.351646000000	-2.141900000000	-0.725917000000	O	0.091300000000	-1.164700000000	3.640900000000
W	2.658301000000	1.299536000000	-2.840136000000	W	3.567100000000	0.856300000000	-2.399300000000
C	3.173727000000	1.505201000000	-4.720160000000	C	4.849100000000	1.960700000000	-3.460200000000
C	4.467548000000	0.525183000000	-2.508782000000	C	4.726200000000	-0.713600000000	-2.823400000000
C	3.416458000000	3.117240000000	-2.524795000000	C	4.693500000000	1.196800000000	-0.779300000000
O	3.442798000000	1.613105000000	-5.855722000000	O	5.301500000000	1.404700000000	0.196900000000
O	3.818863000000	4.193302000000	-2.314319000000	O	5.558900000000	2.625000000000	-4.110000000000
O	5.503645000000	0.034214000000	-2.287216000000	O	5.358100000000	-1.660500000000	-3.089900000000
				C	-3.502500000000	1.147800000000	1.808800000000
				C	-2.987500000000	1.330100000000	2.889700000000
				H	-2.559700000000	1.472100000000	3.857500000000
				H	-3.970500000000	1.011800000000	0.858000000000

### CO-anti-W@Ind-TS(2,3)

E = -5611.87 kcal mol<sup>-1</sup> -56.58 cm<sup>-1</sup>

C	1.686900000000	-0.105300000000	-3.498600000000
C	1.589400000000	-0.483300000000	-2.117500000000
C	1.507900000000	0.525000000000	-1.140900000000
C	1.589100000000	1.928000000000	-1.526100000000
C	1.714300000000	2.291700000000	-2.886900000000
C	1.734900000000	1.255500000000	-3.878400000000
C	1.529100000000	2.717400000000	-0.303600000000
C	1.417600000000	1.875200000000	0.771400000000
C	1.323500000000	0.464200000000	0.334300000000
Rh	-0.709300000000	0.287400000000	1.020300000000
C	-1.544400000000	0.912700000000	-0.796900000000
C	-2.090600000000	-0.090300000000	-1.518900000000
C	-1.891700000000	-1.433500000000	-0.965900000000
C	-1.240000000000	-1.513800000000	0.213000000000
H	1.591700000000	3.800100000000	-0.268300000000

### CO-anti-W@Ind-3

E = -5617.94 kcal mol<sup>-1</sup>

C	1.660066000000	-0.215951000000	-3.452824000000
C	1.555643000000	-0.597370000000	-2.077853000000
C	1.465693000000	0.414437000000	-1.102372000000
C	1.512922000000	1.818531000000	-1.488916000000
C	1.622444000000	2.174834000000	-2.860909000000
C	1.629923000000	1.146943000000	-3.850799000000
C	1.466567000000	2.604656000000	-0.274266000000
C	1.391787000000	1.754740000000	0.811784000000
C	1.296661000000	0.353579000000	0.368619000000
Rh	-0.787045000000	0.428550000000	1.079698000000
C	-1.527126000000	0.758670000000	-0.853838000000

C	-1.925742000000	-0.357750000000	-1.506233000000	C	1.433878000000	1.781023000000	0.841287000000
C	-1.769000000000	-1.599194000000	-0.762212000000	C	1.337864000000	0.377295000000	0.405168000000
C	-1.268328000000	-1.497618000000	0.489313000000	Rh	-0.764965000000	0.374580000000	1.115659000000
H	1.516266000000	3.688022000000	-0.237619000000	C	-1.631884000000	0.791270000000	-0.780161000000
H	1.496202000000	2.068182000000	1.844737000000	C	-1.899233000000	-0.338665000000	-1.505321000000
H	1.810658000000	-0.435698000000	0.910688000000	C	-1.676097000000	-1.578574000000	-0.816940000000
H	-2.356184000000	-0.352153000000	-2.510198000000	C	-1.146217000000	-1.502260000000	0.438152000000
H	-1.632710000000	1.763245000000	-1.271981000000	H	1.540560000000	3.711207000000	-0.210235000000
H	-1.143740000000	-2.328294000000	1.182221000000	H	1.523428000000	2.095957000000	1.875236000000
H	-2.058780000000	-2.566230000000	-1.181957000000	H	1.869896000000	-0.402695000000	0.943242000000
H	1.535184000000	-1.646094000000	-1.801539000000	H	-2.266389000000	-0.315663000000	-2.533243000000
H	1.732537000000	-0.987997000000	-4.212725000000	H	-1.739307000000	1.798607000000	-1.181388000000
H	1.688987000000	1.406067000000	-4.902614000000	H	-1.012617000000	-2.363127000000	1.092437000000
H	1.661508000000	3.218045000000	-3.161334000000	H	-1.931125000000	-2.541860000000	-1.265367000000
C	-0.210218000000	-0.235175000000	2.832217000000	H	1.533537000000	-1.626795000000	-1.766875000000
O	0.066278000000	-0.791263000000	3.805333000000	H	1.693683000000	-0.973347000000	-4.182695000000
W	3.559222000000	0.814332000000	-2.411984000000	H	1.654057000000	1.420443000000	-4.873673000000
C	4.780541000000	2.219180000000	-3.099788000000	H	1.650284000000	3.235254000000	-3.133800000000
C	4.765116000000	-0.499928000000	-3.278928000000	C	-0.198052000000	-0.289012000000	2.849104000000
C	4.689612000000	0.690142000000	-0.778847000000	O	0.084840000000	-0.811624000000	3.839138000000
O	5.297881000000	0.619260000000	0.216694000000	W	3.555120000000	0.822260000000	-2.410604000000
O	5.461488000000	3.069610000000	-3.525792000000	C	4.771974000000	2.190640000000	-3.174139000000
O	5.433868000000	-1.294377000000	-3.816428000000	C	4.744218000000	-0.537043000000	-3.229774000000
C	-3.069203000000	0.776609000000	1.351283000000	C	4.706188000000	0.772270000000	-0.788804000000
C	-2.512030000000	1.535676000000	2.145211000000	O	5.326915000000	0.745526000000	0.201482000000
H	-2.315724000000	2.221584000000	2.944511000000	O	5.450517000000	3.019573000000	-3.644450000000
H	-3.761122000000	0.213252000000	0.760130000000	O	5.401714000000	-1.360164000000	-3.737705000000
				C	-2.993838000000	1.043535000000	0.909840000000
				C	-2.413317000000	1.490607000000	1.934962000000
				H	-2.506088000000	1.914506000000	2.920366000000
				H	-3.876583000000	0.728687000000	0.384783000000

### CO-anti-W@Ind-TS(3,b)

E = -5615.38 kcal mol<sup>-1</sup> -272.8 cm<sup>-1</sup>

C	1.636186000000	-0.199737000000	-3.423130000000
C	1.551799000000	-0.578552000000	-2.044628000000
C	1.485019000000	0.434105000000	-1.068282000000
C	1.526605000000	1.838283000000	-1.459139000000
C	1.613332000000	2.192572000000	-2.831307000000
C	1.608492000000	1.162024000000	-3.820990000000
C	1.494830000000	2.627673000000	-0.243845000000

### CO-anti-W@Ind-b

E = -5636.95 kcal mol<sup>-1</sup>

C	1.615151000000	-0.137368000000	-3.397480000000
C	1.580279000000	-0.540834000000	-2.027431000000
C	1.553109000000	0.456264000000	-1.024261000000

C	1.570081000000	1.869176000000	-1.393466000000
C	1.621118000000	2.243859000000	-2.765790000000
C	1.575247000000	1.234207000000	-3.771971000000
C	1.539283000000	2.637076000000	-0.169019000000
C	1.504535000000	1.766190000000	0.902738000000
C	1.441013000000	0.379116000000	0.439036000000
Rh	-0.713914000000	0.229992000000	1.158118000000
C	-1.689581000000	0.694194000000	-0.726589000000
C	-2.252997000000	-0.562452000000	-1.249748000000
C	-2.190666000000	-1.661478000000	-0.427237000000
C	-1.496352000000	-1.489345000000	0.793276000000
H	1.566172000000	3.720106000000	-0.115303000000
H	1.588953000000	2.063081000000	1.942746000000
H	1.936178000000	-0.420827000000	0.983614000000
H	-2.720932000000	-0.611897000000	-2.236173000000
H	-1.205159000000	1.323052000000	-1.479494000000
H	-1.456798000000	-2.293029000000	1.531549000000
H	-2.659576000000	-2.615191000000	-0.677890000000
H	1.574888000000	-1.595356000000	-1.770548000000
H	1.644953000000	-0.896987000000	-4.172753000000
H	1.584385000000	1.509980000000	-4.821160000000
H	1.646017000000	3.291923000000	-3.050953000000
C	-0.298433000000	-0.182187000000	3.023865000000
O	-0.170955000000	-0.490319000000	4.128489000000
W	3.577337000000	0.868037000000	-2.447261000000
C	4.767289000000	2.301550000000	-3.123744000000
C	4.723348000000	-0.406333000000	-3.439520000000
C	4.795937000000	0.658101000000	-0.890406000000
O	5.461042000000	0.535530000000	0.063583000000
O	5.430161000000	3.170638000000	-3.542363000000
O	5.353774000000	-1.179653000000	-4.050777000000
C	-2.728109000000	1.486393000000	0.106863000000
C	-2.456323000000	1.291354000000	1.391721000000
H	-2.929277000000	1.663926000000	2.295790000000
H	-3.516145000000	2.096011000000	-0.347977000000

### CO-anti-W@Ind-TS(b,h)

$$E = -5635.5 \text{ kcal mol}^{-1} \quad -227.56 \text{ cm}^{-1}$$

C	1.650752000000	-0.269396000000	-3.378331000000
C	1.642612000000	-0.662681000000	-2.008619000000
C	1.569113000000	0.341526000000	-1.007950000000
C	1.535714000000	1.750497000000	-1.387649000000
C	1.569775000000	2.115210000000	-2.768339000000
C	1.546065000000	1.100724000000	-3.764509000000
C	1.477885000000	2.524815000000	-0.173363000000
C	1.486403000000	1.653300000000	0.909512000000
C	1.466123000000	0.270592000000	0.447315000000
Rh	-0.728823000000	0.334100000000	1.182612000000
C	-1.763766000000	0.761878000000	-0.866292000000
C	-1.908353000000	-0.561148000000	-1.358332000000
C	-1.955284000000	-1.657330000000	-0.471839000000
C	-1.454546000000	-1.456559000000	0.800727000000
H	1.456941000000	3.608034000000	-0.124167000000
H	1.604901000000	1.959618000000	1.943333000000
H	1.923219000000	-0.539796000000	1.007263000000
H	-1.896273000000	-0.747882000000	-2.436048000000
H	-1.419670000000	1.497983000000	-1.595783000000
H	-1.436315000000	-2.256422000000	1.541790000000
H	-2.296095000000	-2.640621000000	-0.801413000000
H	1.693892000000	-1.714122000000	-1.744083000000
H	1.707527000000	-1.032394000000	-4.148909000000
H	1.536287000000	1.367611000000	-4.816031000000
H	1.554207000000	3.161561000000	-3.060882000000
C	-0.438346000000	-0.030820000000	3.008325000000
O	-0.300098000000	-0.299831000000	4.124683000000
W	3.578368000000	0.821984000000	-2.469986000000
C	4.712581000000	2.375623000000	-2.949309000000
C	4.747551000000	-0.251445000000	-3.649252000000
C	4.822733000000	0.420155000000	-0.971786000000
O	5.503408000000	0.177873000000	-0.052268000000
O	5.342598000000	3.315169000000	-3.250779000000
O	5.395624000000	-0.903065000000	-4.374587000000
C	-2.826071000000	1.354353000000	0.089960000000

C	-2.560282000000	1.235746000000	1.378905000000	W	0.294234000000	5.392313000000	2.697066000000
H	-3.133767000000	1.535839000000	2.249762000000	C	0.905319000000	5.384947000000	4.593583000000
H	-3.697960000000	1.837022000000	-0.364554000000	C	-1.251709000000	6.521977000000	3.252700000000
				C	1.330894000000	7.049219000000	2.463401000000
				O	1.274402000000	5.329513000000	5.700679000000
				O	1.965600000000	8.016753000000	2.283485000000
				O	-2.189474000000	7.153146000000	3.546702000000

### CO-anti-W@Ind-(h)

$$E = -5664.4 \text{ kcal mol}^{-1}$$

C	1.298172000000	3.245555000000	2.239501000000
C	-0.072438000000	2.888125000000	2.499877000000
C	-1.145537000000	3.522703000000	1.739468000000
C	-0.824343000000	4.503848000000	0.736888000000
C	0.535306000000	4.732654000000	0.411175000000
C	1.591434000000	4.099402000000	1.149086000000
C	-2.395592000000	2.945999000000	2.190208000000
C	-2.096225000000	2.079972000000	3.297613000000
C	-0.695982000000	1.968779000000	3.439915000000
Rh	-1.468273000000	0.975245000000	1.353004000000
C	-1.747624000000	1.195968000000	-0.658437000000
C	-1.994624000000	0.335906000000	-1.665524000000
C	-0.376163000000	-0.527102000000	1.103499000000
O	0.336568000000	-1.430804000000	1.009509000000
C	-3.165803000000	-0.159928000000	1.349329000000
C	-3.567081000000	-1.187718000000	0.580362000000
C	-2.982900000000	-1.744280000000	-0.630667000000
C	-2.306119000000	-1.083154000000	-1.606465000000
H	-3.382466000000	3.273312000000	1.888753000000
H	-3.204886000000	-2.796921000000	-0.810137000000
H	-4.468358000000	-1.705417000000	0.928586000000
H	-2.038289000000	-1.656841000000	-2.494682000000
H	-1.930503000000	0.746601000000	-2.679269000000
H	-3.770817000000	0.110026000000	2.216267000000
H	-1.553433000000	2.243506000000	-0.911349000000
H	-2.829259000000	1.581899000000	3.920177000000
H	-0.172457000000	1.388129000000	4.189214000000
H	-1.612545000000	5.007852000000	0.186932000000
H	0.786703000000	5.426252000000	-0.384748000000
H	2.623777000000	4.323075000000	0.901284000000
H	2.101317000000	2.797219000000	2.815877000000

### CO-anti-W@Ind-TS(h,4)

$$E = -5662.63 \text{ kcal mol}^{-1} \quad -254.33 \text{ cm}^{-1}$$

C	1.284399000000	3.261283000000	2.110737000000
C	-0.071738000000	2.902436000000	2.426757000000
C	-1.174277000000	3.564062000000	1.745963000000
C	-0.903284000000	4.570023000000	0.756107000000
C	0.439538000000	4.812878000000	0.374238000000
C	1.527705000000	4.157210000000	1.041407000000
C	-2.404264000000	2.966393000000	2.238863000000
C	-2.066987000000	2.072948000000	3.307222000000
C	-0.655628000000	1.932795000000	3.351311000000
Rh	-1.506375000000	0.996304000000	1.364741000000
C	-1.983803000000	1.114862000000	-0.632883000000
C	-1.903407000000	0.204982000000	-1.637182000000
C	-0.423644000000	-0.532353000000	1.212941000000
O	0.311701000000	-1.424554000000	1.231958000000
C	-3.293059000000	0.045022000000	0.987938000000
C	-3.552987000000	-1.161328000000	0.427779000000
C	-2.772460000000	-1.853482000000	-0.565671000000
C	-2.014890000000	-1.224676000000	-1.519587000000
H	-3.402684000000	3.300701000000	1.984052000000
H	-2.925007000000	-2.928348000000	-0.659220000000
H	-4.494351000000	-1.640525000000	0.716353000000
H	-1.603215000000	-1.828434000000	-2.327740000000
H	-1.798566000000	0.596125000000	-2.654462000000
H	-4.067546000000	0.533214000000	1.581929000000
H	-2.085552000000	2.173357000000	-0.889233000000
H	-2.771444000000	1.572387000000	3.959801000000
H	-0.096063000000	1.338907000000	4.063391000000

H	-1.716760000000	5.089510000000	0.259740000000	C	-1.247806000000	-0.126251000000	-1.924604000000
H	0.652764000000	5.531897000000	-0.410121000000	C	-3.647656000000	-0.661608000000	-0.540299000000
H	2.547839000000	4.389299000000	0.753914000000	C	-2.663473000000	-1.666861000000	-0.670450000000
H	2.113158000000	2.791240000000	2.630779000000	C	-1.481652000000	-1.406020000000	-1.351674000000
W	0.301668000000	5.393924000000	2.692109000000	C	0.791060000000	2.030919000000	1.507405000000
C	0.973785000000	5.312630000000	4.565083000000	C	-1.012782000000	0.626886000000	1.834114000000
C	-1.212822000000	6.512588000000	3.342787000000	C	-0.627052000000	1.992518000000	1.747934000000
C	1.342961000000	7.052728000000	2.479952000000	Rh	-0.293797000000	1.344860000000	-0.311467000000
O	1.377581000000	5.212475000000	5.657129000000	W	1.677065000000	-0.397171000000	4.012727000000
O	1.977762000000	8.021975000000	2.310340000000	C	3.243964000000	0.297670000000	5.008548000000
O	-2.135043000000	7.138858000000	3.693267000000	C	0.524297000000	0.805755000000	5.095690000000
				C	1.498493000000	-1.762547000000	5.438705000000
				O	1.394899000000	-2.606673000000	6.242607000000
				O	4.196414000000	0.703546000000	5.554480000000
				O	-0.187158000000	1.531805000000	5.675754000000

### CO-anti-W@Ind-4

E = -5710.81 kcal mol<sup>-1</sup>

H	-1.278035000000	2.851103000000	1.858420000000
H	-2.020198000000	0.272162000000	2.014438000000
C	0.394059000000	-1.562684000000	2.261036000000
H	-4.194111000000	1.372500000000	-0.986222000000
H	-4.581293000000	-0.883612000000	-0.027884000000
H	-2.843591000000	-2.655538000000	-0.253839000000
H	1.389446000000	2.933323000000	1.466333000000
C	2.653194000000	0.186549000000	1.866713000000
H	-2.158145000000	1.814799000000	-2.333988000000
H	-0.741470000000	-2.191394000000	-1.486351000000
H	-0.447985000000	-0.012792000000	-2.651219000000
C	2.850321000000	-1.220355000000	2.066997000000
C	1.738519000000	-2.067553000000	2.297464000000
H	3.509257000000	0.838746000000	1.721769000000
H	3.856089000000	-1.625936000000	2.093282000000
H	1.903187000000	-3.122749000000	2.492059000000
H	-0.444501000000	-2.232434000000	2.421726000000
C	0.570596000000	2.450619000000	-1.538070000000
O	1.120286000000	3.198635000000	-2.240069000000
C	1.338080000000	0.698842000000	1.807909000000
C	0.193978000000	-0.188149000000	2.013271000000
C	-3.430403000000	0.602801000000	-1.071176000000
C	-2.228379000000	0.892558000000	-1.765771000000



# Appendix C

## Associated to Chapter 5

**Table C1.** Cartesian coordinates (in Å) and ADF total energies (in kcal mol<sup>-1</sup>) of all stationary points, as well as imaginary frequencies of transition states (in cm<sup>-1</sup>) along the Path I catalyzed by CpNRh, computed at ZORA-BLYP/TZ2P.

<b>CpN-1</b>			
$E = -4415.13 \text{ kcal mol}^{-1}$			
C	1.845141000000	-0.473739000000	0.039566000000
C	1.920600000000	0.393261000000	-1.138221000000
C	1.348639000000	1.672311000000	-0.752009000000
C	0.942439000000	1.545117000000	0.649248000000
C	1.448244000000	0.311964000000	1.165766000000
Rh	-0.444816000000	-0.215479000000	0.110805000000
C	-1.314363000000	-1.940410000000	-0.827106000000
C	-0.609490000000	-2.323094000000	0.141956000000
C	-2.010815000000	0.805610000000	1.096891000000
C	-2.436699000000	0.568583000000	-0.062810000000
H	0.561821000000	2.361609000000	1.253225000000
H	1.504807000000	0.022406000000	2.207855000000
H	2.274372000000	-1.468133000000	0.096616000000
H	-3.199027000000	0.525902000000	-0.820895000000
H	-2.073700000000	1.236642000000	2.081844000000
H	-0.144651000000	-3.066922000000	0.766862000000
H	-2.031404000000	-2.087093000000	-1.615770000000
C	1.263699000000	2.709267000000	-1.662569000000
C	2.390426000000	0.190801000000	-2.422681000000
C	1.756709000000	2.527196000000	-2.986461000000
C	2.327689000000	1.251269000000	-3.371591000000
H	2.812971000000	-0.767000000000	-2.722684000000
H	0.828788000000	3.668069000000	-1.384215000000
C	1.710599000000	3.570691000000	-3.954697000000
C	2.816783000000	1.099337000000	-4.700561000000
C	2.194614000000	3.383998000000	-5.235344000000
C	2.753253000000	2.135838000000	-5.612068000000
H	1.282555000000	4.529803000000	-3.666194000000
H	2.148014000000	4.194767000000	-5.959467000000
H	3.131729000000	1.997146000000	-6.622718000000
H	3.246872000000	0.141615000000	-4.990634000000
<b>CpN-TS(1,2)</b>			
$E = -4399.03 \text{ kcal mol}^{-1} \quad -440.26 \text{ cm}^{-1}$			
C	1.908653000000	-0.306334000000	0.264229000000
C	1.945849000000	0.478358000000	-0.966452000000
C	1.326574000000	1.771059000000	-0.678616000000
C	0.912343000000	1.746981000000	0.707003000000
C	1.383670000000	0.532809000000	1.300844000000
Rh	-0.319557000000	-0.168862000000	0.067192000000
C	-1.850378000000	-1.149840000000	-1.143645000000
C	-0.898331000000	-1.950690000000	-0.809643000000
C	-1.832666000000	-0.103417000000	1.418362000000
C	-2.491335000000	0.052206000000	0.321284000000
H	0.447633000000	2.568023000000	1.240559000000
H	1.360985000000	0.292400000000	2.357093000000
H	2.391023000000	-1.264963000000	0.412588000000
H	-3.368074000000	0.528772000000	-0.096137000000
H	-1.867940000000	-0.135789000000	2.496930000000
H	-0.459469000000	-2.913956000000	-1.020027000000
H	-2.556010000000	-0.888730000000	-1.921162000000

C	1.211285000000	2.731378000000	-1.682616000000	C	4.111537000000	-2.720055000000	-0.882924000000
C	2.422992000000	0.198210000000	-2.246065000000	H	1.578190000000	-3.576804000000	1.324397000000
C	1.709443000000	2.461846000000	-2.977397000000	H	4.451625000000	-0.722366000000	-1.670727000000
C	2.324916000000	1.173552000000	-3.264467000000	C	5.194267000000	-3.334464000000	-1.573045000000
H	2.883947000000	-0.762752000000	-2.469507000000	C	3.602595000000	-4.924722000000	0.111732000000
H	0.748567000000	3.695592000000	-1.477722000000	C	5.465650000000	-4.681459000000	-1.424023000000
C	1.631133000000	3.425818000000	-4.030457000000	C	4.663446000000	-5.484372000000	-0.574364000000
C	2.820702000000	0.936151000000	-4.583966000000	H	5.812531000000	-2.720665000000	-2.226182000000
C	2.121632000000	3.153998000000	-5.288257000000	H	6.298331000000	-5.131013000000	-1.960783000000
C	2.723547000000	1.894039000000	-5.568664000000	H	4.885383000000	-6.543673000000	-0.465523000000
H	1.171779000000	4.390042000000	-3.817357000000	H	2.984701000000	-5.540664000000	0.763168000000
H	2.051002000000	3.902332000000	-6.074922000000				
H	3.106665000000	1.691832000000	-6.566731000000				
H	3.281441000000	-0.026985000000	-4.798988000000				

## CpN-2

$$E = -4437.81 \text{ kcal mol}^{-1}$$

C	1.214542000000	0.638825000000	0.695989000000	C	4.145283000000	-2.818871000000	-0.639119000000
C	0.868365000000	-0.737433000000	1.064402000000	C	3.856310000000	-1.449179000000	-0.869474000000
C	1.941941000000	-1.599397000000	0.545830000000	C	2.748492000000	-0.867106000000	-0.269727000000
C	2.778654000000	-0.768641000000	-0.308597000000	C	1.865983000000	-1.658609000000	0.577410000000
C	2.268397000000	0.600354000000	-0.222497000000	C	2.129471000000	-3.003608000000	0.800320000000
Rh	0.160735000000	-0.528962000000	-0.897324000000	C	3.269134000000	-3.607489000000	0.209441000000
C	-1.529493000000	0.581945000000	-0.773428000000	C	2.211410000000	0.490752000000	-0.298802000000
C	-2.673604000000	-0.078459000000	-1.044362000000	C	1.123715000000	0.562301000000	0.596499000000
C	-2.522643000000	-1.526512000000	-1.275363000000	C	0.784294000000	-0.774666000000	1.019461000000
C	-1.252145000000	-1.977498000000	-1.192261000000	Rh	0.140050000000	-0.596211000000	-1.095891000000
H	2.696378000000	1.456800000000	-0.731629000000	C	-1.374647000000	-1.996192000000	-0.867518000000
H	0.707011000000	1.526157000000	1.053815000000	C	-2.612401000000	-1.476382000000	-0.721547000000
H	0.186362000000	-1.014594000000	1.860899000000	C	-2.671115000000	-0.022267000000	-0.767688000000
H	-1.464612000000	1.652563000000	-0.566526000000	C	-1.484355000000	0.599695000000	-0.929345000000
H	-0.983831000000	-3.032874000000	-1.301181000000	H	2.668554000000	1.333437000000	-0.804908000000
H	-3.644493000000	0.420430000000	-1.098680000000	H	0.601242000000	1.463326000000	0.892615000000
H	-3.384958000000	-2.162852000000	-1.488217000000	H	0.046125000000	-1.017809000000	1.773784000000
C	2.199532000000	-2.953346000000	0.683740000000	H	-1.335018000000	1.676650000000	-1.010506000000
C	3.826188000000	-1.331401000000	-1.020025000000	H	-1.148756000000	-3.064693000000	-0.877741000000
C	3.291050000000	-3.541457000000	-0.014888000000	H	-3.609000000000	0.531077000000	-0.684332000000
				H	-3.506633000000	-2.085880000000	-0.575599000000
				H	1.476959000000	-3.601514000000	1.434396000000
				H	4.517456000000	-0.865661000000	-1.508438000000

## CpN-3

$$E = -4967.37 \text{ kcal mol}^{-1}$$

C	4.145283000000	-2.818871000000	-0.639119000000
C	3.856310000000	-1.449179000000	-0.869474000000
C	2.748492000000	-0.867106000000	-0.269727000000
C	1.865983000000	-1.658609000000	0.577410000000
C	2.129471000000	-3.003608000000	0.800320000000
C	3.269134000000	-3.607489000000	0.209441000000
C	2.211410000000	0.490752000000	-0.298802000000
C	1.123715000000	0.562301000000	0.596499000000
C	0.784294000000	-0.774666000000	1.019461000000
Rh	0.140050000000	-0.596211000000	-1.095891000000
C	-1.374647000000	-1.996192000000	-0.867518000000
C	-2.612401000000	-1.476382000000	-0.721547000000
C	-2.671115000000	-0.022267000000	-0.767688000000
C	-1.484355000000	0.599695000000	-0.929345000000
H	2.668554000000	1.333437000000	-0.804908000000
H	0.601242000000	1.463326000000	0.892615000000
H	0.046125000000	-1.017809000000	1.773784000000
H	-1.335018000000	1.676650000000	-1.010506000000
H	-1.148756000000	-3.064693000000	-0.877741000000
H	-3.609000000000	0.531077000000	-0.684332000000
H	-3.506633000000	-2.085880000000	-0.575599000000
H	1.476959000000	-3.601514000000	1.434396000000
H	4.517456000000	-0.865661000000	-1.508438000000

C	-0.086275000000	-1.160531000000	-3.155970000000	H	4.315850000000	-0.612804000000	-1.426719000000
C	0.469160000000	-0.038064000000	-3.162999000000	C	-0.748199000000	-2.069670000000	-2.320354000000
H	0.892426000000	0.846009000000	-3.604655000000	C	-0.091125000000	-1.167157000000	-2.962352000000
H	-0.578869000000	-2.016052000000	-3.581886000000	H	0.341534000000	-0.829433000000	-3.888985000000
C	5.284622000000	-3.454406000000	-1.217251000000	H	-1.188522000000	-3.053249000000	-2.327240000000
C	3.588806000000	-4.981166000000	0.426737000000	C	5.374595000000	-3.110015000000	-1.363481000000
C	5.557178000000	-4.785718000000	-0.982599000000	C	3.929066000000	-4.939713000000	0.213591000000
C	4.700260000000	-5.557326000000	-0.151629000000	C	5.800190000000	-4.413461000000	-1.244652000000
H	5.942460000000	-2.863976000000	-1.853370000000	C	5.068619000000	-5.339937000000	-0.446256000000
H	6.430914000000	-5.251015000000	-1.433904000000	H	5.935373000000	-2.403204000000	-1.973334000000
H	4.925191000000	-6.606850000000	0.025950000000	H	6.699299000000	-4.743155000000	-1.761114000000
H	2.932953000000	-5.572966000000	1.063487000000	H	5.416614000000	-6.367245000000	-0.361151000000
				H	3.371254000000	-5.648008000000	0.824547000000

### CpN-TS(3,4)

$$E = -4960.55 \text{ kcal mol}^{-1} \quad -313.704 \text{ cm}^{-1}$$

C	4.195508000000	-2.648326000000	-0.697601000000
C	3.752395000000	-1.312797000000	-0.811660000000
C	2.608588000000	-0.898551000000	-0.127854000000
C	1.860032000000	-1.848451000000	0.693042000000
C	2.282254000000	-3.174903000000	0.795142000000
C	3.447651000000	-3.595927000000	0.119036000000
C	1.918279000000	0.375612000000	-0.047720000000
C	0.857060000000	0.253604000000	0.912395000000
C	0.734861000000	-1.129041000000	1.263972000000
Rh	0.123205000000	-0.762216000000	-0.920218000000
C	-1.903192000000	-1.193387000000	-0.724825000000
C	-2.704284000000	-0.184199000000	-1.171821000000
C	-2.049763000000	0.895255000000	-1.858684000000
C	-0.695888000000	0.809955000000	-1.964239000000
H	2.261846000000	1.304877000000	-0.486582000000
H	0.256313000000	1.065000000000	1.304073000000
H	0.024528000000	-1.534139000000	1.974880000000
H	-0.073132000000	1.548568000000	-2.465149000000
H	-2.275789000000	-2.066858000000	-0.193148000000
H	-2.613885000000	1.718859000000	-2.300019000000
H	-3.787975000000	-0.206922000000	-1.044506000000
H	1.728999000000	-3.888801000000	1.403379000000

### CpN-4

$$E = -5034.02 \text{ kcal mol}^{-1}$$

C	1.946582000000	0.297752000000	-0.687466000000
C	1.952103000000	0.183086000000	0.758579000000
C	0.887855000000	1.082676000000	1.254625000000
C	0.482065000000	1.957804000000	0.177429000000
C	0.879197000000	1.263757000000	-1.027369000000
Rh	-0.834269000000	0.349739000000	0.054555000000
C	-2.028261000000	-1.318980000000	1.143363000000
C	-1.689667000000	-1.856655000000	-0.122808000000
C	-2.042502000000	-1.117742000000	-1.279088000000
C	-2.860084000000	0.049854000000	-1.180106000000
C	-3.299332000000	0.506733000000	0.082681000000
C	-2.845470000000	-0.151473000000	1.247595000000
H	0.746297000000	1.308659000000	2.307790000000
H	0.069478000000	2.958007000000	0.258441000000
H	0.730150000000	1.653210000000	-2.030551000000
H	-1.699583000000	-1.821992000000	2.048631000000
H	-1.109554000000	-2.770430000000	-0.202078000000
H	-1.724821000000	-1.464271000000	-2.258674000000
H	-3.125685000000	0.219787000000	2.229235000000
H	-3.941563000000	1.379647000000	0.159018000000
H	-3.151870000000	0.577241000000	-2.083817000000

C	2.820817000000	-0.431325000000	-1.453281000000	C	-2.557585000000	2.289225000000	-0.053627000000
C	2.831707000000	-0.657031000000	1.393250000000	C	-3.473945000000	1.210900000000	-0.092570000000
C	3.753049000000	-1.323928000000	-0.819423000000	C	-3.181607000000	0.074051000000	-0.830070000000
C	3.758602000000	-1.437946000000	0.619581000000	H	-1.002522000000	-2.572039000000	1.659556000000
H	2.823604000000	-0.352535000000	-2.540129000000	H	1.659716000000	-2.579431000000	1.153658000000
H	2.842784000000	-0.750503000000	2.478879000000	C	2.914586000000	0.054832000000	1.937728000000
C	4.676572000000	-2.098439000000	-1.565337000000	H	-0.266208000000	1.139078000000	-2.285806000000
C	4.687236000000	-2.319777000000	1.227120000000	H	-0.688127000000	3.070320000000	-0.773406000000
C	5.573561000000	-2.953607000000	-0.939408000000	H	-2.796606000000	3.180110000000	0.523576000000
C	5.578952000000	-3.065108000000	0.467473000000	H	-1.732392000000	-0.024109000000	2.155804000000
H	4.674422000000	-2.011726000000	-2.651399000000	C	0.693292000000	1.727632000000	2.603419000000
H	6.274008000000	-3.537750000000	-1.532977000000	H	-1.843357000000	-0.819029000000	-2.281425000000
H	6.283437000000	-3.735156000000	0.956227000000	H	-4.415045000000	1.282723000000	0.449192000000
H	4.693346000000	-2.405283000000	2.313262000000	H	-3.896018000000	-0.745060000000	-0.881187000000
				H	0.179998000000	-3.143769000000	-1.801603000000
				H	1.857536000000	-0.558234000000	-2.601804000000
				C	2.020042000000	2.228429000000	2.741548000000
C	1.619394000000	-0.417911000000	1.828491000000	C	3.146395000000	1.380755000000	2.403903000000
C	1.064344000000	-1.700477000000	1.378228000000	H	-0.146351000000	2.374343000000	2.852909000000
C	-0.349153000000	-1.707945000000	1.666828000000	H	3.764710000000	-0.574486000000	1.678637000000
C	-0.726765000000	-0.359509000000	1.928967000000	C	2.280113000000	3.547813000000	3.209720000000
C	0.488578000000	0.430805000000	2.168290000000	C	4.461402000000	1.905343000000	2.554178000000
Rh	-0.004646000000	-0.650972000000	-0.220630000000	C	4.673406000000	3.192744000000	3.010461000000
C	0.477645000000	-2.113698000000	-1.692641000000	C	3.571840000000	4.021936000000	3.341628000000
C	1.152085000000	-1.093400000000	-1.987580000000	H	1.434957000000	4.185241000000	3.466441000000
C	-1.964793000000	-0.020314000000	-1.557415000000	H	3.747029000000	5.034031000000	3.700650000000
C	-1.058414000000	1.074806000000	-1.546772000000	H	5.686968000000	3.573726000000	3.116997000000
C	-1.373016000000	2.225244000000	-0.771686000000	H	5.307922000000	1.268291000000	2.301312000000

## CpN-5

E = -5556.38 kcal mol<sup>-1</sup>

C	1.619394000000	-0.417911000000	1.828491000000	C	3.146395000000	1.380755000000	2.403903000000
C	1.064344000000	-1.700477000000	1.378228000000	H	-0.146351000000	2.374343000000	2.852909000000
C	-0.349153000000	-1.707945000000	1.666828000000	H	3.764710000000	-0.574486000000	1.678637000000
C	-0.726765000000	-0.359509000000	1.928967000000	C	2.280113000000	3.547813000000	3.209720000000
C	0.488578000000	0.430805000000	2.168290000000	C	4.461402000000	1.905343000000	2.554178000000
Rh	-0.004646000000	-0.650972000000	-0.220630000000	C	4.673406000000	3.192744000000	3.010461000000
C	0.477645000000	-2.113698000000	-1.692641000000	C	3.571840000000	4.021936000000	3.341628000000
C	1.152085000000	-1.093400000000	-1.987580000000	H	1.434957000000	4.185241000000	3.466441000000
C	-1.964793000000	-0.020314000000	-1.557415000000	H	3.747029000000	5.034031000000	3.700650000000
C	-1.058414000000	1.074806000000	-1.546772000000	H	5.686968000000	3.573726000000	3.116997000000
C	-1.373016000000	2.225244000000	-0.771686000000	H	5.307922000000	1.268291000000	2.301312000000

**Table C2.** Cartesian coordinates (in Å) and ADF total energies (in kcal mol<sup>-1</sup>) of all stationary points, as well as imaginary frequencies of transition states (in cm<sup>-1</sup>) along the Path I catalyzed by FNRh, computed at ZORA-BLYP/TZ2P

**FN-1**

E = -4412.38 kcal mol<sup>-1</sup>

C	1.866529000000	-0.455824000000	0.009835000000
C	1.744055000000	0.367839000000	-1.184999000000
C	1.271615000000	1.675113000000	-0.778527000000
C	1.248975000000	1.706579000000	0.687475000000
C	1.707360000000	0.418080000000	1.163939000000
Rh	-0.294190000000	-0.151453000000	-0.031334000000
C	-0.895622000000	-2.112882000000	-0.628373000000
C	-0.916501000000	-2.086443000000	0.627884000000
C	-2.250897000000	0.622904000000	0.543890000000
C	-2.229053000000	0.597920000000	-0.703421000000
H	2.294931000000	-1.452442000000	0.037895000000
H	-2.593522000000	0.729479000000	-1.706106000000
H	-2.649941000000	0.793429000000	1.527335000000
H	-1.063158000000	-2.515678000000	1.604539000000
H	-1.010162000000	-2.582717000000	-1.590514000000
C	1.023337000000	2.668510000000	-1.752422000000
C	1.971461000000	0.098403000000	-2.556673000000
C	1.265361000000	2.376831000000	-3.089229000000
C	1.742259000000	1.102689000000	-3.487704000000
H	2.335166000000	-0.878074000000	-2.869767000000
H	1.929650000000	0.912049000000	-4.542287000000
H	1.094758000000	3.139989000000	-3.845580000000
H	0.667040000000	3.653622000000	-1.459324000000
C	0.971629000000	2.740564000000	1.609772000000
C	1.891816000000	0.207505000000	2.552206000000
C	1.171887000000	2.506398000000	2.964724000000
C	1.634818000000	1.250623000000	3.431873000000
H	0.978780000000	3.301144000000	3.682153000000
H	1.789272000000	1.105319000000	4.498947000000
H	2.244721000000	-0.754567000000	2.917837000000
H	0.625539000000	3.712115000000	1.263902000000

**FN-TS(1,2)**

E = -4396.67 kcal mol<sup>-1</sup> -415.628 cm<sup>-1</sup>

C	1.964950000000	-0.402467000000	-0.113585000000
C	1.658139000000	0.497783000000	-1.205414000000
C	1.219972000000	1.768921000000	-0.642535000000
C	1.386288000000	1.695637000000	0.801948000000
C	1.880010000000	0.372407000000	1.118944000000
Rh	-0.247196000000	-0.263293000000	-0.099133000000
C	-0.869413000000	-1.992887000000	0.783232000000
C	-1.835620000000	-1.169660000000	1.030119000000
C	-2.363323000000	-0.039139000000	-0.550017000000
C	-1.617390000000	-0.299669000000	-1.571836000000
H	2.452257000000	-1.365459000000	-0.213250000000
H	-1.534722000000	-0.450148000000	-2.638913000000
H	-3.256759000000	0.483211000000	-0.235272000000
H	-2.591258000000	-0.889738000000	1.752161000000
H	-0.463260000000	-2.967605000000	1.007798000000
C	0.837243000000	2.825643000000	-1.504163000000
C	1.739677000000	0.351866000000	-2.623049000000
C	0.914139000000	2.642516000000	-2.874802000000
C	1.374432000000	1.412654000000	-3.429265000000
H	2.093558000000	-0.582247000000	-3.054238000000
H	1.442267000000	1.314585000000	-4.510893000000
H	0.631679000000	3.451646000000	-3.544666000000
H	0.503557000000	3.776424000000	-1.093706000000
C	1.185484000000	2.639369000000	1.828025000000
C	2.164724000000	0.036925000000	2.463143000000
C	1.484380000000	2.285441000000	3.140223000000
C	1.972093000000	0.993324000000	3.453034000000
H	1.346968000000	3.010593000000	3.939349000000
H	2.201646000000	0.748989000000	4.488161000000
H	2.538414000000	-0.953517000000	2.715006000000
H	0.814264000000	3.636097000000	1.598492000000

**FN-2**

$$E = -4441.52 \text{ kcal mol}^{-1}$$

C 1.174137000000 0.942140000000 0.432610000000  
C 0.732609000000 -0.469382000000 0.623998000000  
C 1.948982000000 -1.283926000000 0.340372000000  
C 2.985776000000 -0.433175000000 -0.151242000000  
C 2.502093000000 0.956187000000 -0.094860000000  
Rh -0.181396000000 -0.684713000000 -1.208427000000  
C -2.021012000000 0.014410000000 -0.830569000000  
C -2.957831000000 -0.953115000000 -0.727328000000  
C -2.451123000000 -2.332580000000 -0.823952000000  
C -1.117238000000 -2.445320000000 -1.003661000000  
H 0.078053000000 -0.732869000000 1.454275000000  
H -2.216831000000 1.087723000000 -0.761667000000  
H -0.570479000000 -3.389295000000 -1.075424000000  
H -4.018993000000 -0.738967000000 -0.583011000000  
H -3.116259000000 -3.195967000000 -0.753644000000  
C 2.171873000000 -2.661933000000 0.467549000000  
C 4.219702000000 -0.970041000000 -0.531547000000  
C 3.415650000000 -3.186945000000 0.094652000000  
C 4.426522000000 -2.350454000000 -0.405820000000  
H 1.391235000000 -3.313427000000 0.853670000000  
H 3.602281000000 -4.253856000000 0.195528000000  
H 5.384879000000 -2.778928000000 -0.691322000000  
H 5.017171000000 -0.330705000000 -0.904907000000  
C 3.125614000000 2.167994000000 -0.406817000000  
C 0.496412000000 2.147690000000 0.661838000000  
C 2.433721000000 3.365476000000 -0.178588000000  
C 1.135417000000 3.356160000000 0.355918000000  
H 4.137369000000 2.190240000000 -0.806743000000  
H 2.911187000000 4.314972000000 -0.411019000000  
H 0.621584000000 4.297858000000 0.535874000000  
H -0.509260000000 2.144848000000 1.075955000000

**FN-3**

$$E = -4968.67 \text{ kcal mol}^{-1}$$

C 4.148665000000 -2.533660000000 -0.461072000000  
C 3.933155000000 -1.187741000000 -0.749026000000  
C 2.779873000000 -0.558251000000 -0.246313000000  
C 1.823660000000 -1.306904000000 0.529520000000  
C 2.064833000000 -2.671058000000 0.806171000000  
C 3.223518000000 -3.266667000000 0.316511000000  
C 2.334384000000 0.834710000000 -0.282951000000  
C 1.109530000000 0.926086000000 0.470662000000  
C 0.702683000000 -0.424715000000 0.880382000000  
Rh 0.081015000000 -0.679471000000 -1.159749000000  
C -1.003135000000 -2.373486000000 -0.897632000000  
C -2.335968000000 -2.202188000000 -0.749400000000  
C -2.777534000000 -0.819715000000 -0.788189000000  
C -1.788170000000 0.084222000000 -0.966636000000  
H -0.002954000000 -0.629148000000 1.678665000000  
H -1.919266000000 1.163912000000 -1.059940000000  
H -0.483012000000 -3.332555000000 -0.934051000000  
H -3.826185000000 -0.534667000000 -0.684505000000  
H -3.027167000000 -3.036308000000 -0.614589000000  
H 1.356364000000 -3.242768000000 1.401328000000  
H 3.424252000000 -4.313095000000 0.536551000000  
H 5.043894000000 -3.028097000000 -0.831861000000  
H 4.657935000000 -0.629541000000 -1.338019000000  
C 0.268694000000 -1.332547000000 -3.231049000000  
C -0.112296000000 -0.145675000000 -3.264928000000  
H -0.483307000000 0.774841000000 -3.677273000000  
H 0.509692000000 -2.316565000000 -3.589763000000  
C 0.511021000000 2.188585000000 0.678920000000  
C 2.916773000000 1.991537000000 -0.832162000000  
C 2.307712000000 3.224928000000 -0.611547000000  
C 1.117215000000 3.321591000000 0.144280000000  
H 2.756057000000 4.128615000000 -1.018650000000  
H 0.670888000000 4.299635000000 0.311557000000  
H 3.839905000000 1.929703000000 -1.404716000000  
H -0.406620000000 2.271000000000 1.256947000000

**FN-TS(3,4)**E = -4959.14 kcal mol<sup>-1</sup> -421.889 cm<sup>-1</sup>

C	4.025018000000	-2.574395000000	-0.626164000000
C	3.775037000000	-1.245592000000	-0.936608000000
C	2.692564000000	-0.584271000000	-0.312219000000
C	1.841885000000	-1.301922000000	0.618881000000
C	2.122423000000	-2.664561000000	0.909367000000
C	3.203556000000	-3.276256000000	0.295986000000
C	2.242604000000	0.801286000000	-0.345161000000
C	1.120176000000	0.921724000000	0.566785000000
C	0.802490000000	-0.398367000000	1.093021000000
Rh	0.199923000000	-0.639919000000	-1.000234000000
C	-0.924373000000	-2.335236000000	-1.174752000000
C	-2.288069000000	-2.151867000000	-1.203172000000
C	-2.702466000000	-0.796176000000	-1.260690000000
C	-1.674203000000	0.118449000000	-1.281370000000
H	0.120851000000	-0.600517000000	1.910609000000
H	-1.817814000000	1.198953000000	-1.292269000000
H	-0.440939000000	-3.309645000000	-1.102827000000
H	-3.748178000000	-0.501078000000	-1.358474000000
H	-2.988678000000	-2.986523000000	-1.254830000000
H	1.501658000000	-3.210690000000	1.616354000000
H	3.434049000000	-4.314627000000	0.525443000000
H	4.864631000000	-3.088558000000	-1.088550000000
H	4.416874000000	-0.712886000000	-1.635090000000
C	-0.065456000000	-1.471408000000	-2.965049000000
C	-0.442902000000	-0.248376000000	-3.017212000000
H	-0.541321000000	0.660861000000	-3.582776000000
H	0.377577000000	-2.320609000000	-3.453628000000
C	0.544692000000	2.200912000000	0.797451000000
C	2.740076000000	1.945608000000	-1.010676000000
C	2.159462000000	3.179843000000	-0.758383000000
C	1.070067000000	3.304093000000	0.145201000000
H	2.544065000000	4.069293000000	-1.252350000000
H	0.645283000000	4.288922000000	0.328867000000
H	3.581882000000	1.862291000000	-1.694879000000
H	-0.287898000000	2.307694000000	1.489423000000

**FN-4**E = -5026.25 kcal mol<sup>-1</sup>

C	1.876080000000	0.577201000000	-0.820518000000
C	1.852658000000	0.525306000000	0.619876000000
C	0.795144000000	1.420608000000	1.083223000000
C	0.377028000000	2.236344000000	-0.053984000000
C	0.928265000000	1.624917000000	-1.246231000000
Rh	-0.539937000000	0.123797000000	0.007993000000
C	-1.587568000000	-1.367592000000	1.115591000000
C	-1.494332000000	-1.876925000000	-0.218455000000
C	-2.243589000000	-1.233697000000	-1.234122000000
C	-3.382735000000	-0.404495000000	-0.903527000000
C	-3.473370000000	0.105000000000	0.362787000000
C	-2.401636000000	-0.193890000000	1.295253000000
H	0.623020000000	1.680282000000	2.123371000000
H	-1.086005000000	-1.853341000000	1.947903000000
H	-0.850152000000	-2.720793000000	-0.449639000000
H	-2.092003000000	-1.541149000000	-2.265838000000
H	-2.430440000000	0.261355000000	2.282851000000
H	-4.287629000000	0.759650000000	0.663808000000
H	-4.121025000000	-0.175745000000	-1.668219000000
C	2.756063000000	-0.246617000000	-1.540961000000
C	2.729059000000	-0.334792000000	1.307871000000
C	3.617371000000	-1.093135000000	-0.837506000000
C	3.607383000000	-1.132351000000	0.572249000000
H	2.780050000000	-0.219304000000	-2.628305000000
H	2.722873000000	-0.374036000000	2.395334000000
H	4.315382000000	-1.723836000000	-1.383897000000
H	4.299234000000	-1.791692000000	1.092229000000
C	-0.441923000000	3.386268000000	-0.162408000000
C	0.627933000000	2.171180000000	-2.514742000000
C	-0.169673000000	3.309318000000	-2.588460000000
C	-0.695307000000	3.916311000000	-1.422669000000
H	1.034730000000	1.724252000000	-3.419255000000
H	-0.391149000000	3.746356000000	-3.559881000000
H	-1.310662000000	4.808171000000	-1.518242000000
H	-0.851067000000	3.852486000000	0.731435000000

**FN-5**E = -5554.30 kcal mol<sup>-1</sup>

C	1.497194000000	-0.310032000000	1.757315000000	H	-2.410804000000	3.597018000000	0.291917000000
C	1.078004000000	-1.682344000000	1.440220000000	C	0.454619000000	1.763462000000	2.588033000000
C	-0.262928000000	-1.862088000000	2.012767000000	H	-1.965578000000	-0.693063000000	-2.189678000000
C	-0.752560000000	-0.565675000000	2.407853000000	H	-4.214541000000	1.882591000000	0.425356000000
C	0.348554000000	0.401532000000	2.254757000000	H	-3.972791000000	-0.274826000000	-0.779569000000
Rh	0.016229000000	-0.763353000000	-0.102781000000	H	-0.236174000000	-3.128945000000	-1.876869000000
C	0.242254000000	-2.200775000000	-1.602847000000	H	2.058205000000	-0.991468000000	-2.244334000000
C	1.163831000000	-1.340447000000	-1.750453000000	C	1.689722000000	2.398486000000	2.455499000000
C	-2.015388000000	0.199638000000	-1.575486000000	C	2.822422000000	1.696957000000	1.987858000000
C	-0.993426000000	1.169845000000	-1.650997000000	H	-0.406759000000	2.311560000000	2.963164000000
C	-1.146207000000	2.397838000000	-0.971549000000	H	1.786884000000	3.447778000000	2.726244000000
C	-2.293575000000	2.646475000000	-0.224667000000	H	3.775248000000	2.215705000000	1.905993000000
C	-3.313878000000	1.677254000000	-0.149630000000	C	-2.049180000000	-0.435121000000	2.938156000000
C	-3.178255000000	0.466686000000	-0.822001000000	C	-1.074179000000	-3.003851000000	2.185692000000
H	1.765825000000	-2.496156000000	1.224911000000	C	-2.832459000000	-1.577594000000	3.099414000000
C	2.735940000000	0.352816000000	1.630740000000	C	-2.346014000000	-2.852227000000	2.733516000000
H	-0.156494000000	1.030213000000	-2.327037000000	H	-2.430331000000	0.538410000000	3.238068000000
H	-0.366811000000	3.152822000000	-1.044886000000	H	-3.830777000000	-1.489643000000	3.522951000000
				H	-2.975967000000	-3.726690000000	2.882060000000
				H	-0.705027000000	-3.987496000000	1.902882000000

**Table C3.** Cartesian coordinates (in Å) and ADF total energies (in kcal mol<sup>-1</sup>) of all stationary points, as well as imaginary frequencies of transition states (in cm<sup>-1</sup>) along the Path II catalyzed by CpNRh(CO), computed at ZORA-BLYP/TZ2P.

**CO-CpN-1**E = -4760.08 kcal mol<sup>-1</sup>

C	2.349927000000	-1.448800000000	-1.688048000000	H	1.680594000000	0.100775000000	1.036131000000
C	2.202225000000	-0.075526000000	-2.162078000000	H	1.908078000000	-2.432053000000	0.207793000000
C	1.613886000000	0.692208000000	-1.090573000000	H	2.788103000000	-2.256172000000	-2.268212000000
C	1.345715000000	-0.239936000000	0.055837000000	H	-1.494536000000	-2.513246000000	-1.697271000000
C	1.888044000000	-1.542857000000	-0.410884000000	H	-1.665231000000	0.687037000000	-2.079862000000
Rh	-0.759872000000	-0.593696000000	0.518766000000	H	-0.267570000000	-1.373973000000	3.364450000000
C	-0.732432000000	-2.516540000000	1.463600000000	H	-0.867489000000	-3.556989000000	1.213642000000
C	-0.488838000000	-1.629827000000	2.340145000000	C	1.442693000000	2.048713000000	-1.225064000000
C	-1.495832000000	-0.244841000000	-1.576359000000	C	2.571511000000	0.525541000000	-3.347428000000

C	1.817419000000	2.704991000000	-2.440681000000	C	2.436821000000	2.027591000000	-3.578137000000
C	2.381052000000	1.930332000000	-3.521747000000	H	3.304779000000	0.088931000000	-4.044287000000
H	3.031593000000	-0.050351000000	-4.149690000000	H	0.829868000000	2.796098000000	-0.607078000000
H	1.006460000000	2.645836000000	-0.425860000000	C	1.435236000000	4.168303000000	-2.868951000000
C	1.645708000000	4.103606000000	-2.620233000000	C	2.793041000000	2.653962000000	-4.806245000000
C	2.741513000000	2.599076000000	-4.722805000000	C	1.796741000000	4.742997000000	-4.073445000000
C	2.007419000000	4.723014000000	-3.804649000000	C	2.482149000000	3.978304000000	-5.050894000000
C	2.559344000000	3.964087000000	-4.864107000000	H	0.908768000000	4.756077000000	-2.118237000000
H	1.221519000000	4.687711000000	-1.804799000000	H	1.556186000000	5.784840000000	-4.274640000000
H	1.868348000000	5.795432000000	-3.923428000000	H	2.763773000000	4.438657000000	-5.995760000000
H	2.841759000000	4.457843000000	-5.791596000000	H	3.320919000000	2.067788000000	-5.557347000000
H	3.168252000000	2.016885000000	-5.538296000000	C	-0.704923000000	0.927130000000	1.612077000000
C	-1.012850000000	1.227983000000	1.089630000000	O	-0.782624000000	1.921499000000	2.212478000000
O	-1.353362000000	2.258306000000	1.500805000000				

## CO-CpN-2

$$E = -4809.24 \text{ kcal mol}^{-1}$$

### CO-CpN-TS(1,2)

$$E = -4745.45 \text{ kcal mol}^{-1} \quad -346.444 \text{ cm}^{-1}$$

C	2.634951000000	-1.215544000000	-1.520508000000
C	2.390003000000	0.106635000000	-2.090547000000
C	1.675249000000	0.880025000000	-1.101918000000
C	1.435609000000	0.003651000000	0.091571000000
C	2.116367000000	-1.271317000000	-0.261495000000
Rh	-0.665541000000	-0.565755000000	0.531272000000
C	-2.318246000000	-2.163551000000	0.756687000000
C	-1.748208000000	-1.745197000000	1.828544000000
C	-0.839609000000	-1.073913000000	-1.522495000000
C	-1.391920000000	-2.126122000000	-1.055659000000
H	1.738529000000	0.433017000000	1.047561000000
H	2.188478000000	-2.117175000000	0.414823000000
H	3.171915000000	-2.014376000000	-2.024555000000
H	-1.576315000000	-3.163770000000	-1.289572000000
H	-0.330681000000	-0.717149000000	-2.405311000000
H	-1.928328000000	-1.707925000000	2.892171000000
H	-3.241839000000	-2.620100000000	0.431923000000
C	1.367942000000	2.199805000000	-1.342968000000
C	2.756080000000	0.667048000000	-3.301336000000
C	1.737887000000	2.808315000000	-2.580646000000

C	2.567635000000	-1.243547000000	-1.418503000000
C	2.465235000000	0.099098000000	-1.983924000000
C	2.077087000000	0.997880000000	-0.900196000000
C	1.983116000000	0.194501000000	0.314993000000
C	2.394230000000	-1.122058000000	0.006910000000
Rh	0.366594000000	-0.968307000000	-1.041757000000
C	-0.622765000000	-3.669125000000	-1.470017000000
C	-0.149335000000	-2.885691000000	-0.482855000000
C	-0.342874000000	-1.751513000000	-2.829788000000
C	-0.728546000000	-3.042232000000	-2.783471000000
H	1.760929000000	0.574820000000	1.304937000000
H	2.513100000000	-1.929360000000	0.719454000000
H	2.939464000000	-2.119070000000	-1.935512000000
H	-1.098231000000	-3.588068000000	-3.653880000000
H	-0.374275000000	-1.121303000000	-3.720251000000
H	-0.037212000000	-3.165207000000	0.564032000000
H	-0.916087000000	-4.706385000000	-1.292616000000
C	1.882194000000	2.356100000000	-1.148654000000
C	2.646875000000	0.596231000000	-3.274556000000
C	2.083006000000	2.869498000000	-2.449494000000
C	2.472965000000	1.974820000000	-3.529720000000

H	2.937915000000	-0.066592000000	-4.087463000000	H	3.824800000000	3.009600000000	-0.540100000000
H	1.592054000000	3.031641000000	-0.345569000000	C	2.882300000000	4.350900000000	-2.710000000000
C	1.916786000000	4.258736000000	-2.743337000000	C	1.492600000000	2.739900000000	-4.541500000000
C	2.673515000000	2.528906000000	-4.832691000000	C	2.359500000000	4.902300000000	-3.866700000000
C	2.119752000000	4.748840000000	-4.013621000000	C	1.659700000000	4.091300000000	-4.791500000000
C	2.502714000000	3.873925000000	-5.070370000000	H	3.424100000000	4.977000000000	-2.002600000000
H	1.624190000000	4.928621000000	-1.936310000000	H	2.487500000000	5.963800000000	-4.068900000000
H	1.987627000000	5.809452000000	-4.216593000000	H	1.253900000000	4.532800000000	-5.699200000000
H	2.659038000000	4.275511000000	-6.069288000000	H	0.954500000000	2.114200000000	-5.252400000000
H	2.965549000000	1.860743000000	-5.641317000000	C	0.137400000000	0.004600000000	0.530400000000
C	-1.352530000000	-0.372385000000	-0.546477000000	O	0.020400000000	0.449800000000	1.589900000000
O	-2.412288000000	-0.027075000000	-0.238836000000	C	-2.543300000000	-0.849900000000	-1.842600000000
				C	-2.287300000000	0.311400000000	-1.605900000000
				H	-2.794400000000	-1.863500000000	-2.067600000000
				H	-2.162600000000	1.353400000000	-1.405700000000

### CO-CpN-TS(2,3)

E = -5306.62 kcal mol<sup>-1</sup> -51. 093 cm<sup>-1</sup>

C	2.265100000000	-1.165000000000	-1.351300000000
C	2.363000000000	0.203800000000	-1.926700000000
C	3.089000000000	1.036100000000	-0.985000000000
C	3.511700000000	0.175400000000	0.117200000000
C	3.044700000000	-1.087100000000	-0.090200000000
Rh	0.149100000000	-0.961500000000	-1.173300000000
C	-0.333700000000	-3.811400000000	-1.038000000000
C	-0.199400000000	-2.742100000000	-0.225400000000
C	0.000700000000	-2.263800000000	-2.811600000000
C	-0.230600000000	-3.552300000000	-2.474200000000
H	4.088700000000	0.511800000000	0.973700000000
H	3.201300000000	-1.939400000000	0.563200000000
H	2.418100000000	-2.035300000000	-1.987600000000
H	-0.358800000000	-4.359300000000	-3.200400000000
H	0.064300000000	-1.945600000000	-3.858100000000
H	-0.263700000000	-2.779900000000	0.861700000000
H	-0.527200000000	-4.812100000000	-0.641800000000
C	3.269100000000	2.379400000000	-1.233800000000
C	1.845400000000	0.745500000000	-3.091200000000
C	2.728100000000	2.968100000000	-2.419600000000
C	2.009600000000	2.142200000000	-3.361600000000
H	1.343900000000	0.122100000000	-3.828600000000

### CO-CpN-3

E = -5309.11 kcal mol<sup>-1</sup>

C	2.128062000000	-1.053380000000	-1.375553000000
C	2.285156000000	0.309712000000	-1.955666000000
C	3.058833000000	1.110075000000	-1.027247000000
C	3.450020000000	0.239188000000	0.078477000000
C	2.931006000000	-1.002828000000	-0.122327000000
Rh	-0.046317000000	-0.994695000000	-1.135982000000
C	-0.134842000000	-3.886683000000	-1.038254000000
C	-0.100759000000	-2.816732000000	-0.216111000000
C	-0.016627000000	-2.305476000000	-2.803020000000
C	-0.072534000000	-3.612252000000	-2.467333000000
H	4.053052000000	0.552461000000	0.925645000000
H	3.063805000000	-1.861193000000	0.528397000000
H	2.295575000000	-1.914335000000	-2.020443000000
H	-0.058511000000	-4.423398000000	-3.198534000000
H	0.048288000000	-1.964341000000	-3.839840000000
H	-0.141136000000	-2.859842000000	0.870952000000
H	-0.207221000000	-4.902797000000	-0.642923000000
C	3.319007000000	2.439121000000	-1.293305000000
C	1.812142000000	0.864656000000	-3.130351000000

C	2.826121000000	3.038500000000	-2.491736000000	H	-0.249609000000	-4.835038000000	-0.714678000000
C	2.066990000000	2.239474000000	-3.427152000000	C	3.319552000000	2.379094000000	-1.271462000000
H	1.261680000000	0.266032000000	-3.853984000000	C	1.793030000000	0.793003000000	-3.085565000000
H	3.909590000000	3.043666000000	-0.605615000000	C	2.780220000000	2.980326000000	-2.450020000000
C	3.069146000000	4.404016000000	-2.806826000000	C	2.011022000000	2.176750000000	-3.372782000000
C	1.599948000000	2.847488000000	-4.624170000000	H	1.243600000000	0.187856000000	-3.803774000000
C	2.595250000000	4.964107000000	-3.979701000000	H	3.914402000000	2.990581000000	-0.593719000000
C	1.854893000000	4.179572000000	-4.897633000000	C	2.986907000000	4.353285000000	-2.756105000000
H	3.641719000000	5.008231000000	-2.104562000000	C	1.499287000000	2.786962000000	-4.549662000000
H	2.792604000000	6.010876000000	-4.201490000000	C	2.468927000000	4.916407000000	-3.909216000000
H	1.488148000000	4.627610000000	-5.818676000000	C	1.719615000000	4.127209000000	-4.815070000000
H	1.031879000000	2.243205000000	-5.330257000000	H	3.566534000000	4.961584000000	-2.063299000000
C	0.095023000000	-0.102689000000	0.606085000000	H	2.638741000000	5.969430000000	-4.124088000000
O	0.119258000000	0.303711000000	1.683840000000	H	1.318197000000	4.577493000000	-5.720399000000
C	-2.123319000000	-0.786936000000	-2.068007000000	H	0.923695000000	2.178809000000	-5.246130000000
C	-2.146673000000	-0.034128000000	-1.090410000000	C	0.106637000000	-0.011492000000	0.605226000000
H	-2.421885000000	-1.348080000000	-2.929482000000	O	0.094788000000	0.425412000000	1.673194000000
H	-2.481296000000	0.656442000000	-0.343560000000	C	-2.086503000000	-1.147746000000	-2.157495000000
				C	-1.857200000000	-0.012244000000	-1.663086000000
				H	-2.761237000000	-1.922825000000	-2.470730000000
				H	-2.257438000000	0.931275000000	-1.333167000000

### CO-CpN-TS(3,b)

$$E = -5306.48 \text{ kcal mol}^{-1} \quad -282.903 \text{ cm}^{-1}$$

C	2.182883000000	-1.123617000000	-1.350100000000
C	2.312643000000	0.235825000000	-1.929016000000
C	3.094791000000	1.043561000000	-1.010443000000
C	3.522380000000	0.171082000000	0.079181000000
C	3.013090000000	-1.076653000000	-0.120712000000
Rh	0.015150000000	-0.928185000000	-1.102373000000
C	-0.186702000000	-3.810684000000	-1.089191000000
C	-0.066618000000	-2.751397000000	-0.237073000000
C	-0.279553000000	-2.176090000000	-2.806551000000
C	-0.245995000000	-3.509361000000	-2.490932000000
H	4.133332000000	0.487645000000	0.919088000000
H	3.164835000000	-1.936087000000	0.524537000000
H	2.276691000000	-1.995355000000	-1.995905000000
H	-0.271669000000	-4.300573000000	-3.243171000000
H	-0.304381000000	-1.816339000000	-3.835376000000
H	-0.084158000000	-2.843872000000	0.848337000000

### CO-CpN-b

$$E = -5326.93 \text{ kcal mol}^{-1}$$

C	2.460517000000	-1.216171000000	-1.360818000000
C	2.450356000000	0.147360000000	-1.916240000000
C	3.141650000000	1.018396000000	-0.973310000000
C	3.640463000000	0.179669000000	0.103698000000
C	3.255069000000	-1.114772000000	-0.126517000000
Rh	0.239965000000	-1.042897000000	-1.078961000000
C	-0.703680000000	-3.754140000000	-0.916020000000
C	-0.370518000000	-2.609401000000	-0.151954000000
C	-0.191862000000	-2.312524000000	-2.796355000000
C	-0.560051000000	-3.639435000000	-2.277127000000
H	4.201674000000	0.538871000000	0.960484000000
H	3.483404000000	-1.965694000000	0.507700000000
H	2.557173000000	-2.092393000000	-1.997472000000

H	-0.728095000000	-4.489193000000	-2.943871000000	H	4.250085000000	0.434069000000	1.002439000000
H	0.472262000000	-2.339571000000	-3.669233000000	H	3.536024000000	-2.074743000000	0.564345000000
H	-0.516424000000	-2.600604000000	0.930183000000	H	2.542610000000	-2.232891000000	-1.916316000000
H	-1.070099000000	-4.663616000000	-0.435253000000	H	0.015166000000	-4.479375000000	-2.841148000000
C	3.221688000000	2.376304000000	-1.210527000000	H	0.182606000000	-2.333917000000	-3.956595000000
C	1.868443000000	0.675467000000	-3.061789000000	H	-0.469691000000	-2.521605000000	0.920964000000
C	2.624927000000	2.938944000000	-2.378259000000	H	-0.770361000000	-4.615983000000	-0.439585000000
C	1.941506000000	2.078177000000	-3.318445000000	C	3.222999000000	2.257079000000	-1.163888000000
H	1.383468000000	0.034643000000	-3.795135000000	C	1.848178000000	0.539772000000	-2.989331000000
H	3.741363000000	3.035323000000	-0.515725000000	C	2.581160000000	2.815691000000	-2.311467000000
C	2.685831000000	4.332648000000	-2.656936000000	C	1.884972000000	1.949863000000	-3.235683000000
C	1.366352000000	2.656208000000	-4.483103000000	H	1.401784000000	-0.108057000000	-3.740653000000
C	2.110431000000	4.861540000000	-3.798190000000	H	3.741673000000	2.925294000000	-0.476883000000
C	1.445328000000	4.016581000000	-4.720737000000	C	2.609589000000	4.211887000000	-2.580258000000
H	3.198679000000	4.984172000000	-1.950893000000	C	1.271700000000	2.524797000000	-4.380711000000
H	2.168623000000	5.930720000000	-3.991434000000	C	1.994087000000	4.739645000000	-3.701492000000
H	0.996711000000	4.441223000000	-5.616239000000	C	1.320763000000	3.888690000000	-4.611198000000
H	0.854951000000	2.005694000000	-5.191176000000	H	3.130772000000	4.866716000000	-1.883393000000
C	0.154686000000	0.110647000000	0.498175000000	H	2.028209000000	5.810986000000	-3.888173000000
O	-0.003971000000	0.725725000000	1.460460000000	H	0.841437000000	4.310193000000	-5.492215000000
C	-1.434676000000	-1.414999000000	-3.042817000000	H	0.752672000000	1.870826000000	-5.079988000000
C	-1.502085000000	-0.524509000000	-2.062215000000	C	0.096463000000	0.207438000000	0.351542000000
H	-2.100448000000	-1.550849000000	-3.902103000000	O	-0.033773000000	0.860663000000	1.296486000000
H	-2.199958000000	0.288114000000	-1.880046000000	C	-1.535784000000	-1.406643000000	-2.940234000000
				C	-1.551280000000	-0.462628000000	-2.016283000000
				H	-2.307000000000	-1.594279000000	-3.695641000000
				H	-2.304801000000	0.289268000000	-1.804458000000

### CO-CpN-TS(b,h)

E = -5325.17 kcal mol<sup>-1</sup> -217.48 cm<sup>-1</sup>

C	2.507607000000	-1.335727000000	-1.304483000000
C	2.487950000000	0.012789000000	-1.865852000000
C	3.177659000000	0.898999000000	-0.927556000000
C	3.688227000000	0.068723000000	0.148980000000
C	3.302843000000	-1.228222000000	-0.074371000000
Rh	0.259184000000	-0.912264000000	-1.142711000000
C	-0.524674000000	-3.661719000000	-0.909991000000
C	-0.330030000000	-2.519031000000	-0.160504000000
C	-0.299209000000	-2.335217000000	-2.974514000000
C	-0.284677000000	-3.575444000000	-2.301015000000

### CO-CpN-h

E = -5355.63 kcal mol<sup>-1</sup>

C	2.527377000000	-1.060970000000	-1.886506000000
C	2.582322000000	0.326168000000	-2.329515000000
C	3.061887000000	1.120547000000	-1.202970000000
C	3.345697000000	0.191556000000	-0.109652000000
C	3.138418000000	-1.122103000000	-0.585220000000
Rh	1.004779000000	-0.284223000000	-0.343053000000
C	-0.912928000000	-2.458077000000	0.782754000000

C	0.276637000000	-2.089418000000	0.273127000000	C	3.249192000000	0.284316000000	-0.046368000000
C	-2.637219000000	-0.787276000000	0.011542000000	C	3.150526000000	-1.051634000000	-0.517425000000
C	-2.159482000000	-1.713223000000	0.884686000000	Rh	1.010085000000	-0.299672000000	-0.337778000000
H	3.778705000000	0.460062000000	0.846647000000	C	-1.001305000000	-2.468533000000	0.639437000000
H	3.355942000000	-2.029285000000	-0.034129000000	C	0.090537000000	-2.121564000000	-0.084420000000
H	2.305852000000	-1.913347000000	-2.517369000000	C	-2.610800000000	-0.639336000000	0.157499000000
H	-2.817584000000	-2.012384000000	1.701721000000	C	-2.139536000000	-1.644036000000	0.961044000000
H	-3.645349000000	-0.410877000000	0.191552000000	H	3.630147000000	0.586105000000	0.922230000000
H	1.083423000000	-2.824411000000	0.256676000000	H	3.392372000000	-1.941915000000	0.050772000000
H	-0.951284000000	-3.470522000000	1.201547000000	H	2.437480000000	-1.891349000000	-2.471485000000
C	3.184890000000	2.502965000000	-1.317532000000	H	-2.746649000000	-1.944603000000	1.814952000000
C	2.249904000000	0.946663000000	-3.530915000000	H	-3.570976000000	-0.189523000000	0.409567000000
C	2.863761000000	3.139950000000	-2.538819000000	H	0.778986000000	-2.904531000000	-0.407838000000
C	2.390271000000	2.348267000000	-3.663878000000	H	-1.055929000000	-3.510343000000	0.973139000000
H	1.897391000000	0.362972000000	-4.379672000000	C	3.088520000000	2.568681000000	-1.307678000000
H	3.541850000000	3.101091000000	-0.480569000000	C	2.347684000000	0.941067000000	-3.542710000000
C	2.996302000000	4.552656000000	-2.706765000000	C	2.821155000000	3.173670000000	-2.561047000000
C	2.082387000000	3.022240000000	-4.885855000000	C	2.446062000000	2.346927000000	-3.695812000000
C	2.686285000000	5.161405000000	-3.902571000000	H	2.065600000000	0.330109000000	-4.398685000000
C	2.224608000000	4.386975000000	-5.004139000000	H	3.368154000000	3.194380000000	-0.461570000000
H	3.350181000000	5.144965000000	-1.864387000000	C	2.914824000000	4.585761000000	-2.747942000000
H	2.793023000000	6.238604000000	-4.010581000000	C	2.190448000000	2.986272000000	-4.946428000000
H	1.982959000000	4.880599000000	-5.943064000000	C	2.657850000000	5.162871000000	-3.973032000000
H	1.728603000000	2.431989000000	-5.729699000000	C	2.291995000000	4.354067000000	-5.083935000000
C	0.217999000000	0.631654000000	1.104697000000	H	3.195386000000	5.205273000000	-1.897525000000
O	-0.190365000000	1.224074000000	2.009050000000	H	2.733405000000	6.241272000000	-4.094778000000
C	-2.003619000000	-0.325043000000	-1.213239000000	H	2.091111000000	4.821417000000	-6.045631000000
C	-0.690770000000	-0.192631000000	-1.488489000000	H	1.910156000000	2.368701000000	-5.798370000000
H	-2.701165000000	-0.024623000000	-2.003330000000	C	0.251758000000	0.538639000000	1.175134000000
H	-0.406178000000	0.140564000000	-2.491488000000	O	-0.082308000000	1.095928000000	2.132746000000
				C	-2.022361000000	-0.278905000000	-1.106899000000
				C	-0.716152000000	-0.384165000000	-1.459554000000
				H	-2.719197000000	0.071638000000	-1.875639000000
				H	-0.443553000000	-0.255870000000	-2.510835000000

### CO-CpN-TS(h,4)

$$E = -5354.35 \text{ kcal mol}^{-1} \quad -235.423 \text{ cm}^{-1}$$

C	2.604086000000	-1.023310000000	-1.843807000000
C	2.630168000000	0.358476000000	-2.313521000000
C	3.009851000000	1.187484000000	-1.176935000000

### CO-CpN-4

$E = -5402.20 \text{ kcal mol}^{-1}$

C	1.182493000000	3.921151000000	2.300987000000	C	-3.205258000000	1.611976000000	-1.544432000000
C	-0.119971000000	3.470218000000	2.378941000000	H	-3.301254000000	3.332002000000	1.219496000000
C	-1.095644000000	3.836344000000	1.366583000000	H	-3.026769000000	2.295349000000	3.687110000000
C	-0.731348000000	4.637450000000	0.301562000000	H	-0.393056000000	2.276164000000	4.288189000000
C	0.604759000000	5.126467000000	0.206857000000	H	-4.875981000000	-0.151745000000	0.861290000000
C	1.574593000000	4.764850000000	1.220346000000	H	-2.633748000000	-1.183597000000	1.099351000000
C	-2.362234000000	3.197667000000	1.743898000000	H	-3.393459000000	2.343912000000	-2.327070000000
C	-2.225752000000	2.647387000000	3.048638000000	H	-5.282455000000	1.529718000000	-0.915135000000
C	-0.817488000000	2.603625000000	3.345755000000	H	1.918689000000	3.645233000000	3.054467000000
Rh	-1.273449000000	1.119949000000	1.769152000000	H	-1.452458000000	4.913134000000	-0.466353000000
C	-1.669569000000	0.136306000000	-0.351531000000	H	-1.110441000000	1.439329000000	-1.996695000000
C	-1.926175000000	1.113123000000	-1.355545000000	H	-0.741223000000	-0.425956000000	-0.394572000000
C	-0.279599000000	-0.302002000000	2.449492000000	C	2.319058000000	6.441341000000	-0.939316000000
O	0.320357000000	-1.164142000000	2.954750000000	C	1.021033000000	5.971782000000	-0.860016000000
C	-2.744058000000	-0.300867000000	0.477668000000	C	3.267713000000	6.086837000000	0.052284000000
C	-4.050142000000	0.218451000000	0.257570000000	H	0.292723000000	6.246784000000	-1.621811000000
C	-4.276754000000	1.152889000000	-0.739956000000	H	4.287182000000	6.460324000000	-0.017736000000
				C	2.900120000000	5.269296000000	1.105003000000
				H	3.629134000000	4.997641000000	1.867161000000
				H	2.616065000000	7.085336000000	-1.764488000000

**Table C4.** Cartesian coordinates (in Å) and ADF total energies (in kcal mol<sup>-1</sup>) of all stationary points, as well as imaginary frequencies of transition states (in cm<sup>-1</sup>) along the Path II catalyzed by FNRh(CO), computed at ZORA-BLYP/TZ2P.

### CO-FN-1

$E = -4766.22 \text{ kcal mol}^{-1}$

C	2.441417000000	-1.482715000000	-1.722255000000	C	-1.334574000000	-1.690045000000	-1.328144000000
C	2.253724000000	-0.086380000000	-2.142440000000	H	1.697557000000	0.022655000000	1.042315000000
C	1.644217000000	0.623068000000	-1.073329000000	H	-1.446269000000	-2.745068000000	-1.488526000000
C	1.358842000000	-0.319911000000	0.063238000000	H	-1.418729000000	0.396003000000	-2.232192000000
C	1.945257000000	-1.621736000000	-0.397011000000	H	-0.549139000000	-1.053766000000	3.492530000000
Rh	-0.752971000000	-0.605860000000	0.541152000000	H	-1.184344000000	-3.435378000000	1.566376000000
C	-0.972058000000	-2.388339000000	1.710698000000	C	1.450981000000	2.002654000000	-1.177840000000
C	-0.708160000000	-1.423190000000	2.491968000000	C	2.626999000000	0.574209000000	-3.317051000000
C	-1.335908000000	-0.479340000000	-1.617415000000	C	1.836989000000	2.664482000000	-2.352564000000
				C	2.409460000000	1.954633000000	-3.418484000000
				H	3.097023000000	0.033865000000	-4.136529000000
				H	0.998374000000	2.566868000000	-0.366141000000

C	-0.992736000000	1.252286000000	0.963444000000	O	-0.613935000000	1.939572000000	2.214432000000
O	-1.373847000000	2.296183000000	1.299153000000	H	1.390097000000	3.672631000000	-2.953667000000
H	1.689168000000	3.738880000000	-2.437734000000	H	2.435025000000	2.283392000000	-4.723525000000
H	2.696918000000	2.482349000000	-4.325495000000	C	2.283579000000	-2.521812000000	0.456311000000
C	2.104894000000	-2.833116000000	0.281713000000	C	3.142360000000	-2.504388000000	-2.242564000000
C	3.053246000000	-2.559900000000	-2.369868000000	C	2.916754000000	-3.642152000000	-0.099121000000
C	2.730120000000	-3.907134000000	-0.367048000000	C	3.335242000000	-3.635844000000	-1.439333000000
C	3.188729000000	-3.775901000000	-1.686350000000	H	1.959348000000	-2.534550000000	1.495010000000
H	1.736772000000	-2.949324000000	1.297627000000	H	3.492207000000	-2.501428000000	-3.273315000000
H	3.438731000000	-2.457133000000	-3.382415000000	H	3.825233000000	-4.514491000000	-1.854000000000
H	3.665025000000	-4.621562000000	-2.178253000000	H	3.088796000000	-4.524303000000	0.514106000000
H	2.859400000000	-4.851916000000	0.156637000000				

## CO-FN-2

### CO-FN-TS(1,2)

$$E = -4753.44 \text{ kcal mol}^{-1} \quad -348.286 \text{ cm}^{-1}$$

C	2.515032000000	-1.380137000000	-1.693475000000
C	2.241638000000	-0.048966000000	-2.254661000000
C	1.624483000000	0.741258000000	-1.245407000000
C	1.429076000000	-0.081705000000	-0.006597000000
C	2.069160000000	-1.393234000000	-0.341719000000
Rh	-0.658604000000	-0.557428000000	0.545419000000
C	-2.335920000000	-2.107503000000	0.839246000000
C	-1.705025000000	-1.718803000000	1.889462000000
C	-0.978519000000	-1.031767000000	-1.499608000000
C	-1.510483000000	-2.084361000000	-1.007682000000
H	1.805796000000	0.381685000000	0.906275000000
H	-1.713733000000	-3.118653000000	-1.242029000000
H	-0.524677000000	-0.677338000000	-2.413154000000
H	-1.844307000000	-1.688108000000	2.959542000000
H	-3.291497000000	-2.527690000000	0.560049000000
C	1.321896000000	2.082718000000	-1.496464000000
C	2.529871000000	0.500855000000	-3.511218000000
C	1.620833000000	2.628733000000	-2.751576000000
C	2.213557000000	1.842490000000	-3.753759000000
H	3.005973000000	-0.096957000000	-4.286369000000
H	0.850616000000	2.697995000000	-0.732458000000
C	-0.598934000000	0.941284000000	1.615167000000

$$E = -4803.75 \text{ kcal mol}^{-1}$$

C	1.838284000000	-1.349947000000	-1.227166000000
C	1.607493000000	-0.024322000000	-1.806092000000
C	1.897497000000	0.955589000000	-0.775538000000
C	2.250449000000	0.247874000000	0.443593000000
C	2.328486000000	-1.149886000000	0.136017000000
Rh	0.026863000000	-0.446161000000	0.046692000000
C	-1.777388000000	-2.688204000000	0.478181000000
C	-0.723142000000	-2.084844000000	1.054925000000
C	-1.607914000000	-0.966249000000	-1.141335000000
C	-2.280936000000	-2.063147000000	-0.744077000000
H	2.577598000000	0.711619000000	1.366632000000
H	-3.139993000000	-2.468647000000	-1.282969000000
H	-1.863038000000	-0.358125000000	-2.010667000000
H	-0.219885000000	-2.391372000000	1.970362000000
H	-2.223901000000	-3.593713000000	0.895329000000
C	1.807789000000	2.338021000000	-1.081670000000
C	1.251223000000	0.400854000000	-3.107283000000
C	1.472601000000	2.721043000000	-2.370769000000
C	1.195742000000	1.759977000000	-3.378121000000
H	1.041640000000	-0.327621000000	-3.887006000000
H	2.021399000000	3.082588000000	-0.317720000000
C	-1.016343000000	0.614496000000	1.151864000000
O	-1.676263000000	1.274640000000	1.836760000000

H	1.420020000000	3.778647000000	-2.619795000000	H	2.196400000000	2.337100000000	-4.386400000000
H	0.939361000000	2.099611000000	-4.379014000000	C	2.368400000000	-2.829300000000	0.423000000000
C	2.788583000000	-2.274844000000	0.883461000000	C	2.993400000000	-2.635600000000	-2.334800000000
C	1.845119000000	-2.655589000000	-1.796945000000	C	2.914900000000	-3.920700000000	-0.266100000000
C	2.782604000000	-3.519127000000	0.290602000000	C	3.216900000000	-3.828300000000	-1.633600000000
C	2.310662000000	-3.712475000000	-1.044280000000	H	2.120700000000	-2.914400000000	1.478800000000
H	3.161614000000	-2.139765000000	1.896385000000	H	3.251700000000	-2.566000000000	-3.389800000000
H	1.497431000000	-2.810431000000	-2.815464000000	H	3.638300000000	-4.687600000000	-2.151100000000
H	2.325101000000	-4.713488000000	-1.468768000000	H	3.106200000000	-4.851500000000	0.263700000000
H	3.150168000000	-4.379480000000	0.846011000000	C	-3.562500000000	0.839400000000	-0.179800000000
				C	-3.040900000000	0.607800000000	-1.244300000000
				H	-4.009800000000	1.047000000000	0.767200000000
				H	-2.633200000000	0.439100000000	-2.216300000000

### CO-FN-TS(2,3)

$$E = -5308.2 \text{ kcal mol}^{-1} \quad -64.137 \text{ cm}^{-1}$$

C	2.453500000000	-1.542400000000	-1.651200000000
C	2.173900000000	-0.167100000000	-2.087400000000
C	1.718100000000	0.576200000000	-0.950800000000
C	1.566100000000	-0.347400000000	0.210300000000
C	2.122200000000	-1.644500000000	-0.272400000000
Rh	-0.564400000000	-0.139300000000	0.189500000000
C	-1.568500000000	-2.700900000000	1.006100000000
C	-1.163700000000	-1.535700000000	1.550500000000
C	-0.840300000000	-1.784200000000	-1.067200000000
C	-1.406900000000	-2.840600000000	-0.446300000000
H	1.880000000000	-0.019900000000	1.200700000000
H	-1.707800000000	-3.760400000000	-0.953600000000
H	-0.637500000000	-1.776700000000	-2.143100000000
H	-1.139800000000	-1.311200000000	2.616100000000
H	-1.976600000000	-3.507600000000	1.621100000000
C	1.483100000000	1.956000000000	-1.065800000000
C	2.336300000000	0.463400000000	-3.321000000000
C	1.653900000000	2.578200000000	-2.313500000000
C	2.065200000000	1.837500000000	-3.428700000000
H	2.687100000000	-0.090900000000	-4.189400000000
H	1.202400000000	2.548800000000	-0.199200000000
C	-0.609100000000	1.267500000000	1.543900000000
O	-0.765400000000	2.005700000000	2.421500000000
H	1.480000000000	3.647400000000	-2.409100000000

### CO-FN-3

$$E = -5313.93 \text{ kcal mol}^{-1}$$

C	2.437533000000	-1.555824000000	-1.585165000000
C	2.140336000000	-0.200897000000	-2.063260000000
C	1.636411000000	0.558219000000	-0.955534000000
C	1.480365000000	-0.333019000000	0.224256000000
C	2.065933000000	-1.632377000000	-0.213715000000
Rh	-0.686894000000	-0.024831000000	0.134279000000
C	-1.388759000000	-2.769108000000	0.780335000000
C	-1.206176000000	-1.573465000000	1.383577000000
C	-0.860432000000	-1.622051000000	-1.221939000000
C	-1.196801000000	-2.805225000000	-0.661229000000
H	1.804303000000	0.028109000000	1.199518000000
H	-1.320538000000	-3.730967000000	-1.227106000000
H	-0.706087000000	-1.485928000000	-2.295141000000
H	-1.342360000000	-1.383127000000	2.447008000000
H	-1.675857000000	-3.655357000000	1.351835000000
C	1.346073000000	1.924859000000	-1.117658000000
C	2.305727000000	0.402840000000	-3.309480000000
C	1.514169000000	2.516387000000	-2.382034000000
C	1.980386000000	1.761359000000	-3.464462000000
H	2.695690000000	-0.160813000000	-4.154967000000
H	1.040616000000	2.535152000000	-0.271226000000

C	-0.574848000000	1.169986000000	1.676609000000	C	1.979384000000	1.787674000000	-3.452560000000
O	-0.546017000000	1.699763000000	2.703599000000	H	2.626471000000	-0.148701000000	-4.169779000000
H	1.299495000000	3.574570000000	-2.513891000000	H	1.104706000000	2.560710000000	-0.240363000000
H	2.112000000000	2.237366000000	-4.433986000000	C	-0.581156000000	1.196296000000	1.698980000000
C	2.300425000000	-2.802052000000	0.510433000000	O	-0.546487000000	1.791203000000	2.689996000000
C	3.011071000000	-2.657144000000	-2.229542000000	H	1.362982000000	3.611160000000	-2.476903000000
C	2.881892000000	-3.900155000000	-0.139473000000	H	2.106016000000	2.267361000000	-4.420958000000
C	3.227763000000	-3.831952000000	-1.498157000000	C	2.275831000000	-2.801559000000	0.492434000000
H	2.023816000000	-2.869041000000	1.560233000000	C	2.922533000000	-2.661120000000	-2.262728000000
H	3.298974000000	-2.605612000000	-3.278051000000	C	2.824877000000	-3.907095000000	-0.173039000000
H	3.677054000000	-4.695722000000	-1.983725000000	C	3.138403000000	-3.841347000000	-1.539514000000
H	3.067473000000	-4.817542000000	0.415596000000	H	2.024785000000	-2.867139000000	1.548682000000
C	-2.569655000000	1.159383000000	-0.552733000000	H	3.186835000000	-2.611009000000	-3.317530000000
C	-2.944208000000	-0.010211000000	-0.584455000000	H	3.561926000000	-4.710899000000	-2.037825000000
H	-2.537726000000	2.229258000000	-0.567855000000	H	3.009279000000	-4.828398000000	0.375927000000
H	-3.443181000000	-0.951698000000	-0.670268000000	C	-2.419919000000	0.948495000000	-0.676035000000
				C	-2.745367000000	-0.221647000000	-0.995624000000
				H	-2.711000000000	1.977200000000	-0.553170000000
				H	-3.454901000000	-0.981421000000	-1.260479000000

### CO-FN-TS(3,b)

$$E = -5311.47 \text{ kcal mol}^{-1} \quad -264.787 \text{ cm}^{-1}$$

C	2.384574000000	-1.551490000000	-1.602174000000
C	2.109879000000	-0.187378000000	-2.067506000000
C	1.647405000000	0.576906000000	-0.946289000000
C	1.498489000000	-0.314620000000	0.232793000000
C	2.045646000000	-1.624013000000	-0.221432000000
Rh	-0.693290000000	-0.014156000000	0.196457000000
C	-1.314835000000	-2.767624000000	0.812535000000
C	-1.097399000000	-1.568961000000	1.422480000000
C	-1.005283000000	-1.583397000000	-1.215068000000
C	-1.210981000000	-2.795434000000	-0.619933000000
H	1.841304000000	0.039857000000	1.203766000000
H	-1.282741000000	-3.730515000000	-1.178672000000
H	-0.877483000000	-1.453030000000	-2.289104000000
H	-1.204427000000	-1.402180000000	2.493624000000
H	-1.561281000000	-3.659774000000	1.392840000000
C	1.390312000000	1.951037000000	-1.094232000000
C	2.268522000000	0.419823000000	-3.313416000000
C	1.553701000000	2.547160000000	-2.355718000000

### CO-FN-b

$$E = -5336.63 \text{ kcal mol}^{-1}$$

C	2.392600000000	-1.630800000000	-1.525900000000
C	2.019500000000	-0.303800000000	-2.006900000000
C	1.695200000000	0.502300000000	-0.851500000000
C	1.754900000000	-0.331300000000	0.353800000000
C	2.252900000000	-1.638400000000	-0.099700000000
Rh	-0.537300000000	-0.034000000000	0.257300000000
C	-1.452300000000	-2.603900000000	0.543300000000
C	-1.391600000000	-1.526400000000	1.325000000000
C	-1.497600000000	-1.523500000000	-1.763100000000
C	-1.025800000000	-2.448600000000	-0.868900000000
H	2.077800000000	0.070700000000	1.311300000000
H	-0.300300000000	-3.174900000000	-1.236000000000
H	-1.110400000000	-1.593700000000	-2.781500000000
H	-1.672800000000	-1.440900000000	2.369700000000
H	-1.731800000000	-3.599300000000	0.897500000000

C	1.325600000000	1.856900000000	-1.032900000000	H	-1.356500000000	-1.790200000000	-2.880500000000
C	1.954000000000	0.247800000000	-3.287900000000	H	-1.846400000000	-1.434100000000	2.290800000000
C	1.268200000000	2.385200000000	-2.332000000000	H	-1.900000000000	-3.592100000000	0.943100000000
C	1.573900000000	1.590100000000	-3.445700000000	C	1.435600000000	2.010600000000	-1.107300000000
H	2.208200000000	-0.348700000000	-4.162700000000	C	1.946500000000	0.297400000000	-3.314600000000
H	1.156200000000	2.507600000000	-0.177600000000	C	1.410200000000	2.501800000000	-2.415700000000
C	-0.647600000000	1.138200000000	1.642000000000	C	1.655000000000	1.652100000000	-3.510000000000
O	-0.756200000000	1.859800000000	2.545600000000	H	2.157400000000	-0.342600000000	-4.169700000000
H	0.998800000000	3.429600000000	-2.473000000000	H	1.261600000000	2.683300000000	-0.269400000000
H	1.528700000000	2.022900000000	-4.442700000000	C	-0.490900000000	1.020600000000	1.665500000000
C	2.575400000000	-2.797000000000	0.622900000000	O	-0.563600000000	1.764600000000	2.553000000000
C	2.822600000000	-2.779900000000	-2.203800000000	H	1.203800000000	3.555600000000	-2.589400000000
C	3.015200000000	-3.932600000000	-0.065500000000	H	1.629600000000	2.057700000000	-4.519200000000
C	3.132000000000	-3.929400000000	-1.468800000000	C	2.536400000000	-2.625400000000	0.699200000000
H	2.483200000000	-2.815700000000	1.707500000000	C	2.695600000000	-2.725200000000	-2.134100000000
H	2.932500000000	-2.779900000000	-3.287100000000	C	2.922200000000	-3.797500000000	0.044200000000
H	3.476800000000	-4.824500000000	-1.982200000000	C	2.994200000000	-3.852500000000	-1.362300000000
H	3.272000000000	-4.832600000000	0.490000000000	H	2.475400000000	-2.598800000000	1.785800000000
C	-2.440000000000	0.308700000000	-0.484200000000	H	2.769400000000	-2.772100000000	-3.219400000000
C	-2.573300000000	-0.519600000000	-1.525900000000	H	3.295000000000	-4.777900000000	-1.848800000000
H	-3.180400000000	1.053100000000	-0.195700000000	H	3.172000000000	-4.682100000000	0.626700000000
H	-3.381000000000	-0.475200000000	-2.263600000000	C	-2.408600000000	0.199600000000	-0.468300000000
				C	-2.594800000000	-0.570000000000	-1.558700000000
				H	-3.088600000000	0.994200000000	-0.164600000000
				H	-3.400500000000	-0.375400000000	-2.275400000000

### CO-FN-TS(b,h)

$$E = -5335.79 \text{ kcal mol}^{-1} \quad -89.40 \text{ cm}^{-1}$$

C	2.320800000000	-1.537500000000	-1.491100000000
C	1.986700000000	-0.215000000000	-2.012200000000
C	1.710400000000	0.643000000000	-0.885900000000
C	1.781400000000	-0.147500000000	0.350300000000
C	2.225300000000	-1.486300000000	-0.060900000000
Rh	-0.480500000000	-0.133200000000	0.267800000000
C	-1.622600000000	-2.631600000000	0.506400000000
C	-1.551400000000	-1.519600000000	1.247800000000
C	-1.665200000000	-1.662500000000	-1.841600000000
C	-1.211200000000	-2.568600000000	-0.919800000000
H	2.152900000000	0.295900000000	1.270500000000
H	-0.548800000000	-3.357500000000	-1.280900000000

### CO-FN-h

$$E = -5352.91 \text{ kcal mol}^{-1}$$

C	2.562350000000	-1.519223000000	-1.612385000000
C	2.296740000000	-0.232528000000	-2.246253000000
C	1.931853000000	0.707352000000	-1.201192000000
C	1.878590000000	-0.011688000000	0.055787000000
C	2.358044000000	-1.357938000000	-0.183787000000
Rh	0.073122000000	-0.923220000000	-1.039779000000
C	-1.834361000000	-3.355297000000	-1.609048000000
C	-0.617866000000	-2.796904000000	-1.454362000000
C	-3.375350000000	-1.512126000000	-2.354649000000

C	-3.127754000000	-2.711901000000	-1.764247000000	C	-1.895627000000	-3.318782000000	-1.623313000000
H	1.742752000000	0.440724000000	1.031188000000	C	-0.668522000000	-2.752039000000	-1.676094000000
H	-3.990386000000	-3.304272000000	-1.456686000000	C	-3.423766000000	-1.441367000000	-2.191872000000
H	-4.419767000000	-1.224008000000	-2.480380000000	C	-3.173929000000	-2.645868000000	-1.596430000000
H	0.256156000000	-3.453484000000	-1.379807000000	H	1.644077000000	0.419335000000	1.031076000000
H	-1.863959000000	-4.450675000000	-1.600298000000	H	-4.019427000000	-3.203937000000	-1.194047000000
C	1.693216000000	2.067535000000	-1.530272000000	H	-4.456718000000	-1.096079000000	-2.236055000000
C	2.400548000000	0.207332000000	-3.584324000000	H	0.208412000000	-3.387785000000	-1.837441000000
C	1.804553000000	2.466545000000	-2.851064000000	H	-1.933298000000	-4.413217000000	-1.637205000000
C	2.148802000000	1.540310000000	-3.874424000000	C	1.664470000000	2.066311000000	-1.518067000000
H	2.674295000000	-0.486698000000	-4.375715000000	C	2.477404000000	0.235753000000	-3.555358000000
H	1.428228000000	2.780853000000	-0.752806000000	C	1.825322000000	2.481037000000	-2.831288000000
C	-1.223142000000	-0.566339000000	0.227627000000	C	2.221603000000	1.570027000000	-3.845294000000
O	-2.039783000000	-0.345352000000	1.017977000000	H	2.793432000000	-0.447511000000	-4.340496000000
H	1.628536000000	3.506540000000	-3.116550000000	H	1.355978000000	2.768033000000	-0.746148000000
H	2.229874000000	1.892348000000	-4.900407000000	C	-1.220104000000	-0.573106000000	0.206863000000
C	2.624319000000	-2.443081000000	0.691870000000	O	-1.997075000000	-0.327287000000	1.030547000000
C	3.012510000000	-2.756184000000	-2.124225000000	H	1.645760000000	3.521137000000	-3.093716000000
C	3.065798000000	-3.641631000000	0.158280000000	H	2.339885000000	1.931024000000	-4.864584000000
C	3.251765000000	-3.800595000000	-1.243100000000	C	2.590541000000	-2.445430000000	0.702407000000
H	2.482913000000	-2.328852000000	1.764462000000	C	3.085240000000	-2.727111000000	-2.097196000000
H	3.170525000000	-2.888986000000	-3.192082000000	C	3.080021000000	-3.631555000000	0.177143000000
H	3.603245000000	-4.756698000000	-1.624493000000	C	3.318303000000	-3.774611000000	-1.215039000000
H	3.277770000000	-4.479844000000	0.818207000000	H	2.405365000000	-2.343548000000	1.769541000000
C	-1.108084000000	-0.421238000000	-2.624842000000	H	3.285488000000	-2.847214000000	-3.159582000000
C	-2.399109000000	-0.619646000000	-2.956018000000	H	3.704438000000	-4.719184000000	-1.591824000000
H	-0.514648000000	0.281384000000	-3.220426000000	H	3.286280000000	-4.469554000000	0.839077000000
H	-2.780211000000	-0.013214000000	-3.785332000000	C	-1.107422000000	-0.636233000000	-2.722985000000
				C	-2.443673000000	-0.677713000000	-2.929485000000
				H	-0.468674000000	-0.126000000000	-3.451665000000
				H	-2.829816000000	-0.095273000000	-3.772709000000

### CO-FN-TS(h,4)

$$E = -5352.46 \text{ kcal mol}^{-1} \quad -180.001 \text{ cm}^{-1}$$

C	2.593189000000	-1.505252000000	-1.591337000000
C	2.328377000000	-0.214614000000	-2.226513000000
C	1.909720000000	0.709349000000	-1.192619000000
C	1.801776000000	-0.027906000000	0.056383000000
C	2.334489000000	-1.361507000000	-0.173465000000
Rh	0.071498000000	-0.935886000000	-1.069234000000

### CO-FN-4

$$E = -5399.92 \text{ kcal mol}^{-1}$$

C	2.134425000000	-1.592516000000	-1.700026000000
C	1.952556000000	-0.334007000000	-2.441460000000
C	2.084827000000	0.749155000000	-1.509588000000

C	2.234736000000	0.185541000000	-0.156388000000	H	2.160173000000	2.905363000000	-1.267826000000
C	2.409488000000	-1.263270000000	-0.325853000000	C	-0.214447000000	0.726388000000	1.327779000000
Rh	0.153010000000	-0.295592000000	-0.139947000000	O	-0.432080000000	1.381724000000	2.269592000000
C	-1.608065000000	-2.948549000000	-0.503566000000	H	1.854454000000	3.344896000000	-3.696949000000
C	-1.823661000000	-1.626825000000	-0.020733000000	H	1.588228000000	1.471713000000	-5.298506000000
C	-1.802020000000	-2.155593000000	-2.791704000000	C	2.765000000000	-2.281910000000	0.584004000000
C	-1.593310000000	-3.206646000000	-1.863737000000	C	2.191531000000	-2.930054000000	-2.128466000000
H	2.654266000000	0.743452000000	0.674613000000	C	2.830629000000	-3.598410000000	0.133796000000
H	-1.434683000000	-4.220560000000	-2.223970000000	C	2.537043000000	-3.920814000000	-1.209792000000
H	-1.800189000000	-2.370121000000	-3.858271000000	H	2.988959000000	-2.037623000000	1.620240000000
H	-2.049644000000	-1.486909000000	1.031783000000	H	1.990346000000	-3.190365000000	-3.165328000000
H	-1.474726000000	-3.757904000000	0.210495000000	H	2.596506000000	-4.957818000000	-1.533703000000
C	2.050667000000	2.078912000000	-1.967051000000	H	3.111511000000	-4.390670000000	0.824255000000
C	1.761002000000	-0.071927000000	-3.805215000000	C	-2.048859000000	-0.569466000000	-0.952760000000
C	1.874788000000	2.320877000000	-3.330235000000	C	-2.031951000000	-0.863859000000	-2.346901000000
C	1.723519000000	1.255660000000	-4.240832000000	H	-2.460130000000	0.379511000000	-0.621952000000
H	1.660439000000	-0.885660000000	-4.520504000000	H	-2.226088000000	-0.065058000000	-3.058987000000

## References

---

- [1] G. Jones, *Compr. Heterocycl. Chem.* **1984**, 2, 395–510; b) K. Tanaka, Transition-Metal-Mediated Aromatic Ring Construction, Wiley, Hoboken, New Jersey, **2013**.
- [2] M. Berthelot, *Ann. Chem. Pharm.* **1867**, 141, 173–184.
- [3] W. Reppe, O. Schlichting, K. Klager, T. Toepel, *Justus Liebigs Ann. Chem.* **1948**, 560, 1–92.
- [4] Y. Wakatsuki, H. Yamazaki, *J. Chem. Soc. Chem. Commun.* **1973**, 280a–280a.
- [5] Y. Wakatsuki, H. Yamazaki, *Bull. Chem. Soc. Jpn.* **1985**, 58, 2715–2716.
- [6] D. Suzuki, H. Urabe, F. Sato, *J. Am. Chem. Soc.* **2001**, 123, 7925–7926.
- [7] T. Takahashi, Y. Li, P. Stepnicka, M. Kitamura, Y. Liu, K. Nakajima, M. Kotora, *J. Am. Chem. Soc.* **2002**, 124, 576–582.
- [8] H. Werner, *Angew. Chem. Int. Ed. Engl.* **1983**, 22, 927–949.
- [9] G. Consiglio, F. Morandini, *Chem. Rev.* **1987**, 87, 761–778.
- [10] E. B. Bauer, *Chem. Soc. Rev.* **2012**, 41, 3153–3167.
- [11] S. Saito, Y. Yamamoto, *Chem. Rev.* **2000**, 100, 2901–2916.
- [12] J. P. Collman, *Univ. Sci. Books* **1987**, 324.
- [13] J. A. Varela, C. Saá, C. *Chem. Rev.* **2003**, 103, 3787–3802.
- [14] H. Bönnemann, *Angew. Chem. Int. Ed. Engl.* **1978**, 17, 505–515.
- [15] H. Bönnemann, *Angew. Chem. Int. Ed. Engl.* **1985**, 24, 248–262.
- [16] G. Schmid, M. Schütz, *Organometallics* **1992**, 11, 1789–1792.
- [17] N. Koga, K. Morokuma, *Chem. Rev.* **1991**, 91, 823–842.
- [18] M. J Calhorda, L. F. Veiros, *Coord. Chem. Rev.* **1999**, 185–186, 37–51.
- [19] M. J. Calhorda, C. C. Romão, L. F. Veiros, *Chem.- Eur. J.* **2002**, 8, 868–875.
- [20] F. Basolo, R. G. Pearson, *John Wiley Sons Inc N. Y.* **1967**.
- [21] H. G. Schuster-Woldan, F. Basolo, *J. Am. Chem. Soc.* **1966**, 88, 1657–1663.
- [22] M. Dalla Tiezza, F. M. Bickelhaupt, L. Orian, *Chemistry Open* **2018**, 143–154.

- 
- [23] S. Kozuch, S. Shaik, *ACC. Chem. Res.* **2011**, *44*, 101–110.
- [24] P. Diversi, G. Ingrosso, A. Lucherini, W. Porzio, M. Zocchi, *Inorg. Chem.* **1980**, *19*, 3590–3597.
- [25] A. Borrini, P. Diversi, G. Ingrosso, A. Lucherini, G. Serra, *J. Mol. Catal.* **1985**, *30*, 181–195.
- [26] K. Abdulla, B. L. Booth, C. Stacey, *J. Organomet. Chem.* **1985**, *293*, 103–114.
- [27] A. J. Hart-Davis, R. J. Mawby, *J. Chem. Soc. A* **1969**, 2403–2407.
- [28] M. E. Rerek, L. N. Ji, F. Basolo, *J. Chem. Soc. Chem. Commun.* **1983**, *21*, 1208–1209.
- [29] P. Cioni, P. Diversi, G. Ingrosso, A. Lucherini, P. Ronca, *J. Mol. Catal.* **1987**, *40*, 337–357.
- [30] P. Diversi, L. Ermini, G. Ingrosso, A. Lucherini, *J. Organomet. Chem.* **1993**, *447*, 291–298.
- [31] A. A. Dahy, K. Yamada, N. Koga, *Organometallics* **2009**, *28*, 3636–3649.
- [32] B. M. Trost, M. C. Ryan, *Angew. Chem. Int. Ed.* **2017**, *56*, 2862–2879.
- [33] C. Bonifaci, A. Ceccon, A. Gambaro, P. Ganis, S. Santi, G. Valle, A. Venzo, *Organometallics* **1993**, *12*, 4211–4214.
- [34] a) C. Bonifaci, A. Ceccon, A. Gambaro, F. Manoli, L. Mantovani, P. Ganis, S. Santi, A. Venzo, *J. Organomet. Chem.* **1998**, *557*, 97–109; b) C. Bonifaci, G. Carta, A. Ceccon, A. Gambaro, S. Santi, A. Venzo, *Organometallics* **1996**, *15*, 1630–1636; c) P. Cecchetto, A. Ceccon, A. Gambaro, S. Santi, P. Ganis, R. Gobetto, G. Valle, A. Venzo, *Organometallics* **1998**, *17*, 752–762.
- [35] A. Ceccon, S. Santi, L. Orian, A. Bisello, *Coord. Chem. Rev.* **2004**, *248*, 683–724.
- [36] A. Ceccon, A. Gambaro, S. Santi, A. Venzo, *J. Mol. Catal.* **1991**, *69*, L1–L6; b) C. Amatore, A. Ceccon, S. Santi, J. N. Verpeaux, *Chem. Eur. J.* **1999**, *5*, 3357–3365; c) L. Mantovani, A. Ceccon, A. Gambaro, S. Santi, P. Ganis, A. Venzo, *Organometallics* **1997**, *16*, 2682–2690.
- [37] J. H. Hardesty, J. B. Koerner, T. A. Albright, G. Y. Lee, *J. Am. Chem. Soc.* **1999**, *121*, 6055–6067.
- [38] K. Kirchner, M. J. Calhorda, R. Schmid, L. F Veiros, *J. Am. Chem. Soc.* **2003**, *125*, 11721–11729.

- 
- [39] M. J. Calhorda, P. J. Costa, K. A. Kirchner, *Inorganica. Chim. Acta* **2011**, *374*, 24–35.
- [40] G. Dazinger, M. Torres-Rodrigues, K. Kirchner, M. J. Calhorda, P. J. Costa, *J. Organomet. Chem.* **2006**, *691*, 4434–4445.
- [41] L. Orian, J. N. P. van Stralen, F. M. Bickelhaupt, *Organometallics* **2007**, *26*, 3816–3830.
- [42] L. Orian, W. J. van Zeist, F. M. Bickelhaupt, *Organometallics* **2008**, *27*, 4028–4030.
- [43] L. Orian, M. Swart, F. M. Bickelhaupt, *ChemPhysChem* **2014**, *15*, 219–228.
- [44] L. Orian, L. P. Wolters, F. M. Bickelhaupt, *Chem. Eur. J.* **2013**, *19*, 13337–13347.
- [45] A. A. Dahy, C. H. Suresh, N. Koga, *Bull. Chem. Soc. Jpn.* **2005**, *78*, 792–803.
- [46] A. A. Dahy, N. Koga, *Organometallics* **2015**, *34*, 4965–4974.
- [47] F. Jensen, Introduction to Computational Chemistry, Wiley-VCH, Weinheim, **1999**.
- [48] R. McWeeny, Methods of Molecular Quantum Mechanics, Academic Press, London, **1992**.
- [49] C. J. Cramer, Essentials of Computational Chemistry: Theories and Models, John Wiley & Sons, Ltd., Chichester, West Sussex, **2004**.
- [50] M. Born, J. R. Oppenheimer, *Ann. Phys.* **1927**, *84*, 457–484.
- [51] a) W. Koch, M. C. Holthausen, A Chemist's Guide to Density Functional Theory, Wiley-VCH, Weinheim, **2002**; b) R. Dreizler, E. Gross, Density Functional Theory. Plenum Press: New York, **1995**.
- [52] E. Schrödinger, *Ann. Phys.* **1926**, *80*, 437–490.
- [53] D. R. Hartree, *Math. Proc. Camb. Philos. Soc.* 1928, *24*, 89–110.
- [54] J. C. Slater, *Phys. Rev.* **1928**, *32*, 339–348.
- [55] a) V. Fock, *Zeitschrift für Physik*, **1930**, *61*, 126–148; b) V. Fock, *Zeitschrift für Physik*, **1930**, *62*, 795–805.
- [56] a) D. Maurice, M. Head-Gordon, *Molecular Physics* **1999**, *96*, 1533–1541; b) M. Head-Gordon, R. J. Rico, M. Oumi, T. J. Lee, *Chem. Phys. Lett.* **1994**, *219*, 21–29.
- [57] H. D. Meyer, U. Manthe, L. S. Cederbaum, *Chem. Phys. Lett.* **1990**, *165*, 73–78.

- 
- [58] a) C. Møller, M. S. Plesset, *Phy. Rev.* **1934**, *46*, 618–622; b) K. Raghavachari, J. A. Pople, *Int. J. Quantum. Chem.* **1978**, *14*, 91–100.
- [59] a) G. D. Purvis, R. J. Bartlett, *J. Chem. Phys.* **1982**, *76*, 1910–1918; b) K. Raghavachari, G. W. Trucks, J. A. Pople, M. Head-Gordon, *Chem. Phys. Lett.* **1989**, *157*, 479–483; c) T. Van Voorhis, M. Head-Gordon, *J. Chem. Phys.* **2001**, *115*, 5033–5040.
- [60] a) V. Magnasco, “Post-Hatree–Fock Methods” Methods of Molecular Quantum Mechanics: An Introduction to Electronic Molecular Structure, John Wiley & Sons, Ltd. **2009**, 133–138 ; b) R. J. Bartlett, J. F. Stanton, Applications of Post-Hatree–Fock Methods: A Tutorial. Reviews in Computational Chemistry, John Wiley & Sons, Inc, **2007**, 65–169.
- [61] P. Hohenberg, W. Kohn, *Phys. Rev.* **1964**, *136*, B864–B871.
- [62] W. Kohn, L. J. Sham, *Phys. Rev.* **1965**, *140*, A1133–A1138.
- [63] a) S. H. Vosko, L. Wilk, M. Nusair, *J. Phys.* **1980**, *58*, 1200–1211; b) A. D. Becke, *J. Chem. Phys.* **2014**, *140*, 18A301; c) R. G. Parr, S. K Ghosh, *Phys. Rev. A* **1995**, *51*, 3564–3570.
- [64] J. P. Perdew, , J. A. Chevary, S. H. Vosko, K. A. Jackson, M. R. Pederson, D. J. Singh, C. Fiolhais, *Phys. Rev. B* **1992**, *46*, 6671–6687.
- [65] D. C. Langreth, M. J. Mehl, *Phys. Rev. B* **1983**, *28*, 1809–1834.
- [66] a) A. D. Becke, *J. Chem. Phys.* **1993**, *98*, 1372–1377; b) J. P. Perdew, M. Ernzerhof, K. Burke, *J. Chem. Phys.* **1996**, *105*, 9982–9985.
- [67] R. G. Parr, W. Yang, Density-functional theory of atoms and molecules, International series of monographs on chemistry, 1. issue, Oxford Univ. Press, New York, NY, **1994**. ISBN 978-0-19-509276-9.
- [68] G. te Velde, F. M. Bickelhaupt, E. J. Baerends, C. Fonseca Guerra, S. J. A. van Gisbergen, J. G. Snijders, T. Ziegler, *J. Comput. Chem.* **2001**, *22*, 931–967.
- [69] a) C. Fonseca Guerra, J. G. Snijders, G. te Velde, E. J. Baerends, *Theor. Chem. Acc.* **1998**, *99*, 391–403.

- 
- [70] E. J. Baerends, T. Ziegler, A. J. Atkins, J. Autschbach, D. Bashford, A. Bérçes, F. M. Bickelhaupt, C. Bo, P. M. Boerritger, L. Cavallo, D. P. Chong, D. V. Chulhai, L. Deng, R. M. Dickson, J. M. Dieterich, D. E. Ellis, M. van Faassen, A. Ghysels, A. Giammona, S. J. A. van Gisbergen, A. W. Götz, S. Gusarov, F. E. Harris, P. van den Hoek, C. R. Jacob, H. Jacobsen, L. Jensen, J. W. Kaminski, G. van Kessel, F. Kootstra, A. Kovalenko, M. Krykunov, E. van Lenthe, D. A. McCormack, A. Michalak, M. Mitoraj, S. M. Morton, J. Neugebauer, V. P. Nicu, L. Noddleman, V. P. Osinga, S. Patchkovskii, M. Pavanello, C. A. Peeples, P. H. T. Philipsen, D. Post, C. C. Pye, W. Ravenek, J. I. Rodríguez, P. Ros, R. Rüger, P. R. T. Schipper, H. van Schoot, G. Schreckenbach, J. S. Seldenthuis, M. Seth, J. G. Snijders, S. Miquel, M. Swart, D. Swerhone, G. te Velde, P. Vernooij, L. Versluis, L. Visscher, O. Visser, F. Wang, T. A. Wesolowski, E. M. van Wezenbeek, G. Wiesnekker, S. K. Wolff, T. K. Woo, A. L. Yakovlev, **ADF2016**, Amsterdam, The Netherlands, **2016**.
- [71] A. D. Becke, *Phys. Rev. A* **1988**, *38*, 3098–3100.
- [72] C. Lee, W. Yang, R. G. Parr, *Phys. Rev. B* **1988**, *37*, 785–789.
- [73] E. van Lenthe, E. J. Baerends, *J. Comput. Chem.* **2003**, *24*, 1142–1156.
- [74] E. van Lenthe, E. J. Baerends, J. G. Snijders, *J. Chem. Phys.* **1994**, *101*, 9783–9792.
- [75] a) E. van Lenthe, E. J. Baerends, J. G. Snijders, *J. Chem. Phys.* **1993**, *99*, 4597–4610; b) E. van Lenthe, A. Ehlers, E. J. Baerends, *J. Chem. Phys.* **1999**, *110*, 8943–8953; c) E. van Lenthe, E. J. Baerends, *J. Comput. Chem.* **2003**, *24*, 1142–1156.
- [76] F. M. Bickelhaupt, K. N. Houk, *Angew. Chem. Int. Ed.* **2017**, *56*, 10070–10086.
- [77] I. Fernández, F. M. Bickelhaupt, *Chem. Soc. Rev.* **2014**, *43*, 4953–4967.
- [78] K. Morokuma, *J. Chem. Phys.* **1971**, *55*, 1236–1244.
- [79] T. Ziegler, A. Rauk, *Theor. Chim. Acta* **1977**, *46*, 1–10.
- [80] a) F. M. Bickelhaupt, *J. Comput. Chem.* **1999**, *20*, 114–128; b) C. M. Weng, F. E. Hong, *Dalton Trans.* **2011**, *40*, 6458–6468.
- [81] J. Wassenaar, E. Jansen, W-J. van Zeist, F. M. Bickelhaupt, M.A. Siegler, A. L. Spek, J. N. H. Reek, *Nat Chem.* **2010**, *2*, 417–421.

- 
- [82] U. Radius, F. M. Bickelhaupt, *Organometallics* **2008**, *27*, 3410–3414.
- [83] a) D. H. Ess, K. N. Houk, *J. Am. Chem. Soc.* **2008**, *130*, 10187–98; b) Y. Cao, Y. Liang, L. Zhang, S. Osuna, A. L. Hoyt, A. L. Briseno, K. N. Houk, *J. Am. Chem. Soc.* **2014**, *136*, 10743–51.
- [84] a) F. Schoenebeck, D. H. Ess, G. O. Jones, K. N. Houk, *J. Am. Chem. Soc.* **2009**, *131*, 8121–8133; b) I. Fernández, F. M. Bickelhaupt, *J. Comput. Chem.* **2014**, *35*, 371–376.
- [85] M. El-Hamdi, W. Tiznado, J. Poater, M. Solà, *J. Org. Chem.* **2011**, *76*, 8913–8921.
- [86] M. Contreras, E. Osorio, F. Ferraro, G. Puga K. J. Donald, J. G. Harrison, G. Merino, W. Tiznado, *Chem. Eur. J.* **2013**, *19*, 2305–2310.
- [87] L. P. Wolters, F. M. Bickelhaupt, *Rev. Comput. Mol. Sci.* **2015**, *5*, 324–343.
- [88] A. Diefenbach, F. M. Bickelhaupt, *J. Chem. Phys.* **2001**, *115*, 4030–4040.
- [89] M. A. van Bochove, M. Swart, F. M. Bickelhaupt, *J. Am. Chem. Soc.* **2006**, *128*, 10738–44.
- [90] F. M. Bickelhaupt, E. J. Baerends, *Rev. Comput. Chem.* **2000**, *15*, 1–86.
- [91] a) J. Hagen, Industrial catalysis: a practical approach. John Wiley & Sons, **2015**; b) M. Boudart, A. Aldag, J. E. Benson, N. A. Dougherty, C. G. Harkins, *J. Catal.* **1966**, *6*, 92–99; c) S. Kozuch, Jan M. L. Martin, *ACS Catal.* **2012**, *2*, 2787–2794.
- [92] a) D. Astruc, Organometallic chemistry and catalysis; Springer: Berlin, New York, **2007**; b) PW. Van Leeuwen, Homogeneous catalysis: understanding the art. Springer Science & Business Media, **2006**.
- [93] a) J. A. Christiansen, *Adv. Catal.* **1953**, *5*, 311–353; b) S. Kozuch, S. Shaik, *J. Am. Chem. Soc.* **2006**, *128*, 3355–3365.
- [94] S. Kozuch, S. Shaik, *J. Phys. Chem. A* **2008**, *112*, 6032–6041.
- [95] C. Amatore, A. Jutand, *J. Organomet. Chem.* **1999**, *576*, 254–278.
- [96] a) S. Kozuch, *ACS Catal.* **2015**, *5*, 5242–5255; b) E. Solel, N. Tarannam, S. Kozuch, *Chem. Commun.* **2019**, *55*, 5306–5322.
- [97] a) S. Kozuch, S. Shaik, *J. Phys. Chem. A* **2008**, *112*, 6032–6041; b) A. Uhe, S. Kozuch, S. Shaik, *J. Comput. Chem.* **2011**, *32*, 978–985.

- 
- [98] T. A. Albright, P. Hofmann, R. Hoffmann, C. P. Lillya, P. A. Dobosh, *J. Am. Chem. Soc.* **1983**, *105*, 3396–3411.
- [99] N. E. Schore, *Chem. Rev.* **1988**, *88*, 1081–1119.
- [100] M. Dalla Tiezza, F. M. Bickelhaupt, L. Orian, *ChemPhysChem* **2018**, *19*, 1766–1773.
- [101] C. Bonifaci, A. Ceccon, A. Gambaro, P. Ganis, L. Mantovani, S. Santi, A. Venzo, *J. Organomet. Chem.* **1994**, *475*, 267–276.
- [102] C. R Groom, I. J Bruno, M. P. Lightfoot, S. C. Ward, *Acta Crystallogr. B* **2016**, *72*, 171–179.
- [103] M. E. Rerek, F. Basolo, *J. Am. Chem. Soc.* **1984**, *106*, 5908–5912.
- [104] I. Fernández, F.M. Bickelhaupt, F. P Cossío, *Chem. Eur. J.* **2012**, *18*, 12395–12403.
- [105] C. Bonifaci, A. Ceccon, S. Santi, C. Mealli, R. W. Zoellner, *Inorganica Chim. Acta* **1995**, *240*, 541–549.
- [106] S. M. Ahmad, M. Dalla Tiezza, L. Orian, *Catalysts* **2019**, *9*, 679.
- [107] J. T. Price, T. S. Sorensen, *Canadian. J. Chem.* **1968**, *46*, 515–522.
- [108] S. L. Mukerjee, R. F. Lang, T. Ju, G. Kiss, C. Hoff, S. P. Nolan, *Inorganic. Chem.* **1992**, *31*, 4885–4889.